Identification, occurrence and fate of transformation products and metabolites of fluoxetine and metformin in the aquatic environment

Dissertation

der Mathematisch-Naturwissenschaftlichen Fakultät

der Eberhard Karls Universität Tübingen

zur Erlangung des Grades eines

Doktors der Naturwissenschaften

(Dr. rer. nat.)

vorgelegt von

Selina Kornelia Tisler

Reutlingen

Tübingen

2019

Gedruckt mit Genehmigung der Mathematisch-Naturwissenschaftlichen Fakultät der Eberhard Karls Universität Tübingen.

Tag der mündlichen Qualifikation:	04. Juli 2019
Dekan:	Prof. Dr. Wolfgang Rosenstiel
1. Berichterstatter:	Prof. Dr. Christian Zwiener
2. Berichterstatter:	Prof. Dr. Stefan B. Haderlein

Contents

Abstract

Nowadays, one of the fundamental challenges in water treatment is the removal of micropollutants. Conventional wastewater treatment plants (WWTPs) are ineffective in the removal of a broad range of micropollutants. Consequently, these compounds and their transformation products (TPs) are released into the aquatic environment where they might undergo further transformation through abiotic (e.g. photolysis) or biotic (e.g. bacteria or fish) degradation. Pharmaceuticals are the largest group of representatives of micropollutants and the ones with the highest concentrations in waste water. They are designed to have certain effects on the human body which can result in unwanted effects of the precursors and the TPs on water organisms. Furthermore, the structure and effect of most of the TPs are still unknown and moreover, a higher toxicity of the TPs than that of their parent compound was already detected for some pharmaceuticals.

This study contributes to the identification of unknown TPs of the pharmaceuticals metformin (MF) and fluoxetine (FLX) in aquatic environment. The biguanide MF is a drug against type 2 diabetes and one of the most consumed pharmaceuticals worldwide. FLX is a drug against depression, with high ecotoxicity in environmental relevant concentrations. For the identification of new TPs, a workflow of liquid chromatography coupled with high resolution mass spectrometry (LC-HRMS) was used.

In the first part of the study, natural transformation of MF was simulated by electrochemical degradation and the occurrence and fate of the identified TPs were investigated in batch experiments with activated sludge. In electrochemical experiments, four new TPs of MF were revealed which were formed by cyclization and demethylation. Three of them (MBG, 2,4-AMT, 2,4-DAT) were detected in effluent samples of WWTPs. For detailed biodegradation information, batch experiments with activated sludge were performed. MF was aerobically transformed completely into the TPs. The well-known metabolite guanyl urea (GU) was the main metabolite (98%) and 2% of MF was degraded into the newly identified TPs.

Furthermore, for the first time, GU degradation in activated sludge was observed, fast under anaerobic conditions and slow under aerobic conditions. The aerobic biodegradability of GU was depending on the microbial community which was influenced by the originating WWTP of the activated sludge.

In the second part of the study, FLX degradation in a sunlight simulation chamber revealed 27 TPs, formed by *O*-dealkylation, hydroxylation, CF_3-substitution and *N*-acylation. The human main metabolite norfluoxetine (NFLX) was a minor TP in photolysis. With increasing pH in ultrapure water, the reactivity of FLX and the primary TPs, formed by *O*-dealkylation, became faster. Taking indirect photolysis into consideration, degradation rates of FLX and primary *O*-dealkylated TPs were even higher, but the general formation rates of TPs, especially for hydroxylated TPs, increased. In zebra fish embryos (96 h postfertilization), seven metabolites known from photodegradation, as well as three new metabolites formed by N-hydroxylation, N-methylation and attachment of an amine group, were identified. The bioconcentration factor of FLX (exposition medium 5 mg/L) was 200, and about 1% of FLX taken up by the embryos was transformed to NFLX.

The study highlights the importance of considering a broad range of environmental relevant TPs of MF and FLX in fresh water systems. Furthermore, differences and similarities between abiotic and biotic formed TPs were revealed and can be helpful for further studies on identification of TPs of other micropollutants.

Zusammenfassung

Die Entfernung von Spurenstoffen ist zu einer der größten Herausforderungen der Abwasserreinigung unserer Zeit geworden. Die anthropogen eingebrachten Stoffe werden häufig unzureichend aus Kläranlagen entfernt und gelangen als Ausgangsstoffe oder als veränderter Stoffe, sogenannte Transformationsprodukte (TPs), in die Oberflächengewässer. Die Substanzen können in der aquatischen Umwelt durch abotische Prozesse, wie z.B. Photoabbau weiter verändert werden, oder von Organismen aufgenommen und in diesen akkumulieren oder weiter transformiert werden. Die Gruppe von Spurenstoffen mit der größten Vielfalt an Stoffen und den höchsten Konzentrationen im Abwasser sind die Arzneimittel. Während diese im menschlichen Stoffwechsel gewollte Effekte auslösen, können die Ausgangssubstanzen oder TPs ungewollte Effekte bei Wasserorganismen hervorrufen. Für manche Substanzen (Bspw. Gabapentin, Diclofenac, Acyclovir) wurde eine höhere Toxizität der TPs als der Ausgangssubstanz nachgewiesen. Des Weiteren wurden eine Vielzahl von TPs noch nicht ausreichend untersucht oder gar identifiziert, weshalb deren Toxizität ungewiss ist. Diese Studie soll anhand von Transformationsprozessen von zwei umweltrelevanten Arzneimitteln bei der Aufklärung der unbekannten TPs in der aquatischen Umwelt Aufschluss geben. Zum einen durch das Biguanid Metformin (MF), welches hauptsächlich gegen Diabetes Typ 2 eingesetzt wird und eines der meist eingenommenen Arzneimittel weltweit ist. Außerdem wurden die TPs des selektiven Serotonin-Wiederaufnahmehemmer Fluoxetin (FLX) untersucht, welcher hauptsächlich gegen Depressionen verschrieben wird und für eine hohe Ökotoxizität in umweltrelevanten Konzentrationen bekannt ist. Mögliche umweltrelevante TPs wurden mit verschiedenen Abbauexperimenten (Elektrochemie, Bioabbau mit Belebtschlamm, Photoabbau, Fischembryo Metabolismus) generiert und anhand eines Workflows mit Flüssigchromatographie gekoppelt an hochauflösende Massenspektrometrie (LC-HRMS) identifiziert.

Im ersten Teil der Arbeit wurden TPs aus elektrochemischem MF Abbau identifiziert und in mikrobiellen Bioabbau-Experimenten untersucht. Mittels elektrochemisch simulierten abiotische und biotische Transformationsprozesse konnten vier neue umweltrelevante

TPs von MF identifiziert werden, welche sich durch Zyklisierung und Demethylierung bildeten. Die neu identifizierten TPs (MBG, 2,4-AMT, 2,4-DAT) konnten im Abstrom von Kläranlagen nachgewiesen werden. Anhand von Batchexperimenten mit Belebtschlamm wurden die biologischen Bildungs- und Abbauprozesse der TPs untersucht. Der aerobe Abbau von MF zeigte eine 1:1 Umwandlung in die TPs, wobei der bekannte Metabolit Guanylharnstoff (GU) das Hauptprodukt war und die elektrochemisch identifizierten TPs weniger als 2% des abgebauten MF darstellten. Es konnte außerdem erstmals die Abbaubarkeit von GU in Belebtschlamm nachgewiesen werden, wobei die Abbauprozesse schneller im anaeroben Milieu abliefen, während im aeroben Milieu die Abbaubarkeit zusätzlich von der Herkunft des Belebtschlamms und somit der mikrobiellen Gemeinschaft, abhängig war.

Im zweiten Teil der Arbeit wurden anhand von Photolyse und Fisch-Metabolismus neue TPs von Fluoxetin identifiziert. Mit einer Sonnensimulationskammer konnten 27 TPs durch direkten und indirekten Photoabbau von FLX identifiziert werden, welche durch *O*-Dealkylierung, Hydroxylierung, CF_3-Subsitution und *N*-acylierung gebildet wurden. Der menschliche Hauptmetabolit Norfluoxetine (NFLX) spielte dabei eine untergeordnete Rolle. In Experimenten mit direkter Photolyse zeigte sich mit zunehmendem pH-Wert eine höhere Abbaurate für FLX sowie für die primären TPs, welche durch Molekülspaltung (O-Dealkylierung) gebildet wurden. In Abbauexperimenten mit Oberflächenwasser anstatt Reinstwasser, zeigte sich der Einfluss der indirekten Photolyse durch die größte gebildete Intensität an hydroxylierte TPs, sowie die höchste Abbaurate von FLX. Eine neue Gruppe von TPs bildete sich durch die CF_3-Substitution, welche bisher in der Literatur nur für eines der sieben identifizierten TPs beschrieben wurde. Auch bei der *N*-acylierung von FLX mit Carboxylsäuren und Aldehyden wurden sieben neue TPs identifiziert, wobei *N*-acylierung bisher nur im biologischen FLX Abbau beschrieben wurde. Im Extrakt von Zebrafisch Embryonen (96 h nach Befruchtung) konnten sieben der abiotischen TPs nachgewiesen werden, sowie drei neue TPs identifiziert werden. Diese bildeten sich durch *N*-hydroxylierung, *N*-methylierung und *N*-acylierung von FLX mit einer Aminogruppe. FLX aus dem Expositionsmedium (5 mg/L) reicherte sich 200-fach in den

Embryonen an, wobei 1% in NFLX umgewandelt und als Hauptmetabolit nachgewiesen werden konnte.

Die in dieser Studie identifizierten TPs mittel LC-HRMS bieten eine umfassende Anzahl an TPs mit mögliche Effekten auf Wasserorganismen, welche für Effektuntersuchungen auf verschiedenen Organismenebenen verwendet werde können. Desweiten konnten Unterschiede und Gemeinsamkeiten der abiotischen und biotischen Transformationsprozessen gezeigt werden, welche für die Identifizierung von TPs von weiteren Spurenstoffen hilfreich sein können.

Danksagung

Diese Studie wurde im Rahmen des Verbundprojekts Effect-Net im Wassernetzwerk Baden-Württemberg durchgeführt, für dessen Förderung durch das Ministerium für Wissenschaft, Forschung und Kunst, ich meinen Dank aussprechen möchte.

Ich möchte mich ganz besonders bei Prof. Dr. Christian Zwiener bedanken, der mir die Promotion durch dieses spannende Thema ermöglichte. Des Weiteren möchte ich mich für seine Unterstützung in Form von fundiertem Rat und neuen Ideen bedanken, auf die ich mich während der ganzen Promotionsphase verlassen konnte. Auch bei der Erstellung von wissenschaftlichen Publikationen konnte ich mich stets auf aufschlussreiche und hilfreiche Kritik verlassen. Danken möchte ich auch Prof. Dr. Stefan B. Haderlein für seine Tätigkeit als Gutachter, sowie Prof. Dr. Rita Triebskorn und Jun.-Prof. Dr. Christiane Zarfl die sich als weitere Prüfer zur Verfügung stellen.

Mein Dank geht außerdem an alle Kollegen der chemischen Umweltanalytik Arbeitsgruppe am Institut für Geowissenschaften in Tübingen. Besonders danken möchte ich Stephanie Nowak, die im Labor und bei administrativen Dingen eine tolle Unterstützung war und mich außerdem in wichtigen Phasen mit essentieller Nervennahrung versorgte. Des Weiteren danke ich Dr. Sylvain Merel und Dr. Martina Werneburg, auf die ich mich immer verlassen konnte, wenn es um Fehlerbehebung der Messgeräte oder konstruktive Diskussionen ging. Außerdem danke ich Boris Bugsel, Zi Wang, Sascha Lege, Maximilian Müller, Dr. Jorge E. Yanez und Rebecca Bauer für das tolle Arbeitsklima. Hilfe habe ich außerdem durch erfolgreiche Abschlussarbeiten erhalten, wofür ich mich bedanken möchte. Das gilt im Besonderen für Johanna Schwenkel, Leontien Best, Patricia Riede, Tobias Junginger, Melanie Weinstein und Klaus Röhler.
Danken möchte ich auch Dr. László Toelgyesi von Agilent Technologies, auf den ich mich immer verlassen konnte wenn unsere Messgeräte einen schlechten Tag hatten.

Des Weiteren möchte ich mich bei dem gesamten Effect-Net Team bedanken, für ein tolles Klima bei den Projekttreffen und dem hohen Stellenwert der Doktoranden, sowie deren Förderung im Projekt. Dabei sind vorallem Prof. Dr. Rita Triebskorn und Prof. Dr. Thomas Braunbeck für ihr Engagement zu erwähnen. Für die gegenseitige Unterstützung und Motivation bedanke ich mich außerdem bei meinen Gefährten Florian Zindler, Stefanie Jacob, Michael Ziegler, Sarah Knoll, Eike Rogall, Siegfried Hohmann, Susanna Mieck und Simon Schaub.

Meinen Freunden möchte ich danken für die Unterstützung und ebenso notwendige Ablenkung, besonders erwähnt werden sollen dabei Jasmin, Katharina, meine Handball-Mädels, die TZWler und die „unglaublichen Vier“.

Schließlich möchte ich meiner Familie für die immerwährende Unterstützung danken. Danke an meine Eltern, Matthias und meinen Bruder Merlin die mir den optimalen Rahmen für die Promotion geschaffen haben und mir immer mit Rat und Tat zur Seite stehen.

List of abbreviations

2,4-AMT	2-amino-4-methylamino-1,3,5-triazine
2,4-DAT	2,4-diamino-1,3,5-triazine
4,2,1-AIMT	4-amino-2-imino-1-methyl-1,2,dihydro-1,3,5-triazine
AcN	Acetonitrile
AMO	Ammonia mono-oxygenase
BDD	Boron-doped diamond electrode
CDOM	Colored dissolved organic matter
EC	Emerging contaminants
EC_{50}	Half-maximal effective concentration
EPA	United States Environmental Protection Agency
FLX	Fluoxetine
FLX-d5	Deuterated internal fluoxetine standard
GU	Guanyl urea
HILIC	Hydrophilic interaction chromatography
Hpf	Hours postfertilization
HRMS	High resolution mass spectrometry
LC	Liquid chromatography
LC_{50}	Half-maximal lethal concentration
MBG	Methylbiguanide
MeOH	Methanol
MF	Metformin

MS/MS	Tandem mass spectrometry with occurring fragmentation
NFLX	Norfluoxetine
OH·	Hydroxyl radicals
QqQ	Triple quadrupole
QTOF	Quadrupol time-of-flight mass spectrometer
ROS	Reactive oxygen species
SSRI	Selective Serotonin Reuptake Inhibitor
TFMP	4-Trifluormethylphenol
TP	Transformation product
WWTP	Waste water treatment plant

List of publications

Paper I

Tisler, Selina; Zwiener, Christian (2018): Formation and occurrence of transformation products of metformin in wastewater and surface water. *Science of The Total Environment,* 628-629, 1121–1129. DOI: 10.1016/j.scitotenv.2018.02.105.

Paper II

Tisler, Selina; Zwiener, Christian (2019): Aerobic and anaerobic formation and biodegradation of guanyl urea and other transformation products of metformin. *Water Research*, *149*, 130–135. DOI: 10.1016/j.watres.2018.11.001

Paper III

Tisler, Selina; Zindler, Florian; Freeling Finnian; Nödler, Karsten; Toelgyesi, László; Braunbeck, Thomas; Zwiener, Christian (2019): Transformation products of fluoxetine formed by photodegradation in water and biodegradation in zebrafish embryos (Danio rerio). *Environmental Science & Technology*, submitted

Author's contribution (Selina Tisler)

Paper I (first author)

The author and Christian Zwiener planned the study. The author performed the sampling campaign, developed the analytical methods, did all the experimental work, evaluated the data, and had the lead role in writing and revising the manuscript. Christian Zwiener provided critical feedback and helped shape the research, analysis and manuscript.

Paper II (first author)

The author planned the study, performed the sampling campaign, did all the experimental work, evaluated the data, and had the lead role in writing and revising the manuscript. Christian Zwiener provided critical feedback and helped shape the research, analysis and manuscript.

Paper III (first author)

The author and Florian Zindler planned the study. The author did all the experimental work of photodegradation and the extraction of the zebrafish embryos. The author did most of the analytical work (95%), including data evaluation and identification of the TPs and had the lead role in writing. All authors provided critical feedback and helped shape the research, analysis and manuscript.

1. Introduction

1.1. Organic micropollutants and their transformation products in the aquatic environment

Over the last few decades, increasing numbers and concentrations of anthropogenic chemicals were detected in the aquatic environment. The US EPA (United States Environmental Protection Agency) divided the so-called emerging contaminants (ECs) into 4 groups: veterinary and human antibiotics, human drugs, industrial and household wastewater products, sex and steroidal hormones. ECs are also often called organic micropollutants. They have several input sources and routes to end up in the aquatic environment, whereas the greatest concern is about pharmaceuticals (human drugs). Pharmaceuticals are the largest group of EC representatives, with more than 5000 available substances (Tijani et al. 2016) and worldwide consumption. The administration of pharmaceuticals results in their excretion in hospitals or households waste water by patients, as an active metabolite or as unmodified substance. Further minor entry sources to waste water are inappropriate disposed pharmaceuticals or accidental spillage at manufacturing sites. Conventional waste water treatment plants (WWTPs) are not specifically designed to eliminate ECs, they are able to remove some ECs efficiently, although there is still a significant group of compounds with recalcitrant behavior (Margot et al. 2015). Furthermore, removal should not be considered as mineralization, which would be the ideal case of elimination.

Removal and transformation of drugs and metabolites in WWTPs depends on the physical-chemical properties of the substance and the process conditions. On the one hand, removal by adsorption on activated sludge is improved by hydrophobicity (high Kow) of the compounds (Pomiès et al. 2013). On the other hand, the major removal pathway for more polar compounds is biodegradation, the susceptibility to that is more complex due to variable molecular structures. In general, compounds including esters, nitriles, aromatic alcohols and unsaturated aliphatic compounds have functional groups that may increase biodegradability (Sipma et al. 2010). In contrast, aromatic amines, halogen groups, nitro and azo groups increase a compound’s persistency (Jones et al.

2002). The important process conditions of the WWTPs for micropollutant removal are the solid retention time (SRT) of the activated sludge and the hydraulic retention time (HRT) of the waste water. With a longer SRT the microbial community is more diverse and adapted to the inflowing waste water, which also depends on the overall load and composition of micropollutants in the waste water (Boonnorat et al. 2014). Furthermore, higher HRT enable greater biodegradation of the organic micropollutants (Petrie et al. 2015). SRT and HRT are variable in WWTPs and optimized for most efficient process conditions in removal and energy-saving.

Commonly, treatment processes are incomplete (Petrie et al. 2015; Luo et al. 2014). As a consequence, organic micropollutants and their transformation products (TPs) or metabolites are emitted from WWTPs into surface water, as the most significant entry route into the aquatic environment (Cooper et al. 2008; Ternes 1998) (Figure 1). Due to metabolic processes, TPs are often more polar than their parent compounds when entering freshwater ecosystems. Subsequent transformation could occur through abiotic processes (e.g. hydrolysis, photolysis) or biodegradation by microorganisms and invertebrates (Aymerich et al. 2016). Both, precursors and TPs, could have a negative impact on water organisms. Some of the TPs are known to be more abundant (Boxall et al. 2004) and even more toxic than their parent compounds. For example, enhanced toxicity to water organisms was reported after UV irradiation of different pharmaceuticals, due to formation of toxic TPs (Herrmann et al. 2015; Wang and Lin 2012; Schulze et al. 2010). Furthermore, most likely the majority of TPs have not even been identified yet (Escher and Fenner 2011). Identification of TPs is a difficult task, especially because of the different formation reactions and quantity at which they are generated. The analytical challenge is to identify those compounds for which analytical standards are not available for. High separation efficiency and a maximum of molecular structural information are required. This is provided by high resolution mass spectrometer (HRMS), coupled with liquid chromatography (LC) or gas chromatography (GC).

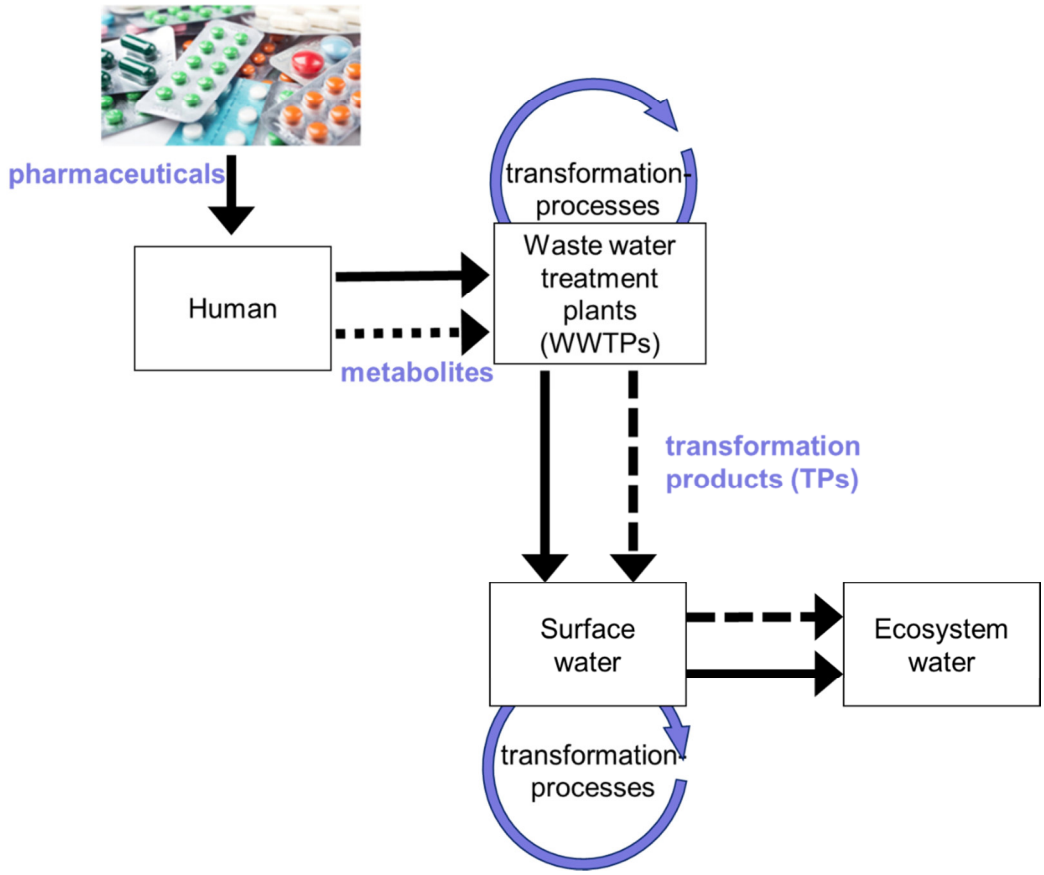

Figure 1: Fate of human pharmaceuticals and their transformation products from uptake to release in the ecosystem water. The arrows and dashed arrows illustrated the pathway of the pharmaceuticals and the metabolites/TPs, respectively.

In this study, the environmental fate of two prevalent pharmaceuticals have been taken into consideration. Metformin (MF) as one of the most prescribed pharmaceuticals worldwide (Ghoshdastidar et al. 2015) and fluoxetine (FLX) with high ecotoxicity in environmental relevant concentrations (Barra Caracciolo et al. 2015; Nałecz-Jawecki 2007).

1.2. Transformation processes of micropollutants in the aquatic environment

Micropollutants can be subjected to various transformation processes in the aquatic environment and are thus converted to one or several products (TPs) or finally mineralized. In the following, common environmental transformation processes are considered. Figure 2 illustrates the occurrence of the various transformation processes during a typical use cycle of pharmaceuticals from the uptake by humans to the discharge into the aquatic environment. The processes can be divided into redox reactions (abiotic and biotic processes), abiotic (hydrolysis, direct and indirect photolysis) and biotic (mammal/fish and microbial) transformation.

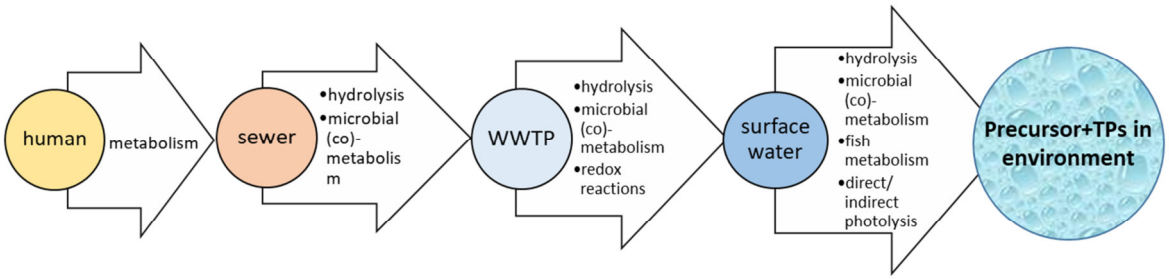

Figure 2: Transformation processes of micropollutants in the environment.

1.2.1. Redox reaction

A redox reaction involves a transfer of electrons between two species, an oxidant accepts electrons and is therefore reduced, and a reductant donates electrons and is oxidized. The thermodynamic favorability of a reaction, which means an overall negative free energy, is determined by the strength of the oxidant and reductant of the contributing half-reactions at standard conditions. In biotic reactions, the redox reaction depends on the major terminal electron accepting process which is determined by the availability of the most favorable electron acceptor (oxygen). At conditions with oxygen depletion, the next most energy recovering electron acceptor (nitrate) is used, down to electron acceptors which are lower on the redox ladder (small oxidation strength) (Grundl et al. 2012). The resulting biotic reactions with micropollutants are explained in chapter 1.2.3 in detail. The biotic redox reactions provide the environmental conditions

for abiotic redox reactions, without mediation by organisms (Tratnyek et al. 2011). However, only a few functional groups are oxidized (e.g. aldehydes to carboxylic acids) or reduced (e.g. dehalogenation of halogenated hydrocarbons) abiotically (Schwarzenbach et al. 2017b). Furthermore, the corresponding half reaction to abiotic oxidation or reduction of a micropollutant is usually unknown. Such reactions can be catalyzed by electrontransfer mediators, which are generated by bulk electron donors and are continuously regenerated by chemical or biological processes. For instance, mediators for oxidation reactions could be Fe(III)-compounds. Oxygen is a very weak oxidant in abiotic processes, due to a one-electron reduction instead of a four-electron reduction, which would needed microbial or light activation (Sigg and Stumm 2011). As a conclusion, natural abiotic redox reactions were not applied in this study, due to reluctant degradation of micropollutants. However, strong oxidants like hydroxyl radicals, which are not stable in water, can be used for intended degradation of substances in an engineered system. Examples for that could be found in contamination remediation and drinking water treatment with ozone or chlorine dioxide. Oxidation reactions may also be used for simulation of natural abiotic oxidation processes and to mimic cytochrome P 450 catalyzed oxidations (Johansson et al. 2007). In this study, electrochemistry was used as a practical tool for fast and easy simulation of natural processes. Electrochemical degradation of micropollutants occur through direct anodic oxidation or indirect oxidation, which is mediated by reactive intermediates that are formed electrochemically. Boron-doped diamond electrodes (BDDs) are suitable for indirect oxidation due to their chemical and electrochemical stability and good conductivity (Comninellis and Chen 2010). BDDs are non-active electrodes, meaning that they induce the electrolytic oxidation of water which formed hydroxyl radicals that do not interact with the anode surface but with organic substances (S) in an electrochemical zone (Figure 3). Due to short lifetime of OH radicals, the reactive chemical zone is very close to the electrode surface. OH· could also form mediators (M_{ox}) by oxidation of indirect agents which are for example salts (chlorine, sulphates and phosphates), ozone or hydrogen peroxide. The mediators could react with the target compounds further away from the electrode and in the bulk of the cell.

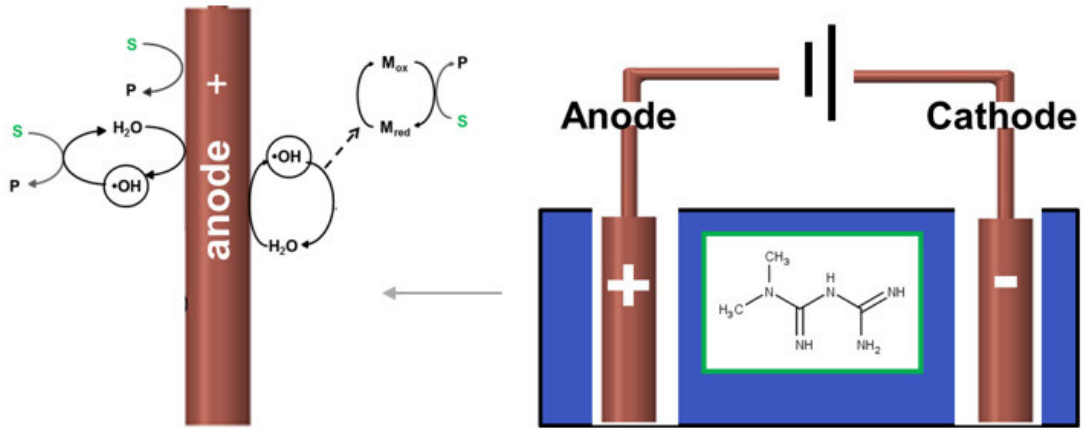

Figure 3: Mechanisms of direct oxidation and mediated oxidation with hydroxyl radicals or via hydroxyl radicals with other oxidants produced from salts, ozone or hydrogen peroxide (reactions derived by Barrera-Díaz et al. (2017)).

1.2.2. Abiotic Transformation

Abiotic transformation processes of environmental relevance are hydrolysis, redox reactions and photolysis. The redox reactions were explained before and represented by electrochemical degradation. The direct and indirect photolysis are linked to the experiments in a sun simulation chamber and hydrolysis is linked indirectly to all experiments, which could occur during experiment time, sample preparation and storage time.

Hydrolysis

A hydrolysis reaction is the formal substitution of a group or atom of an organic molecule by a water molecule (or hydroxide ion). The compound is transformed into a more polar product (Schwarzenbach et al. 2017a). In the aquatic environment, hydrolysis reactions are ubiquitous, since water can react as nucleophile and attack suitable electropositive sites in a molecule. Covalent bonds are polar if the binding partners have different electronegativities (e.g. C and N). Nucleophilic species like

hydroxide anions in base-catalyzed reactions attack the partial positive site, for example of an ester or ether bond. Electrophilic species in acid-catalyzed reactions attack the partial negative site.

Direct photolysis

In photolysis, micropollutants undergo transformation by absorption of photons with a given energy e.g. from ultraviolet (UV) or visible (vis) light, which leads to excitation of electrons from the highest occupied (HOMO) to the lowest unoccupied molecular orbital (LUMO). Often electrons are excited from bonding or nonbonding orbitals (e.g. heteroatoms) to so-called antibonding orbitals. The quantum yield Φ for a given reaction is the ratio of the number of molecules decomposed and the number of photons absorbed. Since not all photons absorbed, the considered reaction Φ is typically a number below 1. The fundamental laws of photochemistry are the Grotthuß Law, which tells that only an absorbed photon can cause a photochemical reaction, and the Stark-Einstein Law which considers that each molecule is excited by absorption by one photon. The light absorption (wavelength range 290-600 nm on earth surface) is mainly achieved in molecules with delocalized π-electron systems (e.g. aromatic rings and conjugated double bonds), so-called chromophores. The properties of chromophores with acid or base functions change with pH value, depending on pKa value. Deprotonation of acidic groups (e.g. phenol) delocalize the negative charge, which typically results in the absorption of longer wavelengths. Protonation of basic groups (e.g. aromatic amines) often results in shifts to shorter wavelengths, due to loss of nonbonding, delocalized electrons in aromatic systems. The excited species is much more reactive than that in an electronic ground state and can undergo different processes: deactivation by radiationless (collisions with solvent molecules) or radiation processes (luminescence) and chemical reactions (bond cleavage). The reactions depend on matrix (pH, oxygen concentration, ionic strength) and functional groups of the substances. General reactions are fragmentation, intramolecular rearrangement, hydrogen atom abstraction or electron transfer (Schwarzenbach et al. 2017a).

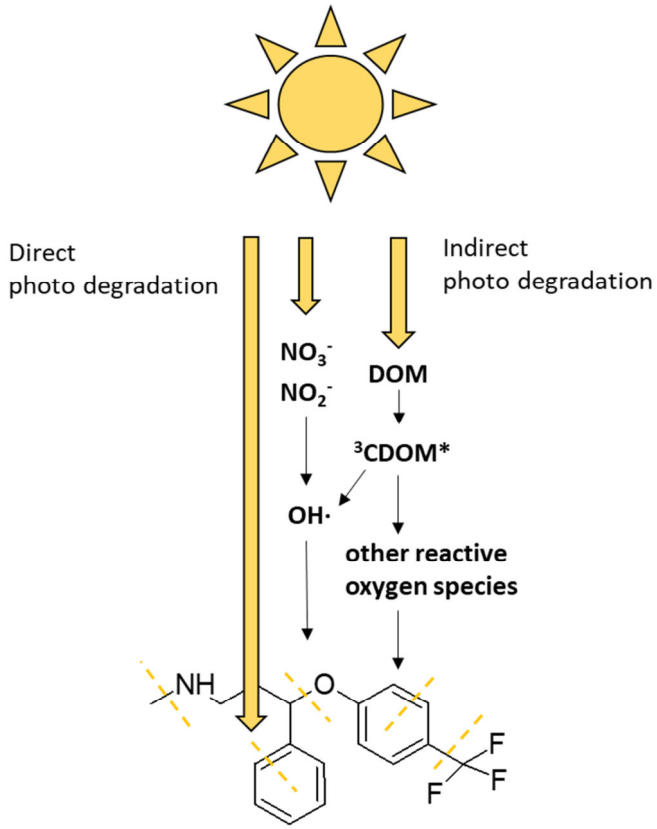

Figure 4: Reaction pathways of direct and indirect photo degradation of fluoxetine (FLX). Dashed lines show possible locations for bond cleavage by photolysis.

Indirect photolysis

In indirect photolysis, organic chemicals are transformed by energy transfer from an initial light adsorbing species, the so-called photosensitizer. The photosensitizer can react with the micropollutants directly or form other reactive oxygen species (ROS), that may react with organic pollutants (Figure 4). ROS are highly reactive, short-lived species (e.g. hydroxyl radicals, ozone, peroxy radicals). They can be formed by colored dissolved organic matter (CDOM), nitrate or nitrite. CDOM are a mixture of diverse molecules which were excited by a photon in the excited singlet state (^{1}CDOM*) and converted into ^{3}CDOM*. The efficiency of this conversion is given by the intersystem crossing quantum yield (Φ_{ISC}). ^{3}CDOM* are reactive on their own and are the source of ROS ($^1O_2$ and possibly OH radicals). The reaction mechanisms of ^{3}CDOM* are less

explored due to the complexity of the mixture and the difficulties to observe and quantify the states (McNeill and Canonica 2016). However, high DOC concentration acts also as inner filter by absorbing light and therefore attenuate the energy input (Stuart and Lapworth 2014). Furthermore, it is known that DOM generally reacts as a net sink for hydroxyl (OH) radicals rather than a source. Due to high formation potential and unselective reactivity, OH radicals are the most important ROS for EC degradation in surface water (Figure 4) (Lam et al. 2003; Wallace et al. 2010) . Well known is the formation of OH radicals by ROS, formed by light absorption of nitrate and nitrite. OH radicals react with organic pollutants primarily in two different ways: a) by electrophilic addition to a double bond or an aromatic ring and b) by abstraction of a hydrogen atom from a carbon bond (Schwarzenbach et al. 2017b) (Figure 5).

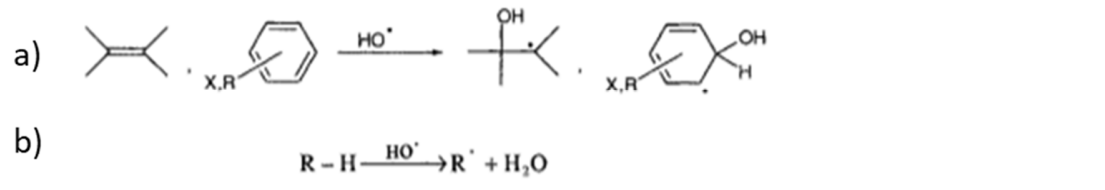

Figure 5: Reaction pathways of micropollutant with hydroxyl radicals (Schwarzenbach et al. 2017b).

1.2.3. Biotransformation

Biotransformation is a chemical modification of a compound by enzymatic catalysis mediated by organisms, which generally leads to the formation of a more hydrophilic product. The primary purpose of metabolic processes is the gain of energy and the built up of endergonic, organic molecules (biomass). Another reason for metabolism can be the transformation to more polar metabolites for easier excretion in mammals and fish, or for a better uptake of non-polar compounds by microorganisms. In this study, zebra fish embryos have been used to represent fish metabolism, and activated sludge for microbial (co)metabolism.

Metabolism in mammal and fish

Biotransformation or metabolism is defined as “the structural modification of drugs and chemicals by enzymatic systems which lead to formation of relatively polar substances in order to be easily excreted from the organism” (Asha and Vidyavathi 2009). However, it can also lead to the formation of metabolites possessing greater pharmacological activity, which may be more toxic than the parent compound to organisms (Pervaiz et al. 2013). Biotransformation reactions are divided into phase I and phase II reactions. In phase I reactions, functional groups are introduced in the molecule or existing groups are modified via oxidation, reduction or hydrolytic reactions. The majority of the drug metabolites are generated by the enzyme system cytochrome P450 (Kebamo and Tesema 2015), which reacts as monooxygenase and catalyzes reactions as N- and O-dealkylation, aromatic hydroxylation and N-oxidation. In phase II reactions, the metabolites of phase I are further transformed by conjugating reactions which include glucuronidation, methylation, acetylation, glutathione and amino acid conjugation (Jancova et al. 2010). Phase II products are typically compounds which are pharmacologically inactive and can be easily excreted. They have typically larger molecular weights than the parent compounds. For example, acetylation is a metabolic pathway for amine functional groups (e.g. FLX), which may be present on the parent xenobiotic, or generated by phase I metabolism. The phase II reaction (acylation) masks an amine with a nonionizable group, often resulting in a less water-soluble substance than the precursor (Franklin 2008).

Zebrafish has become a valuable potential model of higher invertebrates for the evaluation of xenobiotic metabolism. The study of Souza Anselmo et al. (2018) has shown that the metabolic zebrafish enzymes are analogous to those in mammals, performing several phase I and II reactions. The zebrafish embryos are easily obtainable, inexpensive and the brood animal provide a large number of non-adherent and transparent eggs (one female lays 50-200 eggs per day) (Nagel 2002).

Microbial Transformation

Biotransformation of micropollutants in WWTPs is related to reactions induced by the presence of microorganisms in water, such as bacteria. The type of microorganism and chemical compound determine the type of metabolism. Diversity and activity of biomass often determine the degree of degradation. Micropollutants can be used as primary substrate (energy and carbon source), if the concentration levels are sufficiently high. Generally, micropollutants occur at low concentration levels in the µg/L and ng/L range which is often not enough for metabolic processes. Therefore, cometabolism is postulated as the main removal mechanism of organic ECs in environmental and wastewater treatment processes (Fernandez-Fontaina et al. 2014). Microorganisms degrade non-growth substrate in the presence of primary substrates. The presence of primary substrates is necessary for inducing enzymes used in a global metabolic pathway, but they also transform micropollutants by chance. A well-known example is the cometabolism of ECs induced by the enzyme ammonium monooxygenase (AMO), produced by autotrophic aerobic bacteria during nitrification. AMO is the catalyst for the incorporation of hydroxyl functions into molecules of ECs by utilizing oxygen (Chang 1997). Also aerobic heterotrophic transformation processes of ECs are known for biological waste water treatment processes (Alvarino et al. 2016). Both, autotrophic and heterotrophic transformation processes occur under aerobic conditions, which is by far the most efficient redox condition for degradation of a wide range of ECs (Alvarino et al. 2018). However, redox conditions could be aerobic (presence of O_2 as final electron acceptor), anaerobic (absence of O_2 or bound oxygen) or anoxic (absence of O_2, but presence of bound oxygen (NO_2, NO_3)). Some compounds are better biodegradable under anaerobic conditions, due to the presence of strong electron-withdrawing groups (e.g. sulfonyl), which comes along with reductive reactions. Anoxic (dentrification) environment is not especially relevant for biodegradation of ECs (Alvarino et al. 2018).

In general, the resulting metabolites of microorganisms, animals and humans can be similar, due to same pathways (Kebamo and Tesema 2015).

1.3. Occurrence and fate of metformin and fluoxetine

The aim of this chapter is to review the recent literature about occurrence, fate, physiochemical properties and toxicology of MF and FLX, with attention paid especially to TPs/metabolites of chosen pharmaceuticals.

Metformin

The biguanide MF is a drug against type 2 diabetes and one of the most consumed pharmaceuticals worldwide (Ghoshdastidar et al. 2015, 2015; Sebastine and Wakeman 2003). MF is the 14th most commonly prescribed drug in Germany (Grandt and Schubert 2017), number eight in the USA (Marshall 2017), and one of the top three pharmaceuticals in the UK (Jones et al. 2002), with a global increasing prescription trend. It is not metabolized in the human body and is excreted unchanged in the urine with a half-life of 5 h (Gong et al. 2012). Despite of more than 90 % removal of MF in conventional WWTPs (Scheurer et al. 2012), MF concentrations of up to 21 µg/L were detected in WWTP effluents and in the low µg/L range in waste water influenced rivers (Blair et al. 2013; Ruff et al. 2015; Trautwein et al. 2014; Scheurer et al. 2012). Even higher concentrations of the well-known TP guanyl urea (GU), which is formed in activated sludge of WWTPs, were detected in the rivers (up to 25 µg/L) (Scheurer et al. 2012). Lab tests showed a direct correlation between aerobic MF degradation and GU formation (Trautwein et al. 2014). GU is considered as the only bacterial dead-end product of MF (Trautwein et al. 2014; Markiewicz et al. 2017) which is also resistant to further degradation. However, the relation in real WWTPs is inconclusive, some studies revealed well correlation between GU formation and MF degradation (Scheurer et al. 2012; Oosterhuis et al. 2013), other studies showed down to 5 % formed GU from degraded MF on molar basis (Kosma et al. 2015; Trautwein and Kümmerer 2011). Further degradation of GU is not proven so far and no other TPs of MF were detected in WWTP effluent or surface water samples. Other TPs besides GU could be responsible for the incomplete mass balance of MF inflowing and GU outflowing concentrations. In Figure 6 the fate of MF from consumption to release into aquatic environment is depicted. The ecotoxicology for potential TPs is totally unknown, even for GU no effect data were found (Caldwell et al. 2019). Niemuth and Klaper (2015) showed that

wastewater relevant MF concentrations caused intersex individuals in male fish of fathead minnows (*Pimephales promelas*) and similar effects could originate from TPs.

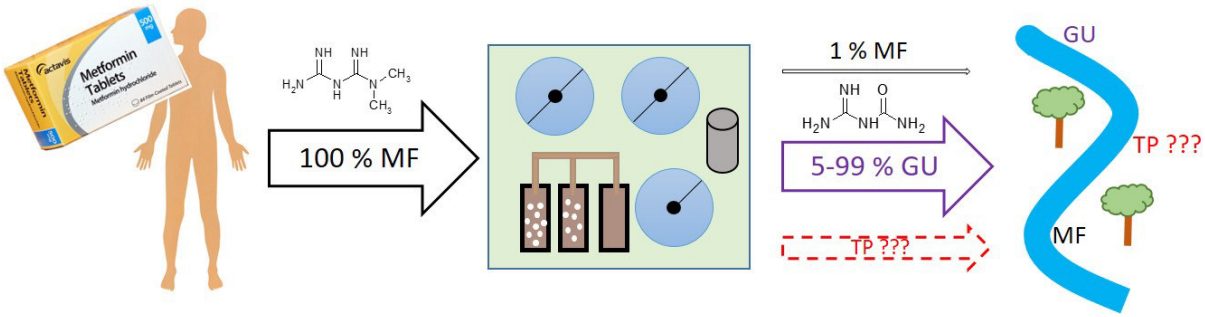

Figure 6: Fate of the antidiabetic metformin (MF) from consumption to release into the aquatic environment. TP= transformation product; GU= guanyl urea

Fluoxetine

Fluoxetine (FLX) is a selective serotonin reuptake inhibitor (SSRI) which is a relatively new group of antidepressants, that became popular quickly. SSRIs delay the reuptake of serotonin and are commonly used to combat depression and anxiety (Peters et al. 2017). FLX hydrochloride (Prozac®) was number twenty of the 200 most prescribed drugs in the USA in 2018 (Agency for Healthcare Research and Quality 2018). FLX is metabolized in the human body to glucuronides and the N-demethylated derivative norfluoxetine (NFLX). FLX is excreted unchanged to 25% (Benfield et al. 1986; Schlüter-Vorberg et al. 2015; Convention 2006) and 20% as NFLX (Nałecz-Jawecki 2007) and furthermore, the glucuronides could be transformed in waste water treatment processes to the origin substances FLX and NFLX. In conventional WWTPs the influent concentration and removal efficiency varied widely from one study to another. Influent concentrations were detected up to 3.5 µg/L (Salgado et al. 2011) and 0.2 µg/L (Baker and Kasprzyk-Hordern 2013), for FLX and NFLX, respectively. Removal efficiency varied between 7% and 80% for both substances in studies from Europe and North America (Lajeunesse et al. 2013; Baker and Kasprzyk-Hordern 2011; Vasskog et al. 2008). In general, FLX and NFLX concentrations in surface water are in the low ng/L range (Metcalfe et al. 2003; Bringolf et al. 2010). However, Metcalfe et al. (2010)

detected up to 141 ng/L FLX in a waste water influenced river in Canada. The substances are even more prevalent in sediment and biota, with 12 ng/g FLX and 7 ng/g NFLX in sediment and 1.6 ng/g FLX and 1.8 ng/g NFLX in the brain of white sucker fish (*Catostomus commersoni*) (Schultz et al. 2010). There are several studies about the toxicity of FLX to aquatic organisms which showed that FLX is one of the most acute toxic pharmaceuticals reported so far (Barra Caracciolo et al. 2015). Reported surface water concentrations were similar to EC_{50} values for female goldfish (Mennigen et al. 2008). In applied bioassays of protozoan *S. ambiguum* and crustacean *T. platyurus* the LC_{50} was 50% more toxic for the TP NFLX than the parent compound (Nałecz-Jawecki 2007). The high toxicity of FLX and the even higher toxicity of its metabolite and TP NFLX highlight the importance of identifying other TPs, which might be formed and/or accumulate in sediment and biota. In Figure 7 the fate of FLX from consumption to release into the aquatic environment is depicted.

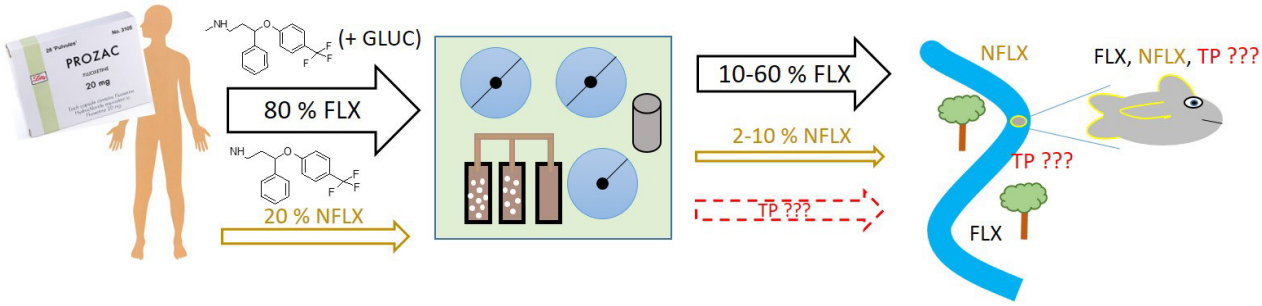

Figure 7: Fate of the antidepressant fluoxetine (FLX) and its metabolite norfluoxetine (NFLX) from consumption to release into the aquatic environment. TP= transformation product

2. Aim of this thesis

This thesis is embedded in the project Effect-Net from the Wassernetzwerk Baden-Württemberg, with the overall aim "*to investigate the influence of antidiabetics (…) and antidepressants as well as their metabolites and transformation products in a multi-scale approach from mode of action at the molecular level to effects on microbial communities"* (Universität Tübingen 2018). Metformin (antidiabetic) and FLX (antidepressant) are representatives of these groups, due to their ubiquitous occurrence in the aquatic environment, their known effect at environmental relevant concentrations (FLX) (Barra Caracciolo et al. 2015) and their persistency in the environment (MF) (Ghoshdastidar et al. 2015).

The goal of this project is to improve the understanding of transformation processes of the pharmaceuticals metformin and fluoxetine, to achieve a mass balance closure in waste water treatment processes and fresh water ecosystems. For this purpose, environmental relevant TPs should be identified by abiotic (hydrolysis, electrochemistry, direct and indirect photolysis) and biotic (biotransformation in fish and microorganism) laboratory experiments, based on measurements with liquid chromatography and high-resolution mass spectrometry (LC-HRMS). In field studies, the identified TPs are screened. The identified TPs should give a comprehensive toolbox about relevant compounds, which can be investigated in the project for effects in a multi-scale approach. Furthermore, the thesis can help to transfer knowledge from abiotic transformation processes (electrochemistry, photodegradation) to biotic metabolism.

Related to the overall aim, three studies were conducted. The major objectives of the studies are detailed below and depicted in Figure 8.

Paper 1 (P1): The aim is to mimic the formation of TPs of MF by electrochemistry, to identify new TPs with relevance for the aquatic environment. For that purpose, MF and the electrochemical identified TPs are screened in WWTPs influent and effluent samples and surface water samples.

Paper 2 (P2): The aim is to investigate the fate of MF and its TPs in biological waste water treatment. In a lab study, batch experiments of MF and GU are treated with

activated sludge under aerobic and anaerobic conditions. Degradation of precursors, and occurrence and fate of TPs are investigated.

Paper 3 (P3): The aim is to identify new TPs of FLX which are formed by photo degradation in water and biodegradation in zebra fish embryos (*Danio rerio*). Differences and similarities between direct, indirect photolysis and biodegradation should be revealed.

Additional results (A): The aim is to investigate the occurrence of FLX and NFLX in surface water sample and associated sediment of rivers in Southwest Germany.

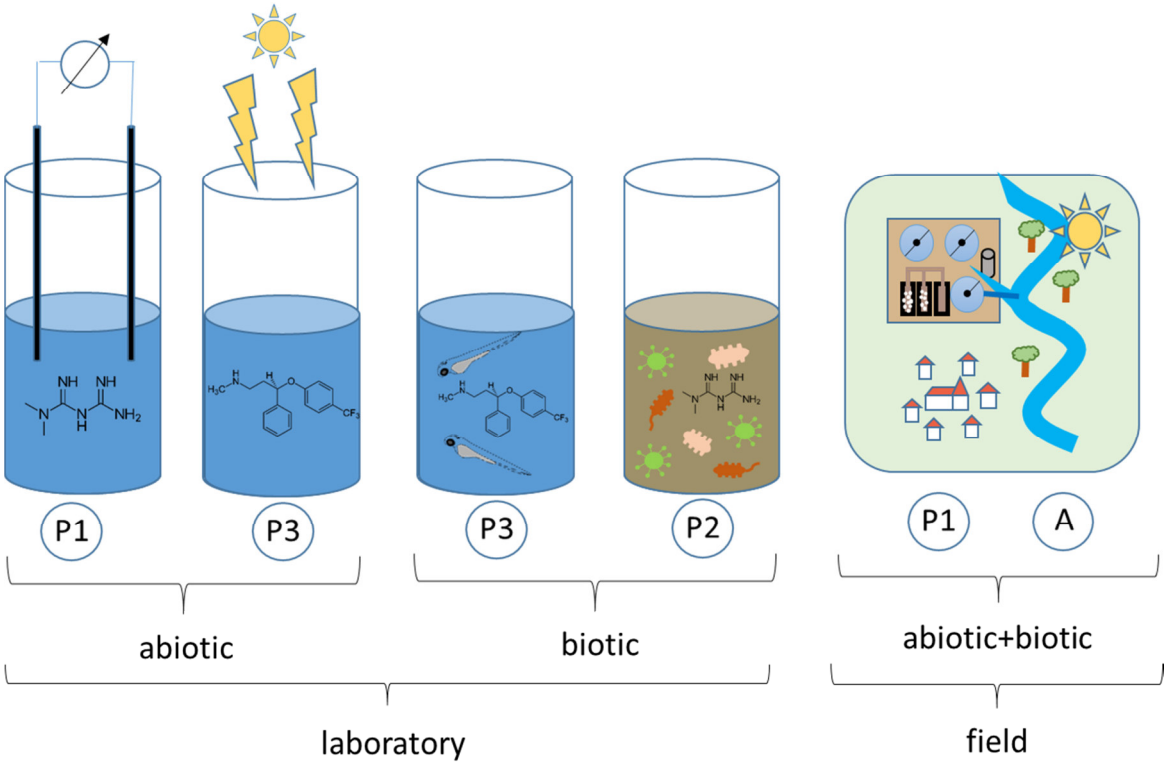

Figure 8: Overview about the conducted abiotic (electrochemistry and photolysis) and biotic (zebra fish embryo and activated sludge) laboratory experiments, and the field studies in published articles P 1-3 and additional results (A).

3. Materials and Methods

3.1. Chemicals

Detailed information about the used chemicals and experimental setup are given in the published articles. Chemical characterization of FLX, MF and its TPs, which were available as analytical standards, are given in Table 1.

Table 1: Target compounds included in this thesis.

Substance	Sum formula	Classification	log Kow	pKa
Fluoxetine (**FLX**)	$C_{17}H_{18}F_3NO$	antidepressant	4.1[a]	9.8[a]
Norfluoxetine (**NFLX**)	$C_{16}H_{16}F_3NO$	TP of FLX	3.8[a]	9.8[a]
4-(trifluormethyl)phenol (**TFMP**)	$C_7H_5F_3O$	TP of FLX	2.7[a]	9.4[a]
α-[2-(Methylamino)ethyl] benzyl alcohol (**TP 166**)	$C_{10}H_{15}NO$	TP of FLX	0.9[b]	14.4[b]
Metformin (**MF**)	$C_4H_{11}N_5$	antidiabetic	-1.8[c]	12.3[c]
Guanyl urea (**GU**)	$C_2H_6N_4O$	TP of MF	-1.9[c]	12.4[c]
1-Methylbiguanide (**MBG**)	$C_3H_9N_5$	TP of MF	-1.8[c]	12.3[b]

[a]HMDB.ca, [b]chemicalize.com, [c]Pubchem.com

3.2. Transformation experiments

In the following, the methods of the applied transformation processes are explained (Figure 9). The four experiments (electrochemistry, biodegradation with activated sludge, photolysis and zebrafish embryo metabolism) show a representative selection for the common natural transformation processes, which are explained in chapter 1.2. Electrochemistry was performed to mimic biotic and abiotic redox processes, batch experiments with activated sludge represent the microbial (co)metabolism and the sun simulation chamber simulates natural sunlight for direct and indirect photolysis. Zebra fish embryos were used as well-established model organisms for fish metabolism.

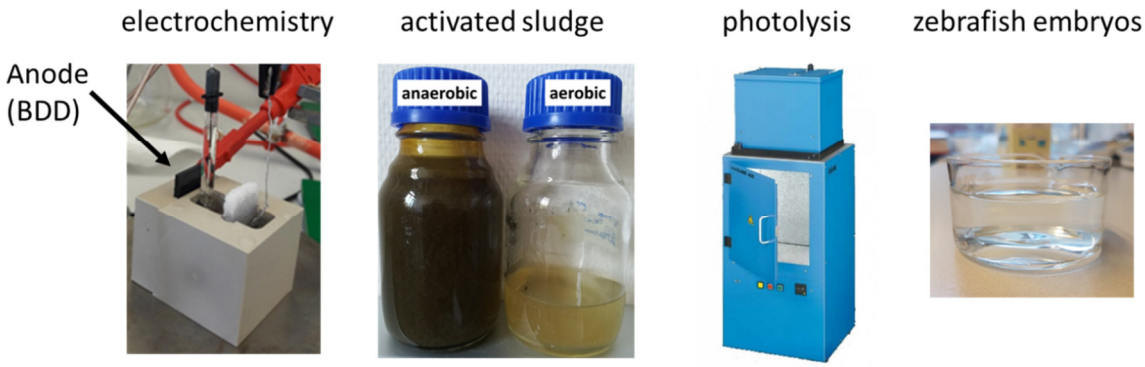

Figure 9: Illustration of the four experiments for transformation product formation.

3.2.1. Electrochemical transformation of metformin

Electrochemical experiments were realized in a 12-ml batch cell of PEEK with a conductive boron-doped-diamond (BDD) working electrode (4 cm x 2 cm, with a 10 µm diamond layer on Niob base from Condias, Itzehoe, Germany). As a counter electrode a 4 mm x 8 mm platinum mesh (Sigma Aldrich, St.Louis, USA) and as reference a Ag/AgCl electrode (3M, MF-2052, BASi, West Lafayette, USA) were used. Oxidative and reductive compartments of the batch cell were separated by a Vycor glass frit. The experiments were performed with 10 mg/L MF in a 20 mM ammonium formate solution which was adjusted either to pH 3 or pH 7 with formic acid or ammonium hydroxide. A constant potential of 1.5 V was applied with a potentiostat (Autolab Potentiostat, PGSTAT 101; Metrohm) for 10 min. More details are given in paper 1.

3.2.2. Degradation of metformin by activated sludge

The biodegradation studies were performed in bottles in the dark at room temperature (22 °C). The experiments were conducted with activated sludge of nitrification basins. For the aerobic biodegradation experiment, 90 ml tap water with 10 ml activated sludge were filled in 250 ml glass bottles. The supernatant of 150 ml air volume and every day mixing with air supply guaranteed sufficient oxygen supply. For the anaerobic degradation experiment the bottles were filled with 250 ml pure activated sludge without

a supernatant of air volume, to guarantee anoxic conditions. All bottles were spiked with MF and/or GU in the concentration range of 5 and 40 mg/L. The dry weight of the aerobic bottle test was 3 g/L and of the anaerobic bottle test was 30 g/L. Every experiment consists of two parallel test bottles and one sterile control (poisoned with 3 g/L sodium azide). More details are given in paper 2.

3.2.3. Photodegradation of fluoxetine

Photochemical experiments were conducted in a sunlight test chamber model "UVACUBE 400" from Hoenle UV Technology (Gräfelfing, Germany) equipped with a SOL 500 RF2 solar simulator and a H2 filter glass. The emission wavelength range covered by the applied solar simulator was between 295 nm and 800 nm with an intensity setting of 1000 W/m^2. Degradation experiments were conducted in ultrapure water for direct photolysis and in surface water for indirect photolysis. Experiments with ultrapure water were performed at pH 6, 8 and 10 in a phosphate-buffered system, and experiments with surface water without pH adjustment (pH 8). The FLX concentration was 15 mg/L and the total irradiation time was 28 h with 9 sampling events. More details are given in paper 3.

3.2.4. Biotransformation of fluoxetine in zebrafish embryos

After spawning, 160 freshly fertilized eggs of wild-type zebrafish (*Danio rerio*) of the Westaquarium strain were collected and divided into two groups (control and exposure group), each of which was transferred into a 70 ml crystallizing dish filled with 60 ml ultrapure water. At 30 h postfertilization (hpf), all embryos were mechanically dechorionated with Dumont no. 5 tweezers. For the exposure group, ultrapure water was replaced by 60 ml of FLX hydrochloride (HCl) test solution (nominal: 5 mg/L FLX HCl) at 48 hpf. For identification of FLX metabolites, embryos and test media were sampled at 96 hpf. For this end, 15 embryos per group were rinsed three times with 5% AcN in water (v/v) as washing procedure. Chemical analysis of FLX and its metabolites in fish was conducted in three replicates, each consisting of five pooled embryos. For

extraction, five pooled embryos were spiked with a mixture of 300 µl AcN and 200 µl of 12 µg/L FLX-d5 (internal standard) aqueous solution. The samples were sonicated (SONOREX®, Bandelin, Berlin, Germany) for 2 × 15 min and stored at 4 °C for 24 h. After another 15 min sonication, the extracts were centrifuged for 15 min at 10.000 rpm (centrifuge 5417 C®, Eppendorf, Hamburg, Germany).

3.3. Water sample collection and preparation (metformin)

WWTP influent and effluent samples were obtained for 7 days (twenty four-hour composite samples) for screening of MF and its TPs. The sample campaign was done at three different WWTPs, which were all located in Southwest Germany and had no advanced treatment technologies. For universal terms, the definition of the WWTPs is WWTP 1,2 and 3 in this thesis, instead of the definition W 1 and 2 (in paper 1+2) to avoid confusion, due to same terms in different papers (Table 2).

Table 2: Wastewater treatment plants (WWTPs) included in this thesis. PE=population equivalent

WWTP	PE	Sampling time	Term paper 1	Term paper 2
1	100000	04/2016 07/2016	W1	W1
2	75000	08/2016	W2	
3	80000	06/2018		W2

For biodegradation studies (paper 2) activated sludge of WWTP 1 in April and July 2016 and of WWTP 3 in June 2018 were obtained. Surface water samples, which were screened for MF and its TP, were collected in November 2016 upstream and downstream of WWTP 1 and 2 and the surrounding area. Sample preparation of all water samples is described in the published articles (paper 1 and 2).

3.4. Sediment sample collection and preparation (fluoxetine)

The method of sediment sampling and extraction are described in detail. Sediment samples were collected from two rivers in Southwest Germany, Neckar (N) and Rhine (R). The four sampling sites of the Neckar, within a sampling distance of 4 km (49.44378-49.43377° N and 8.62142-8.64813° E) were divided into sediment with high TOC (1.4 and 2.6%) (N1) and small TOC (<1%) (N2). The sampling sites of the Rhine were divided into samples of the main sewer R1 (48.975°N, 8.2547 °E and TOC 1.52%), and a tributary R2 (TOC 0.65 and 0.84%), which was 16 km downstream of R1 (49.1211°N, 8.3668 °E). Over the entire distance of the rivers, different WWTP effluents were discharging into the rivers. Each of the four sampling sites (N1,2 and R1,2) was at two sampling locations (a and b), extracted in triplicates.

After sampling, sediment was freeze dried and stored at -80°C for 2 years. Immediately before extraction, the sediment was sieved to 0.5 mm and 2 g dry mass of sediment was weighed into a 15 ml centrifuge tube. After adding 200 µl FLX-d5 (50 µg/L) and drying (24 h room temperature), the first step included adding 5 ml mixture of AcN and MeOH (50:50 v/v) with aqueous ammonium hydroxide solution (adjusted to pH 10) to the tube and mixing. The slurry was sonicated for 15 min (Ultrasonic bath from Bandelin Sonorex, Papenburg, Germany) and afterward centrifuged at 3000 rpm for 10 min (Hermle Z 320 centrifuge, Wehingen, Germany). The supernatants of three steps per tube (15 ml) were filtered (0,45 µm polytetrafluoroethylene filter) and 5 ml were evaporated (40 °C with gently stream of nitrogen), reconstituted in 500 µl AcN:H_2O (50:50 v/v) and transferred into a HPLC vial. The recovery of the method was 101% $\pm$ 10% (n=3) for FLX.

3.5. Analytical methods

For analysis, liquid chromatography (LC) coupled to mass spectrometry was used. Due to high polarity of MF and its TPs, the LC column was a hydrophilic interaction column (HILIC) (Phenomenex LUNA 5 u HILIC 200 Å column (150x 3 mm; 5 µm particle size)). For FLX and its TPs a reversed phase column was used (Agilent Poroshell-120-EC-C18 (2.7 µm, 2.1 × 100 mm)).

For quantification of compounds with available analytical standards a triple quadrupole mass spectrometer (6490 iFunnel Triple Quadrupole LC/MS, Agilent Technologies, Singapore) was used. For identification of new TPs and to qualify identified TPs, a quadrupole time of flight mass spectrometer (6550 iFunnel Q-TOF LC/MS, Agilent Technologies, Singapore) was used. Identification of TPs was done in positive ionization mode for MF and in positive and negative ionization mode for FLX. Detailed information about the analytical methods are given in the published articles. Quantification of FLX and NFLX in sediment was done with the analytical triple quadrupole method described in paper 3.

3.6. Workflow for TP Identification by Nontarget-Screening

Since reference standards are not available for a large number of TPs, the proposed structures of the TPs were identified by a nontarget-screening approach. Nontarget-screening begins with the transformation experiment (chapter 3.2.1-3.2.4), for which the number of possible structures is limited to structures with close relationship to the parent compound. For assigning the elemental composition, high mass resolution and low mass error are essential. This can be achieved with the applied QTOF-MS (Lambropoulou and Nollet 2014). After molecular feature extractions of scan data (*m/z* 100-500), the compound patterns were evaluated in data sets from samples before and after experiments. A fold-change filter of 5 was used to select TPs which were formed during the experiments. Based on accurate mass measurements chemical formulas were assigned with a mass deviation smaller than 10 ppm. Constraints for elemental compositions were selected based on the precursor composition of FLX ($C_{17}H_{18}F_3NO$)

and MF ($C_4H_{11}N_5$). The potential TPs could have similar composition, but vary in the amount of C, H and O atoms. In addition, FLX may lose the three fluorine atoms or add a group with nitrogen to the molecule in fish embryo assays.

Targeted MS/MS was performed to acquire MS/MS fragmentation data for the selected molecular features to facilitate their characterization. In the ideal case, chemical structures were proposed based on MS/MS data, in-source fragmentation, retention time behavior, and literature information. Confirmation can be achieved only for substances with available analytical standards. The workflow is depicted in Figure 10 for the electrochemical degradation experiment of MF.

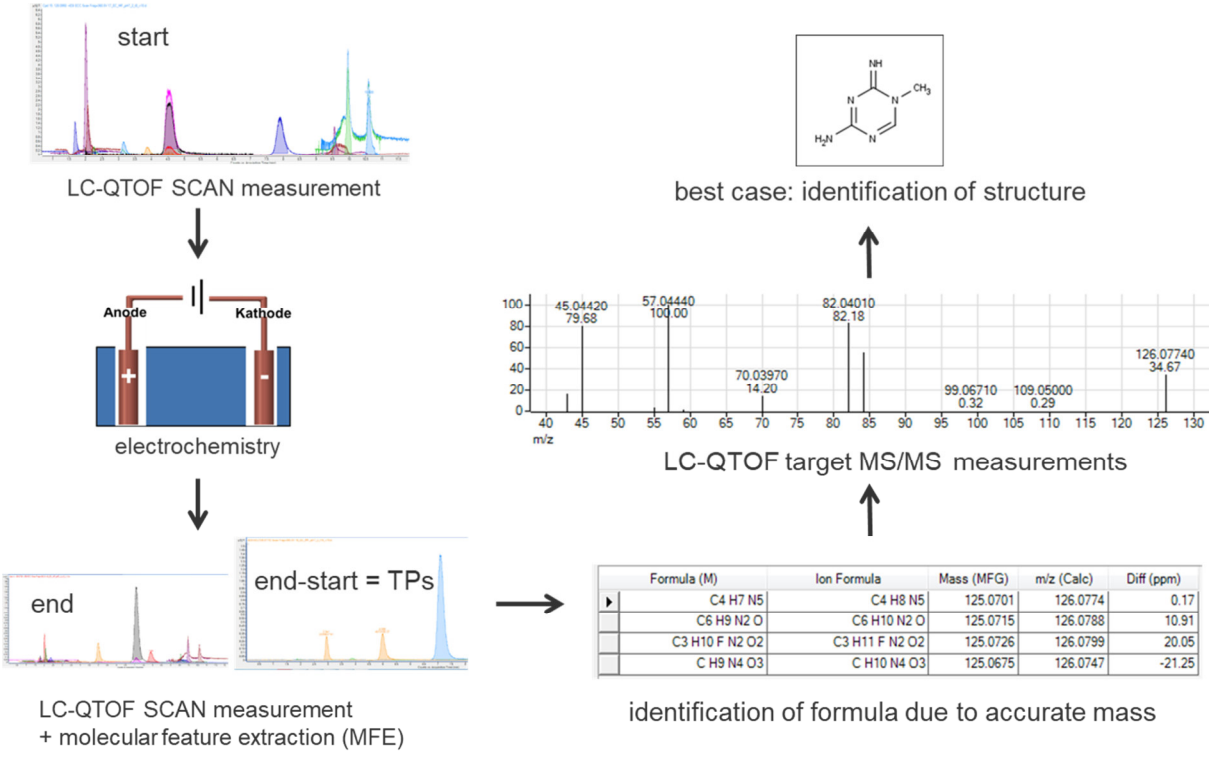

Figure 10: Example of TP identification with non-target screening workflow (TPs of MF with electrochemistry).

4. Results

The results are divided into target analysis (4.1. Occurrence of substances and well-known TPs in the environment) and non-target analysis (4.2. Newly identified TPs and their environmental fate). The chapter 4.1. includes the results of **paper 1** for MF and **additional results** for FLX, which are not published yet. The results in chapter 4.2. can be clearly divided into three chapters for the three published papers.

4.1. Target screening: occurrence of substances and well-known TPs in the environment

Metformin

In **paper 1**, screening of WWTP influent and effluent, surface water and drinking water samples showed the ubiquitous occurrence of MF in the human influenced water cycle. In 24-hours composite influent samples of two WWTPs the MF concentration was between 14 and 95 µg/L and the elimination rate during treatment processes was between 92% and 98%. The fate of GU differed in those two WWTPs. In W2, GU was formed in treatment processes and showed 4 to 25 times higher effluent than influent concentrations, which were in general 25% of the degraded MF on a molar basis. In W1, the well-known TP GU showed unexpected fate which has never been reported before. We observed in 3 days during one week in spring and summer much higher GU concentrations in influent than effluent and moreover, the GU influent was 90% higher than the MF influent concentration. The reason for the high amount of inflowing GU could be other biguanide precursors (Perreault et al. 2013) which were transformed to GU in sewage system. Lower GU effluent than influent concentrations indicate that further degradation processes of GU could play a role in WWTPs, which was investigated in **Paper 2** (chapter 4.2.). Grab samples of rivers in Southwest Germany showed the occurrence of MF already upstream of WWTPs (up to 87 ng/L) and 10 times higher GU (up to 4,5 µg/L) than MF concentrations downstream. Even in tap water samples MF was detected (34 ng/L), which reveals the ubiquitous exposure to MF, not only for water organisms, but also for humans.

Results

Fluoxetine

In **additional results**, FLX and NFLX were analyzed in surface water and sediment samples of Rhine and Neckar. Both substances were detected in the extract of the sediments, but not in surface water samples of our study. Water concentrations of FLX are inconclusive for the estimation of the occurrence in the environment, due to the adsorptive properties of FLX. The antidepressant is more prevalent in fish tissue and sediment (Kwon and Armbrust 2006). In our study, sediment samples of the river Neckar showed FLX concentrations between 0.19 and 0.89 ng/g. Higher values were observed in sediments with higher TOC content (Table 3). The FLX concentration in the sediments of the Rhine river was even higher, with concentrations up to 3.8 ng/g in the main stream and up to 2.3 ng/g in a tributary, despite the TOC content being lower than 1% in the sample of R2 (Table 3). The concentrations of NFLX were up to 0.14 ng/g, with the highest value found in the sediment of the main stream of Rhine.

Table 3: Average concentrations (ng/g) $\pm$ standard deviation (n=3) of FLX and the TP NFLX in sediment samples of Neckar (N) and Rhine (R). LOQ= limit of quantitation (0.02 ng/g)

	TOC	FLX	NFLX
	[%]	[ng/g]	[ng/g]
N 1 a	2.60	0.89$\pm$0.03	0.05$\pm$0.01
N 1 b	1.43	0.58$\pm$0.11	0.04$\pm$0.01
N 2 a	0.15	0.31$\pm$0.16	<LOQ
N 2 b	0.25	0.19$\pm$0.04	<LOQ
R 1 a	1.52	3.79$\pm$0.03	0.14$\pm$0.02
R 1 b	1.52	2.31$\pm$0.06	0.09$\pm$0.02
R 2 a	0.65	1.55$\pm$0.06	0.04$\pm$0.02
R 2 b	0.84	2.25$\pm$0.10	0.08$\pm$0.01

4.2. Non-target screening: newly identified transformation products and their environmental fate

P1: Newly identified transformation products of metformin and occurrence in the environment

In **paper 1**, the generation of MF TPs was conducted by electrochemical oxidation with a boron-doped diamond electrode (BDD). Four TPs have been identified by LC (HILIC) coupled with QTOF-MS. These are methylbiguanide (MBG; $C_3H_9N_5$) formed by demethylation, 2-amino-4-methylamino-1,3,5-triazine (2,4-AMT; $C_4H_7N_5$) formed by cyclization and 4-amino-2-imino-1-methyl-1,2-dihydro-1,3,5-triazine (4,2,1-AIMT; $C_4H_7N_5$) formed by migration of the methyl end group of 2,4-AMT. 2,4-diamino-1,3,5-triazine (2,4-DAT; $C_3H_5N_5$) could be a secondary TP formed by cyclization of MBG or by demethylation of 4,2,1-AIMT and 2,4-AMT. The TPs were already found after gamma radiolysis of MF, identified with low-resolution MS2 (Collin et al. 2004). Our accurate mass measurements and fragmentation data confirmed the proposed TPs. GU could not be formed by electrochemistry. In our study for the first time other TPs than GU were identified in the water cycle. 2,4-AMT and 2,4-DAT were detected in WWTP samples and showed an increasing peak area from influent to effluent. MBG concentration was in average 70 ng/L without a significant trend from influent to effluent which is explainable due to the additional formation process by hydrolysis of MF. In waste water influenced rivers, MBG concentrations up to 31 ng/L were detected and the peak area of 2,4-DAT was in average three times smaller than in effluent samples. 2,4-AMT was not detectable in surface water samples and 4,2,1-AIMT not in any sample. In general, the electrochemical identified TPs of MF played a minor role in the water cycle.

P2: Fate of metformin and its transformation products in biodegradation processes

In **paper 2**, the fate of MF and its TPs in WWT processes was elucidated more closely by aerobic and anaerobic biodegradation batch experiments of MF and GU. MF showed fast biodegradability under aerobic (5 and 12 days for W1 and W3, respectively) and slow biodegradability under anaerobic conditions (both 40 days). In the aerobic experiments, MF was quantitatively transformed to GU (98%). The picture for GU degradation was contrary to that of MF. Anaerobic degradation of GU was completed within 8 days in both experiments, with sludge from W1 and W3. Aerobic GU degradation was depending from the origin of the activated sludge. In W1, 33 days after GU formation, aerobic degradation of GU was completed, whereas in W3 no degradation of GU was observed, even though in W3 2.5 times higher dry mass of sludge was used which results in 2.5 times faster MF degradation. Higher GU influent concentrations to W1, along with better adapted microorganisms could be the reason for GU degradation in experiments with activated sludge from W1. After second spike in experiments of W1, the fast adaption of the microorganisms was shown by faster degradation of GU (5 days). In aerobic MF degradation experiments besides GU, MBG, 2,4-AMT and partially 2,4-DAT were formed. MBG was quickly degraded in turn, whereas the other decreased slightly. MBG can be suspected as an intermediate of GU, but it was excluded, due to easier enzymatic reaction processes for hydroxylation than N-demethylation of MF (Cui and Schröder 2016). The identified TPs beside GU (MBG, 2,4-AMT, 2,4-DAT) were in total less than 2% of degraded MF. Furthermore, adsorption of MF and GU on sludge was observed as an additional removal process with up to 20%. The deficits in mass balance of inflowing MF and outflowing GU in former and current studies can be explained by GU adsorption and degradation processes predominantly and minor by formation of the other TPs.

P3: Newly identified TPs of FLX (abiotic and biotic)

In **paper 3**, the generation of FLX TPs was conducted by photodegradation in water and biodegradation in zebrafish embryos. Photo experiments were conducted with ultrapure water at pH 6, 8 and 10 and with surface water (pH 8). At higher pH values more FLX was degraded due to deprotonation and a higher electron density on the N atom, which

results in a higher reactivity of FLX. Taking indirect photolysis into consideration, degradation rates for surface water samples were even higher. The well-known metabolite and TP norfluoxetine (NFLX) proved to be a minor TP in photolysis (<2% of degraded FLX), due to faster photodegradation of NFLX than FLX. In addition, 26 TPs were detected, which were formed by *O*-dealkylation (twelve TPs), hydroxylation (two TPs), CF_3-substitution (seven TPs) and *N*-acylation with aldehydes (six TPs) and carboxylic acids (five TPs). The TPs were identified due to accurate mass measurements, MS/MS data, literature and characteristic in-source fragments which were formed by cleavage of the 4-Trilfluormethylphenol (TFMP) moiety. TFMP and TP 166 are formed by O-dealkylation and were predominant, with concentrations of 31 % and 19 % of degraded FLX at pH 6, respectively. TP 148, which is also formed by C-O-cleavage and without available analytical standard, also showed the highest peak at pH 6. At higher pH values and in surface water, the mentioned TPs showed less intensities, but secondary TPs formed by demethylation, and unsaturation of TP 166 and 148 showed higher intensities. Hydroxylation of the benzyl ring of FLX and TP 166 could form TPs 326a/b and 182a/b which were one order of magnitude higher in indirect photolysis experiments than in ultrapure water, due to higher amount of attacking hydroxyl radicals. 3 TPs were directly derived from substitution of the CF_3 group, namely TP 286a/b/c and further degradation formed four secondary TPs. Six of the seven TPs have never been described before, whereas four of them were exclusively measured in negative mode, without significant difference between direct and indirect photolysis. Photo induced N-acylated TPs were identified as a new group of FLX TPs. In zebrafish embryos the bioconcentration factor of FLX was found to be 200, and about 1% of FLX taken up by the embryos was transformed to NFLX. The already identified (photolysis) *N*-acylated TPs 338, 364, 352, and 410, could be confirmed in zebra fish embryos. The detection of TFMP at an average concentration of 300 µg/L in zebra fish embryos showed a transformation of FLX by C-O cleavage. Three new metabolites were identified, formed by *N*-hydroxylation, *N*-methylation and the attachment of an amine group. The study demonstrated the importance of considering a broad range of FLX TPs in environmental fate studies.

5. Summary and discussion

TPs are an important issue in assessing the impact of micropollutants on the environment. The goal of this study, to achieve a more detailed understanding of biological and chemical transformation processes and to investigate the environmental relevance of TPs, has been achieved for the pharmaceuticals MF and FLX. For the identification of the TPs a workflow of liquid chromatography coupled with high resolution mass spectrometry (LC-HRMS) was used.

In the following, the most important results are summarized:

- Target screening in WWTP effluent, surface water and even tap water samples confirmed the ubiquitous occurrence of MF. The well-known metabolite GU has shown in three of seven 24-hours composite samples of a WWTP unexpected high concentrations and 90% removal. The GU removal instead of formation has never been reported before. The occurrence of FLX and the well-known metabolite NFLX in sediment were confirmed, with concentrations up to 3.79 ng/g and 0.14 ng/g in extracts of Rhine sediment, respectively.
- With electrochemical degradation of MF four new TPs, which were formed by cyclization and demethylation, were identified. Three of them (MBG, 2,4-AMT, 2,4-DAT) were also detected in effluent samples of WWTPs.
- For detailed information about the TP formation processes of MF in WWTPs, batch experiments with activated sludge were performed. MF was aerobically completely transformed into the TPs. GU was the main metabolite (98%) and less than 2% MF was degraded into the newly identified TPs. Furthermore, for the first time GU degradation in activated sludge was observed, fast under anaerobic conditions and slow under aerobic conditions. In addition, the aerobic biodegradability of GU depended on the microbial community which was influenced from the originating WWTP of the activated sludge.
- Environmental relevant TPs of FLX were identified by FLX degradation in a sunlight simulation chamber. The simulation experiment revealed 27 TPs, formed by *O*-dealkylation, hydroxylation, oxidation of the CF_3-group and *N*-acylation. The *O*-dealkylated TPs were the main TPs in ultrapure water, whereas indirect

photolysis revealed high amounts of hydroxylated TPs. The human metabolite NFLX played a minor role in photolysis. The oxidation of the CF_3-group revealed six of seven TPs which have never been described before and photoinduced N-acylation was a new transformation mechanism, with seven new identified TPs.

- In zebrafish embryos (96 h post fertilization), the relevance of metabolites was shown in fish. The bioconcentration factor of FLX (exposition medium 5 mg/L FLX) was 200 and 1% was transformed to NFLX. Furthermore, seven metabolites known from photodegradation, as well as three new metabolites formed by N-hydroxylation, N-methylation and attachment of an amine group were identified.

All in all, the study indicates that TPs generated by simple batch experiments (electrochemistry) can be qualitatively transferred to a more complex system (experiments with activated sludge and real WWTPs). Three of four TPs of MF, which were detected by LC-HRMS after electrochemical degradation, were analyzed in surface water. TP 126b was not detected in environmental samples. The reason could be fast further degradation of TP 126b to 126a, due to migration of the external methyl-group of the aromatic ring. The study also demonstrates the formation of FLX TPs in environmental relevant processes (photolysis and fish metabolism). In general, the FLX concentration in surface water is smaller than the MF concentration and associated with lower concentration of TPs and difficulties to detect them. Natural matrices make it even more challenging to identify unknown compounds. Consequently, the lab studies were performed at elevated concentration to minimize matrix effects and to enhance peak performance for identification of primary and secondary TPs.

It is demonstrated that the well-known metabolites NFLX and GU are not the main TPs in abiotic and not the sole TPs in biotic processes. TPs formed by common abiotic and biotic transformation processes (demethylation, methylation, hydroxylation, unsaturation) and unexpected ones like N-acylation as abiotic process, CF_3 substitution and splitting at a breaking point and further transformation of both parts of the molecule, (e.g. TFMP, TP 166 and further TPs) should be considered.

The study also shows the limitation of transferability between abiotic and biotic processes. Demethylation was a common transformation process in biotic and abiotic experiments for both compounds (formation of MBG (from MF) and NFLX (from FLX)). However, NFLX was a main metabolite in zebrafish embryos but played a minor role in photolysis. MBG formation was more dominant in the abiotic processes of electrochemistry and hydrolysis. It is remarkable that the formation of GU, the main metabolite of MF, was missing in electrochemistry. The reason for it could be fast further degradation of GU or different biotic than abiotic oxidation processes. FLX TPs formed by hydroxylation and *N*-acylation in photochemical reactions were similar to those formed by biotic transformation (metabolism) in fish. In contrast, the TP with an attached amine group was only detected in fish embryo extract, whereas TPs after C-O cleavage were predominant in photolysis.

In conclusion, the study highlights the importance of considering a broad range of environmental relevant TPs in fresh water systems. TPs may be formed in a high number and concentration in WWTPs and natural systems.

6. Further needs

Based on the knowledge gain of transformation reactions of FLX and MF, the following perspectives are proposed for future work, towards a more comprehensive picture of the environmental fate of organic mic:

- Screenings of FLX TPs should be done with water samples from North America, where the consumption of FLX is higher than in Europe. Furthermore, the sorptive and bioaccumulative properties of FLX/NFLX indicate the importance to investigate the according sediment and biota.
- A further need is the estimation of the concentrations of FLX TPs. For the TPs of MF, without analytical standard, the study showed a solution approach by concentration estimation with an analytical standard of a similar substance. Production of analytical standards or comparison with similar substances should be done for the TPs of FLX.
- Further case studies with different biota (fish in different life stages, benthic flora and fauna), different abiotic processes (advanced treatment technologies, e.g. ozonation) and other micropollutants with similar functional groups should be done towards an extensive knowledge about the environmental fate of micropollutants in general.
- A very important point is the risk assessment of the TPs in aquatic ecosystems. The effects of the environmental relevant TPs, and mixture-effects of precursors and TPs should be evaluated on aquatic organisms, from receptors to biodiversity.

Publication bibliography

Agency for Healthcare Research and Quality (2018): The Top 200 of 2018. Provided by the ClinCalc DrugStats Database. Available online at http://clincalc.com/DrugStats/Top200Drugs.aspx, checked on 9/20/2018.

Alvarino, T.; Komesli, O.; Suarez, S.; Lema, J. M.; Omil, F. (2016): The potential of the innovative SeMPAC process for enhancing the removal of recalcitrant organic micropollutants. *Journal of Hazardous Materials* 308, 29–36. DOI: 10.1016/j.jhazmat.2016.01.040.

Alvarino, T.; Suarez, S.; Lema, J.; Omil, F. (2018): Understanding the sorption and biotransformation of organic micropollutants in innovative biological wastewater treatment technologies.*The Science of the Total Environment* 615, 297–306. DOI: 10.1016/j.scitotenv.2017.09.278.

Asha, Sepuri; Vidyavathi, Maravajhala (2009): Cunninghamella--a microbial model for drug metabolism studies--a review. *Biotechnology Advances* 27 (1), 16–29. DOI: 10.1016/j.biotechadv.2008.07.005.

Aymerich, I.; Acuña, V.; Barceló, D.; García, M. J.; Petrovic, M.; Poch, M. et al. (2016): Attenuation of pharmaceuticals and their transformation products in a wastewater treatment plant and its receiving river ecosystem. *Water Research* 100, 126–136. DOI: 10.1016/j.watres.2016.04.022.

Baker, David R.; Kasprzyk-Hordern, Barbara (2011): Multi-residue analysis of drugs of abuse in wastewater and surface water by solid-phase extraction and liquid chromatography-positive electrospray ionisation tandem mass spectrometry. *Journal of Chromatography. A* 1218 (12), 1620–1631. DOI: 10.1016/j.chroma.2011.01.060.

Baker, David R.; Kasprzyk-Hordern, Barbara (2013): Spatial and temporal occurrence of pharmaceuticals and illicit drugs in the aqueous environment and during wastewater treatment. New developments. *The Science of the Total Environment* 454-455, 442–456. DOI: 10.1016/j.scitotenv.2013.03.043.

Barra Caracciolo, Anna; Topp, Edward; Grenni, Paola (2015): Pharmaceuticals in the environment. Biodegradation and effects on natural microbial communities. A review. *Journal of Pharmaceutical and Biomedical Analysis* 106, 25–36. DOI: 10.1016/j.jpba.2014.11.040.

Barrera-Díaz, C.; Cañizares, P.; Fernández, F. J.; Natividad, R.; Rodrigo, M. A. (2017): Electrochemical Advanced Oxidation Processes. An Overview of the Current Applications to Actual Industrial Effluents. J*ournal of the Mexican Chemical Society* 58 (3). DOI: 10.29356/jmcs.v58i3.133.

Benfield, Paul; Heel, Rennie C.; Lewis, Susan P. (1986): Fluoxetine. *Drugs* 32 (6), 481–508. DOI: 10.2165/00003495-198632060-00002.

Publication bibliography

Blair, Benjamin D.; Crago, Jordan P.; Hedman, Curtis J.; Klaper, Rebecca D. (2013): Pharmaceuticals and personal care products found in the Great Lakes above concentrations of environmental concern. *Chemosphere* 93 (9), 2116–2123. DOI: 10.1016/j.chemosphere.2013.07.057.

Boonnorat, Jarungwit; Chiemchaisri, Chart; Chiemchaisri, Wilai; Yamamoto, Kazuo (2014): Microbial adaptation to biodegrade toxic organic micro-pollutants in membrane bioreactor using different sludge sources. *Bioresource Technology* 165, 50–59. DOI: 10.1016/j.biortech.2014.04.024.

Boxall, Alistair B. A.; Sinclair, Chris J.; Fenner, Kathrin; Kolpin, Dana; Maund, Steve J. (2004): Peer Reviewed. When Synthetic Chemicals Degrade in the Environment. *Environmental Science & Technology* 38 (19), 368A-375A. DOI: 10.1021/es040624v.

Bringolf, Robert B.; Heltsley, Rebecca M.; Newton, Teresa J.; Eads, Chris B.; Fraley, Stephen J.; Shea, Damian; Cope, W. Gregory (2010): Environmental occurrence and reproductive effects of the pharmaceutical fluoxetine in native freshwater mussels. *Environmental Toxicology and Chemistry* 29 (6), 1311–1318. DOI: 10.1002/etc.157.

Caldwell, Daniel J.; D'Aco, Vincent; Davidson, Todd; Kappler, Kelly; Murray-Smith, Richard J.; Owen, Stewart F. et al. (2019): Environmental risk assessment of metformin and its transformation product guanylurea. II. Occurrence in surface waters of Europe and the United States and derivation of predicted no-effect concentrations. *Chemosphere* 216, 855–865. DOI: 10.1016/j.chemosphere.2018.10.038.

Chang, Soon Woong (1997): Cometabolic degradation of polycyclic aromatic hydrocarbons (PAHs) and aromatic ethers by phenol- and ammonia-oxidizing bacteria. Dissertation, checked on 8/9/2017.

Collin, F.; Khoury, H.; Bonnefont-Rousselot, D.; Thérond, P.; Legrand, A.; Jore, D.; Gardès-Albert, M. (2004): Liquid chromatographic/electrospray ionization mass spectrometric identification of the oxidation end-products of metformin in aqueous solutions. *Journal of Mass Spectrometry* 39 (8), 890–902. DOI: 10.1002/jms.656.

Comninellis, Christos; Chen, Guohua (2010): Electrochemistry for the environment. New York, London: Springer.

Convention, United States Pharmacopeial (2006): USP DI. Volume 1, Volume 1. Greenwood Village, CO: Thomson/MICROMEDEX.

Cooper, Emily R.; Siewicki, Thomas C.; Phillips, Karl (2008): Preliminary risk assessment database and risk ranking of pharmaceuticals in the environment. *The Science of the Total Environment* 398 (1-3), 26–33. DOI: 10.1016/j.scitotenv.2008.02.061.

Cui, Hao; Schröder, Peter (2016): Uptake, translocation and possible biodegradation of the antidiabetic agent metformin by hydroponically grown Typha latifolia. *Journal of Hazardous Materials* 308, 355–361. DOI: 10.1016/j.jhazmat.2016.01.054.

Escher, Beate I.; Fenner, Kathrin (2011): Recent advances in environmental risk assessment of transformation products. *Environmental Science & Technology* 45 (9), 3835–3847. DOI: 10.1021/es1030799.

Fernandez-Fontaina, E.; Carballa, M.; Omil, F.; Lema, J. M. (2014): Modelling cometabolic biotransformation of organic micropollutants in nitrifying reactors. *Water Research* 65, 371–383. DOI: 10.1016/j.watres.2014.07.048.

Franklin, Michael R. (2008): Phase II Biotransformation Reactions-N-Acetyltransferase. In S. J. Enna, David B. Bylund (Eds.): XPharm. *The Comprehensive Pharmacology Reference*. Amsterdam, Boston: Elsevier, 1–3.

Ghoshdastidar, Avik J.; Fox, Shannon; Tong, Anthony Z. (2015): The presence of the top prescribed pharmaceuticals in treated sewage effluents and receiving waters in Southwest Nova Scotia, Canada. *Environmental Science and Pollution Research International* 22 (1), 689–700. DOI: 10.1007/s11356-014-3400-z.

Gong, Li; Goswami, Srijib; Giacomini, Kathleen M.; Altman, Russ B.; Klein, Teri E. (2012): Metformin pathways. Pharmacokinetics and pharmacodynamics. *Pharmacogenetics and Genomics* 22 (11), 820–827. DOI: 10.1097/FPC.0b013e3283559b22.

Grandt, Daniel; Schubert, Ingrid (2017): Arzneimittelreport 2017. Barmer GEK. Available online at https://www.barmer.de/blob/121882/fb95b983d313c453d9ebaa01c2ac783d/data/dl-barmer-arzneimittelreport-2017.pdf, updated on 9/7/2017, checked on 2/11/2019.

Grundl, Timothy J.; Haderlein, Stefan; Nurmi, James T.; Tratnyek, Paul G. (2012): Introduction to Aquatic Redox Chemistry. In Paul G. Tratnyek (Ed.): Aquatic redox chemistry, vol. 1071. Washington, D.C: American Chemical Society (ACS Symposium Series, 1071), 1–14.

Herrmann, Manuel; Menz, Jakob; Olsson, Oliver; Kümmerer, Klaus (2015): Identification of phototransformation products of the antiepileptic drug gabapentin. Biodegradability and initial assessment of toxicity. *Water Research* 85, 11–21. DOI: 10.1016/j.watres.2015.08.004.

Jancova, Petra; Anzenbacher, Pavel; Anzenbacherova, Eva (2010): Phase II drug metabolizing enzymes. *Biomedical Papers of the Medical Faculty of the University Palacky, Olomouc, Czechoslovakia* 154 (2), 103–116.

Johansson, Tove; Weidolf, Lars; Jurva, Ulrik (2007): Mimicry of phase I drug metabolism--novel methods for metabolite characterization and synthesis. *Rapid Communications in Mass Spectrometry : RCM* 21 (14), 2323–2331. DOI: 10.1002/rcm.3077.

Jones, O. A. H.; Voulvoulis, N.; Lester, J. N. (2002): Aquatic environmental assessment of the top 25 English prescription pharmaceuticals. *Water Research* 36 (20), 5013–5022.

Kebamo, Selamu; Tesema, Shibiru (2015): The Role of Biotransformation in Drug Discovery and Development. *Journal of Drug Metabolism & Toxicology* 06 (05). DOI: 10.4172/2157-7609.1000196.

Kosma, Christina I.; Lambropoulou, Dimitra A.; Albanis, Triantafyllos A. (2015): Comprehensive study of the antidiabetic drug metformin and its transformation product guanylurea in Greek wastewaters. *Water Research* 70, 436–448. DOI: 10.1016/j.watres.2014.12.010.

Kwon, Jeong-Wook; Armbrust, Kevin L. (2006): Laboratory persistence and fate of fluoxetine in aquatic environments. *Environmental Toxicology and Chemistry* 25 (10), 2561. DOI: 10.1897/05-613R.1.

Lajeunesse, André; Blais, Mireille; Barbeau, Benoît; Sauvé, Sébastien; Gagnon, Christian (2013): Ozone oxidation of antidepressants in wastewater -Treatment evaluation and characterization of new by-products by LC-QToFMS. *Chemistry Central Journal* 7 (1), 15. DOI: 10.1186/1752-153X-7-15.

Lam, Monica W.; Tantuco, Kathleen; Mabury, Scott A. (2003): PhotoFate: A New Approach in Accounting for the Contribution of Indirect Photolysis of Pesticides and Pharmaceuticals in Surface Waters. *Environmental Science & Technology* 37 (5), pp. 899–907. DOI: 10.1021/es025902.

Lambropoulou, Dimitra A.; Nollet, Leo M. L. (2014): Transformation Products of Emerging Contaminants in the Environment. Chichester, United Kingdom: John Wiley and Sons Ltd.

Margot, Jonas; Rossi, Luca; Barry, David A.; Holliger, Christof (2015): A review of the fate of micropollutants in wastewater treatment plants. *WIREs Water* 2 (5),457–487. DOI: 10.1002/wat2.1090.

Markiewicz, Marta; Jungnickel, Christian; Stolte, Stefan; Białk-Bielińska, Anna; Kumirska, Jolanta; Mrozik, Wojciech (2017): Ultimate biodegradability and ecotoxicity of orally administered antidiabetic drugs. *Journal of Hazardous Materials* 333, 154–161. DOI: 10.1016/j.jhazmat.2017.03.030.

Marshall, Sally M. (2017): 60 years of metformin use. A glance at the past and a look to the future. *Diabetologia* 60 (9), 1561–1565. DOI: 10.1007/s00125-017-4343-y.

McNeill, Kristopher; Canonica, Silvio (2016): Triplet state dissolved organic matter in aquatic photochemistry: reaction mechanisms, substrate scope, and photophysical properties. *Environmental Science. Processes & Impacts* 18 (11), 1381–1399. DOI: 10.1039/c6em00408c.

Mennigen, Jan A.; Martyniuk, Christopher J.; Crump, Kate; Xiong, Huiling; Zhao, E.; Popesku, Jason et al. (2008): Effects of fluoxetine on the reproductive axis of female goldfish (Carassius auratus). *Physiological Genomics* 35 (3), 273–282. DOI: 10.1152/physiolgenomics.90263.2008.

Metcalfe, Chris D.; Chu, Shaogang; Judt, Colin; Li, Hongxia; Oakes, Ken D.; Servos, Mark R.; Andrews, David M. (2010): Antidepressants and their metabolites in municipal wastewater, and downstream exposure in an urban watershed. *Environmental Toxicology and Chemistry* 29 (1), 79–89. DOI: 10.1002/etc.27.

Metcalfe, Chris D.; Miao, Xiu-Sheng; Koenig, Brenda G.; Struger, John (2003): Distribution of acidic and neutral drugs in surface waters near sewage treatment plantes in the lower Great Lakes, Canada. *Environmental Toxicology and Chemistry* 22 (12), 2881. DOI: 10.1897/02-627.

Nagel, Roland (2002): DarT. The embryo test with the Zebrafish Danio rerio--a general model in ecotoxicology and toxicology. *ALTEX* 19 Suppl 1, 38–48.

Nałecz-Jawecki, Grzegorz (2007): Evaluation of the in vitro biotransformation of fluoxetine with HPLC, mass spectrometry and ecotoxicological tests. *Chemosphere* 70 (1), 29–35. DOI: 10.1016/j.chemosphere.2007.07.035.

Oosterhuis, Mathijs; Sacher, Frank; Ter Laak, Thomas L. (2013): Prediction of concentration levels of metformin and other high consumption pharmaceuticals in wastewater and regional surface water based on sales data. *The Science of the Total Environment* 442, 380–388. DOI: 10.1016/j.scitotenv.2012.10.046.

Perreault, Nancy N.; Halasz, Annamaria; Thiboutot, Sonia; Ampleman, Guy; Hawari, Jalal (2013): Joint photomicrobial process for the degradation of the insensitive munition N-guanylurea-dinitramide (FOX-12). *Environmental Science & Technology* 47 (10), 5193–5198. DOI: 10.1021/es4006652.

Pervaiz, I.; Ahmad, S.; Madni, M. A.; Ahmad, H.; Khaliq, F. H. (2013): Microbial biotransformation. A tool for drug designing (Review). *Prikladnaia biokhimiia i mikrobiologiia* 49 (5), 435–449.

Peters, Joseph R.; Granek, Elise F.; Rivera, Catherine E. de; Rollins, Matthew (2017): Prozac in the water. Chronic fluoxetine exposure and predation risk interact to shape behaviors in an estuarine crab. *Ecology and Evolution* 7 (21), 9151–9161. DOI: 10.1002/ece3.3453.

Petrie, Bruce; Barden, Ruth; Kasprzyk-Hordern, Barbara (2015): A review on emerging contaminants in wastewaters and the environment. Current knowledge, understudied areas and recommendations for future monitoring. *Water Research* 72, 3–27. DOI: 10.1016/j.watres.2014.08.053.

Pomiès, M.; Choubert, J-M; Wisniewski, C.; Coquery, M. (2013): Modelling of micropollutant removal in biological wastewater treatments: a review. *The Science of the Total Environment* 443, 733–748. DOI: 10.1016/j.scitotenv.2012.11.037.

Ruff, Matthias; Mueller, Miriam S.; Loos, Martin; Singer, Heinz P. (2015): Quantitative target and systematic non-target analysis of polar organic micro-pollutants along the river Rhine using high-resolution mass-spectrometry--Identification of unknown sources and compounds. *Water Research* 87, 145–154. DOI: 10.1016/j.watres.2015.09.017.

Salgado, R.; Marques, R.; Noronha, J. P.; Mexia, J. T.; Carvalho, G.; Oehmen, A.; Reis, M. A. M. (2011): Assessing the diurnal variability of pharmaceutical and personal care products in a full-scale activated sludge plant. *Environmental Pollution (Barking, Essex : 1987)* 159 (10), 2359–2367. DOI: 10.1016/j.envpol.2011.07.004.

Scheurer, Marco; Michel, Amandine; Brauch, Heinz-Jürgen; Ruck, Wolfgang; Sacher, Frank (2012): Occurrence and fate of the antidiabetic drug metformin and its metabolite guanylurea in the environment and during drinking water treatment. *Water Research* 46 (15), 4790–4802. DOI: 10.1016/j.watres.2012.06.019.

Schlüter-Vorberg, Lisa; Prasse, Carsten; Ternes, Thomas A.; Mückter, Harald; Coors, Anja (2015): Toxification by Transformation in Conventional and Advanced Wastewater Treatment. The Antiviral Drug Acyclovir. *Environmental Science & Technology Letters* 2 (12), 342–346. DOI: 10.1021/acs.estlett.5b00291.

Schultz, Melissa M.; Furlong, Edward T.; Kolpin, Dana W.; Werner, Stephen L.; Schoenfuss, Heiko L.; Barber, Larry B. et al. (2010): Antidepressant pharmaceuticals in two U.S. effluent-impacted streams. Occurrence and fate in water and sediment, and selective uptake in fish neural tissue. *Environmental Science & Technology* 44 (6), 1918–1925. DOI: 10.1021/es9022706.

Schulze, Tobias; Weiss, Sara; Schymanski, Emma; Ohe, Peter Carsten von der; Schmitt-Jansen, Mechthild; Altenburger, Rolf et al. (2010): Identification of a phytotoxic photo-transformation product of diclofenac using effect-directed analysis. *Environmental Pollution (Barking, Essex : 1987)* 158 (5), 1461–1466. DOI: 10.1016/j.envpol.2009.12.032.

Schwarzenbach, René P.; Gschwend, P. M.; Imboden, Dieter M. (2017a): Environmental organic chemistry. Third edition. Hoboken, New Jersey: Published by John Wiley & Sons.

Schwarzenbach, René P.; Gschwend, Philip M.; Imboden, Dieter M. (2017b): Environmental organic chemistry. Third edition. Hoboken, New Jersey: Wiley. Available online at http://site.ebrary.com/lib/alltitles/docDetail.action?docID=11282612.

Sebastine, I. M.; Wakeman, R. J. (2003): Consumption and Environmental Hazards of Pharmaceutical Substances in the UK. *Process Safety and Environmental Protection* 81 (4), 229–235. DOI: 10.1205/095758203322299743.

Sigg, Laura; Stumm, Werner (2011): Aquatische Chemie. Einführung in die Chemie natürlicher Gewässer. 5., vollst. überarb. Aufl. Zürich: vdf Hochschul-Verl. (utb.de-Bachelor-Bibliothek, 8463).

Sipma, Jan; Osuna, Begoña; Collado, Neus; Monclús, Hector; Ferrero, Giuliana; Comas, Joaquim; Rodriguez-Roda, Ignasi (2010): Comparison of removal of pharmaceuticals in MBR and activated sludge systems. *Desalination* 250 (2), 653–659. DOI: 10.1016/j.desal.2009.06.073.

Souza Anselmo, Carina de; Sardela, Vinicius Figueiredo; Sousa, Valeria Pereira de; Pereira, Henrique Marcelo Gualberto (2018): Zebrafish (Danio rerio): A valuable tool for predicting the metabolism of xenobiotics in humans? *Comparative Biochemistry and Physiology. Toxicology & Pharmacology : CBP* 212, 34–46. DOI: 10.1016/j.cbpc.2018.06.005.

Stuart, Marianne E.; Lapworth, Dan J. (2014): Transformation Products of Emerging Organic Compounds as Future Groundwater and Drinking Water Contaminants (Wiley Online Books).

Ternes, Thomas A. (1998): Occurrence of drugs in German sewage treatment plants and rivers1Dedicated to Professor Dr. Klaus Haberer on the occasion of his 70th birthday.1. *Water Research* 32 (11), 3245–3260. DOI: 10.1016/S0043-1354(98)00099-2.

Tijani, Jimoh O.; Fatoba, Ojo O.; Babajide, Omotola O.; Petrik, Leslie F. (2016): Pharmaceuticals, endocrine disruptors, personal care products, nanomaterials and perfluorinated pollutants. A review. *Environmental Chemistry Letters* 14 (1), 27–49. DOI: 10.1007/s10311-015-0537-z.

Tratnyek, Paul G.; Grundl, Timothy J.; Haderlein, Stefan B. (2011): Aquatic Redox Chemistry. Washington, DC: American Chemical Society (1071).

Trautwein, Christoph; Berset, Daniel; Wolschke, Hendrik; Kümmerer, Klaus (2014): Occurrence of the antidiabetic drug Metformin and its ultimate transformation product Guanylurea in several compartments of the aquatic cycle. *Environment International* 70C. DOI: 10.1016/j.envint.2014.05.008.

Trautwein, Christoph; Kümmerer, Klaus (2011): Incomplete aerobic degradation of the antidiabetic drug Metformin and identification of the bacterial dead-end transformation product Guanylurea. *Chemosphere* 85 (5), 765–773. DOI: 10.1016/j.chemosphere.2011.06.057.

Universität Tübingen (2018): Effect-Net. Physiologische Ökologie der Tiere. Tübingen. Available online at https://uni-tuebingen.de/fakultaeten/mathematisch-naturwissenschaftliche-fakultaet/fachbereiche/biologie/institute/evolutionecology/lehrbereiche/physiologische-oekologie-der-tiere/research/effect-net/, updated on 8/27/2018, checked on 2/21/2019.

Vasskog, Terje; Anderssen, Trude; Pedersen-Bjergaard, Stig; Kallenborn, Roland; Jensen, Einar (2008): Occurrence of selective serotonin reuptake inhibitors in sewage and receiving waters at Spitsbergen and in Norway. *Journal of Chromatography. A* 1185 (2), 194–205. DOI: 10.1016/j.chroma.2008.01.063.

Wallace, Derek F.; Hand, Laurence H.; Oliver, Robin G. (2010): The role of indirect photolysis in limiting the persistence of crop protection products in surface waters. *Environmental Toxicology and Chemistry* 29 (3), 575–581. DOI: 10.1002/etc.65.

Publication bibliography

Wang, Xiao-Huan; Lin, Angela Yu-Chen (2012): Phototransformation of cephalosporin antibiotics in an aqueous environment results in higher toxicity. *Environmental Science & Technology* 46 (22), 12417–12426. DOI: 10.1021/es301929e.

Reprint of articles included in this thesis

PAPER 1

Formation and occurrence of transformation products of metformin in wastewater and surface water

Selina Tisler, Christian Zwiener

(2018)

The Science of the Total Environment 628-629, 1121–1129

DOI: 10.1016/j.scitotenv.2018.02.105

Science of the Total Environment 628–629 (2018) 1121–1129

Contents lists available at ScienceDirect

Science of the Total Environment

journal homepage: www.elsevier.com/locate/scitotenv

Formation and occurrence of transformation products of metformin in wastewater and surface water

Selina Tisler, Christian Zwiener *

Hölderlinstraße 12, 72074 Tübingen, Germany

HIGHLIGHTS

- Electrochemical generation of metformin (MF) TPs
- Identification of MF TPs by LC-high-resolution MS
- Detection of MF TPs in wastewater and surface water

GRAPHICAL ABSTRACT

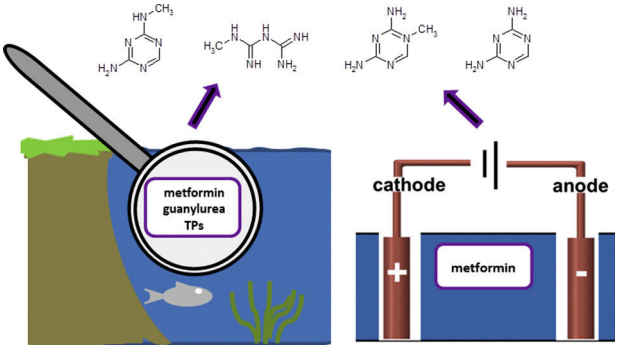

ARTICLE INFO

Article history:
Received 20 December 2017
Received in revised form 9 February 2018
Accepted 9 February 2018
Available online xxxx

Editor: D. Barcelo

Keywords:
Metformin
Guanyl urea
Methylbiguanide
Transformation products
Wastewater treatment
Surface water
High-resolution mass spectrometry
LC-MS

ABSTRACT

The aim of this work was to investigate the occurrence and fate of the antidiabetic metformin (MF) and its transformation products (TPs) in wastewater and surface water samples. New TPs of MF were approached by electrochemical degradation with a boron-doped-diamond electrode (at 1.5 V for 10 min). 2,4-Diamino-1,3,5-triazine (2,4-DAT), methylbiguanide (MBG), 2-amino-4-methylamino-1,3,5-triazine (2,4-AMT) and 4-amino-2-imino-1-methyl-1,2-dihydro-1,3,5-triazine (4,2,1-AIMT) were identified by hydrophilic interaction chromatography (HILIC) with quadrupole time-of-flight mass spectrometry (QTOF-MS) and accurate mass fragmentation. However, the well-known transformation product guanyl urea (GU) could not be formed electrochemically. In samples from wastewater treatment plants (WWTP), 2,4-AMT and 2,4-DAT showed an increasing trend from influents to effluents, which implies formation of the TPs during WWT. MBG is also formed by hydrolysis of MF and therefore didn't show this trend in WWTPs. Compared to GU, the concentrations of other TPs are generally three orders of magnitude lower. MBG and 2,4-DAT were also detected in surface water which was impacted by waste water, while 4,2,1-AIMT could not be detected in any sample. The concentrations of MF were in an expected range for influent (14 to 95 μg/l), effluent (0.7 to 6.5 μg/l), surface water (up to 234 ng/l) and tap water (34 ng/l). GU concentrations, however, were in one of the two investigated WWTP much higher in the influent (between 158 μg/l and 2100 μg/l) than in the effluent (between 26 and 810 μg/l). This is a rather unexpected result which has not been reported yet. Obviously, GU has been already formed in parts of the sewer system from MF or from other biguanide compounds like antidiabetics or disinfection chemicals. Furthermore, lower concentrations of GU in the effluents than in the influents indicate degradation processes of guanyl urea in the waste water treatment.

* Corresponding author.
E-mail address: christian.zwiener@uni-tuebingen.de (C. Zwiener).

https://doi.org/10.1016/j.scitotenv.2018.02.105
0048-9697/

1. Introduction

Micropollutants like pharmaceuticals are ubiquitous in the aquatic environment. Active ingredients and their metabolites are excreted by humans and discharged to waste water. Due to incomplete removal of several pharmaceuticals and their metabolites in municipal wastewater treatment, effluents are major entry pathways to receiving water bodies (Daughton and Kümmerer, 2004). Veterinary drugs can enter the environment via dung and manure used in agriculture. Emphasis should be placed on transformation products (TPs), since they can be more mobile and even more harmful than parent compounds (Hernández et al., 2008). For example, Sinclair and Boxall (2003) noticed that 30% of TPs of pesticides were more toxic to fish, daphnia and algae than the parent pesticides.

A wide spread compound with a well-known TP is the antidiabetic drug metformin (MF). MF is a drug against type 2 diabetes, one of the most prescribed pharmaceuticals worldwide (Ghoshdastidar et al., 2015, Huschek et al., 2004, Jones et al., 2002, Sebastine and Wakeman, 2003) and moreover the only pharmaceutical in the EU which is consumed >1 g per person and year (between 5.9 and 12.1 g) (Roig, 2010). In 2015 worldwide 415 million people suffered from diabetes, 60 million diabetes patients are in Europe alone. Type 2 diabetes is increasing, wherefore 642 million people with diabetes are predicted in 2040 (IDF, 2015). Moreover, clinical studies revealed an additional anticancer effect of MF due to the regulation of glucose metabolism (Salani et al., 2014). A study from 2005 postulated a cancer reduction of 23% in type 2 diabetes patients who were treated with MF (Evans et al., 2005). Consequently, the increasing number of diabetes patients together with the possible anticancer effect will lead to an increasing amount of prescribed and consumed MF.

Previous studies reported MF concentrations up to 129 μg/l in WWTP influents and up to 21 μg/l in WWTP effluents in Germany (Scheurer et al., 2009). The high effluent concentrations of guanyl urea (GU; up to 99 μg/l) are also remarkable. GU is a metabolite of MF which is formed in wastewater treatment processes and has been directly related to the aerobic degradation of MF in lab tests (Trautwein and Kümmerer, 2011). This was also found for waste water treatment plants (WWTPs), where GU formation correlated well with MF degradation (Oosterhuis et al., 2013; Scheurer et al., 2012). On the contrary some selected examples showed no correlation between MF and GU (Trautwein and Kümmerer, 2011; Kosma et al., 2015). A MF removal of 65 μg/l in contrast to a GU formation of only 2 μg/l was found in 24-h mix samples of a sewage treatment plant (600.000 population equivalents) by Trautwein and Kümmerer (2011). This can be interpreted by some further elimination pathways of MF, if GU is considered as the only bacterial dead-end product, which is resistance to further degradation (Trautwein et al., 2014; Markiewicz et al., 2017).

MF and GU were also detected in surface water with concentrations in the low ng/l to the μg/l range (Blair et al., 2013; Kolpin et al., 2002; Ruff et al., 2015; Scheurer et al., 2012; Trautwein et al., 2014). Whereas MF was investigated worldwide, data for GU are primarily available for Germany. In general, GU concentrations in surface water were higher than MF concentrations. Although the substances are ubiquitous in the aquatic environment, information on ecotoxicological effects to water organisms is scarce. For zooplankton and benthos, the acute toxicity of MF is uncritical in the concentration range of WWTP effluents (Fent et al., 2006). However, potential endocrine disrupting effects of MF have been described for adult North American minnows (Niemuth et al., 2015). In general, data on chronic effects in multiple life stages are lacking. An even larger knowledge gap exists for acute and chronic toxicity of GU. For acute *Daphnia magna* immobilization test the EC_{50} value of 40 mg/l for GU was obtained (Markiewicz et al., 2017).

There are also studies about further potential transformation pathways of MF. OH-radical induced oxidation of MF by gamma radiolysis formed eleven primary and secondary oxidation products (Collin et al., 2004; Trouillas et al., 2013). Among them are 4-amino-2-imino-1-methyl-1,2-dihydro-1,3,5-triazine (4,2,1-AIMT), 2-amino-4-methylamino-1,3,5-triazine (2,4-AMT), methylbiguanide (MBG), 2,4-diamino-1,3,5-triazine (2,4-DAT) and biguanide. Scheurer et al. (2012) identified 2,4-AMT as a primary oxidation product of ozonation, whereas Briones et al. (2016) identified MBG as degradation product of MF in plants. Quintao et al. (2016) identified 4,2,1-AIMT and MBG as by-products in photocatalysis, ozonation and chlorination. However so far, no other transformation products of MF than GU have been reported in the water cycle.

Another option to simulate transformation of micropollutants is electrochemistry (EC). The use of EC has demonstrated to be a useful tool for simulating natural oxidation processes such as photo- and biodegradation (Gul et al., 2015). For example, Johansson et al. (2007) used EC to mimic metabolic oxidation performed by CYP 450. EC is advantageous in comparison to classical chemical synthesis of TPs due to no further need of sample preparation and a very fast and simple method (Gul et al., 2015).

The objective of this study is therefore to investigate the occurrence and fate of the antidiabetic MF and its TPs in wastewater and surface water. Our hypothesis is that TPs of MF are relevant contaminants which have to be considered more carefully. For this purpose, an analysis method was established, and identification of potentially new TPs was performed by electrochemical processes and LC high-resolution mass spectrometry.

2. Materials and methods

2.1. Chemicals

Optima LC-MS grade acetonitrile (AcN), formic acid (FA), ammonium formate (NH_4F) and water were purchased from Fisher Chemical. The standards metformin hydrochloride (>98%), guanyl urea sulfate (>98%) were purchased from TCI, 1-methylbiguanide hydrochloride from LGC standards and metformin d6 from Toronto Research Chemicals. Individual stock solutions with a concentration of 1 g/l were prepared in a mixture of AcN and water (1:1). All working solutions of the standards for direct injection were prepared in AcN and tap or ultrapure water (10:1). Calibration and quality control samples for freeze drying were prepared in tap water. Working solution containing 10 μg/l of metformin-D6 was prepared in ultrapure water. Stock and working solutions were stored in the freezer at −20 °C, except of the aqueous metformin-d6 solution which was stored in the refrigerator (4 °C).

2.2. Water sample collection and preparation

Twenty four-hour composite samples of wastewater influents (after first treatment step) and effluents were obtained by flow rate-proportional sampling from waste water treatment plant 1 (W1) (100.000 population equivalent plus hospitals, no advanced treatment steps) in April and July 2016. In August, time- proportional samples were obtained from W2 (75.000 population equivalent), where biological treatment is subdivided into an activated sludge system and in a nitrification/denitrification step with a trickling filter. No further advanced treatment steps are applied. The composite samples were taken from 7 consecutive days from both waste water treatment plants (WWTPs), which are located in Southwest Germany. Surface water samples were investigated from three tributary streams of the river Neckar by collecting individual grab samples on the same day in November 2016. The samples of river 1 and river 2 were collected upstream and downstream of two other WWTPs. Sampling points of river 1 are all upstream of W1. River 3 is a rather pristine surface water from a forest without any waste water impact.

River and WWTP samples were immediately cooled, filtered and stored at 4 °C. In the laboratory, all samples were filtered with syringe filters with regenerated cellulose (Captiva, pore size: 0.2 μm, Agilent

Technologies, Germany). Subsequently 1 ml aliquots were transferred to HPLC vials and 100 µl of an internal stock solution of MF-D6 (10 µg/l) were added. The aliquots were stored at −20 °C and freeze-dried within 2 weeks (freeze-dryer alpha 1–4; Christ, Osterode, Germany). The samples were immediately reconstituted with 100 µl ultrapure water and 900 µl AcN and measured by LC-MS.

2.3. Electrochemical oxidation of metformin

An electrochemical oxidation process was applied to generate TPs. Generated TPs are largely similar to TPs and metabolites which are formed in the environment (Johansson et al., 2007). Electrochemical experiments were realized in a 12-ml batch cell of PEEK with a conductive boron-doped-diamond (BDD) working electrode (4 cm × 2 cm, with a 10 µm diamond layer on Niob base from Condias, Itzehoe, Germany). As a counter electrode a 4 mm × 8 mm platinum mesh (Sigma Aldrich, St. Louis, USA) and as reference a Ag/AgCl electrode (3M, MF-2052, BASi, West Lafayette, USA) was used. Oxidative and reductive compartments of the batch cell were separated by a Vycor glass frit. The experiments were performed with 10 mg/l MF in a 20 mM NH_4F solution which was adjusted either to pH 3 or pH 7 with FA or ammonium hydroxide. Adequate mixing of the solution was guaranteed through gentle magnetic stirring with 320 cycles per minute. A constant potential of 1.5 V was applied with a potentiostat (Autolab Potentiostat, PGSTAT 101; Metrohm) for 10 min.

The experiments were performed in triplicates for both pH values. After each experiment, the BDD electrode was cleaned electrochemically with 150 pulses of alternating potential between +2 V and −2 V over a period of 5 min. The collected samples before ($t = 0$ min) and after ($t = 10$ min) the experiments were stored at 4 °C in the dark and analyzed by LC-ESI-QTOF after dilution with AcN (1:10) within 24 h.

2.4. LC-ESI-QqQ analysis

Target screening was performed by LC-MS using a 1260 Infinity HPLC system (Agilent Technologies, Germany) with a triple quadrupole mass spectrometer (QqQ-MS). A Phenomenex LUNA 5 u HILIC 200 A column (150 × 3 mm; 5 µm particle size), at a flow rate of 0.5 ml/min was used for separation at 40 °C. Eluent A was an aqueous buffer with 15 mM NH_4F and 0.1% FA; eluent B was AcN with 0.1% FA. Gradient elution was used: 0–4 min 95% B, decrease to 50% B within 4 min, held for 6 min at 50% B. After switching back to the starting conditions, post time was 8 min.

Samples (composition of 90% AcN and 10% H2O) were kept in the autosampler at 10 °C and the injection volume was 10 µl for standards, tap water and surface water samples. Due to matrix effects and high concentrations of MF and GU, injection volume for WWTP samples was 1 µl.

A method calibration including freeze drying was typically performed between 0.05 µg/l and 5 µg/l in tap water with deuterated MF (D6) as an internal standard. Only concentrations in tap water samples were analyzed by external calibration in ultrapure water, ranging from 1 ng/l to 100 ng/l.

Quantification of MF, GU and MBG was achieved after LC separation with a 6490 triple quadrupole mass spectrometer (Agilent Technologies, Germany) using the positive ionization mode. The ESI source with the Agilent Jet Stream technology was operated under conditions given in Table S1. The data recorded were processed with the software Mass Hunter. For quantification and confirmation two MRM transitions were monitored for each analyte in the dynamic MRM mode. Details are given in Table 1.

2.5. LC-ESI-QTOF-MS analysis

LC-QTOF-MS measurements were used for fragmentation data and qualification of electrochemical generated TPs. LC operating parameters were the same as used described above. For high-resolution mass spectrometry with a 6550 quadrupole-time-of-flight (QTOF) instrument (Agilent Technologies) a scan range of m/z 50–1000 with 3 spectra/s and similar parameters as described in Table S1 were used, except of a lower nebulizer pressure (35 psi) and a higher capillary voltage (3000 V). Fragmentation data were acquired by the automated fragmentation mode (auto MS/MS; precursor isolation width at about 4 Da) and an all-ion fragmentation (AIF) mode without any precursor selection (scan range m/z 100 to 1000 at three different collision energies (10 eV, 20 eV and 40 eV)). Quantitative analysis was based on extracted ion chromatograms of the accurate masses and retention times at a mass isolation window of 10 ppm (e.g. m/z 126.0774 at 2.8 min, m/z 112.0618 at 3.6 min, m/z 116.0931 at 6.0 min) and an external calibration for MBG (TP 116) in the range of 10 ng/l and 500 ng/l.

3. Results and discussion

3.1. Identification of electrochemically generated TPs

The generation of MF TPs was investigated by electrochemical oxidation at pH 3 and 7 and a potential of 1.5 V. The used boron doped diamond anode is a nonactive electrode wherefore indirect oxidation is the main reaction mechanism (Alfaro et al., 2006). OH-radicals were generated due to a used potential which was in the region of water decomposition (Comninellis and Chen, 2010). Four TPs of MF have been identified by LC-high-resolution-MS after electrochemical degradation. These are TP 112, TP 116, and the two isobaric compounds TP 126a and TP 126b (Fig. 1) which were already described after gamma radiolysis and analyzed by low-resolution MS2 (Collin et al., 2004; Trouillas et al., 2013). Our identification is based on accurate mass (AM) and AM fragmentation, which allowed the assignment of chemical formulas with very high mass accuracy below 3 ppm for all 4 TPs (Table 2).

TP 116 (C3H9N5) was the most abundant TP. Its fragmentation pattern resembles that of MF shifted by 14.0157 Da to lower mass (loss of methyl). This indicates the occurrence of methylbiguanide (MBG) which was finally confirmed by the retention time and AM fragmentation patterns at 3 collision energies of an authentic standard (Fig. S1). Noticeable was the occurrence of MBG in the samples before starting the electrochemical degradation. The experiments showed 0.6% and 0.3% of MBG in the starting sample compared with the endpoint sample for pH 3 and pH 7 respectively. A discussion about possible reasons is given in Section 3.2.

TP 112 (C3H5N5) is a secondary oxidation product and could be formed by dehydrogenation of methylbiguanide (TP 116; C3H9N5). Its AM fragmentation is dominated by the loss of CH2N2 (42.018 Da) and the occurrence of m/z 43.0282 $[CH2N2 + H]^+$, which is typical for amino-triazines and confirms together with the

Table 1
Compound-specific operating parameters of the target MRM method.

	Metformin	Metformin D6	Guanyl urea	1-Methylbiguanide
Precursor ion (m/z)	130	136	103.1	116
Product ion (Quan/Qual) (m/z)	60/71.1	60/77.1	60/86	60/56.9
Collision energy (setpoint in V)	10/30	10/30	10/5	10/20
Cell accelerator voltage (V)	6/6	6/6	5/5	6/3

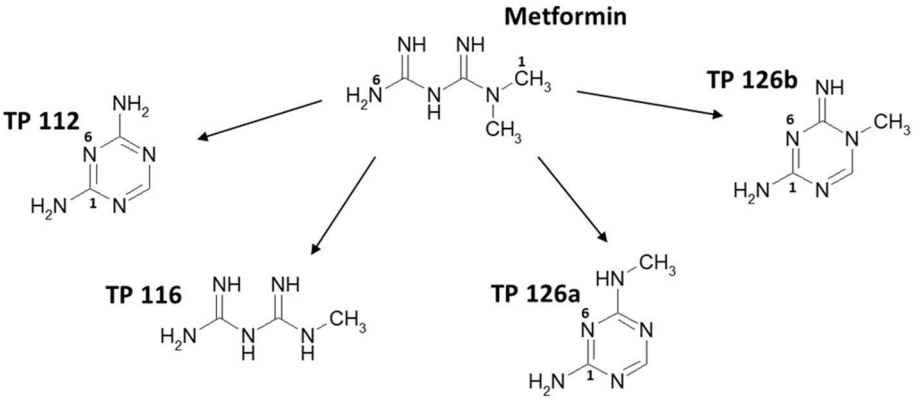

Fig. 1. Proposed structures for electrochemical degradation products. TP 116 (MBG) has been confirmed by an authentic standard, TPs 112, 126a and 126b by accurate mass fragmentation. – TP 112: 2,4-diamino-1,3,5-triazine (2,4-DAT); TP 126a: 2-amino-4-methylamino-1,3,5-triazine (2,4-AMT); TP 126b: 4-amino-2-imino-1-methyl-1,2-dihydro-1,3,5-triazine (4,2,1-AIMT).

loss of HCN (27.0109 Da) the proposed structure of 2,4-diamino-1,3,5-triazine (2,4-DAT) (Fig. 2a). 2,4-DAT was already suggested by Collin et al., 2004, but could not be validated in their work by mass fragmentation.

TP 126a and TP 126b at retention times 2.9 min and 4.8 min are isobars for which the chemical formula C4H7N5 could be assigned. Also for the TPs 126 a triazine structure was proposed in the literature formed from MF by the loss of 4 hydrogen atoms due to cyclization and formation of a double bond (Collin et al., 2004). The proposed reaction pathway for TP 126b is radical formation by H abstraction at C1 of the methyl group by an OH-radical and intramolecular reaction with N6 at the imine group. TP 126a is generated by the migration of a methyl group from TP 126b (Collin et al., 2004). TPs 126 could be also precursors of TP 112 due to a demethylation reaction. The proposed structures are 4-amino-2-imino-1-methyl-1,2-dihydro-1,3,5-triazine (4,2,1-AIMT) and 2-amino-4-methylamino-1,3,5-triazine (2,4-AMT). However, Collin et al. (2004) obtained a CID spectrum only for the mixture of the two TPs 126 by infusion MS.

In this study, we obtained AM fragmentation patterns for both TPs 126 (Fig. 2, Fig. S2 and S3), which are rather similar and confirm the triazine structure by abundant losses of 42. The major differences are the relatively high abundance of *m/z* 57.0444 $[C2H5N2]^+$ for TP 126a, the occurrence of *m/z* 42.0330 $[C2H4N]^+$ and an increased abundance of *m/z* 99.0659 due to the loss of HCN for TP 126b. Calculated log *P* values reveal 4,2,1-AIMT as the more polar analyte (Table S5). Based on the elution behavior on HILIC and RP columns TP 126a could be assigned to 2,4-AMT and TP 126b to 4,2,1-AIMT. This is in accordance with the occurrence of the fragment $[C2H4N]^+$ and the higher abundance of the loss of HCN of TP 126b.

Generally, the electrochemical formation of 4,2,1-AIMT was more abundant than that of 2,4-AMT, 100 times at pH 3 and ten times at pH 7. It was also reported by Trouillas et al. (2013), that higher pH values favored the formation of 2,4-AMT (TP 126a).

At pH 7 the intensity of all TPs was elevated which can be explained by more efficient generation of OH radicals (Comninellis and Chen, 2010). Interestingly, GU could not be formed electrochemically. In further experiments, electrochemical degradation of GU was tested. No TPs from GU have been identified.

3.2. Optimization of the analytical method

MF and related TPs were separated on a HILIC column due to their polar character. This requires a rather non-polar solvent like acetonitrile (AcN) in the samples and the LC eluent. Experiments with different percentages of water in the sample between 0.1% and 20% showed an increasing response of MF for increasing water content. The response of GU was not affected. The effect was independent of the MF concentration in the sample. Therefore, solubility effects could be ruled out. For further measurements we used 10% water and 90% acetonitrile in the samples, where the response reached a plateau (Fig. S6 and S7). Higher water content should be avoided due to peak broadening. For this reason, water samples were freeze dried and reconstituted in 10% water and 90% acetonitrile.

N-Methylbiguanide (MBG, TP 116) is already known as an impurity of metformin (Klaczkow and Anuszewska (2010), Raghava Raju et al. (2013)). We recognized the parameters storage time, temperature and pH as critical for TP formation in aqueous MF solutions. After 0, 4 and 7 days at room temperature and a pH of about 6 we found 18 ng/l, 28 ng/l and 33 ng/l MBG, which is at maximum 0.03% of MF concentration in the solution. At pH 6 we observed <0.01% MBG after 0.5 h at room temperature with a clear trend to higher values at lower pH values and at pH 9 (Fig. S5). These results prove that MBG can also be formed by hydrolysis of MF.

The TPs formed electrochemically were measured by LC-QTOF-MS due to higher signal selectivity compared to LC-QqQ-MS. High-resolution MS data of QTOF-MS showed higher signal to noise ratios than the mass transitions at unit-resolution of QqQ-MS. For TP 112, TP

Table 2
Characteristics of electrochemically generated TPs of MF.

Name of TP	Proposed compound	Chemical formula	Retention time HILIC (min)	accurate mass *m/z*	Δm (ppm)
TP 112	2,4-Diamino-1,3,5-triazine (2,4-DAT)	C3H5N5	3.8	112.0619	0.9
TP 116	Methylbiguanide (MBG)	C3H9N5	6.8	116.0932	0.9
TP 126a	2-Amino-4-methylamino-1,3,5-triazine (2,4-AMT)	C4H7N5	2.9	126.0770	3.2
TP 126b	4-Amino-2-imino-1-metyhl-1,2-dihydro-1,3,5-triazine (4,2,1-AIMT)	C4H7N5	4.8	126.0774	0.0

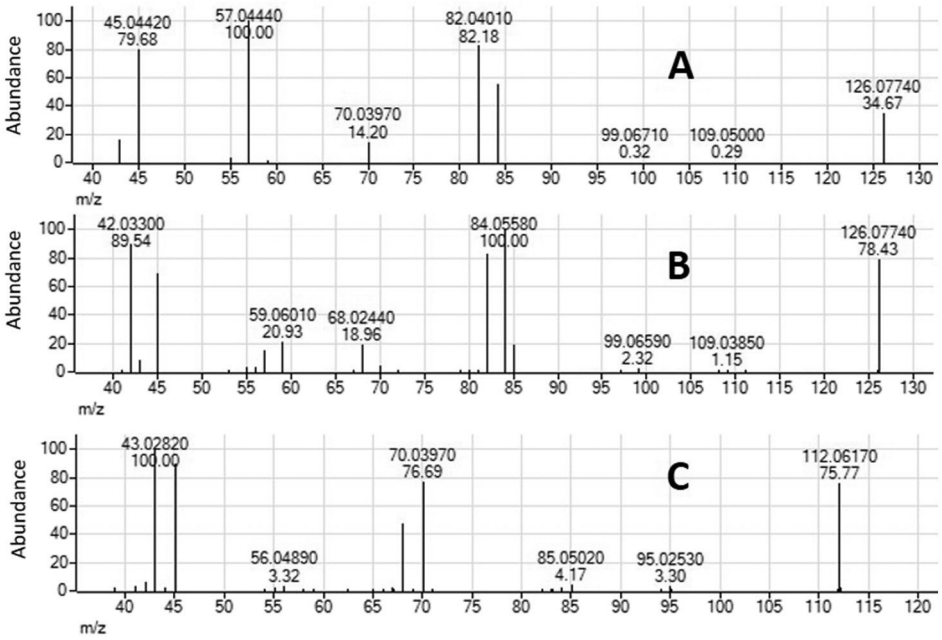

Fig. 2. AM fragmentation patterns of TP 126a (A), TP 126b (B) and TP 112 (C) at 20 eV.

126a and b only a qualitative measurement of the peak response was possible. Substances with available standards were measured quantitatively, TP 116 were measured on QTOF-MS, MF and GU on QqQ-MS. The mean method recoveries in tap water were 96% for MF, 70% for GU and 80% for MBG (Table 3) with relative standard deviations (RSD) in the range of 7% ($n = 4$). In ultrapure water the recovery of MF was only 63%. The RSDs for replicate LC-MS measurements were in the range of 1 to 2% ($n = 8$) on the same day (intraday variation) (Table S2). LOQs are reported for the lowest calibration level and are 1 ng/l for MF and 10 ng/l for GU and MBG.

3.3. Metformin in WWTP

The influent concentrations of MF in the wastewater treatment plants W1 and W2 were between 14 and 95 μg/l (0.11 and 0.74 μmol/l) (Fig. 3) and therefore in the same range reported previously (Scheurer et al., 2012). Increasing influent concentrations of MF could be correlated with the quantity and age of the population together with the size of hospitals (Kosma et al., 2015; Ghoshdastidar et al., 2015; Santos et al., 2013). In our case the wastewater of W1 is from several hospitals and about 100.000 people with an average age of 39 years, that of W2 from 75.000 people with an average age of 43.8 years. However, differences in influent concentrations may be dominated by dilution during rainfall events, since increasing MF concentrations correlate well with decreasing rainfall in April (5 mm), July (2 mm) and August (0.5 mm) (Table S3). Biodegradation of MF in the sewer system due to different residence times, for example in storm-water retention basins, would be another reason for lower MF concentrations in the influents. Biodegradation of MF should be correlated well with the formation of GU. Elimination of MF during wastewater treatment was in the range of 92% (W1, April) and 98% (W2, August). This results in a median effluent concentration of MF of 0.017 μmol/l for W1 and of 1.6 μg/l for W2. Removal efficiency is dependent on specific properties and adaptation of the activated sludge and the residence time, which will change with varying inflow rates (e.g. for dry weather and rainfall conditions). Our data do not support the postulated indirect correlation of removal efficiency and inflow mass of MF (Briones et al., 2016), since we observed highest removal efficiency at highest inflow concentrations.

Table 3
Method recoveries for freeze-dried samples (R(FD)) in tap water (TW); metformin and guanyl urea were measured by QqQ-MS and methylbiguanide by QTOF-MS.

	R (FD) [%]	RSD (FD) (n = 4) [%]	LOQ [ng/l]
Metformin	96	6.4	1
Guanyl urea	70	6.8	10
Methylbiguanide	80	–	10

3.4. Guanyl urea in WWTP

The results of WWTP W2 show that GU is generally formed in WWT, since the effluent concentrations of GU are in the range between 0.09 μmol/l and 0.25 μmol/l and are therefore 4 to 25 times higher than the influent concentrations which are between 0.01 μmol/l and 0.05 μmol/l (Fig. 4 and Fig. S10). Further measurements after single treatment steps in plant W2 clearly showed that GU was formed in the activated sludge process. GU is proposed to be formed quantitatively from biodegradation of MF (Trautwein and Kümmerer, 2011). Our results show that only 25% on a molar basis of degraded MF could be found as GU which confirms the findings that GU was formed in the range between 17% and 95% of removed MF in Greek WWTPs (Kosma et al., 2015). Reasons for that could be other biotic or abiotic removal processes of MF like biodegradation pathways which form other TPs (see electrochemical TPs), adsorption to activated sludge, or complex formation with heavy metals (Donia and Awad, 1995). Another possibility would be further biodegradation of GU under conditions of activated sludge treatment, even if in manometric respiratory tests GU was not further degraded (Trautwein and Kümmerer, 2011).

The results for GU concentrations in WWTP W1 show a different picture. We observed on 3 days during a week in July (19, 21 and 22) much higher GU concentrations in the influent (between 1.55 μmol/l and 20.6 μmol/l) compared to the effluent of W1 (between 0.25 and 7.94 μmol/l) (Fig. S9). The same trend was observed on 3 out of 7 days for sampling week in April (Fig. 4B, Fig. S8). In general the influents of both sampling weeks of W1 (Fig. 4) were characterized by about 90% higher GU than MF concentrations. This observation was independent of the volume of daily treated waste water, since the molar loads (mol/day) showed a similar picture (Table S4). This is a rather unexpected result which has not been reported yet in the literature. Obviously, GU has been

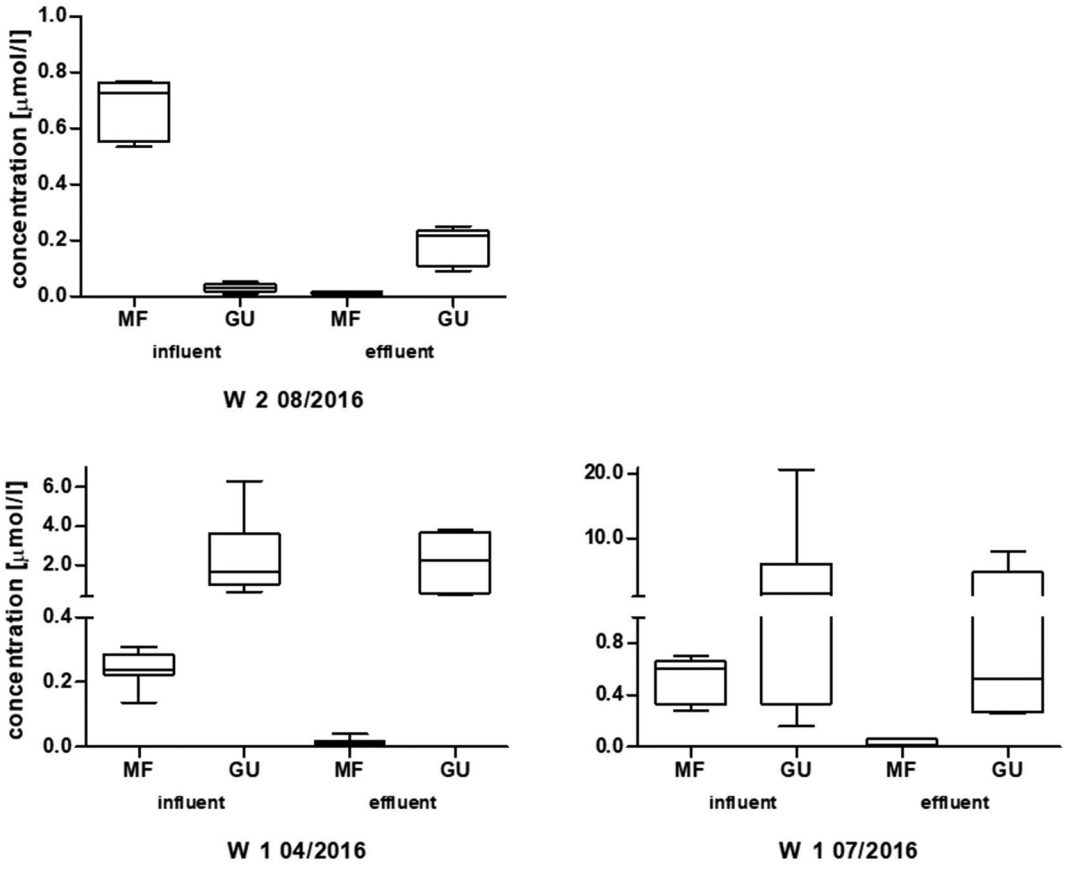

Fig. 3. Box-and-whisker plots for MF and GU concentrations (µmol/l) in influent and effluent samples of two WWTPs (W1, W2) from sampling campaigns in April, July and August. Median concentrations are given for 24-hour composite samples taken on 7 consecutive days.

already formed in parts of the sewer system, which has a total length of 400 km and hydraulic retention times of the sewage water between 10 h and 39 h. Such high GU concentrations formed from MF have been never detected in WWT processes. Therefore we speculate that there are some additional biguanide precursors of GU, for example from disinfection chemicals. In Germany, 3.7 million liter disinfectant were applied in the year 2015 (MTD-Verlag, 2016), with biguanides as an important compound class. Despite further GU formation from degraded MF in WWT of W1, effluent concentrations of GU are reduced in comparison to influent concentrations, which means a further GU removal in W1.

3.5. Occurrence of other TPs in wastewater treatment

In samples from WWTPs the following oxidation products of MF have been detected for the first time: 2,4-DAT (TP 112), MBG (TP 116) and 2,4-AMT (TP 126a). In wastewater treatment (WWT) MBG (TP 116) showed no significant formation or removal over one week in

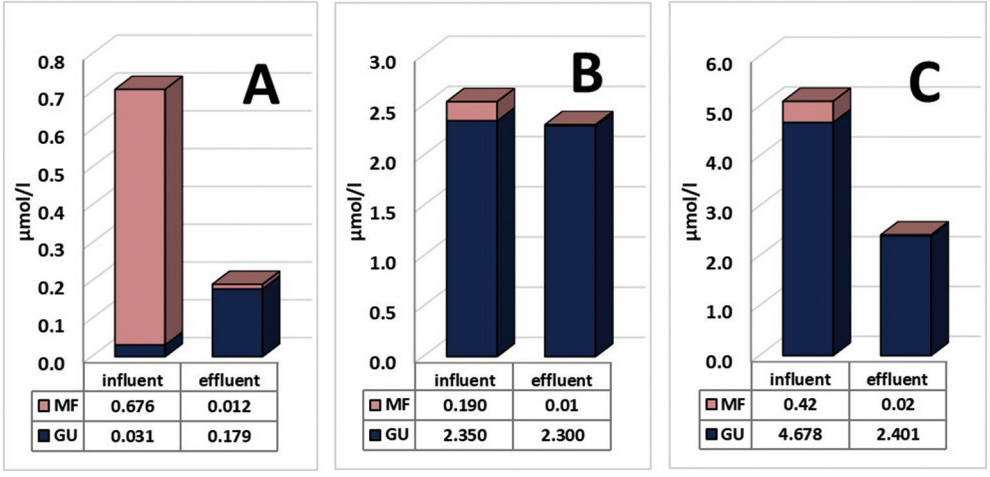

Fig. 4. Average MF and GU concentrations (µmol/l) in influent and effluent of 24-hour composite samples taken on 7 consecutive days from W2 in August (A) and W1 in April (B) and July (C) 2016.

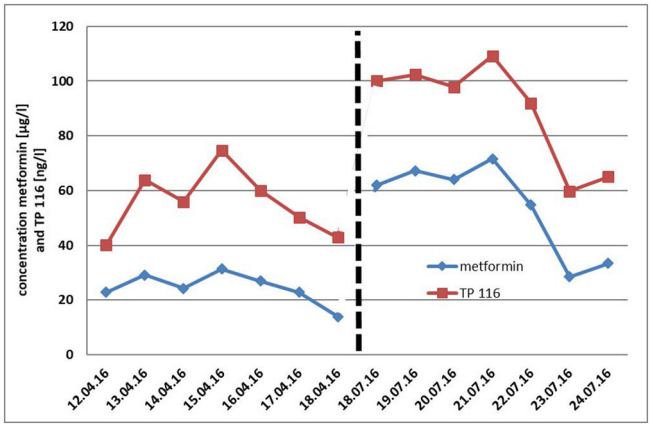

Fig. 5. Concentration trends of MBG (TP 116) and metformin (MF) in W1 for a week in April (left) and in August (right).

April and July in W1 (Fig. 6). The concentrations of MBG range from 35 to 122 ng/l. In fact, MBG is directly correlated to MF concentrations in the influents of W1 and typically occurs at 0.05% of MF (Fig. 5). This indicates MBG as a direct product of MF degradation. In our lab experiments MBG was formed by hydrolysis of MF in the range of 0.01% to 0.03% of MF depending on pH and reaction time. At pH 8 of the wastewater very small amounts of MBG are expected to occur due to hydrolysis. This makes it reasonable to assume that the hydrolysis is more efficient under the prevailing conditions in wastewater or that abiotic and biotic processes finally lead to the MBG formation in the influent of W1.

The effluents of W1 (July) and W2 (August) compared to the influents indicate the removal of MBG during WWT (Fig. S11). Since MBG is derived from MF only by the loss of a methyl group it can be considered as an intermediate of MF degradation to GU. However due to the dynamics of MBG in the WWT processes, no simple production and removal relation is apparent.

The two further TPs 2,4-DAT (TP 112) and 2,4-AMT (TP 126a) showed similar increasing response trends from influents to effluents for plant W1 which means that 2,4-DAT and 2,4-AMT are formed in WWT (Fig. 6). However, in W2 the influent concentrations of 2,4-AMT vary over a wide range during August, so that the 2,4-AMT formation is only observed on 3 days out of 7 (Fig. S11). Since no standards are available for both TPs, only relative intensities for 2,4-DAT and 2,4-AMT can be reported so far. 4,2,1-AIMT (TP 126b) could not be detected in any of the samples.

The average effluent concentration of 2,4-DAT (TP 112) was for all samples higher than the influent concentration (Fig. 6), for W1 it was 2.2 times and for W2 2.7 times higher (Fig. S11). Therefore, it is likely, that 2,4-DAT is formed during the waste water treatment processes. Although 2,4-DAT is a secondary TP, neither the possible precursors 2,4-AMT (TP 126a) nor MBG (TP 116) showed a good correlation with 2,4-DAT. Interestingly, 2,4-DAT in effluents showed a good correlation with MF influent on a weekly basis.

3.6. Occurrence of metformin and the TPs GU, MBG and 2,4-DAT in surface and drinking water

Grab samples were collected from three different tributaries of the river Neckar. MF could be detected in river 1 and 2 at lower concentrations in upstream samples (89 ng/l and 67 ng/l) compared to downstream samples of WWTPs W3 and W4 (234 ng/l and 103 ng/l) (Table 4). A further increase of MF concentration was observed 15 km downstream of W3 (from 234 ng/l to 470 ng/l) which can be interpreted as input from further sources like untreated wastewater from storm-water overflow or sewer leakages from urban areas. This is consistent with the occurrence of MF in upstream samples of W3

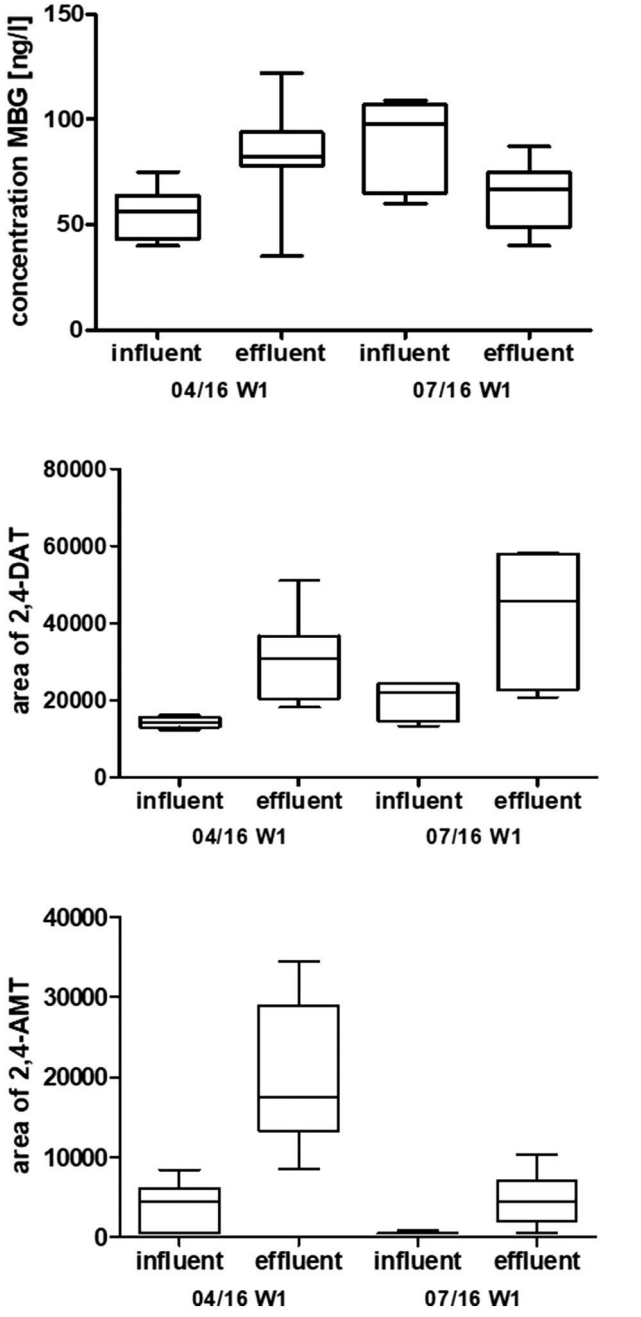

Fig. 6. Box-and-whisker plots for MBG (TP 116), 2,4-DAT (TP 112) and 2,4-AMT (TP 126a) in WWTP W1. Median concentrations are given for seven 24-hour composite samples taken on seven consecutive days.

and W4, because the river shouldn't receive any input from WWTP effluents. The GU concentrations were in both upstream samples (A and D) below the detection limit of 10 ng/l. The occurrence of MF in absence

Table 4
Concentrations of metformin and its TPs guanyl urea (GU) and methylbiguanide (MBG) in surface and drinking water.

	MF [ng/l]	GU [ng/l]	MBG [ngl/l]
A River 1, upstream of W3	89	<LOQ	<LOQ
B River 1 at 0.1 km downstream of W3	234	4502	29
C River 1 at 15 km downstream of W3	470	3723	31
D River 2, upstream of W4	67	<LOQ	<LOQ
E River 2, downstream of W4	103	4402	11
F River 3	<LOQ	<LOQ	<LOQ
Drinking water	34	<LOQ	<LOQ

of GU supports the assumption of an untreated wastewater input in upstream samples (Scheurer et al., 2012). Relatively high GU concentrations of 4500 ng/l and 4400 ng/l were detected downstream of W3 and W4 which reveals its input via treated wastewater. The GU concentration 15 km downstream of W3 was decreased only slightly to 83%. The TPs MBG and 2,4-DAT were detected only in downstream samples of W3 and W4 which reveals their input from WWTPs. MBG concentrations were with 29 ng/l and 11 ng/l in the range of 10% of the corresponding MF concentrations and were not further decreased 15 km downstream of W3. The 2,4-DAT response was in all three downstream samples in the same range, which is about 40% of the response found in WWTP effluents. 2,4-AMT and 4,2,1-AIMT could not be detected in any of the samples.

River 3 was used to show the natural background. The catchment of river 3 is in a forest of a natural reserve and doesn't receive any wastewater. Consequently, neither MF nor any TPs have been observed. In drinking water which is produced from a large surface water resource (Lake Constance), a low background concentration of 34 ng/l of metformin has been observed and confirms the findings of other authors (Trautwein et al., 2014).

4. Conclusions

In this study, we investigated the occurrence and fate of metformin (MF) and its transformation products (TPS) in wastewater and surface water. From the results obtained the following conclusions can be drawn:

- Electrochemistry with a boron doped diamond electrode is useful to generate transformation products (TPs) of metformin for identification by LC-QTOF-MS. 2,4-Diamino-1,3,5-triazine (2,4-DAT), methylbiguanide (MBG), 2-amino-4-methylamino-1,3,5-triazine (2,4-AMT) and 4-amino-2-imino-1-methyl-1,2-dihydro-1,3,5-triazine (4,2,1-AIMT) could be identified.
- Guanyl urea could not be generated electrochemically.
- In WWTP samples, 2,4-AMT and 2,4-DAT showed an increasing trend from influents to effluents, which implies their formation during WWT. MBG is also formed by hydrolysis from MF and didn't show this trend.
- MBG and 2,4-DAT were also detected in surface water which was impacted by wastewater.
- TPs other than GU played a minor role in wastewater and surface water samples, but should be considered if other treatment techniques are applied in water treatment.
- GU showed unexpected high concentrations in some WWTP influents which were 40 times higher than those of MF. This could be due to high input of MF or other compounds which are characterized by a biguanide moiety (e.g. disinfectants).

Further research should focus on sources and fate of high GU levels in WWTP influents. Batch experiments with sludge from different WWTP for testing biodegradation of GU should be included. Furthermore, biodegradation and photolysis experiments under controlled conditions should be performed considering all 5 TPs. This is also important if other water treatment techniques are applied.

Acknowledgements

This research was performed within the framework of the project “Effect Network in Water Research” funded by the Ministry of Science, Research and Arts (grant number 33-5733-25-11t32/2) of the Land of Baden-Württemberg, Germany.

Appendix A. Supplementary data

Supplementary data to this article can be found online at https://doi.org/10.1016/j.scitotenv.2018.02.105.

References

Alfaro, Marco Antonio Quiroz, Ferro, Sergio, Martínez-Huitle, Carlos Alberto, Vong, Yunny Meas, 2006. Boron doped diamond electrode for the wastewater treatment. J. Braz. Chem. Soc. 17 (2), 227–236.
Blair, B.D., Crago, J.P., Hedman, C.J., Klaper, R.D., 2013. Pharmaceuticals and personal care products found in the Great Lakes above concentrations of environmental concern. Chemosphere 93 (9), 2116–2123.
Briones, R.M., Sarmah, A.K., Padhye, L.P., 2016. A global perspective on the use, occurrence, fate and effects of anti-diabetic drug metformin in natural and engineered ecosystems. Environ. Pollut. 219, 1007–1020.
Collin, F., Khoury, H., Bonnefont-Rousselot, D., Therond, P., Legrand, A., Jore, D., Gardes-Albert, M., 2004. Liquid chromatographic/electrospray ionization mass spectrometric identification of the oxidation end-products of metformin in aqueous solutions. J. Mass Spectrom. 39 (8), 890–902.
Comninellis, C., Chen, G., 2010. Electrochemistry for the Environment. Springer, New York.
Daughton, C.G., Kümmerer, K., 2004. Pharmaceuticals in the environment. Spring 463–495.
Donia, A.M., Awad, M.K., 1995. Thermal stabilities, electronic properties and structures of metformin-metal complexes. J. Therm. Anal. 44 (6), 1493–1498.
Evans, J.M., Donnelly, L.A., Emslie-Smith, A.M., Alessi, D.R., Morris, A.D., 2005. Metformin and reduced risk of cancer in diabetic patients. BMJ 330 (7503), 1304–1305.
Fent, K., Weston, A.A., Caminada, D., 2006. Ecotoxicology of human pharmaceuticals. Aquat. Toxicol. 76 (2), 122–159.
Ghoshdastidar, A.J., Fox, S., Tong, A.Z., 2015. The presence of the top prescribed pharmaceuticals in treated sewage effluents and receiving waters in Southwest Nova Scotia, Canada. Environ. Sci. Pollut. Res. Int. 22 (1), 689–700.
Gul, T., Bischoff, R., Permentier, H.P., 2015. Electrosynthesis methods and approaches for the preparative production of metabolites from parent drugs. Trends Anal. Chem. 70, 58–66.
Hernández, F., Ibáñez, M., Pozo, Ó.J., Sancho, J.V., 2008. Investigating the presence of pesticide transformation products in water by using liquid chromatography-mass spectrometry with different mass analyzers. J. Mass Spectrom. 43 (2), 173–184.
Huschek, G., Hansen, P.D., Maurer, H.H., Krengel, D., Kayser, A., 2004. Environmental risk assessment of medicinal products for human use according to European Commission recommendations. Environ. Toxicol. 19 (3), 226–240.
IDF, 2015. In: Federation, I.D. (Ed.), Diabetes Atlas, Seventh Edition.
Johansson, T., Weidolf, L., Jurva, U., 2007. Mimicry of phase I drug metabolism – novel methods for metabolite characterization and synthesis. Rapid Commun. Mass Spectrom. 21 (14), 2323–2331.
Jones, O.A.H., Voulvoulis, N., Lester, J.N., 2002. Aquatic environmental assessment of the top 25 English prescription pharmaceuticals. Water Res. 36 (20), 5013–5022.
Klaczkow, G., Anuszewska, E.L., 2010. Determination of impurities in medical products containing metformin hydrochloride. Acta Pol. Pharm. 67 (6), 593–598.
Kolpin, D.W., Furlong, E.T., Meyer, M.T., Thurman, E.M., Zaugg, S.D., Barber, L.B., Buxton, H.T., 2002. Pharmaceuticals, hormones, and other organic wastewater contaminants in U.S. streams, 1999–2000: a national reconnaissance. Environ. Sci. Technol. 36 (6), 1202–1211.
Kosma, C.I., Lambropoulou, D.A., Albanis, T.A., 2015. Comprehensive study of the antidiabetic drug metformin and its transformation product guanylurea in Greek wastewaters. Water Res. 70, 436–448.
Markiewicz, M., Jungnickel, C., Stolte, S., Białk-Bielińska, A., Kumirska, J., Mrozik, W., 2017. Ultimate biodegradability and ecotoxicity of orally administered antidiabetic drugs. J. Hazard. Mater. 333, 154–161.
MTD-Verlag, 2016. IMS-Analyse Desinfektionsmittel-Markt. Retrieved February 6, 2018, from. https://www.mtd.de/welt-der-medizinprodukte/marktzahlen/733-mtd-3-2016-ims-analyse-desinfektionsmittel-markt.
Niemuth, N.J., Jordan, R., Crago, J., Blanksma, C., Johnson, R., Klaper, R.D., 2015. Metformin exposure at environmentally relevant concentrations causes potential endocrine disruption in adult male fish. Environ. Toxicol. Chem. 34 (2), 291–296.
Oosterhuis, M., Sacher, F., ter Laak, T.L., 2013. Prediction of concentration levels of metformin and other high consumption pharmaceuticals in wastewater and regional surface water based on sales data. Sci. Total Environ. 442, 380–388.
Quintao, F.J., Freitas, J.R., de Tatima Machado, C., Aquino, S.F., de Queiroz Silva, S., de Cassia Franco Afonso, R.J., 2016. Characterization of metformin by-products under photolysis, photocatalysis, ozonation and chlorination by high-performance liquid chromatography coupled to high-resolution mass spectrometry. Rapid Commun. Mass Spectrom. 30 (21), 2360–2368.
Raghava Raju, T., Jagan Mohan, T., Bhavani Prasad, S., Suresh Kumar, P., Someswara Rao, N., Mrutyunjaya Rao, I., 2013. Development, validation and resolving mass balance issue by using alternative oxidizing reagents for the determination of metformin hydrochloride impurities in api and pharmaceutical dosage forms. Asian J. Pharm. Clin. Res. 6 (8), 107–115.
Roig, B., 2010. Pharmaceuticals in the Environment- Current Knowledge and Need Assessment to Reduce Presence and Impact. IWA, London.
Ruff, M., Mueller, M.S., Loos, M., Singer, H.P., 2015. Quantitative target and systematic non-target analysis of polar organic micro-pollutants along the river Rhine using high-resolution mass-spectrometry – identification of unknown sources and compounds. Water Res. 87, 145–154.
Salani, B., Del Rio, A., Marini, C., Sambuceti, G., Cordera, R., Maggi, D., 2014. Metformin, cancer and glucose metabolism. Endocr. Relat. Cancer 21 (6), R461–471.
Santos, L.H., Gros, M., Rodriguez-Mozaz, S., Delerue-Matos, C., Pena, A., Barcelo, D., Montenegro, M.C., 2013. Contribution of hospital effluents to the load of pharmaceuticals in urban wastewaters: identification of ecologically relevant pharmaceuticals. Sci. Total Environ. 461-462, 302–316.

Scheurer, M., Sacher, F., Brauch, H.J., 2009. Occurrence of the antidiabetic drug metformin in sewage and surface waters in Germany. J. Environ. Monit. 11 (9), 1608–1613.
Scheurer, M., Michel, A., Brauch, H.-J., Ruck, W., Sacher, F., 2012. Occurrence and fate of the antidiabetic drug metformin and its metabolite guanylurea in the environment and during drinking water treatment. Water Res. 46 (15), 4790–4802.
Sebastine, I.M., Wakeman, R.J., 2003. Consumption and environmental hazards of pharmaceutical substances in the UK. Process. Saf. Environ. Prot. 81 (4), 229–235.
Sinclair, C.J., Boxall, A.B.A., 2003. Assessing the ecotoxicity of pesticide transformation products. Environ. Sci. Technol. 37 (20), 4617–4625.
Trautwein, C., Kümmerer, K., 2011. Incomplete aerobic degradation of the antidiabetic drug metformin and identification of the bacterial dead-end transformation product Guanylurea. Chemosphere 85 (5), 765–773.
Trautwein, C., Berset, J.D., Wolschke, H., Kummerer, K., 2014. Occurrence of the antidiabetic drug Metformin and its ultimate transformation product Guanylurea in several compartments of the aquatic cycle. Environ. Int. 70, 203–212.
Trouillas, P., Marchetti, C., Bonnefont-Rousselot, D., Lazzaroni, R., Jore, D., Gardes-Albert, M., Collin, F., 2013. Mechanism of one-electron oxidation of metformin in aqueous solution. Phys. Chem. Chem. Phys. 15 (24), 9871–9878.

Supplementary Information

Formation and occurrence of transformation products of metformin in wastewater and surface water

Selina Tisler, Christian Zwiener*

*Corresponding author

Hölderlinstraße 12, 72074 Tübingen, Germany

Tel.: 004970712974702, Email: christian.zwiener@uni-tuebingen.de

Table S 1: Operating parameters of the triple quadrupole mass spectrometer (QqQ-MS).

Parameter	**Set point**
Gas temperature	150 °C
Gas flow	16 l/min
Nebulizer	45 psi
Sheath gas heater	400 °C
Sheath gas flow	12 l/min
Capillary voltage	1500 V
Ion funnel high/low pressure RF	90/70 V
Fragmentor voltage	380 V

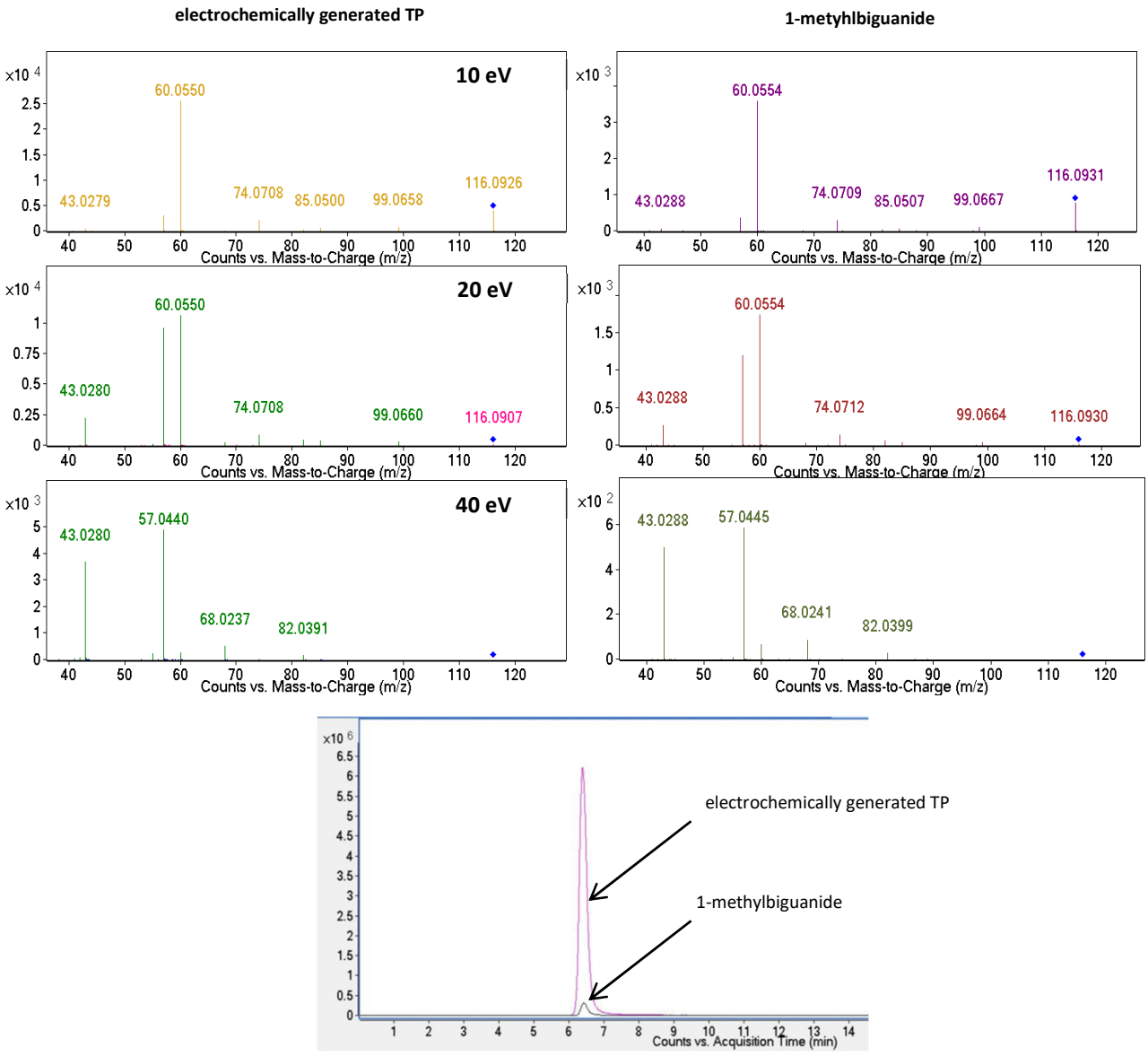

Figure S 1: Fragmentation pattern (@10eV, 20eV and 40eV) and retention time of the electrochemically generated TP 116 in comparison to the standard 1-methylbiguanide (MBG) measured by QTOF-MS.

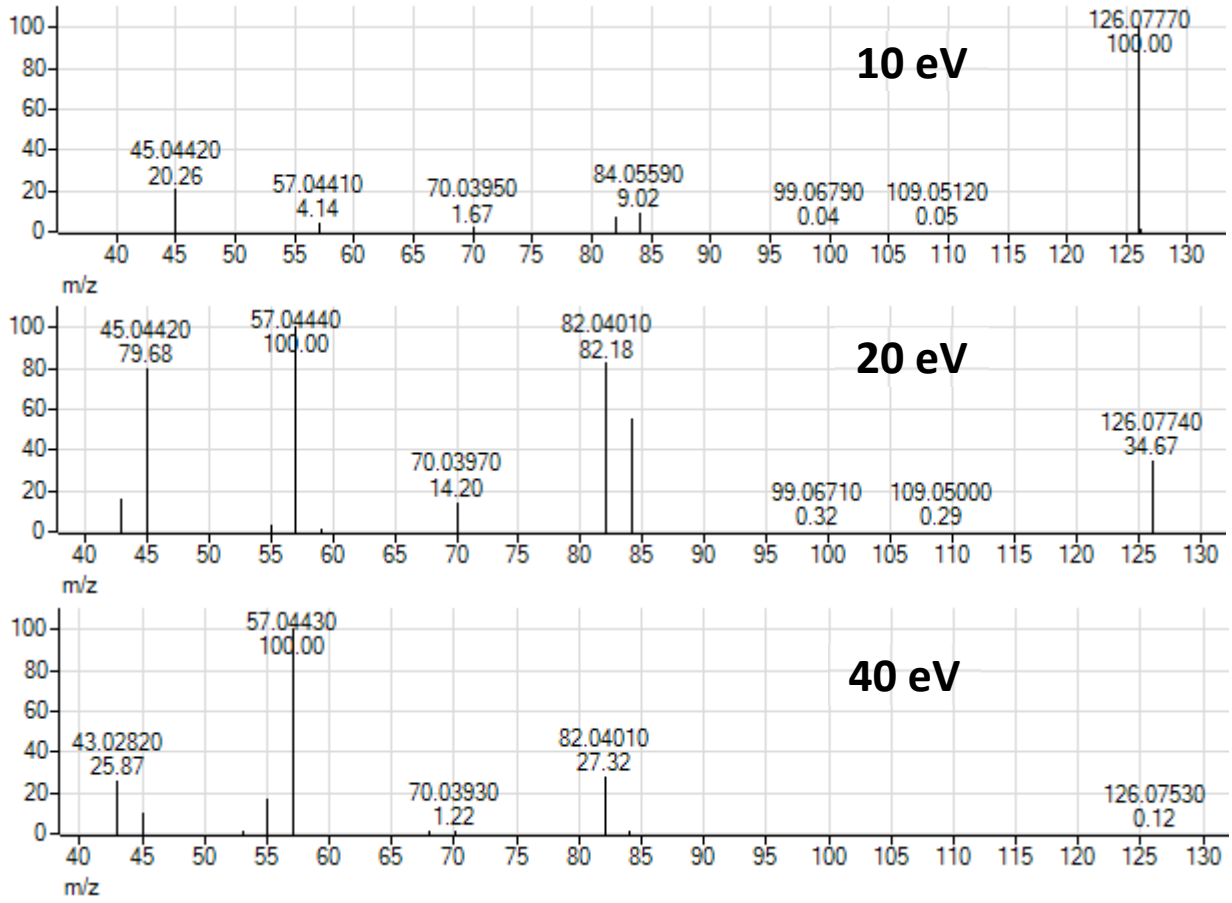

Figure S 2: Fragmentation pattern (@10eV, 20eV and 40eV) of TP 126a measured by QTOF-MS.

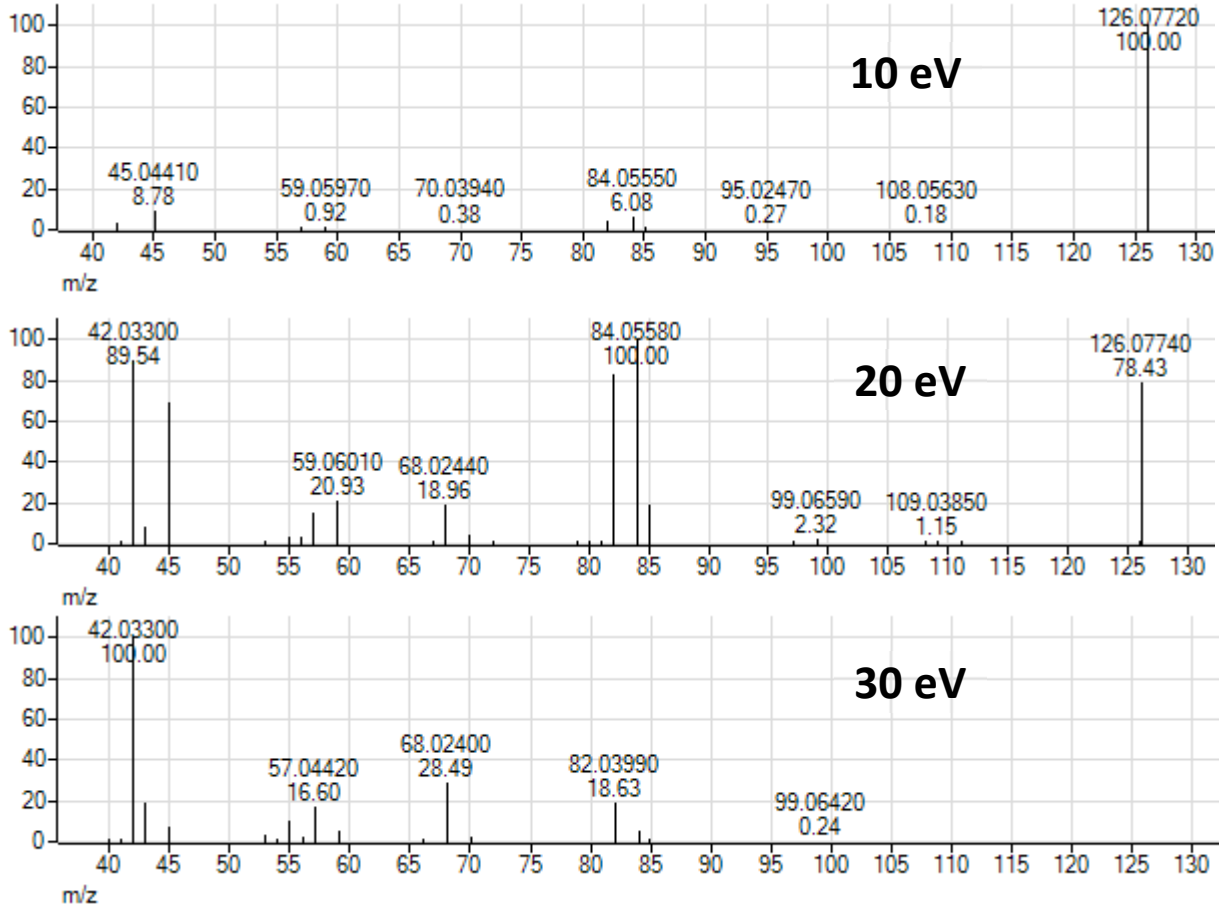

Figure S 3: Fragmentation pattern (@10eV, 20eV and 40eV) of TP 126b measured by QTOF-MS.

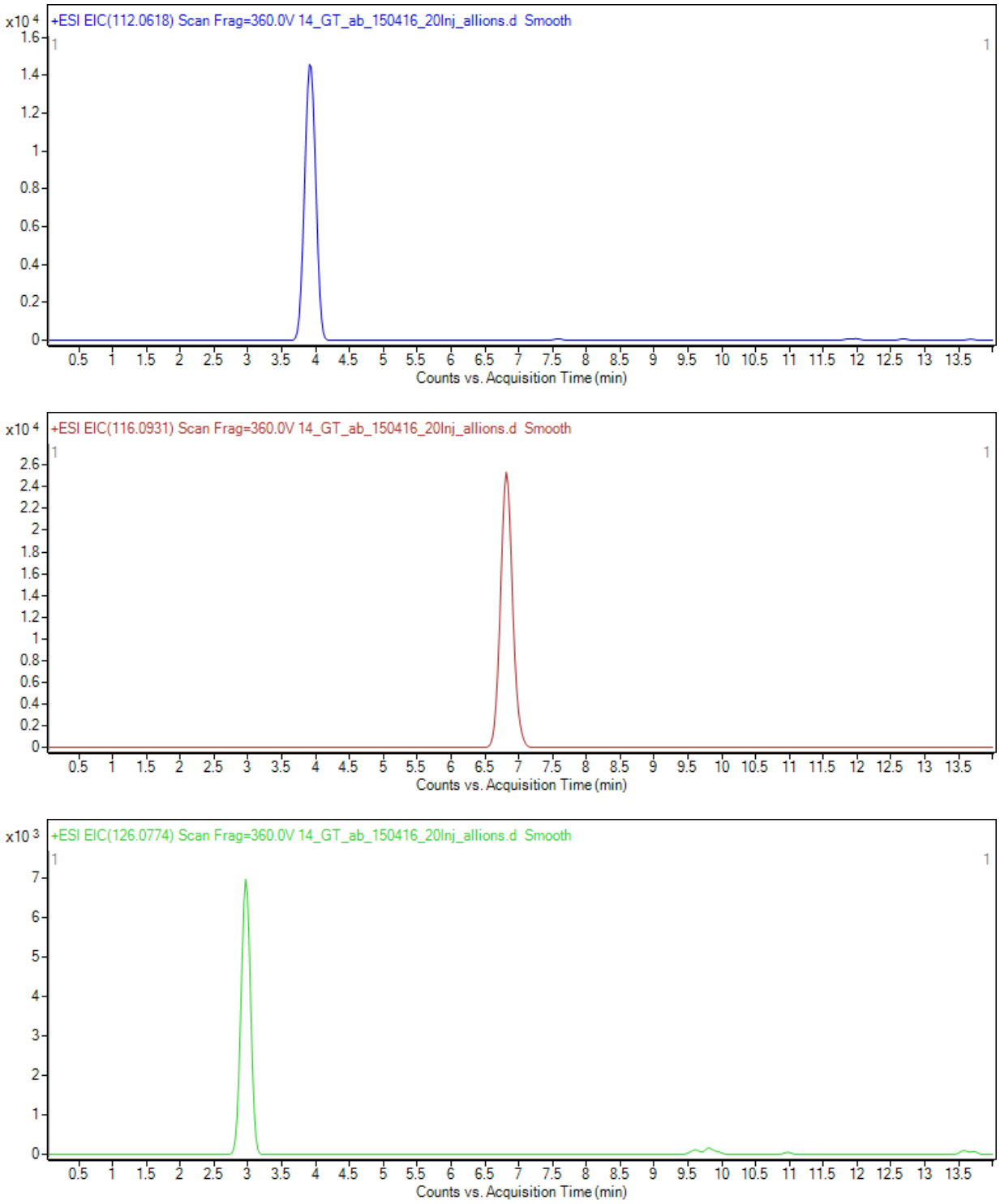

Figure S 4: Extracted ion chromatograms (EIC) of TP 126a, TP 112 and TP 116 in the effluent sample (15.04.2016) of WWTP 1 measured by QTOF-MS.

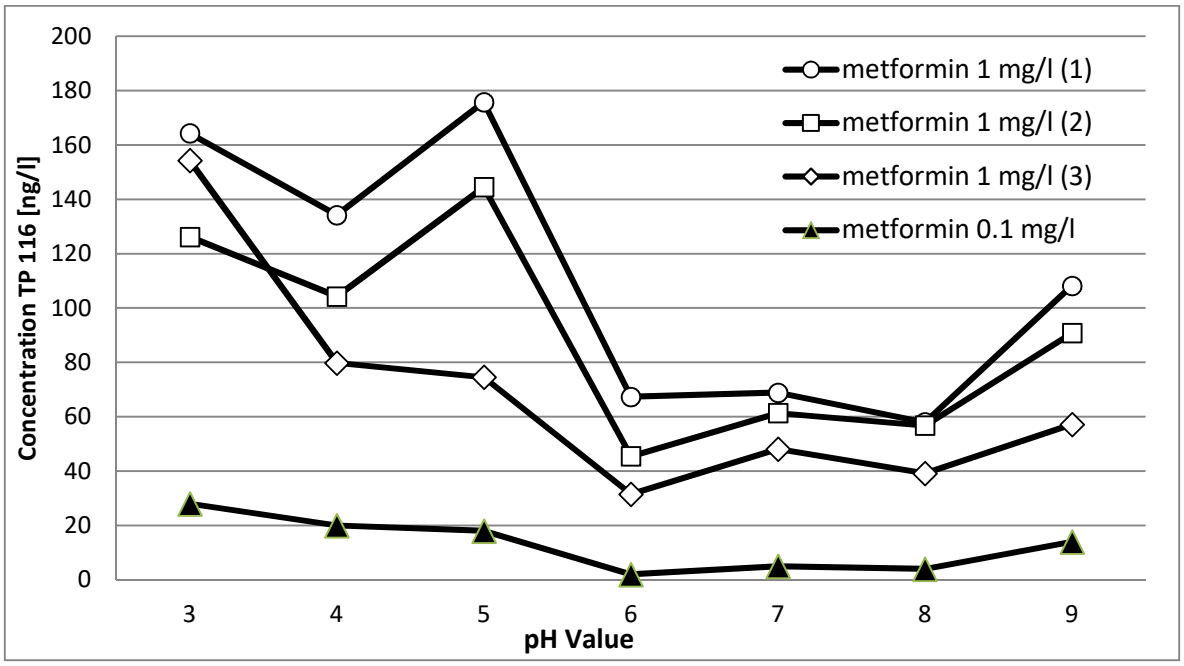

Figure S 5: Concentrations of measured TP 116 in freeze-dried samples spiked with 0.1 and 1 mg/l metformin at different pH values.

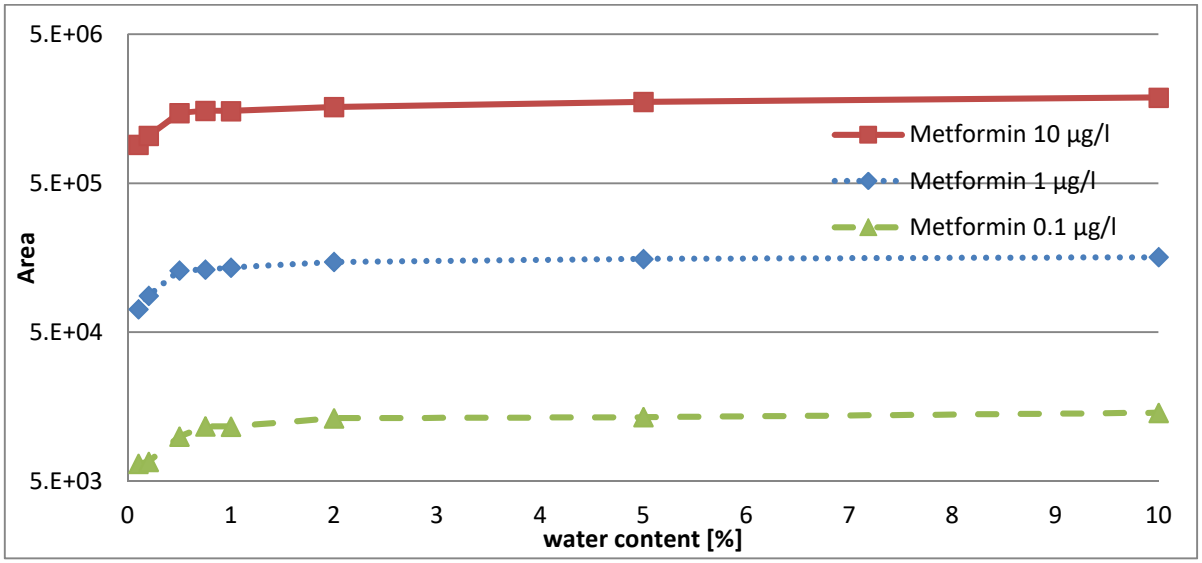

Figure S 6: Effect of water content of samples on the response of metformin 0.1, 1 and 10 µg/l.

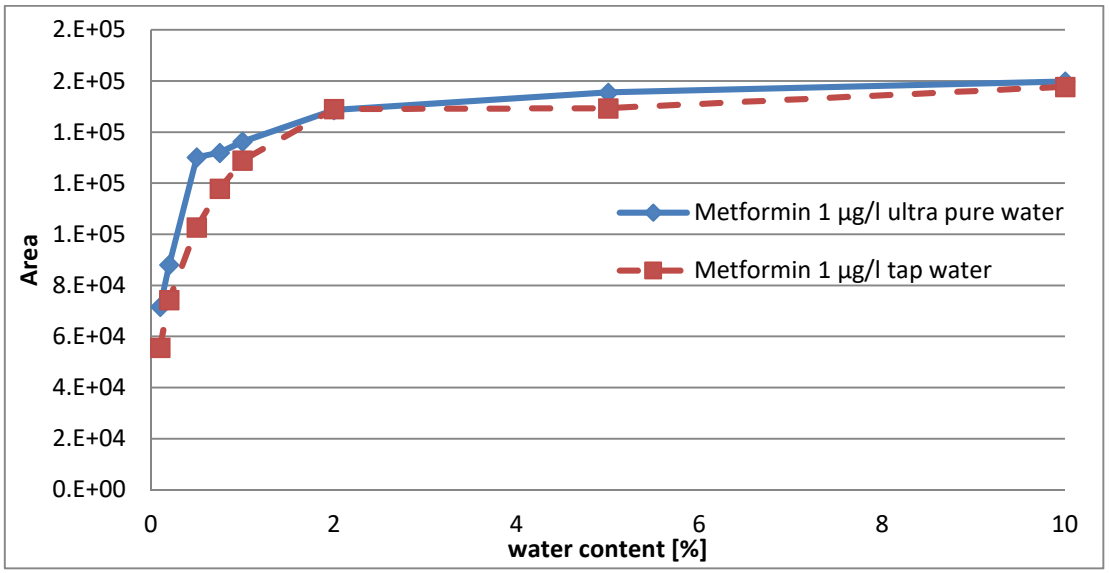

Figure S 7: Effect of water content of samples on the response of metformin at 1 µg/l in ultra-pure water and tap water.

Table S 2: Intraday variations (RSD_r) and interday variations (RSD_R) of metformin and guanyl urea measured by QqQ-MS and of TP 116 measured by QTOF-MS.

	RSD_r [%]	RSD_R [%]
	(n=8)	(MF n=6; GU+TP 116 n=4)
Metformin	0.9	5.5
Guanyl urea	2.1	9.5
Methylbiguanide (TP 116)	1.2	7.0

Table S 3: Rainfall data of Southwest Germany for the 3 sampling weeks

Year 2016	Precipitation [l/(m² d)]
11.04.	0
12.04.	10
13.04.	2
14.04.	0
15.04.	3
16.04.	14
17.04.	6
18.04.	0
17.07.	0
18.07.	0
19.07.	0
20.07.	0
21.07.	9
22.07.	2
23.07.	3
24.07.	1
22.08.	0
23.08.	0
24.08.	0
25.08.	0
26.08.	0
27.08.	3.5
28.08..	0

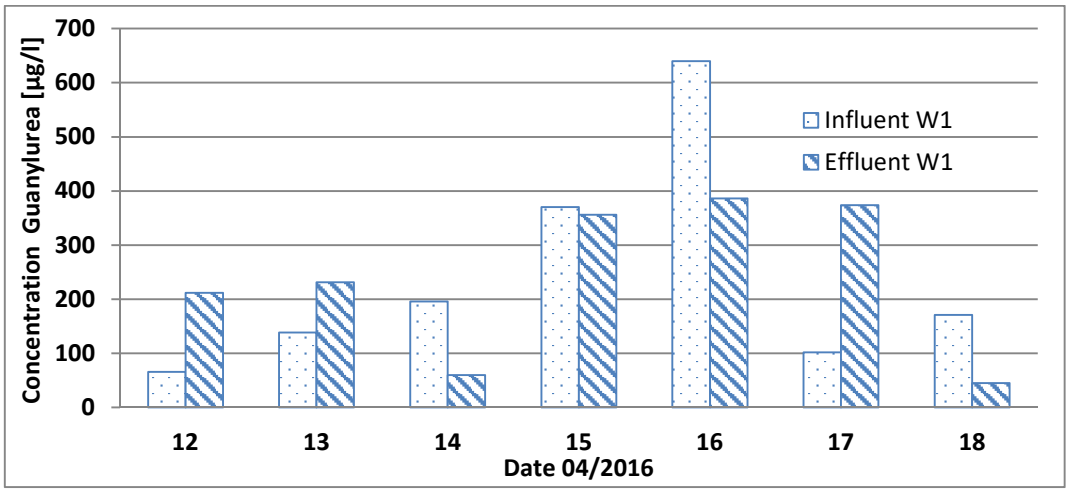

Figure S 8: GU concentrations in 24-h-composite samples of WWTP 1 during a week in April 2016.

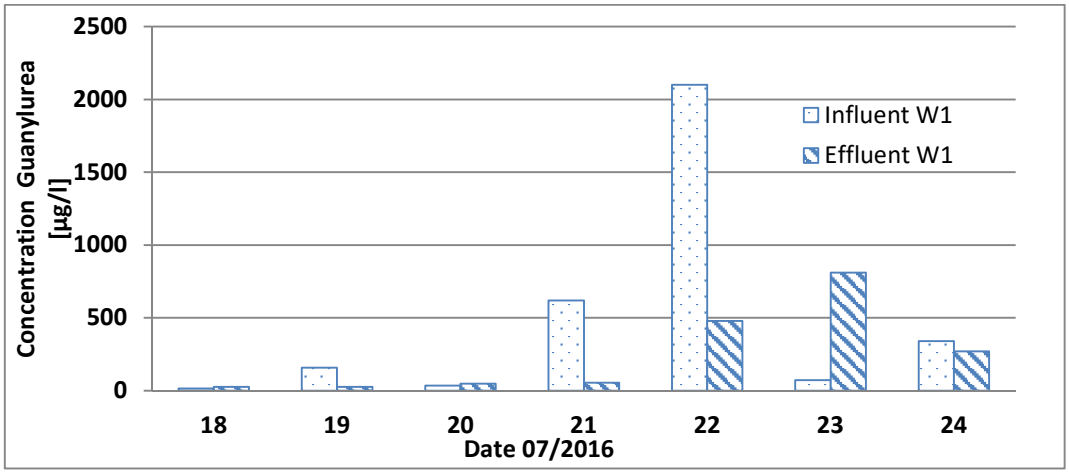

Figure S 9: GU concentrations in 24-h-composite samples of WWTP 1 during a week in July 2016.

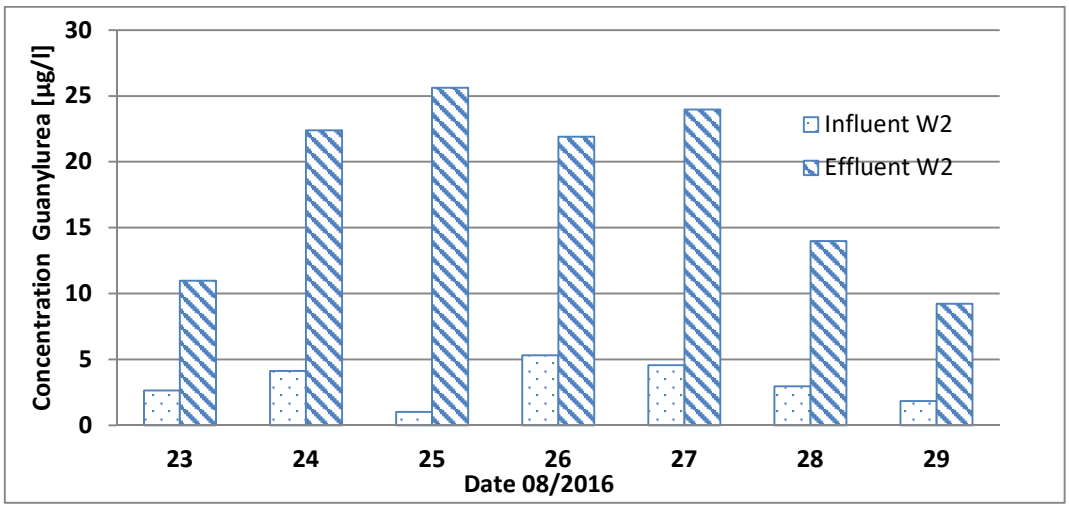

Figure S 10: GU concentrations in 24-h-composite samples of WWTP 2 during a week in August 2016.

Table S 4: Guanyl urea concentrations in influent and effluent and daily wastewater volume of WWTP 2.

	Guanyl urea [µg/l]		Volume [l]
2016	**Influent**	**Effluent**	
12.04.	66	212	5.40E+07
13.04.	138	231	6.30E+07
14.04.	196	60	3.57E+07
15.04.	370	356	4.88E+07
16.04.	640	386	6.95E+07
17.04.	102	374	1.10E+08
18.04.	171	45	8.21E+07
18.07.	16	27	3.35E+07
19.07.	158	26	3.18E+07
20.07.	34	48	3.23E+07
21.07.	620	54	3.45E+07
22.07.	2100	480	4.64E+07
23.07.	72	810	6.52E+07
24.07.	340	270	3.75E+07

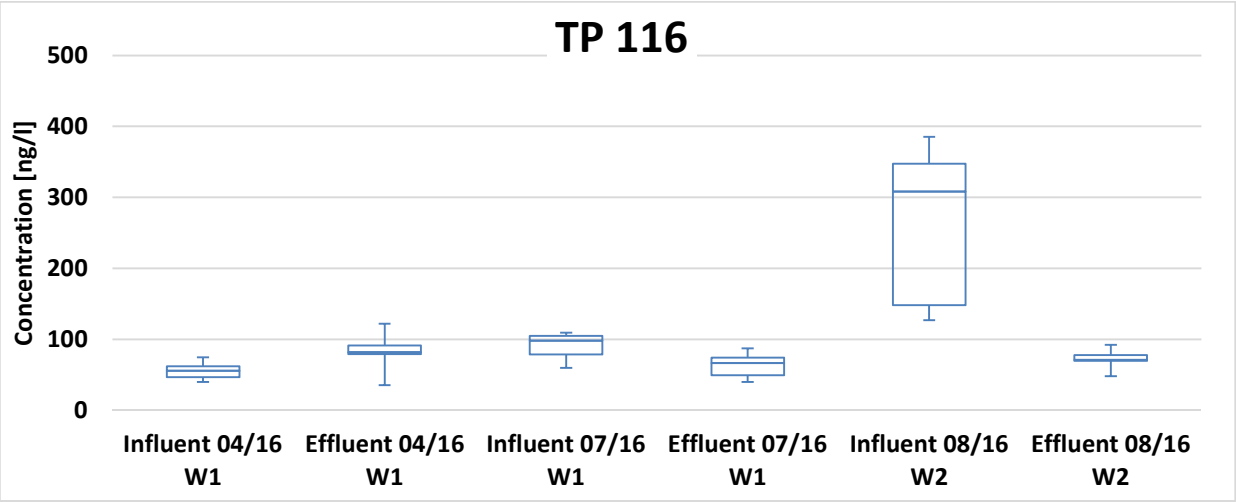

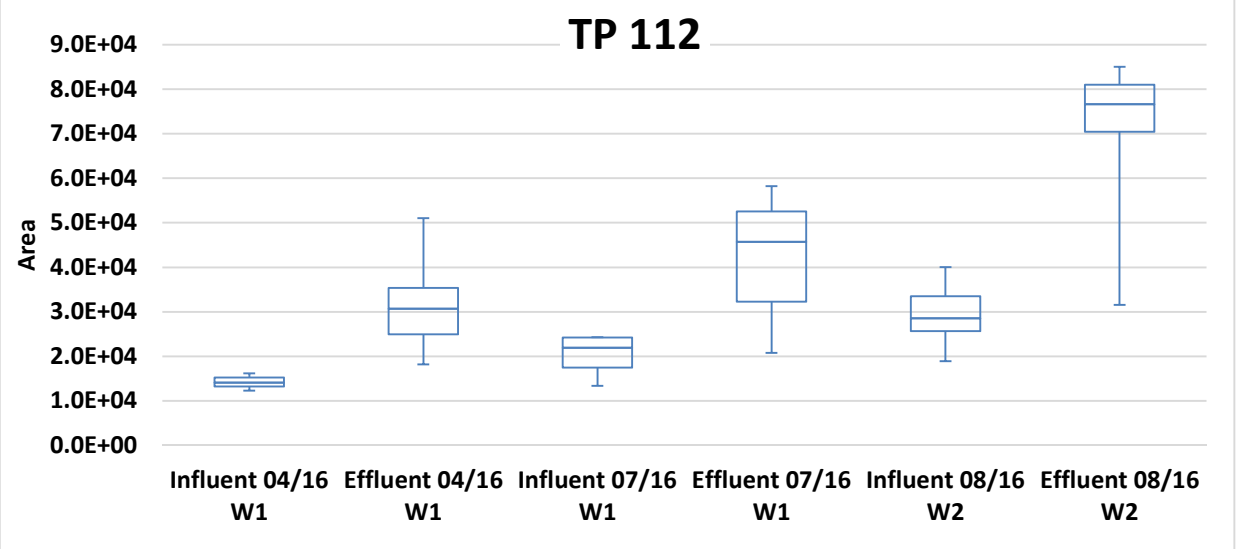

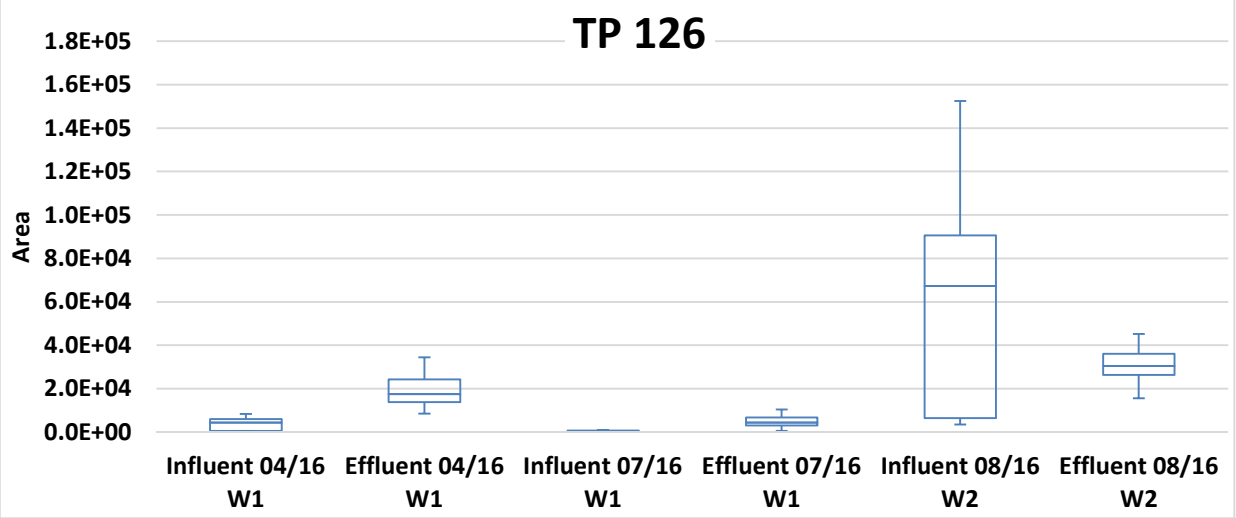

Figure S 11: Concentrations of TP 116 and responses of TP 126 and TP 112 24-h-composite-samples of W1 and W2. The boxes and whiskers represent each the data of7 consecutive days.

Table S 5: Calculated log P values for TP 126a and TP 126b obtained from different algorithms.

Name		SMILE code	Log P			Log D (pH7)
			A	B	C	D
2,4-AMT	TP 126a	CNc1ncnc(N)n1	-0.29	-0.34	-0.23	-0.14
4,2,1-AIMT	TP 126b	C1=NC(=NC(N1C)=N)N	-1.25	-1.79	-0.75	-1.05

A: http://www.molinspiration.com/services/logp.html;

B: http://www.vcclab.org/web/pt/;

C: meteor software;

D: https://disco.chemaxon.com/apps/demos/logd/

PAPER 2

Aerobic and anaerobic formation and biodegradation of guanyl urea and other transformation products of metformin

Selina Tisler, Christian Zwiener

(2019)

Water Research 149, 130-135

DOI: 10.1016/j.watres.2018.11.001

Water Research 149 (2019) 130–135

Contents lists available at ScienceDirect

Water Research

journal homepage: www.elsevier.com/locate/watres

Aerobic and anaerobic formation and biodegradation of guanyl urea and other transformation products of metformin

Selina Tisler, Christian Zwiener*

Hölderlinstraße 12, 72074 Tübingen, Germany

ARTICLE INFO

Article history:
Received 1 August 2018
Received in revised form
25 October 2018
Accepted 1 November 2018
Available online 5 November 2018

Keywords:
Guanyl urea
Waste water treatment
Transformation products
Biodegradation
Antidiabetic
Metformin

ABSTRACT

The aim of the study was to investigate the biodegradability of guanyl urea (GU) and the behavior of other transformation products (TPs) of Metformin (MF). Most biodegradation studies of MF with activated sludge of waste water treatment plants (WWTPs) showed GU as the only bacterial dead-end metabolite without further degradation. In this study, batch experiments with activated sludge revealed biodegradability of GU. GU degradation was much faster under anaerobic than under aerobic conditions. Degradation kinetics for MF was much slower under anaerobic conditions. Adsorptive removal of up to 20% was an additional elimination process of MF and GU. The batch experiments were conducted with sludge of 2 WWTPs, WWTP 1 showed decreasing concentrations of GU from influent to effluent and the other increasing concentrations. This indicates a different adaption of the sludge to GU and may explain the better GU degradation capability of the sludge from WWTP 1. Furthermore, the biodegradation potential of MF was confirmed and in addition, occurrence of the TPs methylbiguanide (MBG), 2-amino-4-methylamino-1,3,5-triazine (2,4-AMT) and the secondary TP 2,4-diamino-1,3,5-triazine (2,4-DAT) was observed in batch experiments with activated sludge of WWTP 1. After fast formation, degradation in turn was slower, especially for 2,4-AMT. In general, TPs played a minor role in MF and GU degradation.

1. Introduction

Pharmaceuticals are designed to be relatively stable and polar compounds. Consequently, they are metabolized incompletely in the human body and are excreted as original substance or modified metabolite into the sewage system. Certain compounds are not quantitatively removed and enter in the surface waters, including human metabolites and transformation products (TPs) generated in WWTP. Metformin (MF) a drug against type 2 diabetes, is a principal representative for these substances, a so-called micro pollutant. MF is one of the most prescribed pharmaceuticals worldwide (Ghoshdastidar et al., 2015; Huschek et al., 2004; Jones et al., 2002) with a well-known bacterial transformation product guanyl urea (GU).

Due to this fact, MF concentrations in waste water are very high in comparison to other pharmaceuticals. Different studies for Germany and the Netherlands showed an average influent WWTP concentration of 61 μg/l for 10 different WWTPs (Tisler and Zwiener, 2018; Oosterhuis et al., 2013; Scheurer et al., 2012). High removal efficiency of MF (95%) leads to effluent concentrations lower than 2 μg/l. Nevertheless MF is also one of the most deposited pharmaceuticals into the aquatic environment (Oosterhuis et al., 2013), and ubiquitously detected in surface waters. Bradley et al., (2016) detected MF in 89% of 59 investigated shallow streams in the US. No pharmaceutical was more prevalent. In Germany the concentrations in surface waters ranged from low ng/l up to 5 μg/l (Scheurer et al., 2012; Trautwein and Kümmerer, 2011; Tisler and Zwiener, 2018). The well-known TP GU is even more prevalent, with concentrations up to 28 μg/l (Scheurer et al., 2012) in waste water-affected rivers. Trautwein and Kümmerer (2011) showed that the formation of GU is directly correlated with the removal of MF in the biological treatment processes. Furthermore, GU is called a bacterial dead-end TP without further degradation. As a result, GU increased from low μg/l concentrations in influents to 99 μg/l in effluents (Scheurer et al., 2012). On the contrary some studies showed no direct correlation between MF and GU, where molar GU concentrations in effluents were significantly lower than MF concentrations in influents (Kosma et al., 2015). Even more remarkable was the degradation of GU in a WWTP of Germany, where the

* Corresponding author. Hölderlinstraße 12, 72074 Tübingen, Germany.
E-mail address: christian.zwiener@uni-tuebingen.de (C. Zwiener).

https://doi.org/10.1016/j.watres.2018.11.001
0043-1354/

average influent concentrations (477 μg/l) were higher than the effluents (244 μg/l) for an entire sampling week, while MF degradation was efficient (97%) (Tisler and Zwiener, 2018). It seems that in- and output of GU is strongly dependent on the characteristics and operating parameters of the WWTP. From that two questions arise: 1) Is GU really a bacterial end product without further transformation? 2) Are there any other TPs which are formed during the WWT processes? Therefore, it is important to investigate aerobic and anaerobic biodegradation processes for GU formation and further removal and to identify possible TPs formed during MF degradation. For example a temporary deficit in the mass balance of MF and GU could be observed in a biodegradation experiment between days 4 and 15 (Markiewicz et al., 2017). This may be explained by the formation and subsequent degradation of intermediates. The occurrence of other TPs of MF is a further indication. For example, 3 further TPs of MF (2,4-diamino-1,3,5-triazine, 2,4-DAT; 2-amino-4-methylamino-1,3,5-triazine, 2,4-AMT; methylbiguanide, MGB) have been detected in waste water and surface water (Tisler and Zwiener, 2018). The aim of this study is therefore to answer the two questions on GU biodegradation and the occurrence of further TPs during metformin degradation.

2. Materials and methods

2.1. Chemicals

Optima LC-MS grade acetonitrile (AcN), formic acid (FA), ammonium formate (NH_4F) and water were purchased from Fisher Chemical. The standards metformin hydrochloride (>98%), guanyl urea sulfate (>98%), melamine (>98%) were purchased from TCI, 1-methylbiguanide hydrochloride from LGC standards and metformin d6 from Toronto Research Chemicals. Sodium azide for the experiments was purchased from *Merckmillipore*. Individual stock solutions with a concentration of 1 g/l were prepared in water. All working solutions of the standards for direct injection were prepared in AcN and tap or ultrapure water (10:1). Working solution containing 10 μg/l of metformin-D6 was prepared in ultrapure water. Stock and working solutions were stored in the freezer at −20 °C, except of the aqueous metformin-d6 solution which was stored in the refrigerator (4 °C).

2.2. Water sample collection and preparation

24-h composite samples of wastewater influents (after technical treatment step) and effluents were obtained by flow rate-proportional sampling from waste water treatment plant 1 (W1) (100.000 population equivalent plus hospitals) in April and July 2016. In June 2018, time-proportional samples were obtained from W2 (80.000 population equivalent). Both plants are located in Southwest Germany and run nitrification and upstream denitrification processes without further advanced treatment steps. The composite samples were taken from 7 consecutive days from W1 and W2. The samples were immediately cooled, filtered and stored at 4 °C. All samples were filtered with syringe filters with regenerated cellulose (Captiva, pore size: 0.2 μm, Agilent Technologies, Germany). Subsequently the samples were diluted with the factor 10 and 100 in ACN vials and 100 μl of an internal stock solution of MF-D6 (10 μg/l) was added.

2.3. Biodegradation studies

The biodegradation studies were performed in bottles in the dark at room temperature (22 °C). The experiments were conducted with activated sludge of nitrification basins. The sludge was obtained from the two waste water treatment plants (WWTPs) which were also screened for MF and its TPs in influent and effluent water. For the aerobic biodegradation experiment with inoculum of W1, 90 ml tap water with 10 ml activated sludge were filled in 250 ml glass bottles. The supernatant of 150 ml air volume and every day mixing with air supply guaranteed the sufficient oxygen supply. The experiment is described with MF_GU_aer_1a in Table 1. Experiment MF_GU_aer_1b was the same set up with higher spiked MF and GU concentration, conducted two years before. For the anaerobic degradation experiment the bottles were filled with 250 ml pure activated sludge without a supernatant of air volume, to guarantee anoxic conditions. 6 mg/l MF and 8 mg/l GU were spiked into the bottles of the experiments MF_anaer_1 and GU_anaer_1, respectively. For sampling, the bottles were opened and closed immediately after sampling. The dry weight of the aerobic bottle test was 3 g/l and of the anaerobic bottle test was 30 g/l. Similar experiments were conducted with inoculum of W2. For experiment MF_aer_2 and MF_f_anaer_2, 120 ml tap water and 40 ml activated sludge were filled in 250 ml glass bottles. The only difference between the two experiments was, that MF_aer_2 was mixed uncovered every day to guarantee oxygen supply. An overview of all experiments is illustrated in Table 1. Every experiment consists of two parallel test bottles and one sterile control. A bottle poisoned with 3 g/l sodium azide was used as sterile control. MF and GU concentrations were between 5 and 40 mg/l, spiked from an aqueous standard solution. For controlling the experiment conditions, O_2-concentration, pH-value and nitrate values were monitored. Samples were measured with a dilution factor of 100. Oxygen concentration was measured with *WTW* Oxi 330 electrode and pH value with *Mettler Toledo* InLab Pro-ISM electrode. Nitrate concentrations were estimated semiquantitative with NO_3^-*M-quant*^{TM} test stripes 10–500 mg/l from *Merck*.

2.4. Instrumental analysis

Target screening was performed by LC-MS using a 1290 Infinity HPLC system (Agilent Technologies, Germany) with a triple quadrupole mass spectrometer (QqQ-MS). A Phenomenex LUNA 3 u HILIC 200 A column (100 × 3 mm; 5 μm particle size) at a flow rate of 0.45 ml/min was used for separation. Eluent A was an aqueous buffer with 15 mM NH_4F and 0.1% FA; eluent B was AcN with 0.1% FA. Gradient elution was used: 0–4 min 95% B, decrease to 50% B within 4 min, held for 6 min at 50% B. After switching back to the starting conditions, post time was 8 min.

The Injection volume of samples was 10 μl for standards and waste water samples. 1 μl was injected of 100 time diluted samples from biodegradation experiment. All samples were analyzed with the same external calibration, which was performed between 10 ng/l and 10 μg/l with deuterated MF (D6) as internal standard. Quantification was achieved after LC separation with a 6490 triple quadrupole mass spectrometer (Agilent Technologies, Germany) using the positive ionization mode. The ESI source with the Agilent Jet Stream technology was operated under conditions given in Table S 2. The data recorded were processed with the software Mass Hunter. For quantification and confirmation two MRM transitions were monitored for each analyte in the dynamic MRM mode. Additional information regarding the analysis are given in Table S 3, S 4 and S 5. In addition to MF and its TPs (Tisler and Zwiener, 2018), melamine (MAM) was measured for quantitative estimation of TPs without available analytical standards (Fig. 1). Due to comparison of the response of MAM to the TPs with a similar structure, an assumption of the concentration of 2,4-diamino-1,3,5-triazine (2,4-DAT), 2-amino-4-methylamino-1,3,5-triazine (2,4-AMT), 4-amino-2-imino-1-methyl-1,2-dihydro-1,3,5-triazine (4,2,1-AIMT) was performed.

LC-QTOF-MS measurements were used for screening of

Table 1
Overview of the conducted experiments with the spiked MF and GU concentrations, dry weight of the experiment solution and O_2-concentration during the entire experiment. Every experiment consists of two parallel test bottles and one sterile control.

Experiment	Spike level (mg/L)		Dry weight [g/l] and % (v/v) sludge/liquid	O_2-concentration [mg/l]	WWTP
	MF	GU			
MF_GU_aer_1a	5	13	3 g/l (10%)	4.4 and 7.7	W1 2018
MF_GU_aer_1b	40	40	3 g/l (10%)	5.0 and 6.8	W1 2016
MF_anaer_1	6		30 g/l (100%)	≥0.5	W1 2018
GU_anaer_1		8	30 g/l (10%)	≥0.5	W1 2018
MF_aer_2	9		8 g/l (25%)	2.2 and 4.7	W2 2018
MF_f_anaer_2	9		8 g/l (25%)	0.3 and 3.2	W2 2018

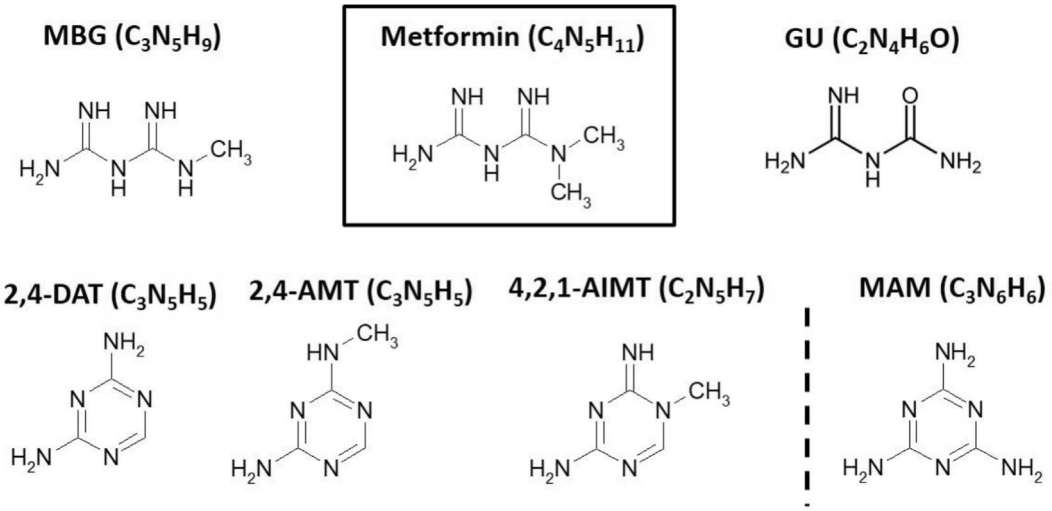

Fig. 1. Chemical structures and formula of metformin (MF) and the analyzed TPs guanyl urea (GU), methylbiguanide (MBG), 2,4-diamino-1,3,5-triazine (2,4-DAT), 2-amino-4-methylamino-1,3,5-triazine (2,4-AMT), and 4-amino-2-imino-1-methyl-1,2-dihydro-1,3,5-triazine (4,2,1-AIMT). Melamine (MAM) was used to estimate the response for all amino-triazine TPs for which no analytical standards were available.

guanidine and non-target screening of possible TPs of GU in the test bottles. LC operating parameters were the same as used described above. For high-resolution mass spectrometry with a 6550 quadrupole-time-of-flight (QTOF) instrument (Agilent Technologies) a scan range of m/z 50–1000 with 3 spectra/s and similar parameters as described in Table S1 were used, except of a lower nebulizer pressure (35 psi) and a higher capillary voltage (3000 V).

3. Results and discussion

3.1. Lab experiments for aerobic degradation of MF and GU with activated sludge

Lab experiments for aerobic biodegradation should give an improved understanding of the fate of GU in biological treatment processes. For the experiments, activated sludge from two WWTPs with different inflowing and outflowing GU concentrations were applied. In general, measurements of sampling weeks with 24 - hour composite samples revealed GU degradation in W1 and GU formation in W2 (S 1).

3.1.1. Activated sludge from W1

In the aerobic lab experiment MF_GU_aer_1a with activated sludge from WWTP W1 degradation of 5 mg/l MF started between day 5 and 7 and within 5 days 99% of MF were degraded (day 12) (Fig. 2). Sterile controls showed no loss of MF, measured concentrations fluctuated around 6% during the experiments (Figure S 3). Simultaneously, GU formation started between day 5 and 7 and reached after 12 days a concentration of 90% of degraded MF on a molar basis. In the following days GU concentration reached a plateau at 42 µmol/l which resembles exactly the amount of spiked MF (41 µmol/l) plus the initial concentration of GU in the activated sludge (1 µmol/l) (Fig. 2). Therefore, MF is quantitatively transformed to GU which stays stable until day 35. Then, degradation of GU started at day 35, which is 23 days after GU was formed (Fig. 2). After further 10 days GU was almost completely degraded (98%). To check the GU degradation potential of the adapted sludge, a further spike of GU (125 µmol/l) was added 15 days later. Again complete

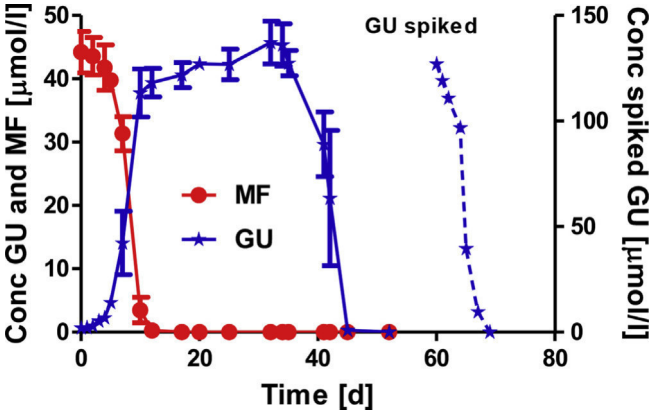

Fig. 2. Aerobic biodegradation of MF and GU in experiment MF_GU_aer_1a. Initial MF concentration $c_0 = 41$ µmol/l, after 60 days 125 µmol/l GU were spiked (Error bars show the range of duplicates).

GU degradation was observed within 5 days without any lag phase. Therefore, GU appears to be readily biodegradable in this system.

After 3 days, formation of MBG started and reached a maximum at 0.05 μmol/l at day 7 (Fig. 3). Within 5 days 85% of MBG were degraded and at day 17 MBG was no longer detectable. The low percentage of MBG (0.12%) compared to degraded MF implies that MBG is an intermediate. Its formation could be the rate limiting step, followed by a fast further degradation process to GU. Previous studies on cytochrome P450 dependent degradation of compounds of the guanidine class found Michaelis-Menten constants (K_m) for the *N*-demethylation which were much higher than those for *N*-hydroxylation (Kawata et al., 1983; Clement et al., 1994). High K_m values imply low enzyme affinity, therefore *N*-demethylation is much more difficult than *N*-hydroxylation (Cui and Schröder, 2016). That means, hydroxylation with subsequent oxidation should occur in contrast to demethylation of MF to GU. Hydroxylated or oxidized intermediates of MF other than GU were not detected.

The cyclized 2,4-AMT was detected at maximum concentrations of 0.37 μmol/l after 7 days, which was about 1% of the initial MF concentration. Further degradation of 2,4-AMT was much slower. Even after 45 days about 0.08 μmol/l 2,4-AMT were still detectable (Fig. 3). TP 2,4-DAT and 4,2,1-AIMT could not be detected.

The oxygen concentrations were between 4.5 and 7.7 mg/l during the experiment, pH was between 7.7 and 8 without significant changes. Nitrate concentrations increased within the first 17 days from 10 mg/l to 25 mg/l. In controls without additional MF the same trend was observed, indicating aerobic turnover of the biomass of the activated sludge. However, at day 70 the final nitrate concentration reached 1.3 mmol/l (80 mg/L), which equals complete MF and GU mineralization. The complete mineralization of the formed and spiked amount of GU (165 μmol/l) can form 660 μmol/L or 40.9 mg/L nitrate, which resembles well the increase of 55 mg/L nitrate. A previous study showed aerobic biodegradation of guanyl urea with the soil isolate Variovorax strain VC1 (Perreault et al., 2013). Transformation products were ammonia, guanidine and CO2, whereas in our study no guanidine was detectable. A non-target screening in the mass range between 50 and 1000 showed also no other substances which could be TPs of GU.

Another similar experiment with 40 mg/l initial MF concentration and activated sludge from W1 was conducted two years before (MF_GU_aer_1b) and showed similar results (Figure S.1). Between day 13 and 21 MF was quantitatively transformed into GU and after 47 days GU was completely degraded. Spiked GU also showed degradation during 12 days. Also MBG formation and further degradation showed a similar trend, with the highest amount of MGB at day 6. The maximum amount of 2,4-AMT was at day 21. Interestingly, also the secondary TP 2,4-DAT has been formed in this experiment, but only with 5% of 2,4-AMT (Figure S2). These results reveal the degradability of GU in activated sludge processes.

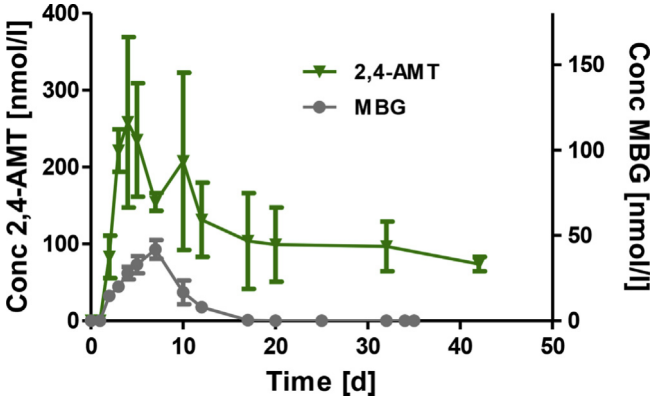

Fig. 3. Time curve of 2,4-AMT and MBG during aerobic biodegradation experiment of MF_GU_aer_1a (Error bars show the range of duplicates).

Real samples from the full-scale plant W1 also confirm these results, since ten times higher GU than MF concentrations in the influent correspond to much lower effluent concentrations of GU (Tisler and Zwiener, 2018). This can be only explained by GU degradation in the treatment process. The TPs 2,4-AMT and 2,4-DAT showed increasing concentrations from influents to effluents of W1, for MBG no noticeable trend was detectable and 4,2,1-AIMT was not detected.

With further lab experiments, we checked whether anaerobic processes during denitrification contribute to MF degradation, GU formation and further degradation (1.2 and 1.3).

3.1.2. Activated sludge from W2

In a lab experiment with activated sludge from the other sewage treatment plant W2, 9 mg/l MF was completely transformed into GU already after 5 days (MF_aer_2) (Figure S 4). In MF_aer_2 we used 2.5 times higher dry mass of sludge (8 g/l) concentration compared to MF_aer_1a, which may explain the faster degradation kinetics (Figure S4). After 36 days of the experiment and therefore 31 days after GU formation, no further biodegradation of GU was detectable. In contrast, GU degradation in MF_GU_aer_1a started already after 23 days even with much less biomass. Remarkable was also, that no further TPs were detected in experiment MF_aer_2. Oxygen concentrations were between 2.2 and 4.7 mg/L and pH between 7.1 and 7.5. The results from the full-scale plant W2 also resemble those of the lab experiments. WWTP W2 shows a rather quantitative MF degradation (99%), but GU increases from the influent with 6 μg/L to the effluent with 34 μg/L. The TPs MBG, 2,4-AMT and 2,4-DAT all showed a decreasing trend from influents to effluents in W2 (S 1).

The major difference in experiment MF_GU_aer_1 and MF_aer_2 was the source of sludge from two different WWTPs with two different input characteristics of GU. W2 is characterized by GU formation of 29% degraded MF on a molar base in the treatment process. In contrast, W1 showed partially high GU concentrations already in the influents and GU removal in the treatment process, which means a net GU degradation whereas W2 is characterized by GU formation. This indicates a different adaption of the sludge to GU and may explain the better GU degradation capability of the sludge from W1.

Noticeable was also the occurrence of other TPs only in the experiment with less dry mass MF_GU_aer_1. Recent experiments with even ten time less dry mass of sludge (0.4 g/l) and a similar set up showed a temporary deficit in mass balance (35%) of degraded MF and formed GU for 10 days (Markiewicz et al., 2017). However, no other TPs have been measured.

3.2. Anaerobic degradation of MF and formation of TPs with activated sludge

In an anaerobic lab experiment with 30 g/l activated sludge from W1 and 6 mg/l MF, only a small decrease of 23% MF occurred during the first 30 days (Fig. 4). A part of MF decrease was due to sorption, since in sterile controls a 19% drop of MF was observed. After 30 days, MF degradation kinetics considerably increased and after 40 days no further MF was detectable. Degradation kinetics was much slower in the anaerobic compared to the aerobic experiment, even if the sludge concentration was 10 times higher. A recent study with different soils showed the same trend, fast degradation processes under aerobic conditions and very slow degradation of MF under anaerobic conditions (Mrozik and Stefańska, 2014). Furthermore, we studied the concentration trends of the TPs GU, MBG and 2,4-AMT. All three TPs occurred only below 1% of MF at maximum

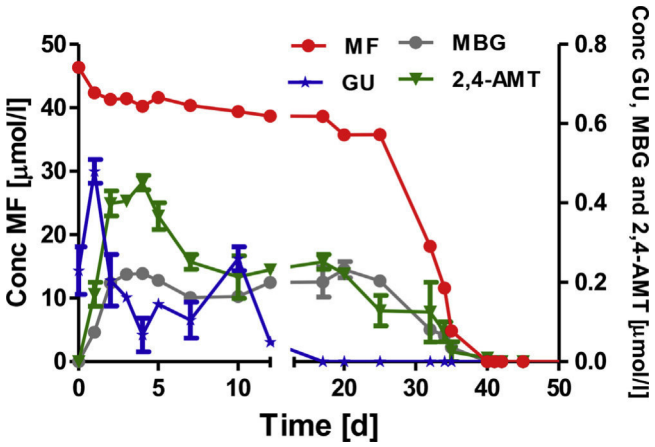

Fig. 4. Anerobic biodegradation of MF and occurrence of the TPs GU, MBG and 2,4-AMT over 55 days with activated sludge of W1 (MF_anaer_1) (Error bars show the range of duplicates).

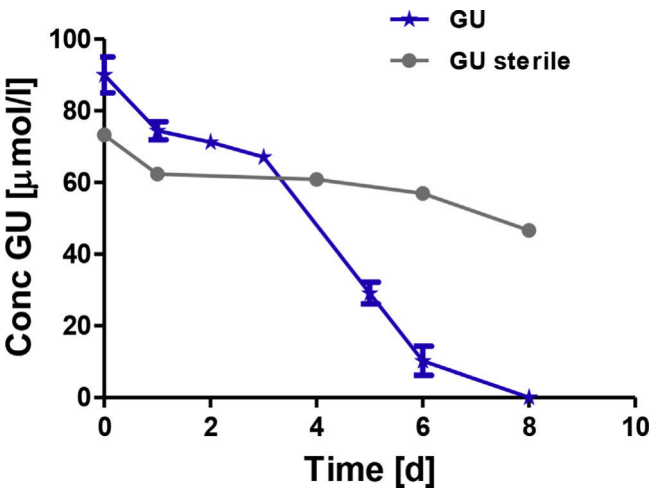

Fig. 5. Anaerobic biodegradation of GU spiked to anaerobic sludge from W1 (GU_anaer_1) (Error bars show the range of duplicates).

whereas about 23% of MF have been degraded. GU concentrations showed peaks after one and 10 days 2,4-AMT and MBG concentrations were time shifted and peaked after 3 and 18 days. All three TPs were consecutively degraded. GU degraded rather rapidly after each peak and was completely degraded after 17 days. Complete degradation of MBG and 2,4-AMT took 40 days. The occurrence of the TP maxima correlated well with our sampling activity and therefore we assume that small amounts of oxygen were introduced into the system which triggered aerobic MF degradation and TP formation until oxygen was again consumed. However, measured oxygen concentrations were below 0.5 mg/l and nitrate was below 10 mg/l during the entire experiment. The aerobic degradation explained the slight decrease of MF (4%) at the beginning and the occurrence of GU, MBG and 2,4-AMT (Figure S 3).

Another, not strictly anaerobic experiment was conducted with an initial MF concentration of 9 mg/l and 8 g/l of dry mass from WWTP W2 (MF_f_anaer_2) (Figure S 5). Oxygen concentrations were lower than 1 mg/l in the first 8 days and increased to a maximum value of 3.2 mg/l after 21 days. After 23 days the oxygen concentration was again lower than 1 mg/l. Here also GU and MBG showed peaks at higher oxygen concentration (increasing TP formation) and degradation during low oxygen content, similar to the previously described experiment MF_anaer_1.2,4-AMT was formed slowly during the experiment with a maximum value of 4 µmol/l at day 14 and only incomplete degradation of 57% during 24 days without fluctuations. Due to much smaller amounts of formed GU (10%) compared to the amount of degraded MF, it can be concluded that still anaerobic biodegradation was the more dominant process in this not strictly anaerobic experiment MF_f_anaer_2.

3.3. *Anaerobic degradation of GU with sludge from WWTP W1*

In a third experiment, 8 mg/l GU was directly spiked to fresh anaerobic sludge from WWTP W1 (GU_anaer_1). After a lag phase of 3 days, anaerobic biodegradation of GU started and 8 days later no further GU was detectable (Fig. 5). This result of GU degradation corresponds with the fast GU degradation in the anaerobic parts of the experiments MF_anaer_1 and MF_f_anaer_2. After the first day, GU concentrations in sludge and in the sterile controls dropped similarly by 15%, indicating adsorption processes. Due to the high concentration of microorganisms and effective degradation processes of GU under anaerobic conditions, it seems that the sterile control was not toxic enough. A slight decrease of GU in the sterile control was also detectable during the complete experiment.

4. Conclusions

In this study, we investigated the formation and biodegradation of GU in aerobic and anaerobic lab experiments with MF. From the results the following conclusions can be drawn:

- Good biodegradability of GU under anaerobic conditions was observed. Under aerobic conditions microorganisms needs a long time for adaption.
- Biodegradability of GU depends on the microbial community of the activated sludge. Depending on influent composition of WWTP, microorganisms could be better adapted to GU.
- Biodegradation of MF was fast under aerobic conditions and slower under anaerobic conditions
- TP MBG is quickly formed and degraded during aerobic MF degradation.
- TP 2,4-AMT was also formed during aerobic MF degradation with very slow degradation in turn, 2,4-DAT is formed in a second step.
- Adsorption to sludge of MF and GU could be an additional elimination process. Adsorptive removal of up to 20% of the initial amount could be observed, despite the low log P values of MF and GU.
- Deficits in mass balance of WWTPs between inflowing MF concentration and outflowing GU concentration seems to be predominantly determined by GU degradation and not by other TPs.

Declaration of interests

The authors declare that they have no known competing financial interests or personal relationships that could have appeared to influence the work reported in this paper.

Acknowledgements

This research was performed within the framework of the project “Effect Network in Water Research” funded by the Ministry of Science, Research and Arts (grant number 33-5733-25-11t32/2) of the Land ofBaden-Württemberg, Germany.

Appendix A. Supplementary data

Supplementary data to this article can be found online at https://doi.org/10.1016/j.watres.2018.11.001.

References

Bradley, Paul M., Journey, Celeste A., Button, Daniel T., Carlisle, Daren M., Clark, Jimmy M., Mahler, Barbara J., et al., 2016. Metformin and other pharmaceuticals widespread in wadeable streams of the southeastern United States. Environ. Sci. Technol. Lett. 3 (6), 243–249. https://doi.org/10.1021/acs.estlett.6b00170.

Clement, B., Schultze-Mosgau, M.H., Richter, P.H., Besch, A., 1994. Cytochrome P450-dependent N-hydroxylation of an aminoguanidine (amidinohydrazone) and microsomal retroreduction of the N-hydroxylated product. Xenobiotica; Fate Foreign Comp. Biol. Syst. 24 (7), 671–688. https://doi.org/10.3109/00498259409043269.

Cui, Hao, Schröder, Peter, 2016. Uptake, translocation and possible biodegradation of the antidiabetic agent metformin by hydroponically grown Typha latifolia. J. Hazard Mater. 308, 355–361. https://doi.org/10.1016/j.jhazmat.2016.01.054.

Ghoshdastidar, Avik J., Fox, Shannon, Tong, Anthony Z., 2015. The presence of the top prescribed pharmaceuticals in treated sewage effluents and receiving waters in Southwest Nova Scotia, Canada. Environ. Sci. Pollut. Res. Int. 22 (1), 689–700. https://doi.org/10.1007/s11356-014-3400-z.

Huschek, Gerd, Hansen, Peter D., Maurer, Hans H., Krengel, Dietmar, Kayser, Anja, 2004. Environmental risk assessment of medicinal products for human use according to European Commission recommendations. Environ. Toxicol. 19 (3), 226–240. https://doi.org/10.1002/tox.20015.

Jones, O., Voulvoulis, N., lester, J., 2002. Aquatic environmental assessment of the top 25 English prescription pharmaceuticals. Water Res. 36 (20), 5013–5022. https://doi.org/10.1016/S0043-1354(02)00227-0.

Kawata, S., Sugiyama, T., Imai, Y., Minami, Y., Tarui, S., Okamoto, M., Yamano, T., 1983. Hepatic microsomal cytochrome p-450-dependent N-demethylation of methylguanidine. Biochem. Pharmacol. 32 (24), 3723–3728.

Kosma, Christina I., Lambropoulou, Dimitra A., Albanis, Triantafyllos A., 2015. Comprehensive study of the antidiabetic drug metformin and its transformation product guanylurea in Greek wastewaters. Water Res. 70, 436–448. https://doi.org/10.1016/j.watres.2014.12.010.

Markiewicz, Marta, Jungnickel, Christian, Stolte, Stefan, Białk-Bielińska, Anna, Kumirska, Jolanta, Mrozik, Wojciech, 2017. Primary degradation of antidiabetic drugs. J. Hazard Mater. 324 (Pt B), 428–435. https://doi.org/10.1016/j.jhazmat.2016.11.008.

Mrozik, Wojciech, Stefańska, Justyna, 2014. Adsorption and biodegradation of antidiabetic pharmaceuticals in soils. In: Chemosphere, vol. 95, pp. 281–288. https://doi.org/10.1016/j.chemosphere.2013.09.012.

Oosterhuis, Mathijs, Sacher, Frank, Ter Laak, Thomas, L., 2013. Prediction of concentration levels of metformin and other high consumption pharmaceuticals in wastewater and regional surface water based on sales data. Sci. Total Environ. 442, 380–388. https://doi.org/10.1016/j.scitotenv.2012.10.046.

Perreault, Nancy N., Halasz, Annamaria, Thiboutot, Sonia, Ampleman, Guy, Hawari, Jalal, 2013. Joint photomicrobial process for the degradation of the insensitive munition N-guanylurea-dinitramide (FOX-12). Environ. Sci. Technol. 47 (10), 5193–5198. https://doi.org/10.1021/es4006652.

Scheurer, Marco, Michel, Amandine, Brauch, Heinz-Jürgen, Ruck, Wolfgang, Sacher, Frank, 2012. Occurrence and fate of the antidiabetic drug metformin and its metabolite guanylurea in the environment and during drinking water treatment. Water Res. 46 (15), 4790–4802. https://doi.org/10.1016/j.watres.2012.06.019.

Tisler, Selina, Zwiener, Christian, 2018. Formation and occurrence of transformation products of metformin in wastewater and surface water. Sci. Total Environ. 628–629, 1121–1129. https://doi.org/10.1016/j.scitotenv.2018.02.105.

Trautwein, Christoph, Kümmerer, Klaus, 2011. Incomplete aerobic degradation of the antidiabetic drug Metformin and identification of the bacterial dead-end transformation product Guanylurea. Chemosphere 85 (5), 765–773. https://doi.org/10.1016/j.chemosphere.2011.06.057.

Supplementary Information

Aerobic and Anaerobic Formation and Biodegradation of Guanyl Urea and other Transformation Products of Metformin

Selina Tisler, Christian Zwiener*

*Corresponding author

Hölderlinstraße 12, 72074 Tübingen, Germany

Tel.: 004970712974702, Email: christian.zwiener@uni-tuebingen.de

S 1. Screening of MF and its TPs in WWTPs

In June 2018, 24-hour composite samples of wastewater influent and effluent were obtained from 7 consecutive days of W2, to have a better background knowledge of the fate and occurrence of MF and its TPs in real waste water treatment (WWT) processes. Results of WWTP composite samples of W1 in 2016 were already published (Tisler and Zwiener 2018).

W2 showed similar results for MF than W1, with high removal efficiency (99 %) and effluent concentrations lower than 1 µg/l. In comparison to former studies, GU concentrations in influents were relatively high, which may be due to abundant GU input sources or may indicate formation of GU from precursors in the sewer system (Table S 1). Higher effluent than influent concentrations of GU in W2 revealed further formation during the treatment processes. GU was detected in the effluents at levels which resemble, about 29 % of degraded MF on a molar base. GU degradation could be started by microorganism due to high GU influent concentrations which comes along with longer adaption time.

In W2 the concentrations of MBG were decreasing from 0.59 µg/l to 0.33 µg/l during WWT. MBG showed higher concentration in W2 than in W1 (0.075 µg/l) which could be due to higher MF influent concentrations in W2 and thus higher MBG formation rate due to hydrolysis of MF (Tisler and Zwiener 2018). Concentrations of 2,4-AMT and 2,4-DAT have been estimated based on the molar response of

melamine. Melamine has an amino-triazine and therefore exactly matches the core structure of 2,4-AMT and 2,4-DAT. The different responses of the TPs indicated the importance of using standards with similar structures. MF and MBG had a similar molar response, the molar response of MAM was around 20 times and of GU around 30 times smaller (Table S2). Estimated concentrations of 2,4-AMT and 2,4-DAT were both decreasing from influent to effluent. 4,2,1-AIMT was not detected. An overall elimination ratio during WWT is in the range of 46% and 68% respectively, and the sum of degradation and formation processes due to MF degradation. In comparison, W1 showed increasing concentrations from influent to effluent of 2,4-AMT and 2,4-DAT, but 4,2,1-AIMT was also not detected. The results clearly showed that molar GU concentrations in effluents are generally lower than the eliminated MF and other TPs besides GU were detected. Biodegradation experiments with sludge of the investigated WWTP should help to get more information about the molar ratio between MF and its TPs.

Table S 1: Concentrations of MF and its TPs in W2 (* Concentrations estimated based on the response of melamine.

	Influent conc [µg/l] ([nmol/l])	Effluent conc [µg/l] ([nmol/l])	Elimination/ Formation
MF	139.19 (1079)	0.32 (3)	99 % ↓
GU	6.40 (63)	34.03 (334)	81 % ↑
MBG	0.59	0.33	62 % ↓
2,4-AMT	0.68*	0.37*	46 % ↓
2,4-DAT	0.83*	0.27*	68 % ↓

S 2. LC-QqQ Operating Parameters

Table S 2: Operating parameters of the triple quadrupole mass spectrometer (QqQ-MS).

Parameter	**Set point**
Gas temperature	150 °C
Gas flow	16 l/min
Nebulizer gas pressure	45 psi
Sheath gas heater	400 °C
Sheath gas flow	12 l/min
Capillary voltage	1500 V
Ion funnel high/low pressure RF	90/70 V
Fragmentor voltage	380 V

Table S 3: MRM transitions and retention times of MF (metformin); MF D6 (deuterated MF); GU (guanyl urea); MBG (methylbiguanide); 2,4-AMT (2-amino-4-methylamino-1,3,5-triazine); 4,2,1-AIMT (4-amino-2-imino-1-methyl-1,2-dihydro-1,3,5-triazine); 2,4-DAT (2,4-diamino-1,3,5-triazine) and MAM (melamine)

	MF	MF D6	GU	MBG	2,4-AMT	4,2,1-AIMT	2,4-DAT	MAM
Precursor ion (m/z)	130	136	103	116	126	126	112	127
Product ion (Quan/Qual) (m/z)	60/71.1	60/77.1	60/86	60/56.9	57/45	57/45	70/68	85/68
Collision energy (setpoint in V)	10/30	10/30	10/5	10/20	30/20	30/20	10/30	20/32

Collision cell accelerator voltage (V)	6/6	6/6	5/5	6/3	6/6	6/6	6/6	6/6
Retention time (min)	2.9	2.9	4.4	3.8	1.8	3.4	3.2	4.1

Table S 4: intraday variations (RSD) with 1 µg/l standard and LOQ of MF, GU, MBG, MAM refer to QqQ

	RSD [%]	LOQ [ng/l]
	(n=4)	
MF	3.6	1
GU	4.5	10
MBG	3.8	1
MAM	3.7	10

Table S 5: Relative peak area (PA) per nnmol/l of the compounds metformin (MF), methylbiguanide (MBG), guanyl urea (GU) and melamine (MAM).

	$\frac{PA * L}{nmol}$
MF	1753
MBG	1984
GU	66
MAM	119

S 3. Additional graphs for biodegradation experiments of GU and MF

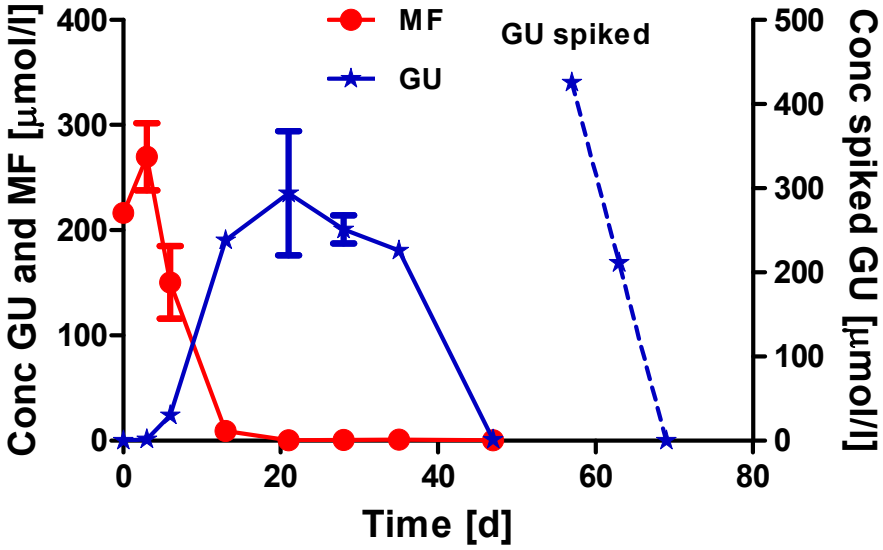

Figure S 1: Aerobic biodegradation of MF and GU with activated sludge from W1 (MF_GU_aer_1b). Error bars show range of duplicates.

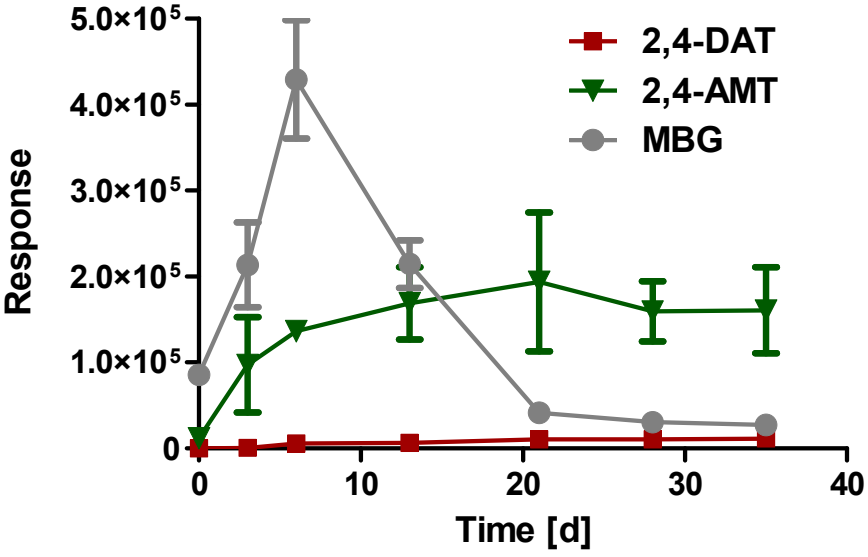

Figure S 2: TP formation during aerobic biodegradation experiment of MF with activated sludge from W1 (MF_GU_aer_1b). Error bars show range of duplicates.

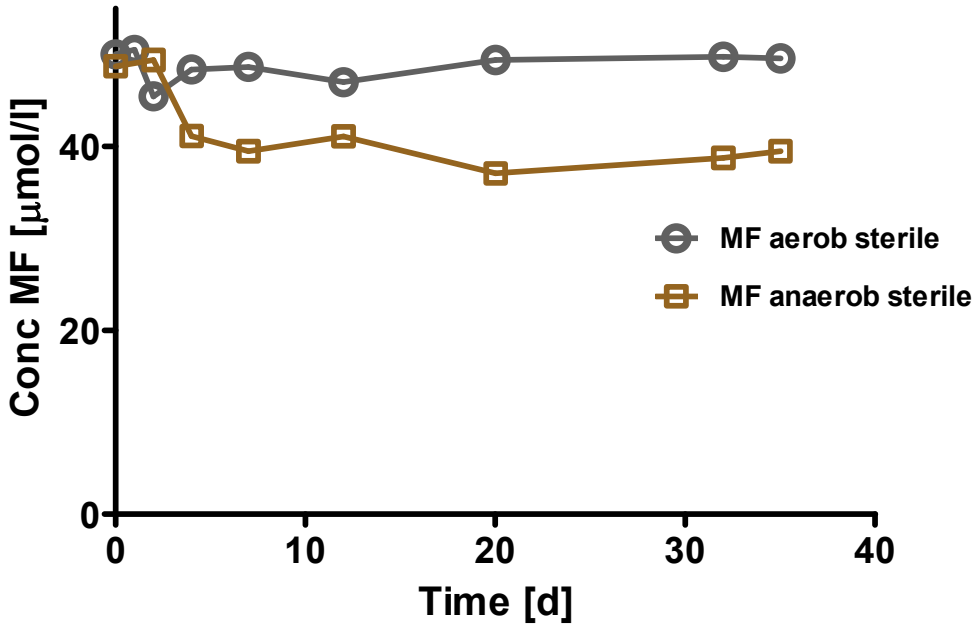

Figure S 3: sterile control of aerob MF degradation experiment (MF_GU_aer_1a) and anerob degradation experiment (MF_anaer_1). Error bars show range of duplicates.

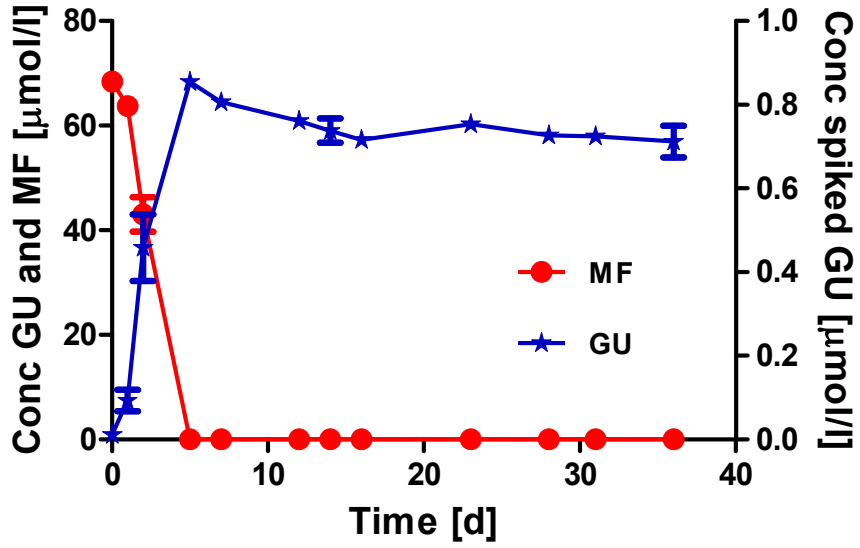

Figure S 4: aerobic biodegradation experiment of MF (MF_aer_2). Error bars show range of duplicates.

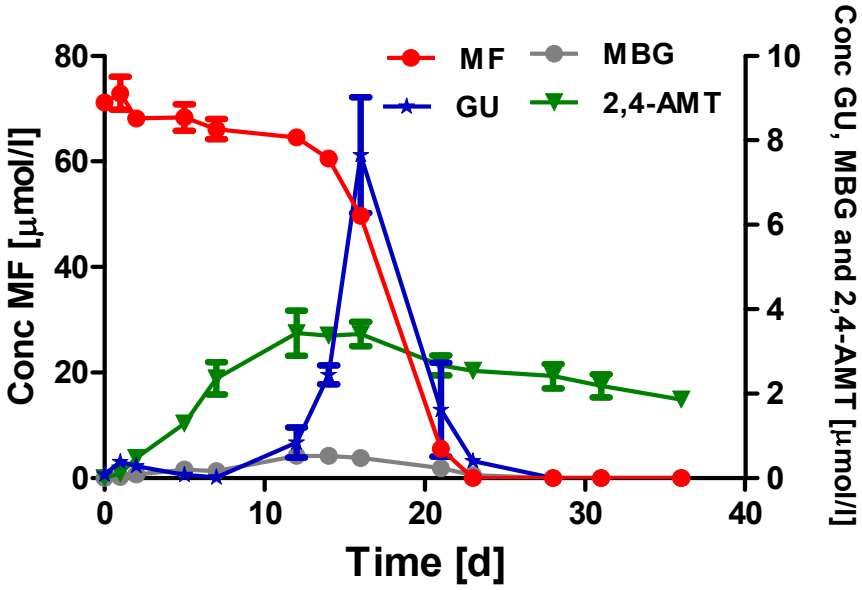

Figure S 5: facultative anaerobic biodegradation experiment with MF (MF_f_anaer_2). Error bars show range of duplicates.

PAPER 3

Transformation products of fluoxetine formed by photodegradation in water and biodegradation in zebrafish embryos (Danio rerio)

Selina Tisler, Florian Zindler, Finnian Freeling, Karsten Nödler, László Toelgyesi, Thomas Braunbeck, Christian Zwiener

(2019)

Transformation products of fluoxetine formed by photodegradation in water and biodegradation in zebrafish embryos (*Danio rerio*)

Selina Tisler[1], Florian Zindler[2], Finnian Freeling[3], Karsten Nödler[3], László Toelgyesi[4], Thomas Braunbeck[2], Christian Zwiener[1]

[1]Environmental Analytical Chemistry, ZAG, University of Tübingen, Germany

[2]Aquatic Ecology & Toxicology, Centre for Organismal Studies, University of Heidelberg, Germany

[3]TZW: DVGW-Technologiezentrum Wasser, Karlsruhe, Germany

[4]Agilent Technologies, Waldbronn, Germany

Abstract

The present study investigates the transformation of the antidepressant fluoxetine (FLX) by photo and biodegradation and shows similarities and differences in transformation products (TPs). TPs were identified using LC-high resolution mass spectrometry (LC-HRMS) with positive and negative electrospray ionization. In a sunlight simulator, photodegradation was carried out using ultra-pure water (pH 6, 8, and 10) and surface water (pH 8) to study the effect of direct and indirect photolysis, respectively. The well-known metabolite and TP norfluoxetine (NFLX) proved to be a minor TP in photolysis (≥2% of degraded FLX). In addition, 26 TPs were detected, which were formed by *O*-dealkylation (twelve TPs), hydroxylation (two TPs), CF_3-substitution (seven TPs) and *N*-acylation with aldehydes (six TPs) and carboxylic acids (five TPs). Higher pH favors the neutral species of FLX and the

neutral/anionic species of primary TPs and therefore photodegradation. In zebrafish embryos the bioconcentration factor of FLX was found to be 200, and about 1% of FLX taken up by the embryos was transformed to NFLX. Seven metabolites known from photodegradation and formed by hydrolysis, hydroxylation and N-acylation as well as three new metabolites formed by *N*-hydroxylation, *N*-methylation and attachment of an amine group were identified in zebrafish embryos.

Table of Contents (TOC)/Abstract Art

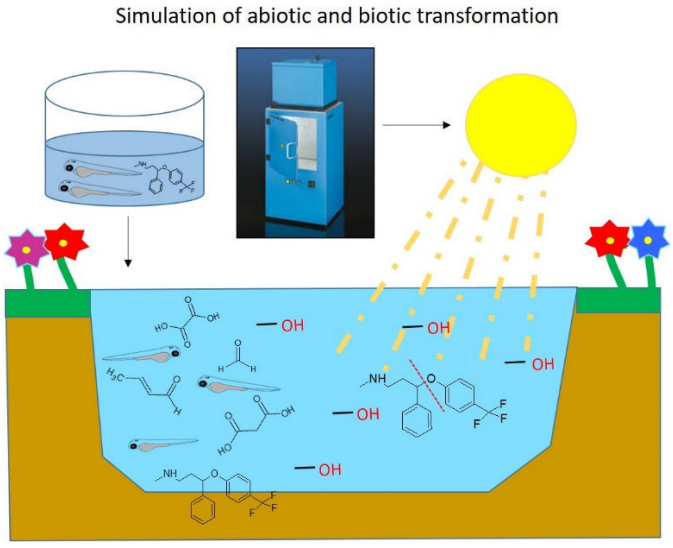

1. Introduction

In developed countries, consumption of antidepressants has grown by more than 60% over the past decade[1]. Among antidepressants, the selective serotonin reuptake inhibitors (SSRIs) represent a relatively new group of active ingredients which quickly became popular. In the United States of America (USA), fluoxetine hydrochloride (Prozac®) is a high-volume prescription SSRI drug. In the first half of 2018, fluoxetine (FLX) was number twenty out of the 200 most prescribed drugs in the USA[2]. In humans, FLX is metabolized mainly to glucuronides and *N*-demethylated derivative norfluoxetine (NFLX)[3]. Since 25% FLX is excreted unchanged[4,5] and 20% released as NFLX[6], main input sources for FLX and NFLX to enter surface waters are waste water treatment plants (WWTPs) with effluent

concentrations up to 930 ng/L[7] and 20 ng/L[8], respectively. FLX concentrations up to 99 ng/L were detected in waste-water dominated rivers in USA and Canada[9,10], and up to 90 ng/l in the Pacific Ocean (USA)[11]. In sediments, FLX and NFLX are even more prevalent with 12 ng/g and 7 ng/g, respectively. In the brains of white sucker (*Catostomus commersoni*) 1.6 ng/g and 1.8 ng/g were reported for FLX and NFLX in fresh weight[12]. There are several studies about the toxicity of FLX in fish[13–19] and invertebrates[20], which documented FLX as one of the most acutely toxic pharmaceuticals reported so far[6]. Furthermore, literature suggests several effects of FLX at environmentally relevant concentrations. In zebra mussels (*Dreissena polymorpha*) exposed for six days to 20 ng/L FLX, both the number of oocytes per follicle and the sperma density decreased by 40% and 21%, respectively[21]. A FLX concentration of 1 µg/L was found to be significantly impacting the mating behavior of fathead minnow (*Pimephales promelas*), specifically nest building and defending in male fish. Moreover, NFLX was reported to be pharmacologically more active in humans than the parent compound[22]. In bioassays with the protozoan *Spirostomum ambiguum* and the crustacean *Thamnocephalus platyurus*, the 24 h LC 50 was approx. 0.5 mg/L, with NFLX being more toxic by 50% than FLX in both bioassays[6]. Tests with *Tetrahymena thermophila* reported the S-enantiomer of NFLX to be ten times more toxic than S-FLX[23]. The high toxicity of FLX and the even higher toxicity of its metabolite and transformation product (TP) NFLX highlight the importance of other TPs, which might be formed and/or accumulate in sediment and biota. Several studies of other pharmaceuticals revealed increasing toxicity after UV irradiation in surface water, due to formation of toxic TPs[24–26].

Various studies on FLX degradation by means of advanced oxidation processes revealed TPs formed by hydroxylation and *O*-dealkylation (cleavage of the C-O bond)[27–30]. In addition, Lam et al. (2005)[29] identified one triple-defluorinated TP, where the CF_3 moiety was hydrolyzed to a carboxyl group (COOH) by photodegradation. However, in these studies, structural elucidation was solely done in electrospray ionization (ESI) (+) mode. TPs containing acidic functional groups, which typically show the highest

sensitivity in the negative electrospray ionization (ESI (−)) mode, were insufficiently considered. Furthermore, biologically formed metabolites apart from NFLX have very rarely been described in the literature. Gulde et al. (2016)[31] identified *N*-acylation as additional biotransformation process in activated sludge. Hence, further studies on biotic and abiotic degradation pathways seem necessary, since TPs/metabolites might also have effects in aquatic ecosystems. Photolysis is the dominant process for FLX degradation in rivers[23] and - as an advanced oxidation process - it tends to simulate biotic CYP450 reactions[32,33]. In the present study, the focus was on direct and indirect photochemical degradation of FLX at three selected pH-values to advance our knowledge of abiotically formed TPs. Furthermore, zebrafish (*Danio rerio*) embryos were exposed to FLX and the findings of biologically formed metabolites were compared with abiotic TPs. The zebrafish is often applied as model organism for assessing xenobiotic metabolism[34]. Identification of TPs/metabolites was performed by LC-high resolution mass spectrometry (HRMS).

2. Materials and Methods

Chemicals

Fluoxetine hydrochloride (FLX HCl), α-[2-(methylamino)ethyl]benzyl alcohol (TP 166), 4-(trifluoromethyl)phenol (TFMP) and trifluoroacetate (TFA; sodium salt) (all ≥96.5% purity) were purchased from Sigma-Aldrich (St.Louis, MO, USA). The deuterated internal standard (IS) FLX-d5 (hydrochloride) was purchased from Cayman Chemicals via Biomol (Hamburg, Germany), the IS TFA-$^{13}C_2$ was obtained from TRC (Toronto, Canada). Optima LC-MS grade acetonitrile (AcN), water, acetic acid (AA) and formic acid (FA) were obtained from Fisher Scientific (Schwerte, Germany). For chemical analysis and photodegradation experiments, individual stock solutions at concentration of 1 g/L were prepared in a mixture of AcN and water (1:1 v/v). Working standard solution containing 50 µg/L of FLX-

d5 was prepared in pure water. Stock and working solutions were stored at -20 °C, while the aqueous FLX-d5 solution was stored at 4 °C.

Photodegradation experiment

Photochemical experiments were conducted in a sunlight test chamber model "UVACUBE 400" from Hoenle UV Technology (Gräfelfing, Germany) equipped with a SOL 500 RF2 solar simulator and a H2 filter glass. The emission wavelength range covered by the applied solar simulator was between 295 nm and 3000 nm with an intensity setting of 1000 W/m^2. The experiments were initiated at 23°C and the test chamber was heated up to 29 °C by radiation of the lamp over the 28 h exposure time. Degradation experiments were conducted in ultrapure water for direct photolysis and in surface water for indirect photolysis. The surface water (SW) was collected on August 30, 2018, from the tributary Ammer of the river Neckar in Tübingen, Germany (48.523852° N, 9.056876° E). The pH of the surface water was not adjusted (pH 8.3). Additional chemical-physical properties of the water are given in Table S1.

Experiments with ultrapure water were performed at pH 6, 8 and 10 in a phosphate-buffered system. For pH-adjustment, diluted NaOH or HCl solutions were added to a 12 mM Na_2HPO_4 solution. For all photolysis experiments, 1 ml of FLX HCl aqueous stock solution was added to 60 mL of the surface water or to pH adjusted ultrapure water, to obtain a final concentration of 15 mg/L FLX. Experiments were conducted in triplicate and with one control sample, which was kept in the dark (Table S 2). In all experiments, the total irradiation time was 28 h with 9 sampling events (t= 0, 1, 2, 4, 6, 8, 13, 24, 28 h).

Pseudo first order rate constant k was obtained for FLX by solving equation (1) for each triplicate per experiment. The final k was computed as the average of the k-values obtained.

$$k = \frac{-\ln(\frac{c}{c_0})}{t} \quad (1)$$

The calculation of normalized peak areas, of the substances (TPs) for which no analytical standards were available, is given in chapter S. 4.

Biotransformation of FLX in the zebrafish embryo

Wild-type zebrafish (*Danio rerio*) of the Westaquarium strain were kept at the fish facilities of the Aquatic Ecology and Toxicology Group at the University of Heidelberg (licensed under no. 35-9185.64/BH). Details of fish maintenance, breeding conditions and embryo rearing are described comprehensively by Lammer et al. (2009)[35]. After spawning, 160 freshly fertilized eggs were collected and divided into two groups (control and exposure group), each of which was transferred into a 70 ml crystallizing dish filled with 60 ml ultrapure water. At 30 h postfertilization (hpf), all embryos were mechanically dechorionated with Dumont no. 5 tweezers. For the exposure group, ultrapure water was replaced by 60 ml of FLX HCl test solution (nominal: 5 mg/L FLX HCl) at 48 hpf. Throughout the entire experiment, embryos were kept at 26 ± 1 °C and pH 7.2 under a 10/14 h dark/light regime, and test solution were replaced each day for both controls and exposure groups. For identification of FLX metabolites, embryos and test media were sampled at 96 hpf. For this end, 15 embryos per group were rinsed three times with 5% AcN in water (v/v) as washing procedure. Subsequently, embryos were transferred into 2 ml Eppendorf cups, surplus acetonitrile-solution was removed, and embryos were euthanized in liquid nitrogen prior to storage at −80 °C. Chemical analysis of FLX and its metabolites in fish was conducted in three replicates, each consisting of five pooled embryos. For extraction, five pooled embryos were spiked with a mixture of 300 µl AcN and 200 µl of 12 µg/l FLX-d5 aqueous solution. The samples were sonicated (SONOREX®, Bandelin, Berlin, Germany) for 2 × 15 min and stored at 4 °C for 24 h. After another 15 min sonication, extracts were centrifuged for 15 min at 10.000 rpm (centrifuge 5417 C®, Eppendorf, Hamburg, Germany). The supernatant was analyzed for FLX and FLX related compounds directly after extraction. For calculation of the bioconcentration factor (BCF) and pseudo BCF, the volume of embryos at 96 hpf was estimated at 500 nl[36]. The pseudo BCF is the ratio of

the concentration of a metabolite in organism to the concentration of the initial precursor in water. The BCF and pseudo BCF were calculated as follows:

$$BCF = \frac{C_{fish\_FLX}}{C_{water\_FLX}} \quad (3)$$

$$pseudo\ BCF = \frac{C_{fish\_NFLX}}{C_{water\_FLX}} \quad (4)$$

where C_{fish_FLX} (mg/L) and C_{fish_NFLX} (mg/L) are the concentrations of FLX and NFLX determined in zebrafish embryos, respectively. C_{water_FLX} (mg/L) is the concentration of FLX measured in the water.

Analytical Methods

Identification of TPs by HRMS. For the chemical analysis of TPs a liquid chromatography system (1290 Infinity I LC System, Agilent Technologies, Waldbronn, Germany) coupled to a quadrupole time of flight mass spectrometer (6550 iFunnel Q-TOF LC/MS, Agilent Technologies) was used. An Agilent Poroshell-120-EC-C18 (2.7 µm, 2.1 × 100 mm) column at a flow rate of 0.4 ml/min was used for separation, and column temperature was maintained at 40 °C. Eluent A and B were water and acetonitrile, respectively. For ESI (+), 0.1 % formic acid was added to both eluents, while for ESI (−) 0.1 % acetic acid was added to both eluents. In addition, for ESI (−), eluent A was an aqueous buffer of 0.1 mM ammonium acetate. Gradient elution was used for both modes: 0–1 min 5% B, linear increase to 100% B within 7 min, hold for 7 min at 100% B. After switching back to the starting conditions, post-time of 3 min was employed. Injection volume was 5 µl and for HRMS-analysis, the eluent was diverted to waste between minute 4.4 and 4.8 to prevent high FLX concentrations contaminating the ion source. Samples were measured with a scan range of *m/z* 50-1000 and at 5 spectra/sec acquisition speed. Additional information on the instrument parameters is given in Table S 3. MS-MS fragmentation data were acquired by targeted

fragmentation mode (targeted MS/MS; precursor isolation width was set to narrow (1.3 Da) and fixed collision energies have been employed (10, 20 and 40 eV)).

Target-analysis. Quantification of 5 µl of diluted samples (factor 100-1000) were performed after LC separation using a triple quadrupole mass spectrometer (6490 iFunnel Triple Quadrupole LC/MS, Agilent Technologies) in ESI(+) mode for FLX, NFLX and TP 166 and in ESI (−) mode for TFMP (details are given in Table S 4-6). Ion exchange LC-MS/MS in ESI (−) was applied for the determination of trifluoroacetate (TFA) according to the method described by Scheurer et al. (2017)[37].

Workflow for TP Identification by Nontarget-Screening

Molecular feature extractions of the scan data (*m/z* 100-500) were performed using the MassHunter Qualitative Analysis Software (version B.07.00, Agilent Technologies). Compound patterns in data sets from samples before and after irradiation or exposure to zebrafish embryos were evaluated with the Mass Profiler Software (version B.08.00 Agilent Technologies). A fold-change filter of 5 was used to select TPs formed during the experiments, and based on accurate mass measurements chemical formulas were assigned with a mass deviation smaller than 10 ppm. Constraints for elemental compositions were selected based on the precursor composition of FLX ($C_{17}H_{18}F_3NO$) and potential TPs derived from FLX: 0–25 C, 0–35 H, 0–6 O, 0–3 F, 0–1 N for photolysis and for zebrafish experiments the same ranges for C, H, O and F but 0–2 N. Hereafter, targeted MS/MS was performed to acquire MS/MS fragmentation data for the selected molecular features to facilitate their characterization. Chemical structures were proposed based on MS/MS data, in-source fragmentation, retention time behavior, and literature information[20,28,29,31]. Confidence levels for the identification are given in Schymanski et al. (2014)[38] and are defined in chapter S. 5.

3. Results and Discussion

FLX degradation and NFLX formation by photolysis

The degradation of FLX by photolysis during the 28 h experimental period in the artificial buffer systems was strongly pH-dependent. The observed pseudo-first order rate constants for direct photolysis of FLX were 0.003, 0.005 and 0.020 h^{-1} resulting in 8, 14 and 42% degraded FLX after 28 h at pH 6, 8 and 10, respectively (Figure S 1). This can be explained by a larger fraction of neutral FLX at higher pH (Table S 2) and therefore the higher electron density on the secondary amine group, compared to the cationic form. A higher reactivity of the neutral form was also shown by Zhao et al. (2017), who observed a similar pH-dependence of FLX degradation during ozonation. In our experiment with surface water, an increased degradation rate constant of 0.027 h^{-1} was observed. The presence of 31 mg/L NO_3^- in the surface water could be the reason for enhanced FLX degradation due to production of hydroxyl radicals, which are predominantly responsible for indirect photodegradation[39,40]. The pH shifted from 8.3 to 7.7 during the 28 h reaction time which was also found in control experiments with surface water without any spiked FLX. No pH change was observed for buffered ultrapure water. After 28 h in surface water, 0.5% of the degraded molar FLX concentration was detected as the TP NFLX. The approaches based on buffered ultrapure water showed 0.4, 0.9 and 2.1% NFLX for pH 6, 8 and 10, respectively (Table S 7). A recent study of Yin et al. (2017) identified NFLX as a photodegradation product only at high pH between 10 and 12. This is in accordance with the positive correlation between the NFLX concentration and the pH value observed in our study. Kwon et al. (2006)[41] showed that photodegradation of NFLX was more than twice as fast as that of FLX, which reveals NFLX as an intermediate during the photolysis of FLX. This is in line with the small amounts of NFLX detected in our study and implies that further TPs of FLX were most likely present. Control experiments in the dark showed negligible (< 4%) losses of FLX in all matrices and no formation of TPs. Therefore, sorption, biodegradation, and non-photolytic abiotic degradation of FLX could be excluded.

TPs formed by *O*-dealkylation and/or hydroxylation

After direct photolysis with simulated sunlight, ten TPs of FLX formed by *O*-dealkylation, and subsequent reactions were detected using positive and negative ESI coupled to HRMS (8 TPs by ESI (+), TFMP and TFA in ESI (−) mode (Figure 2)). The C-O bond cleavage of FLX primarily produces 3-(methylamino)-1-phenyl-1-propanol (TP 166) and 4-(trifluoromethyl)phenol (TFMP). Both TPs showed the highest yield at the lowest pH value on a molar basis compared to degraded FLX (Figure 1). TP 166 yield 19% and TFMP 31% of degraded FLX on a molar basis at pH 6. Assuming a pK_a-value of 10.4 for TP 166 (corresponding acid) and a pK_s-value of 8.7 for TFMP, at pH 10 fast subsequent photodegradation of the species with higher electron density could be the reason for the small amount observed for TP 166 (5%) and TFMP (0.3%). At high pH values the neutral species of TP 166 and the anionic species of TFMP were dominant. A former study with photolysis of 3-trifluoromethyl-4-nitrophenol (TFM), a related substance to TFMP, also revealed faster degradation of TFM at pH 9 than at pH 7 due to an excited state of the deprotonated anion[42]. The samples of indirect photolysis and direct photolysis (both at pH 8.3 at t_0) formed similar amounts of TP 166 (10%; 9%) and TFMP (0.003%; 0.002%) referred to degraded FLX on a molar basis, respectively. In literature, further hydrolysis of TFMP to 4-(difluoromethylene)-2,5-cyclohexadien-1-one (DFCH) was described by the loss of hydrogen fluoride[42]. In our study, DFCH was neither detected with accurate mass screening in ESI (+) nor in ESI (−). Wawryniuk et al. (2018)[43], and Drzewicz et al. (2018)[44] detected TFMP as a TP of FLX formed by direct photodegradation and degradation with potassium ferrate, respectively. Scheurer et al. (2017)[37] observed a substantial transformation of FLX to TFA during ozonation, which was also observed in our photodegradation experiments. TFA occurrence during direct photolysis was in average 0.3% and independent of pH and during indirect photolysis 1.5% of degraded FLX (Figure 1, Table S 8). Since TFA can be considered as a mineralization dead-end product, it will presumably occur in low amounts only, if photodegradation is incomplete and the concentrations of intermediates are still increasing. In indirect photolysis TFA

concentration was higher, due to faster degradation of FLX and hence a more advanced degradation of intermediates which may finally form TFA.

TP 166 has been described as a common TP of FLX in advanced oxidation processes[27–30]. Further TPs of FLX are formed by reactions acting on the benzyl moiety (Figure 2). Demethylation of TP 166 or *O*-dealkylation of NFLX[28] formed TP 152 and further oxidation created TP 150 and TP 146. Indirect photodegradation showed the largest increase for TP 152. TP 150 and TP 146 had a maximum intensity after 21 h and showed a decreasing trend thereafter (Figure S 3), which means hydroxyl radical-mediated indirect photolysis further degraded the TPs successively. The signal intensities of all three TPs showed an increasing trend over 28 h in direct photolysis with the highest signal intensities at pH 10 for TP 152 and at pH 8 for the subsequent TPs 150 and 146.

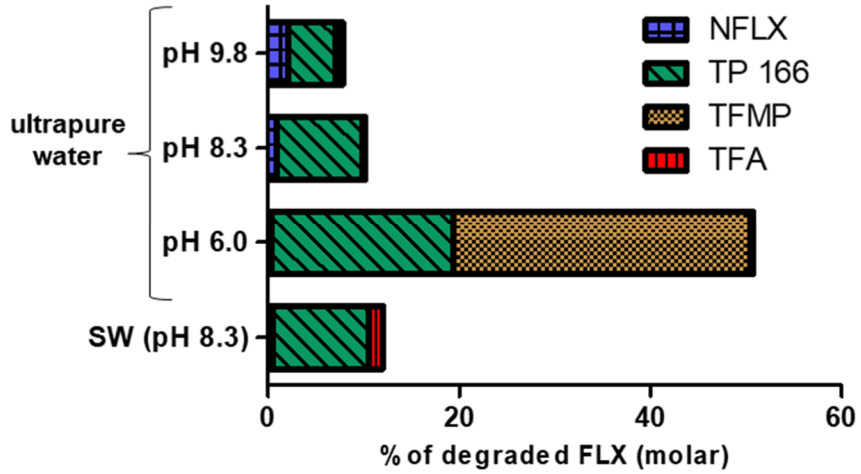

Figure 1: Sum of TPs (mol/L) in percent of degraded FLX (mol/L) for direct (ultrapure water) and indirect photolysis (SW=surface water). 8, 14, 42, 54% FLX was degraded after 28 h in ultrapure water (pH 6, 8, 10) and SW, respectively.

TPs 326a and b are hydroxyl products of FLX and were measured in ESI (+) mode at retention times of 4.7 min and 4.9 min, respectively. Both TPs showed the characteristic MS fragment *m/z* 44.05 (C_2H_6N) of the unchanged alkylamine side chain. TP 326a was also detected in ESI (−) and showed the original TFMP moiety (*m/z* 161.0217) as fragment. The observed fragments suggest that hydroxylation occurred on the benzyl moiety of FLX. TP 326b showed lower intensity and was not detectable in ESI (−) but showed a similar fragmentation pattern as observed for TP 326a in ESI (+). TPs 182a and b (1.3 min and 1.6 min) may be formed by hydroxylation of TP 166 or by dealkylation of TPs 326 a and b. Due to the hydroxyl radical chemistry during indirect photolysis, all four hydroxylated TPs were formed in amounts of one order of magnitude higher than during direct photolysis. The hydroxy-FLX (TP 326) and TP 182 were also identified in previous oxidation studies[27,28,28–30]. TP 148 may be formed by loss of water from TP 166. Due to in-source fragmentation, TP 148 was not detectable *per se*, but in form of the in-source fragments *m/z* 117.07 (C_9H_9) and *m/z* 91.0548 (C_7H_7). A decrease of sheath gas temperature in the ESI source from 400 to 300 °C revealed the precursor TP 148, which co-eluted as a double peak with the in-source fragments *m/z* 117 and 91. Direct photolysis experiments at pH 6 showed the highest intensities for TFMP and TP 148 with still increasing trend after 28 h. Likewise, an in-source fragment of FLX was detected as *m/z* 148.1121 $(C_{10}H_{14}N)^+$.

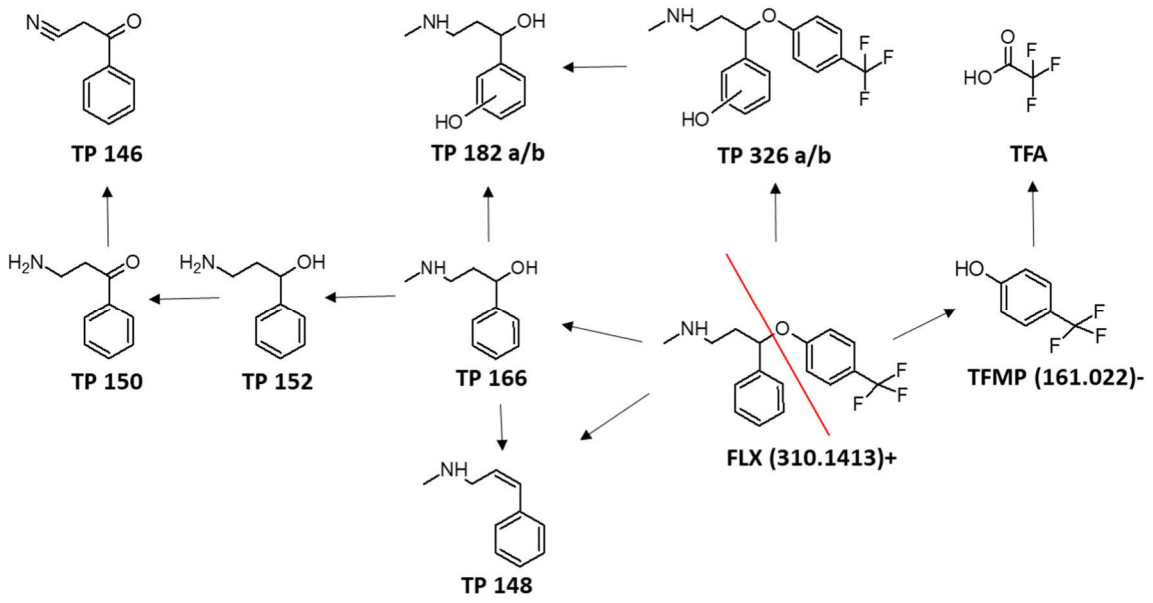

255

256 Figure 2: Scheme for *O*-dealkylated, hydroxylated TPs as well as further oxidation TPs of direct and
257 indirect FLX-photolysis. TFMP and TFA were measured by ESI (−), all other TPs by ESI (+), TP 326a by
258 both.

259 **TPs formed by substitution of the CF_3 moiety**

260 Seven TPs were derived from substitution of the -CF_3 group and further hydroxylation and *O*-
261 dealkylation (Figure 3), three TPs were detected in ESI (+) and four in ESI (−). TP 286a was formed by
262 nucleophilic substitution reaction of -CF_3 to –COOH which already has been described for other
263 compounds with -CF_3 groups[42,45]. We identified TP 286a with the MS fragment *m/z* 268.1332 formed by
264 water loss (*m/z* 18.0106) according to Lam et al. (2005)[29]. The present study is the first to detect TP 286a
265 also by ESI (−) and HRMS, confirming the structure proposed. Likewise, the present study describes for
266 the first time five additional TPs derived *via* substitution of the –CF_3 group. TP 286b (RT 3.7 min) and TP
267 286c [M-H] (RT 4.4 min) are constitutional isomers of TP 286a (RT 3.5 min). TP 286b was not detected in
268 ESI (−) mode, but the MS fragments revealed an unchanged alkylamine moiety (fragment *m/z* $(44.05)^+$)
269 and an intense fragment at *m/z* 185.1153 $(C_{10}H_{17}O_3)^+$ which originated from the oxidized phenol moiety

of FLX after loss of the phenyl and methylamine groups (Figure 3 and chapter S 4). In contrast to TP 286b, TP 286a showed main fragments at *m/z* 237.0921 $(C_{16}H_{13}O_2)^+$ and *m/z* 268.1332 $(C_{17}H_{18}NO_2)^+$. TP 286c [M-H] was only detectable in ESI (−) mode at pH 10 and occurred after indirect photolysis. Considering that the main fragment *m/z* 150.0556 $(C_8H_8NO_2)^-$ shows connection of 2 oxygen atoms to the alkylamine side chain and the observed higher retention time of TP 286c than that of the isomers, the formation of hydroxylamine is assumed. Merel et al. (2017)[46] showed that oxygen attached to nitrogen had a higher retention time than the precursors. TP 286a and b showed inversed abundance trends with increasing pH: the higher the pH, the less TP 286a and the more TP 286b were formed (Figures S 3). Further degradation of TP 286a to TP 272 and TP 139 could be the reason for the low intensity observed. Demethylation formed the secondary TP 272, which had the same fragment *m/z* 237.0921 and *O*-dealkylation of both TPs (TP 286a and 272) resulted in TP 139. The highest intensities of TP 272 and TP 139 were observed at pH 8 and pH 10, respectively, which supported the assumption of further degradation of TP 286a. Indirect photolysis had no significant influence on the amount of TPs 286 and 272, but the formation of TP 139 was observed to be 2-4 times higher. Further hydroxylation of TP 286a could form TP 318b, which was confirmed by the fragment of hydroxylation on the carboxylic acid side, *m/z* 169.0139 $(C_7H_5O_5)^-$. TP 286b, which was only detected in ESI (+) mode, could be excluded as a precursor of TP 318b due to the ESI (−) in-source fragment *m/z* 284.1295 $(C_{17}H_{19}NO_3)$. No in-source fragment was detected for TP 318a, which could be the hydroxyl-TP of TP 286b. The same pH-dependent formation trend as their suspected precursors confirmed the assumption of TP 286a as a precursor for TP 318b. In general, peak intensities of both TPs 318 (a/b) were one order of magnitude higher with indirect photolysis, which was expected due to the higher abundance of hydroxyl radicals.

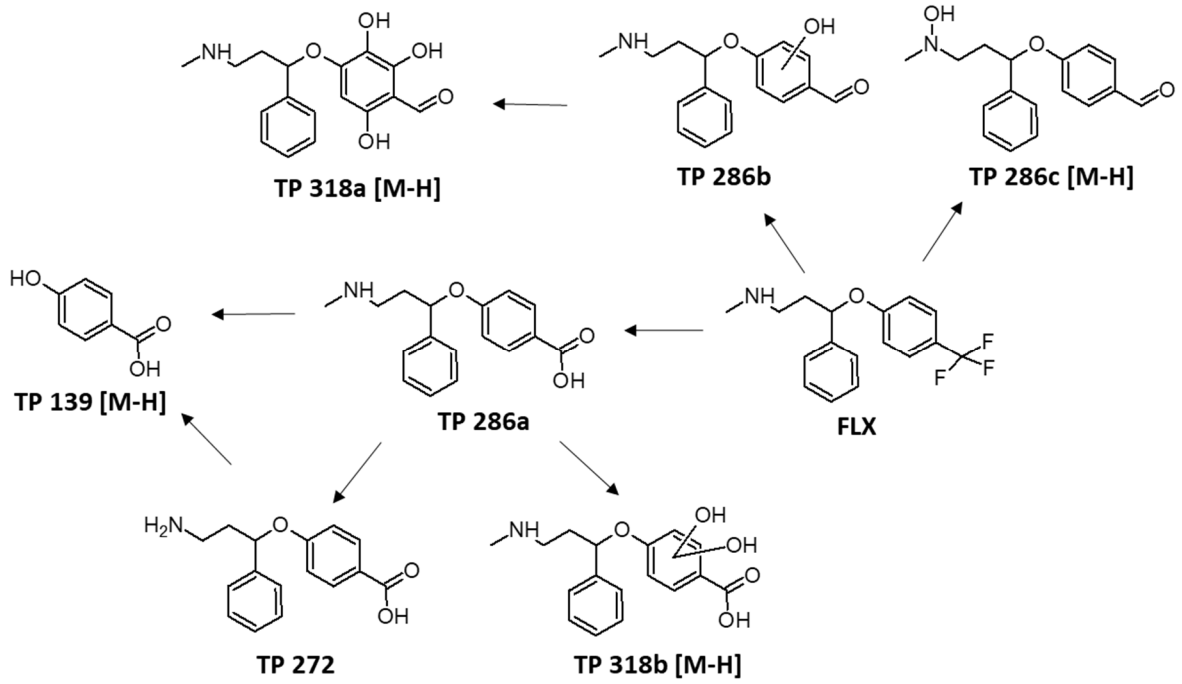

Figure 3: Seven transformation products (TPs) derived by CF_3 substitution. TP 286a/c, 139 and 318a/b were measured by ESI (−), while TP 286a/b and 272 were seen with ESI (+).

Transformation products formed by *N*-acylation

Various *N*-acylation reactions are known for primary and secondary amines in biotic systems. *N*-formylation, *N*-propionylation, *N*-malonylation and *N*-succinylation were observed for metabolism of xenobiotics in lysine residues of proteins[47]. Gulde et al. (2016) observed *N*-succinylation and N-acetylation reactions in activated sludge systems for FLX and *N*-propionylation and *N*-succinylation reactions were assumed for NFLX. We observed photo-induced *N*-acylation which, to the best of our knowledge, has never been observed before for amines in general. We assume that *N*-acylation reactions occurred with aldehydes or carboxylic acids during photolysis, ignoring the possibility that reactions may occur with subsequent cleavage of a longer-chained substituent. Most of the TPs showed a characteristic in-source fragment (IF) formed by cleavage of the TFMP moiety. The measured

intensities of the precursors were higher than the intensities of the IFs, whereas Gulde et al. (2016)[31] analyzed predominantly the IFs.

Six TPs were detected after *N*-acylation with aldehydes in ESI (+) mode (Figure 4). Out of these, TP 352 (*N*-acetylation) and TP 338 (*N*-formylation) have been already described in literature[31]. *N*-propionylation of FLX resulted in TP 366 and subsequent oxidation in TP 364, which can also be directly formed by adducts of acryl aldehyde. Two peaks of TP 378 at retention times 6.46 min and 6.82 min were identified, which may be formed by adducts of croton aldehyde, 3-butenal or methacrolein. The characteristic IF *m/z* 216.1378 $(C_{14}H_{18}NO)^+$ and the fragment *m/z* 96.0807 $(C_6H_{10}N)^+$ were observed for TP 378a. TP 378b, however, showed other fragmentation reactions, with *m/z* 121.0504 $(C_7H_7NO)^+$ and 251.1623 $(C_{13}H_{22}F_3O)^+$ formed by loss of the substituted side as the most abundant fragments. However, differentiation of croton aldehyde, 3-butenal or methacrolein as the specific substituent was not possible for both TPs.

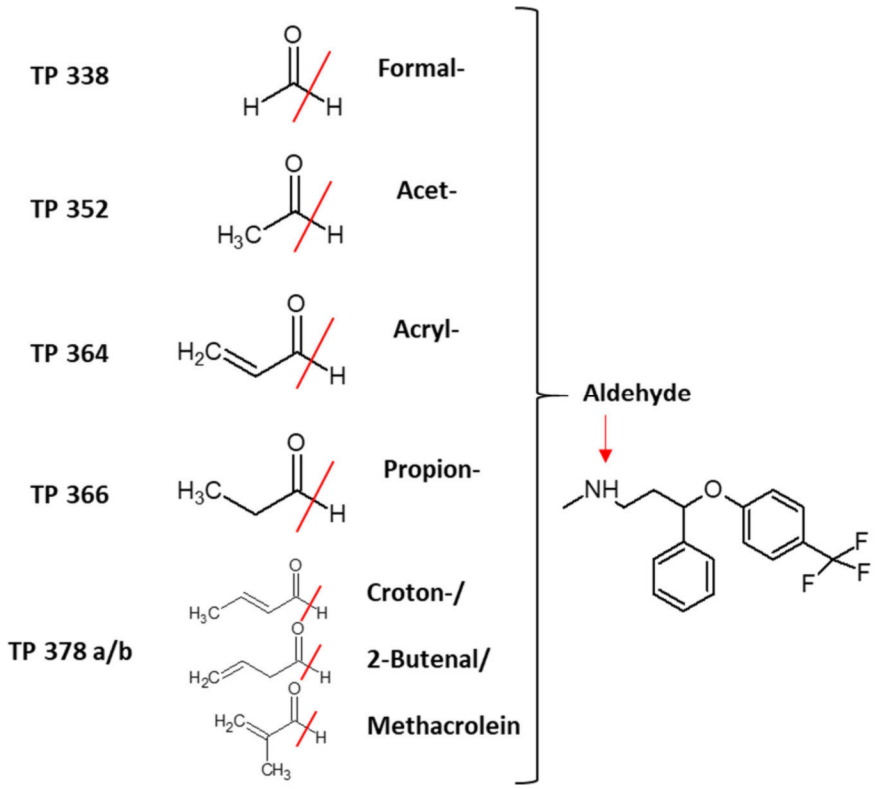

Figure 4: Formation of transformation products via *N*-acylation of FLX with aldehydes. For *N*-acylation of TP 378 a/b, three aldehydes are possible substituents.

Reactions with carboxylic acids revealed five TPs, three of which were measured in ESI (+) mode, one in ESI (−) mode (TP 382), and another one in both modes (TP 430) (Figure S 2). *N*-oxalylation, *N*-malonylation, *N*-fumarylation and *N*-succinylation were proposed to form TPs 382, 396, 410 and 408, respectively. The characteristic IFs (*m/z* 234.1125, 248.1285, 246.1116) were detected for the TPs 396, 410 and 408 in ESI (+)). TP 382 $(M\text{-}H)^-$ showed the unchanged TFMP fragment at *m/z* 161.0216. TP 430 is assumed to be formed by reaction with hydroxybenzoic acid. Detection in ESI (+) and ESI (−) mode confirmed the attached hydroxyl group, which could be attached to the benzoic acid ring or benzyl ring. Hydroxylation on the TFMP side is very unlikely, due to the unimpaired TFMP fragment. In activated

329 sludge systems, TP 396 and TP 410 have already been described as products of *N*-succinylation of FLX
330 and NFLX[31].

331 Except for TP 378a, all *N*-acylated TPs showed fast formation during indirect photolysis in surface water
332 samples (Figure 5 and S 8). Formation curves of TPs during indirect photolysis by reactions with
333 aldehydes (TP 338, 352, 364, 366) leveled off after 12 h (Figure 5), while for TP 378b, a typical curve for
334 intermediates was found with a maximum at 8 h. The amount of TPs formed by reactions with carboxyl
335 acids were still increasing even after 28 h (Figure S 8). The formation of compounds during direct
336 photolysis was often delayed by 8 h (TP 366, 378 a/b, 382 [M-H], 408 and 410), but showed a linear
337 increase thereafter. Whilst the formation of TPs 338 and 364 were delayed only by 2 h, the formation of
338 TPs 430 and 352 started immediately at pH 8 and 10. The delayed generation of TPs by direct photolysis
339 can be interpreted by formation of intermediates and precursors of the TPs such as aldehydes and acids
340 for the adduct formation. Aldehydes and carboxylic acids are common compounds in surface water,
341 which are formed by natural processes and occur during indirect photolysis[48–51]. Although in ultrapure
342 water the concentrations of aldehydes and acids should be low, they may be formed during oxidation
343 processes from FLX as shown by Zhao et al. (2017)[28], who detected maleic acid, oxalic acid,
344 formaldehyde, acetaldehyde, acrolein, and formic acid during the ozonation of FLX. Zhao et al. (2017)[28]
345 revealed higher FLX transformation into small molecules at elevated pH, but also faster degradation of
346 the aldehydes and acids in turn. Advanced oxidation processes at increased pH produces increased
347 hydroxyl radicals which enhanced the reaction rates and the formation of oxidized products. The role of
348 hydroxyl radicals on TP formation from FLX can be derived from the results shown for TPs 366, 378 b,
349 382, 408, and 410 (Figure 5). In any cases, indirect photolysis in surface water showed the fastest
350 formation, followed by direct photolysis at pH 10 compared to pH 6 and 8. The higher degradation
351 potential during indirect photolysis leads to a stagnation of TP formation or, in the case of TP 378b, even
352 to subsequent degradation. Thus, TP 378b shows a typical pattern of an intermediate, which is further

353 degraded at a rate similar to its formation (Figure 5). Graphs of *N*-acylated TPs, normalized to FLX
354 degradation rate, are given in Figures S 7 and S 9 and revealed similar yield of TPs after 28 h for most of
355 the TPs at pH 8 and 10. With 8%, the degradation of FLX at pH 6 was not sufficient to support the
356 formation of most of the TPs. In contrast, TP 430 showed significant formation under all photolysis
357 experiments. As illustrated in the normalized graph (Figure S 9), the *N*-acetylation product, TP 352,
358 showed that the highest yield at pH 6 after 28 h. This could be due to the fast degradation of
359 acetaldehyde at high pH values, as already discussed above.

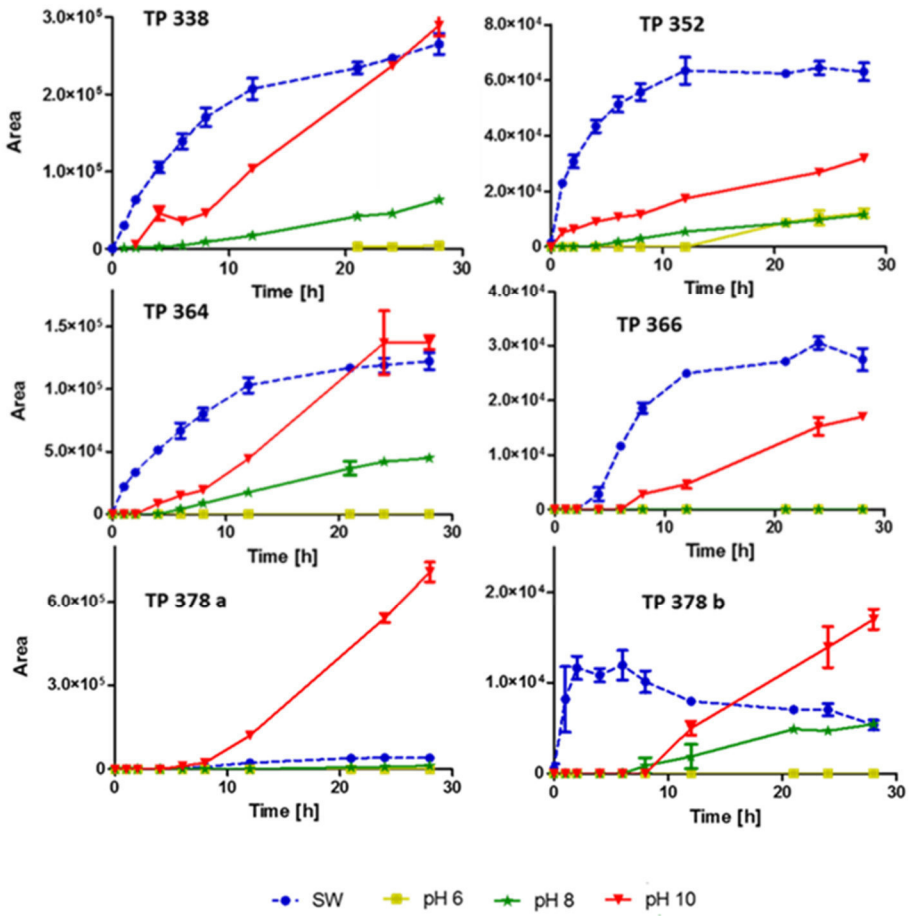

360

361 Figure 5: Progress of transformation products formation by *N*-acylation with aldehydes during direct
362 photolysis pH 6, 8, and 10 and during indirect photolysis (SW). Note the different scales of y-axes.

363

Uptake and transformation of FLX in zebrafish embryos

The concentration of FLX in zebrafish embryos (*D. rerio*) exposed to 5 mg/L of FLX HCl for 48 h was in average 472 mg/L (n=3), assuming a volume of 500 nl per embryo[36]. The bioconcentration factor (BCF) of FLX was 200, and 1% of FLX taken up by the embryos was transformed to NFLX (4.8 mg/L). In literature, the BCF values reported for FLX vary considerably, depending on organism, concentration, pH, time and transformation rate to NFLX[52,53]. Nakamura et al. (2008) postulated BCFs of 8.8, 30, and 260 in the whole body and 330, 580, and 3100 in the liver of Japanese medaka (*Oryzias latipes*) juveniles at pH 7, 8, and 9, respectively. Pseudo BCFs for FLX metabolized to NFLX were up to ten times higher than the BCFs mentioned for FLX. In our study, a BCF of 200 at pH 7.8 was in the same range for zebrafish embryos, but with less transformation to NFLX than in medaka found by Nakamura et al. (2018)[53]. A possible explanation for this observation could be an impaired biotransformation due to the high (5 mg/L) FLX concentration. On the one hand, FLX has been shown to inhibit FLX metabolizing enzymes in human[22,54], and, on the other hand, further in-house experiments demonstrated acute toxicity by FLX at slightly higher test concentrations (approx. > 7 mg/L; details not shown).

In zebrafish embryos, three new metabolites and seven metabolites already described as TPs formed by photolysis were identified (Section 3.2). The already identified (photolysis) *N*-acylated TPs 338, 364, 352, and 410, could be confirmed in zebra fish embryos. TP 338 dominated with intensities one order of magnitude higher than the three other TPs. The detection of TFMP at an average of 300 µg/L in zebra fish embryos showed transformation of FLX by C-O cleavage. Exposed and non-exposed zebra fish embryos showed the same concentration of TFA (average 240 µg/L), which was, therefore, not related to the exposure to FLX. Potential contamination of the test media for exposed and non-exposed fish embryos by TFA is a possible explanation for the observed concentrations. However, the medium was not analyzed for TFA. TP 326c, 409 and 324 were identified, which, to the best of our knowledge, have never been described before. In addition to the hydroxy-FLX TPs 326a and 326b, a third TP 326c was

identified in zebra fish embryos with the highest abundance among all three TPs 326. Based on the increased retention time observed in comparison to TPs 326a and 326b, TP 326c is assumed to be the hydroxylamine derivative of FLX (Figure 6). This is further supported by the occurrence of an abundant fragment with *m/z* 60.0446 $(C_2H_6NO)^+$ compared to *m/z* 44.0486 $(C_2H_6N)^+$ for TPs 326a and 326b. For TP 409 with the exact mass of *m/z* 409.2071, the chemical formula $C_{22}H_{27}F_3N_2O_2$ could be assigned. TP 409 can be an *N*-acylation product of L-valine (Figure 6), which is deduced by Mishra et al. (2017)[55], who detected L-valine as a metabolite of FLX in zebrafish embryos. A modification of the propylamine side chain of FLX was confirmed by the appearance of the IF *m/z* 247.1799 and the fragment *m/z* 143.1178 $(C_7H_{15}N_2O)^+$. For the TP with *m/z* 324.157, methylation of FLX was assumed with the proposed formula $C_{18}H_{20}F_3NO$ (Figure 6). Evidence for TP 324 was once more the IF (*m/z* 162.1263)$^+$ and modification of fragment *m/z* 44.05 to 58.0657 $(C_3H_8N)^+$.

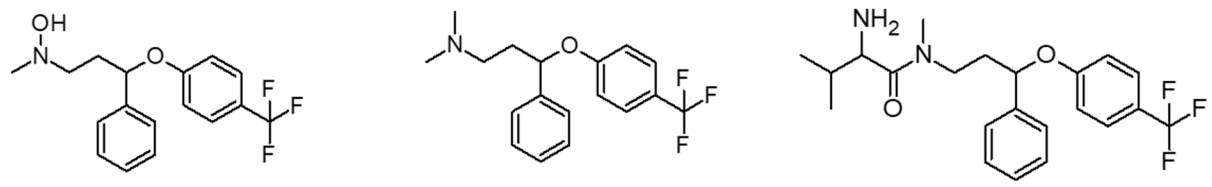

TP 326c ($C_{17}H_{18}F_3NO_2$) TP 324 ($C_{18}H_{20}F_3NO$) TP 409 ($C_{22}H_{27}F_3N_2O_2$)

Figure 6: Proposed structures of metabolites unique to metabolism in zebrafish (*Danio rerio*) embryos, which were not detected as TPs in the photolysis experiments.

Environmental implications

The present investigation illustrates the susceptibility of FLX to photodegradation with a predominance of pathways of *O*-dealkylation, hydroxylation, oxidation of the CF_3-group and *N*-acylation. A higher abundance of most of the TPs in the experiments with surface water than in experiments with ultrapure water underlines the environmental significance of our study. The formation of 27 different TPs, along with low concentrations of NFLX, highlights the importance of considering a broad range of TPs in

abiotic FLX degradation processes. In general, TPs may be more toxic than their respective parent compounds, which is confirmed for NFLX[6,22,23]. The study also demonstrated similarities between abiotic and biotic degradation of FLX. TPs formed by hydroxylation and *N*-acetylation in photochemical reactions corresponded to metabolites formed by biotic transformation (metabolism) in fish. In contrast, metabolite characterized by an attached amine group was only detected in fish embryo extracts, whereas C-O cleavage TPs were predominant in photolysis. Further research should be undertaken to reveal the dead-end degradation products after FLX photodegradation, which could also play an important role in the environment. The present study suggests TFA to be one of these.

Acknowledgement

This research was performed within the framework of the project "Effect Network in Water Research" funded by the Ministry of Science, Research and Art (grants number 33-5733-25-11t32/2) of the Land Baden-Württemberg, Germany. The authors thank Clarissa Glaser for providing data of the river Ammer.

Associated content

Supporting information. Tables showing general information about the operating parameters. Figures showing the progress over time of the TPs during photolysis. In addition, a list of all identified TPs, including MS/MS data, confidence level, formula and attributed reactions, is given.

References

(1) *Health at a Glance 2017*; OECD, 2017.

(2) Agency for Healthcare Research and Quality (AHRQ). The Top 200 of 2018: Provided by the ClinCalc DrugStats Database. http://clincalc.com/DrugStats/Top200Drugs.aspx (accessed September 20, 2018).

(3) Hiemke, C.; Härtter, S. Pharmacokinetics of selective serotonin reuptake inhibitors. *Pharmacology & Therapeutics* **2000**, *85*, 11–28.

(4) Benfield, P.; Heel, R. C.; Lewis, S. P. Fluoxetine. A review of its pharmacodynamic and pharmacokinetic properties, and therapeutic efficacy in depressive illness. *Drugs* **1986**, *32*, 481–508.

(5) Convention, U. S. P. *USP DI. Volume 1, Volume 1*; Thomson/MICROMEDEX: Greenwood Village, CO, 2006.

(6) Nałecz-Jawecki, G. Evaluation of the in vitro biotransformation of fluoxetine with HPLC, mass spectrometry and ecotoxicological tests. *Chemosphere* **2007**, *70*, 29–35.

(7) Bueno, M.; Agüera, A.; Gomez Ramos, M. J.; Dolores Hernando, M.; Garcia-Reyes, J. F.; Fernández-Alba, A. Application of Liquid Chromatography/Quadrupole-Linear Ion Trap Mass Spectrometry and Time-of-Flight Mass Spectrometry to the Determination of Pharmaceuticals and Related Contaminants in Wastewater. *Analytical Chemistry* **2007**, *79,* DOI: 10.1021/ac0715672.

(8) Baker, D. R.; Kasprzyk-Hordern, B. Spatial and temporal occurrence of pharmaceuticals and illicit drugs in the aqueous environment and during wastewater treatment: New developments. *Science of The Total Environment* **2013**, *454-455*, 442–456.

(9) Metcalfe, C. D.; Miao, X.-S.; Koenig, B. G.; Struger, J. Distribution of acidic and neutral drugs in surface waters near sewage treatment plants in the lower Great Lakes, Canada. *Environmental Toxicology and Chemistry* **2003**, *22*, 2881–2889.

(10) Bringolf, R. B.; Heltsley, R. M.; Newton, T. J.; Eads, C. B.; Fraley, S. J.; Shea, D.; Cope, W. G. ce freshwater mussels. *Environmental Toxicology and Chemistry* **2010**, *29*, 1311–1318.

(11) Nödler, K.; Voutsa, D.; Licha, T. Polar organic micropollutants in the coastal environment of different marine systems. *Marine Pollution Pulletin* **2014**, *85*, 50–59.

(12) Schultz, M. M.; Furlong, E. T.; Kolpin, D. W.; Werner, S. L.; Schoenfuss, H. L.; Barber, L. B.; Blazer, V. S.; Norris, D. O.; Vajda, A. M. Antidepressant Pharmaceuticals in Two U.S. Effluent-Impacted Streams:

Occurrence and Fate in Water and Sediment, and Selective Uptake in Fish Neural Tissue. *Environmental Science & Technology* **2010**, *44*, 1918–1925.

(13) Barry, M. J. Effects of fluoxetine on the swimming and behavioural responses of the Arabian killifish. *Ecotoxicology* **2013**, *22*, 425–432.

(14) Lynn, S. E.; Egar, J. M.; Walker, B. G.; Sperry, T. S.; Ramenofsky, M. Fish on Prozac: A simple, noninvasive physiology laboratory investigating the mechanisms of aggressive behavior in Betta splendens. *Advances in Physiology Education* **2007**, *31*, 358–363.

(15) Kohlert, J. G.; Mangan, B. P.; Kodra, C.; Drako, L.; Long, E.; Simpson, H. Decreased aggressive and locomotor behaviors in Betta splendens after exposure to fluoxetine. *Psychological Reports* **2012**, *110*, 51–62.

(16) Dzieweczynski, T. L.; Hebert, O. L. Fluoxetine alters behavioral consistency of aggression and courtship in male Siamese fighting fish, Betta splendens. *Physiology & Behavior* **2012**, *107*, 92–97.

(17) Mennigen, J. A.; Sassine, J.; Trudeau, V. L.; Moon, T. W. Waterborne fluoxetine disrupts feeding and energy metabolism in the goldfish Carassius auratus. *Aquatic Toxicology* **2010**, *100*, 128–137.

(18) Schultz, M. M.; Painter, M. M.; Bartell, S. E.; Logue, A.; Furlong, E. T.; Werner, S. L.; Schoenfuss, H. L. Selective uptake and biological consequences of environmentally relevant antidepressant pharmaceutical exposures on male fathead minnows. *Aquatic Toxicology* **2011**, *104*, 38–47.

(19) Brodin, T.; Piovano, S.; Fick, J.; Klaminder, J.; Heynen, M.; Jonsson, M. Ecological effects of pharmaceuticals in aquatic systems--impacts through behavioural alterations. *Philosophical Transactions of the Royal Society of London. Series B, Biological sciences* **2014**, *369,* DOI: 10.1098/rstb.2013.0580.

(20) Silva, L. J.G.; Lino, C. M.; Meisel, L. M.; Pena, A. Selective serotonin re-uptake inhibitors (SSRIs) in the aquatic environment: An ecopharmacovigilance approach. *Science of The Total Environment* **2012**, *437*, 185–195.

(21) Lazzara, R.; Blázquez, M.; Porte, C.; Barata, C. Low environmental levels of fluoxetine induce spawning and changes in endogenous estradiol levels in the zebra mussel Dreissena polymorpha. *Aquatic Toxicology* **2012**, *106-107*, 123–130.

(22) Stokes, P. E.; Holtz, A. Fluoxetine tenth anniversary update: The progress continues. *Clinical Therapeutics* **1997**, *19*, 1135–1250.

(23) Andrés-Costa, M. J.; Proctor, K.; Sabatini, M. T.; Gee, A. P.; Lewis, S. E.; Pico, Y.; Kasprzyk-Hordern, B. Enantioselective transformation of fluoxetine in water and its ecotoxicological relevance. *Scientific Reports* **2017**, *7*, 15777.

(24) Herrmann, M.; Menz, J.; Olsson, O.; Kümmerer, K. Identification of phototransformation products of the antiepileptic drug gabapentin: Biodegradability and initial assessment of toxicity. *Water Research* **2015**, *85*, 11–21.

(25) Schulze, T.; Weiss, S.; Schymanski, E.; Ohe, P. C. von der; Schmitt-Jansen, M.; Altenburger, R.; Streck, G.; Brack, W. Identification of a phytotoxic photo-transformation product of diclofenac using effect-directed analysis. *Environmental Pollution* **2010**, *158*, 1461–1466.

(26) Wang, X.-H.; Lin, A. Y.-C. Phototransformation of cephalosporin antibiotics in an aqueous environment results in higher toxicity. *Environmental Science & Technology* **2012**, *46*, 12417–12426.

(27) Silva, V. H. O.; Dos Santos Batista, A. P.; Silva Costa Teixeira, A. C.; Borrely, S. I. Degradation and acute toxicity removal of the antidepressant Fluoxetine (Prozac(®)) in aqueous systems by electron beam irradiation. *Environmental Science and Pollution Research International* **2016**, *23*, 11927–11936.

(28) Zhao, Y.; Yu, G.; Chen, S.; Zhang, S.; Wang, B.; Huang, J.; Deng, S.; Wang, Y. Ozonation of antidepressant fluoxetine and its metabolite product norfluoxetine: Kinetics, intermediates and toxicity. *Chemical Engineering Journal* **2017**, *316*, 951–963.

(29) Lam, M. W.; Young, C. J.; Mabury, S. A. Aqueous Photochemical Reaction Kinetics and Transformations of Fluoxetine. *Environmental Science & Technology* **2005**, *39*, 513–522.

(30) Méndez-Arriaga, F.; Otsu, T.; Oyama, T.; Gimenez, J.; Esplugas, S.; Hidaka, H.; Serpone, N. Photooxidation of the antidepressant drug Fluoxetine (Prozac®) in aqueous media by hybrid catalytic/ozonation processes. *Water Research* **2011**, *45*, 2782–2794.

(31) Gulde, R.; Meier, U.; Schymanski, E. L.; Kohler, H.-P. E.; Helbling, D. E.; Derrer, S.; Rentsch, D.; Fenner, K. Systematic Exploration of Biotransformation Reactions of Amine-Containing Micropollutants in Activated Sludge. *Environmental Science & Technology* **2016**, *50*, 2908–2920.

(32) Bussy, U.; Boujtita, M. Advances in the electrochemical simulation of oxidation reactions mediated by cytochrome p450. *Chemical Research in Toxicology* **2014**, *27*, 1652–1668.

(33) Tisler, S.; Zwiener, C. Aerobic and anaerobic formation and biodegradation of guanyl urea and other transformation products of metformin. *Water Research* **2019**, *149*, 130–135.

(34) Souza Anselmo, C. de; Sardela, V. F.; Sousa, V. P. de; Pereira, H. M. G. Zebrafish (Danio rerio): A valuable tool for predicting the metabolism of xenobiotics in humans? *Comparative Biochemistry and Physiology. Toxicology & Pharmacology : CBP* **2018**, *212*, 34–46.

(35) Lammer, E.; Carr, G. J.; Wendler, K.; Rawlings, J. M.; Belanger, S. E.; Braunbeck, T. Is the fish embryo toxicity test (FET) with the zebrafish (Danio rerio) a potential alternative for the fish acute toxicity test? *Comparative Biochemistry and Physiology. Toxicology & Pharmacology : CBP* **2009**, *149*, 196–209.

(36) Brox, S.; Seiwert, B.; Küster, E.; Reemtsma, T. Toxicokinetics of Polar Chemicals in Zebrafish Embryo (Danio rerio): Influence of Physicochemical Properties and of Biological Processes. *Environmental Science & Technology* **2016**, *50*, 10264–10272.

(37) Scheurer, M.; Nödler, K.; Freeling, F.; Janda, J.; Happel, O.; Riegel, M.; Müller, U.; Storck, F. R.; Fleig, M.; Lange, F. T. *et al.* Small, mobile, persistent: Trifluoroacetate in the water cycle - Overlooked sources, pathways, and consequences for drinking water supply. *Water Research* **2017**, *126*, 460–471.

(38) Schymanski, E. L.; Jeon, J.; Gulde, R.; Fenner, K.; Ruff, M.; Singer, H. P.; Hollender, J. Identifying small molecules via high resolution mass spectrometry: Communicating confidence. *Environmental Science & Technology* **2014**, *48*, 2097–2098.

(39) Zhang, Y.; Zhang, J.; Xiao, Y.; Chang, V. W. C.; Lim, T.-T. Direct and indirect photodegradation pathways of cytostatic drugs under UV germicidal irradiation: Process kinetics and influences of water matrix species and oxidant dosing. *Journal of Hazardous Materials* **2017**, *324*, 481–488.

(40) Chen, Y.; Zhang, K.; Zuo, Y. Direct and indirect photodegradation of estriol in the presence of humic acid, nitrate and iron complexes in water solutions. *The Science of the Total Environment* **2013**, *463-464*, 802–809.

(41) Kwon, J.-W.; Armbrust, K. L. LABORATORY PERSISTENCE AND FATE OF FLUOXETINE IN AQUATIC ENVIRONMENTS. *Environ Toxicol Chem* **2006**, *25*, 2561.

(42) Ellis, D. A.; Mabury, S. A. The Aqueous Photolysis of TFM and Related Trifluoromethylphenols. An Alternate Source of Trifluoroacetic Acid in the Environment. *Environmental Science & Technology* **2000**, *34*, 632–637.

(43) Wawryniuk, M.; Drobniewska, A.; Sikorska, K.; Nałęcz-Jawecki, G. Influence of photolabile pharmaceuticals on the photodegradation and toxicity of fluoxetine and fluvoxamine. *Environmental Science and Pollution Research International* **2018**, *25*, 6890–6898.

(44) Drzewicz, P.; Drobniewska, A.; Sikorska, K.; Nałęcz-Jawecki, G. Analytical and ecotoxicological studies on degradation of fluoxetine and fluvoxamine by potassium ferrate. *Environmental Technology* **2018**, 1–11.

(45) Boscá, F.; Cuquerella, M. C.; Marín, M. L.; Miranda, M. A. Photochemistry of 2-hydroxy-4-trifluoromethylbenzoic acid, major metabolite of the photosensitizing platelet antiaggregant drug triflusal. *Photochemistry and Photobiology* **2001**, *73*, 463–468.

(46) Merel, S.; Lege, S.; Yanez Heras, J. E.; Zwiener, C. Assessment of N-Oxide Formation during Wastewater Ozonation. *Environmental Science & Technology* **2017**, *51*, 410–417.

(47) Choudhary, C.; Weinert, B. T.; Nishida, Y.; Verdin, E.; Mann, M. The growing landscape of lysine acetylation links metabolism and cell signalling. *Nature Reviews. Molecular Cell Biology* **2014**, *15*, 536–550.

(48) Peña, R. M.; García, S.; Herrero, C.; Losada, M.; Vázquez, A.; Lucas, T. Organic acids and aldehydes in rainwater in a northwest region of Spain. *Atmospheric Environment* **2002**, *36*, 5277–5288.

(49) Altemose, B.; Gong, J.; Zhu, T.; Hu, M.; Zhang, L.; Cheng, H.; Zhang, L.; Tong, J.; Kipen, H. M.; Strickland, P. O. *et al.* Aldehydes in Relation to Air Pollution Sources: A Case Study around the Beijing Olympics. *Atmospheric Environment* **2015**, *109*, 61–69.

(50) Röhrl, A.; Lammel, G. Determination of malic acid and other C4 dicarboxylic acids in atmospheric aerosol samples. *Chemosphere* **2002**, *46*, 1195–1199.

(51) Dąbrowska, A.; Nawrocki, J.; Szeląg-Wasielewska, E. Appearance of aldehydes in the surface layer of lake waters. *Environmental Monitoring and Assessment* **2014**, *186*, 4569–4580.

(52) Pan, C.; Yang, M.; Xu, H.; Xu, B.; Jiang, L.; Wu, M. Tissue bioconcentration and effects of fluoxetine in zebrafish (Danio rerio) and red crucian cap (Carassius auratus) after short-term and long-term exposure. *Chemosphere* **2018**, *205*, 8–14.

(53) Nakamura, Y.; Yamamoto, H.; Sekizawa, J.; Kondo, T.; Hirai, N.; Tatarazako, N. The effects of pH on fluoxetine in Japanese medaka (Oryzias latipes): Acute toxicity in fish larvae and bioaccumulation in juvenile fish. *Chemosphere* **2008**, *70*, 865–873.

(54) Jeppesen, U.; Gram, L. F.; Vistisen, K.; Loft, S.; Poulsen, H. E.; Brøsen, K. Dose-dependent inhibition of CYP1A2, CYP2C19 and CYP2D6 by citalopram, fluoxetine, fluvoxamine and paroxetine. *European Journal of Clinical Pharmacology* **1996**, *51*, 73–78.

(55) Mishra, P.; Gong, Z.; Kelly, B. C. Assessing biological effects of fluoxetine in developing zebrafish embryos using gas chromatography-mass spectrometry based metabolomics. *Chemosphere* **2017**, *188*, 157–167.

Supplementary Information

Transformation products of fluoxetine formed by photodegradation in water and biodegradation in zebrafish embryos

Selina Tisler[1], Florian Zindler[2], Finnian Freeling[3], Karsten Nödler[3], László Toelgyesi[4], Thomas Braunbeck[2], Christian Zwiener[1]

[1]Environmental Analytical Chemistry, ZAG, University of Tübingen, Germany

[2]Aquatic Ecology & Toxicology, Centre for Organismal Studies, University of Heidelberg, Germany

[3]TZW: DVGW-Technologiezentrum Wasser

[4]Agilent Technologies, Waldbronn, Germany

Table of Contents

S.1 General information

Table S 1: Parameters of the Ammer river (water used for indirect photolysis).

Parameter	**Value**
Chloride	67 mg/L
Nitrate	31 mg/L
Sulfate	288 mg/L
DOC	2.35 mg/L
pH	8.3
Conductivity (temperature-compensated)	1235 µS/cm

Table S 2: Matrices tested for photochemical FLX-degradation and resulting speciation of FLX.

Experiment name	**Matrix**	**pH value**		**Fraction of the**
		Start	**End**	**protonated (i. e.**
		t = 0 h	**t = 28 h**	**cationic) species***
pH 6	H_2O + phosphate buffer	6.0	6.0	1
pH 8	H_2O + phosphate buffer	8.3	8.3	0.95
pH 10	H_2O + phosphate buffer	9.8	9.8	0.37
Surface water (SW)	Surface water	8.3	7.7	0.95

*using pK_a of FLX (corresponding acid) = 9.6 (ACD/pKa GALAS model, ACD/Percepta, ACD/Labs Release 2016.2)

Table S 3: Operating parameters of the quadrupole time of flight MS (Agilent 6550 QTOF) in positive and negative mode.

Parameter	**Set point**
Gas temperature	150 °C
Gas flow	16 L/min
Nebulizer gas pressure	40 psi
Sheath gas heater	350 °C
Sheath gas flow	12 l/min
Capillary voltage	3200 V
Nozzle voltage	300 V

Table S 4: Operating parameters of the triple quadrupole MS (Agilent 6490 QqQ) in positive mode.

Parameter	**Set point**
Gas temperature	250 °C
Gas flow	14 L/min
Nebulizer gas pressure	45 psi
Sheath gas heater	300 °C
Sheath gas flow	12 L/min
Capillary voltage	3500 V
Nozzle voltage	0 V

Table S 5: MRM transitions and retention times of FLX (fluoxetine); FLX-d5 (deuterated FLX); NFLX (norfluoxetine) and α-[2-(methylamino)ethyl]benzyl alcohol (TP 166). Collision cell accelerator voltage was 5 V for each transition.

	FLX	FLX-d5	NFLX	TP 166
Precursor ion (m/z)	310	315	296	166
Product ion (Quan/Qual) (m/z)	148.1/43.9	143/43.9	134/30	148/43.9
Collision energy (setpoint in V)	5/20	5/15	0/10	5/15
Retention time (min)	6.6	6.6	8.2	2.0

Table S 6: Intraday variations (RSD) with 1 µg/L standard and Limit of quantification (LOQ) of FLX, NFLX, TP 166 refer to QqQ. LOQ is calculated with a signal to noise ratio higher than 10.

	RSD [%]	LOQ [ng/L]
	(n=4)	
FLX	8	10
NFLX	10	100
TP 166	5	10

S. 2 FLX degradation

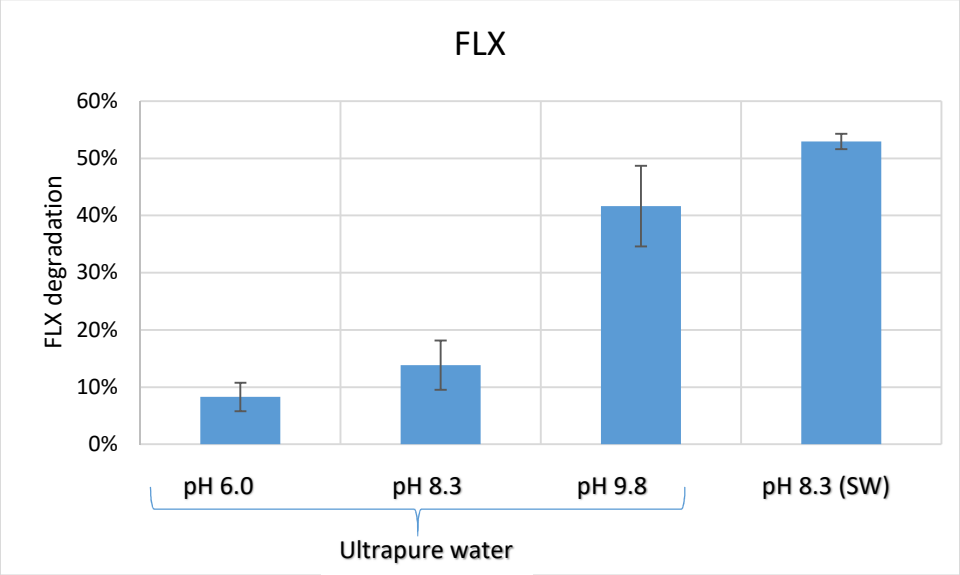

Figure S 1: FLX degradation for direct photolysis (experiments based on ultrapure water) and indirect photolysis (SW) after 28 h.

Table S 7: FLX degradation during photolysis (µmol/L and %) and formation of NFLX and TP 166 absolute (µg/L and µmol/L) and relative to µmol/L FLX degradation.

	FLX		NFLX 28 h			TP 166 28 h		
	c [µmol/L]	degradation [%]	*ß* [µg/L]	c [µmol/L]	% of FLX	*ß* [µg/L]	c [µmol/L]	% of FLX
SW	28	54	43	0.15	**0.5**	473	2.9	**10**
pH 6	3.6	7	4.5	0.015	**0.4**	110	0.7	**19**
pH 8	8	14	20.1	0.07	**0.9**	119	0.7	**9**
pH 10	22	42	138	0.47	**2.1**	181	1.1	**5**

Table S 8: FLX degradation during photolysis (µmol/L and %) and formation of TFMP and TFA absolute (µg/L and µmol/L) and relative to µmol/L FLX degradation.

	FLX		TFMP 28 h			TFA 28 h		
	c [µmol/L]	degradation [%]	β [µg/L]	c [µmol/L]	% of FLX	β [µg/L]	c [µmol/L]	% of FLX
SW	28	54	1.3	0.008	**0.02**	71	0.44	**1.5**
pH 6	3.6	7	182	1.13	**31**	2	0.01	**0.34**
pH 8	8	14	0.34	0.002	**0.03**	3.3	0.02	**0.26**
pH 10	22	42	9.4	0.06	**0.3**	16	0.1	**0.4**

S. 3 Overview of all TPs

Table S 9: Identified TPs from photodegradation (P) and metabolites from zebrafish embryos (E)

Name	Accurate mass (m/z)	Insource fragments (IF) m/z	Chemical formula	Δppm	Photo(P)/ Embryo (E)	LC-retention time (min)
NFLX	296.1367	134.0966	C16H16F3NO	0	P	4.42
TFMP	161.022		C7H5F3O		P/E	5.02
TP 139 [M-H]	137.024		C7H6O3		P	2.79
TP 146	146.06		C9H7NO	4	P	1.46
TP 148	148.1121	117.07, 91.09	C10H13N	3	P	3.1
TP 150	150.0913		C9H11NO	7	P	2.37
TP 152	152.107		C9H13NO	4	P	1.71
TP 166	166.1226 (+)			3	P	2.21
TP 182a	182.1176			5	P	1.25
TP 182b	182.1176			5	P	1.62
TP 272	272.1281		C16H17NO3	1	P	3.44
TP 286a	286.1438		C17H19NO3	3	P	2.93
	284.1292			0		
TP 286b	286.1438		C17H19NO3	2	P	3.72
TP 286c [M-H]	284.1292		C17H19NO3	0	P	4.33
TP 316a [M-H]	316.119		C17H19NO5	0	P	3.19
TP 316b [M-H]	316.119		C17H19NO5	0	P	3.43
TP 324	324.157	162.1263	C18H20F3NO		E	4.59
TP 326a	326.1367		C17H18F3NO2	4	P/E	4.69
TP 326b	326.1367		C17H18F3NO2	0	P/E	4.9
TP 326c	326.1367		C17H18 F3NO2	0	E	5.51
TP 338	338.1362	176.1074	C18H18F3NO2	0	P/E	6.82
TP 352	352.152	268.1339	C19H20F3NO2	2	P/E	6.87
TP 364	364.1519	202.1221	C20H20F3NO2	1	P/E	6.64
TP 366	366.1672	204.1383	C20H22F3NO2	4	P	5.05
TP 378a	378.1675	216.1385	C21H22F3NO2	1	P	6.42
TP 378b	378.1675		C21H22F3NO2	1	P	6.85
TP 382 [M-H]	380.1115		C19H18F3NO4		P	6.18

TP 396	396.1419	234.1125	C20H21F3NO4	1	P	6.63
TP 408	408.1417	246.1116	C21H20F3NO4	0	P	6.62
TP 409	409.2071	247.1799	C22H27F3N2O2		E	5.68
TP 410	410.1547	248.1285	C21H22F3NO4	0	P/E	6.56

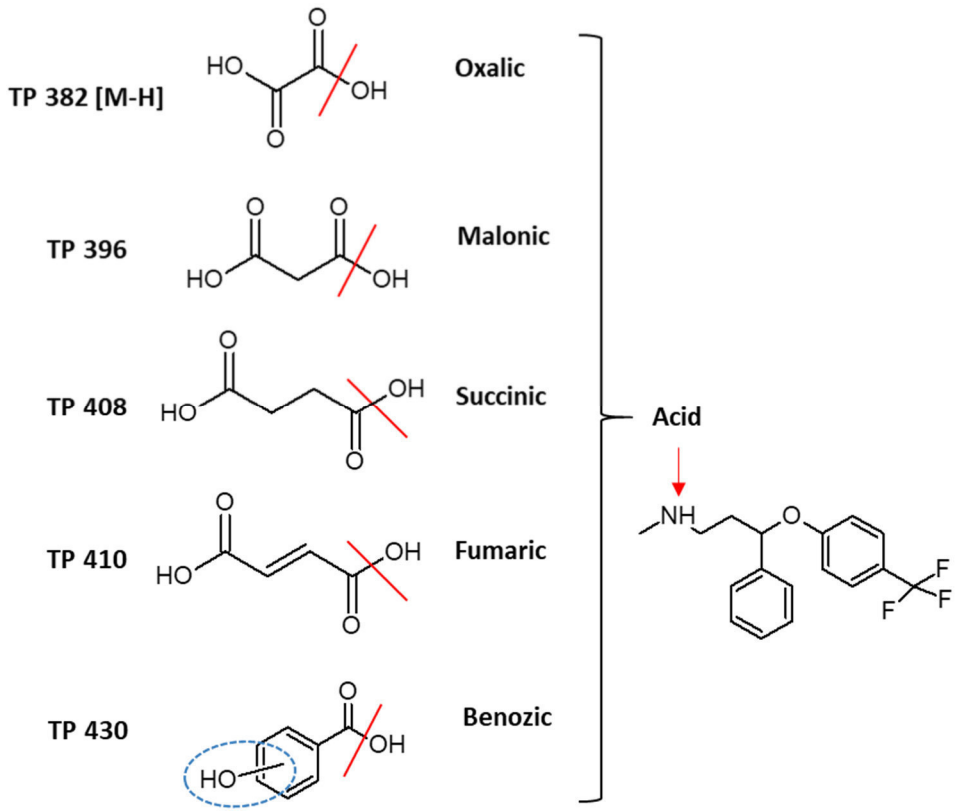

Figure S 2: Formation of transformation products via *N*-acylation of FLX with carboxylic acids. For TP 430 the hydroxylation of the benzyl ring instead of the benzoic acid ring could also be possible.

S. 4 Progress of TPs during photolysis

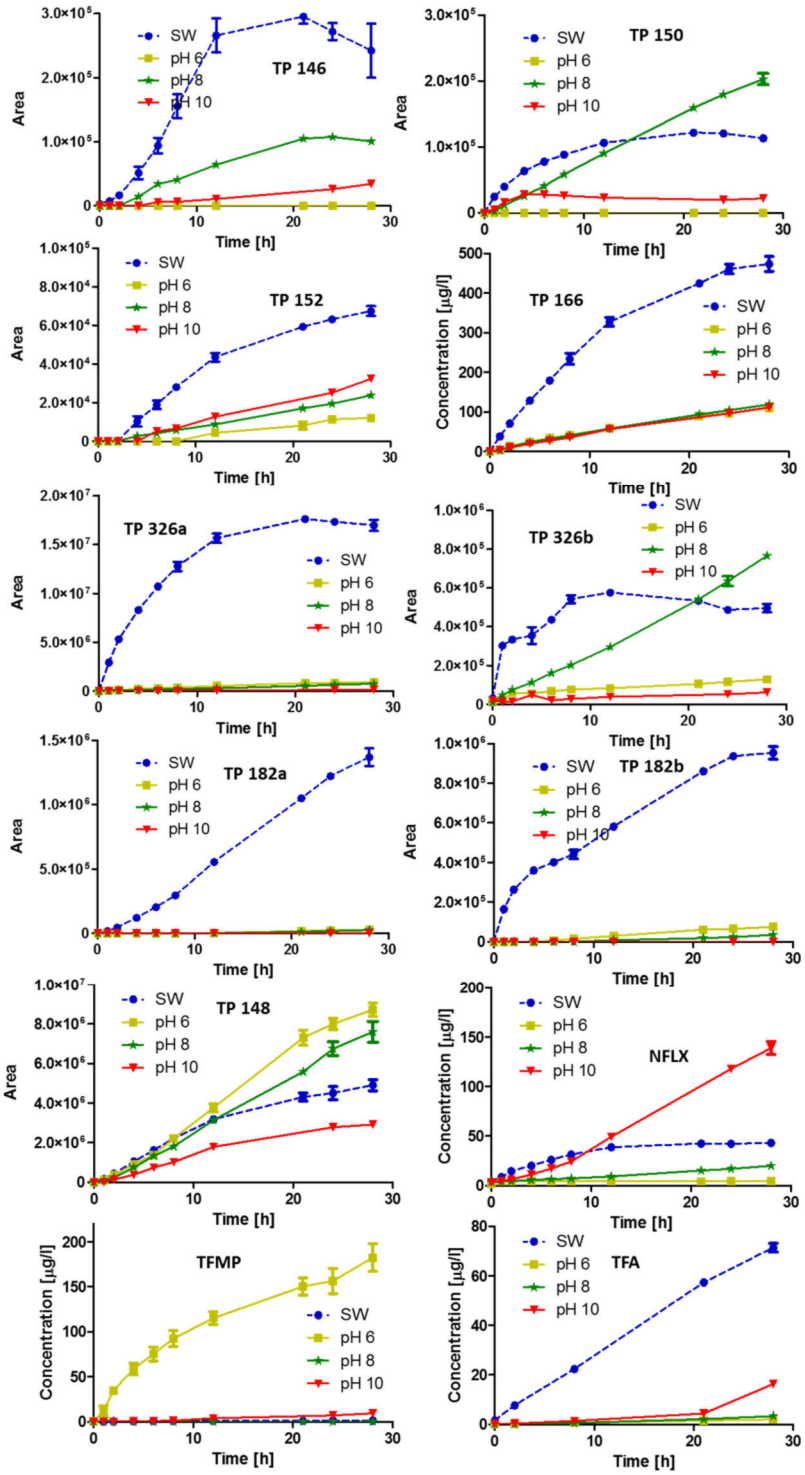

Figure S 3: Progress of transformation products via *O*-dealkylation and/or hydroxylation in direct photolysis experiment (pH 6, 8, and 10) and in indirect photolysis experiment (SW). Note that scalings of y-axes are different. The area of TP 148 is depicted as area of the in source fragment 117.

Normalized peak areas $A_{exp,N}$ of the substances (TPs) for which no analytical standards were available, measurements conducted with LC-QTOF, were calculated as follows for the experimental period of 28 h:

$$A_{exp,N} = \frac{A_{exp}}{\frac{(\%\ degradation,28\ h)}{100}} \quad (1)$$

where A_{exp} is the average measured peak area of a triplicate result set. $A_{exp,N}$ of the four experiments (surface water (SW), pH 6, 8 and 10) were calculated for each TP and the highest $A_{exp,N}$ of each TP was set to 1 and the other three $A_{exp,N}$ were accordingly based on that value.

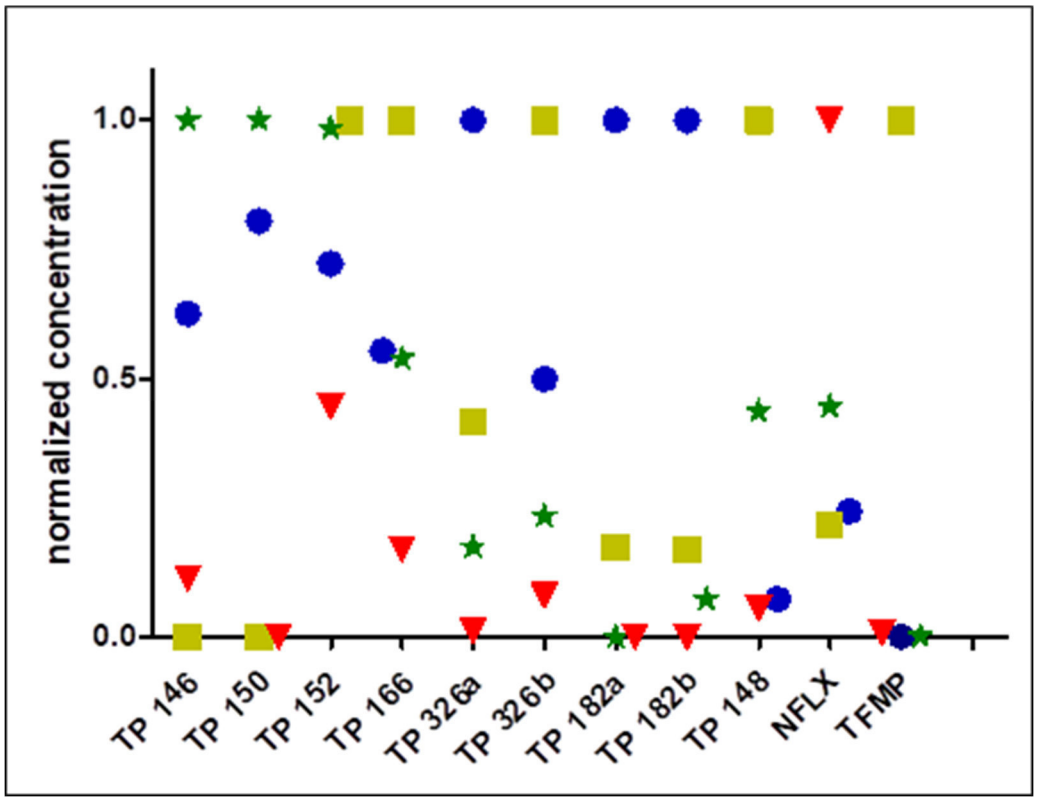

Figure S 4: Normalized concentration of TPs via *O*-dealkylation and/or hydroxylation during direct photolysis (pH 6, 8 and 10) and indirect photolysis (SW) after 28 h.

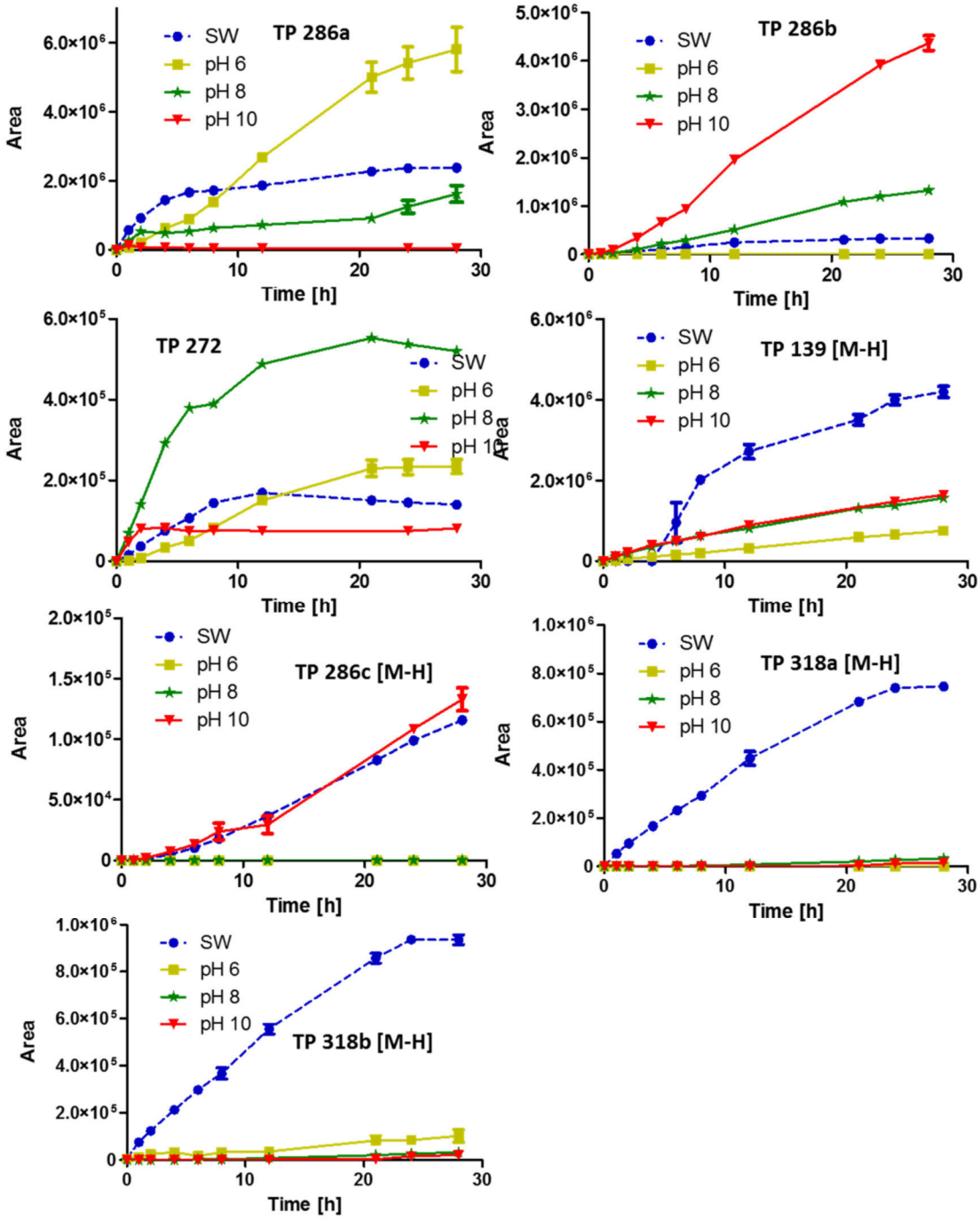

Figure S 5: Progress of transformation products via –CF3 substitution in direct photolysis experiment (pH 6, 8, and 10) and in indirect photolysis experiment (SW). Note that scalings of y-axes are different.

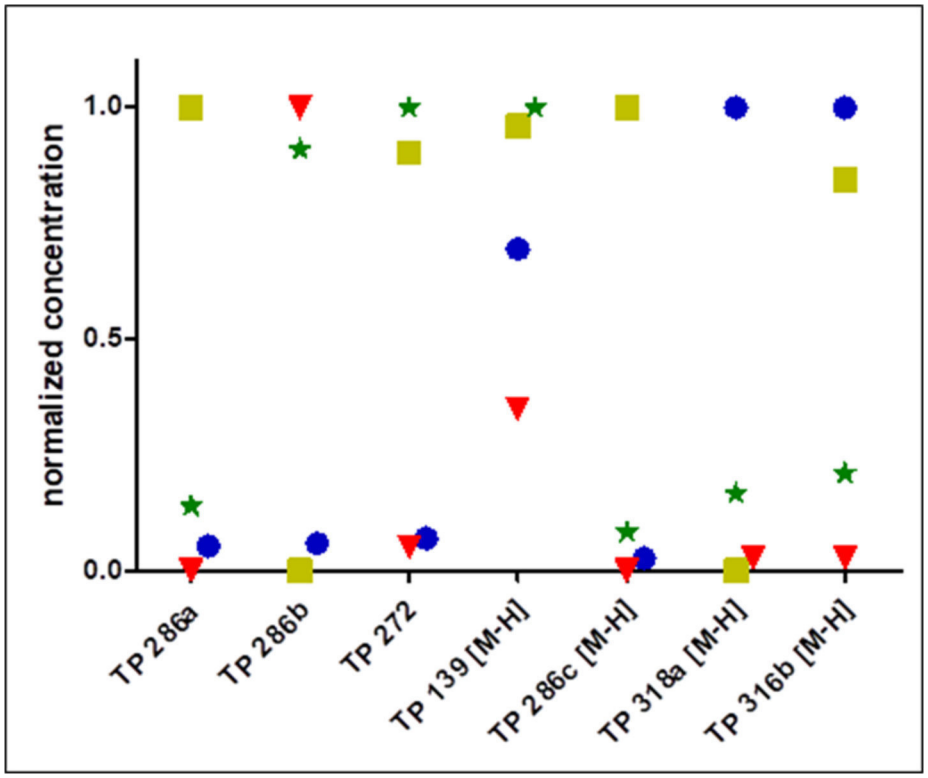

Figure S 6: Normalized peak areas of TPs via –CF3 substitution during direct photolysis (pH 6,8 and 10) and indirect photolysis (SW) after 28 h.

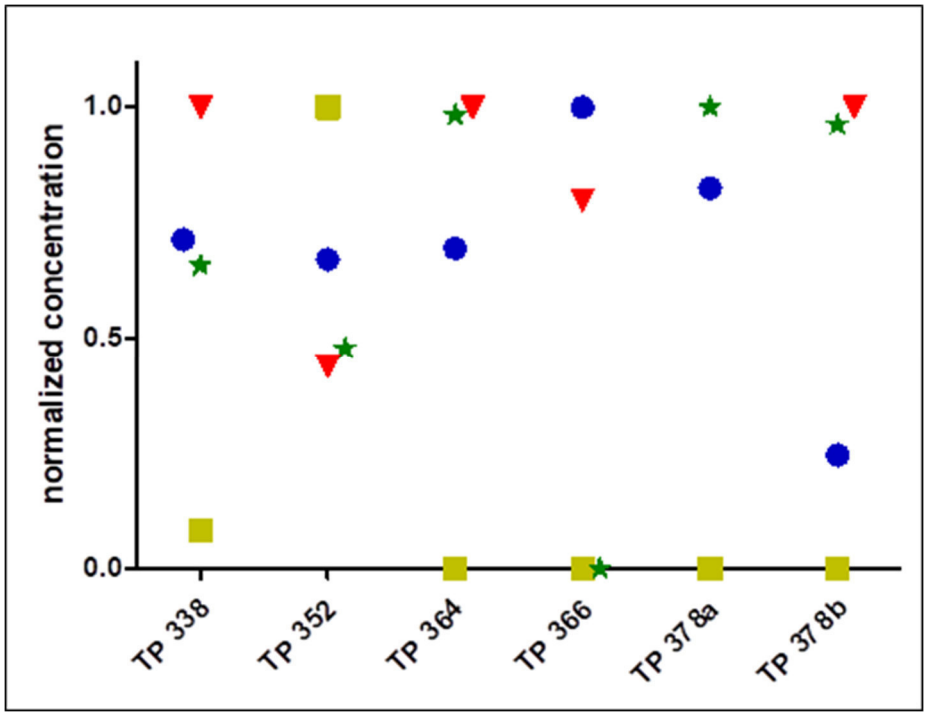

Figure S 7: Normalized peak areas of TPs via N-acylation with aldehydes in direct photolysis (pH 6,8 and 10) and in indirect photolysis experiment (SW) after 28 h.

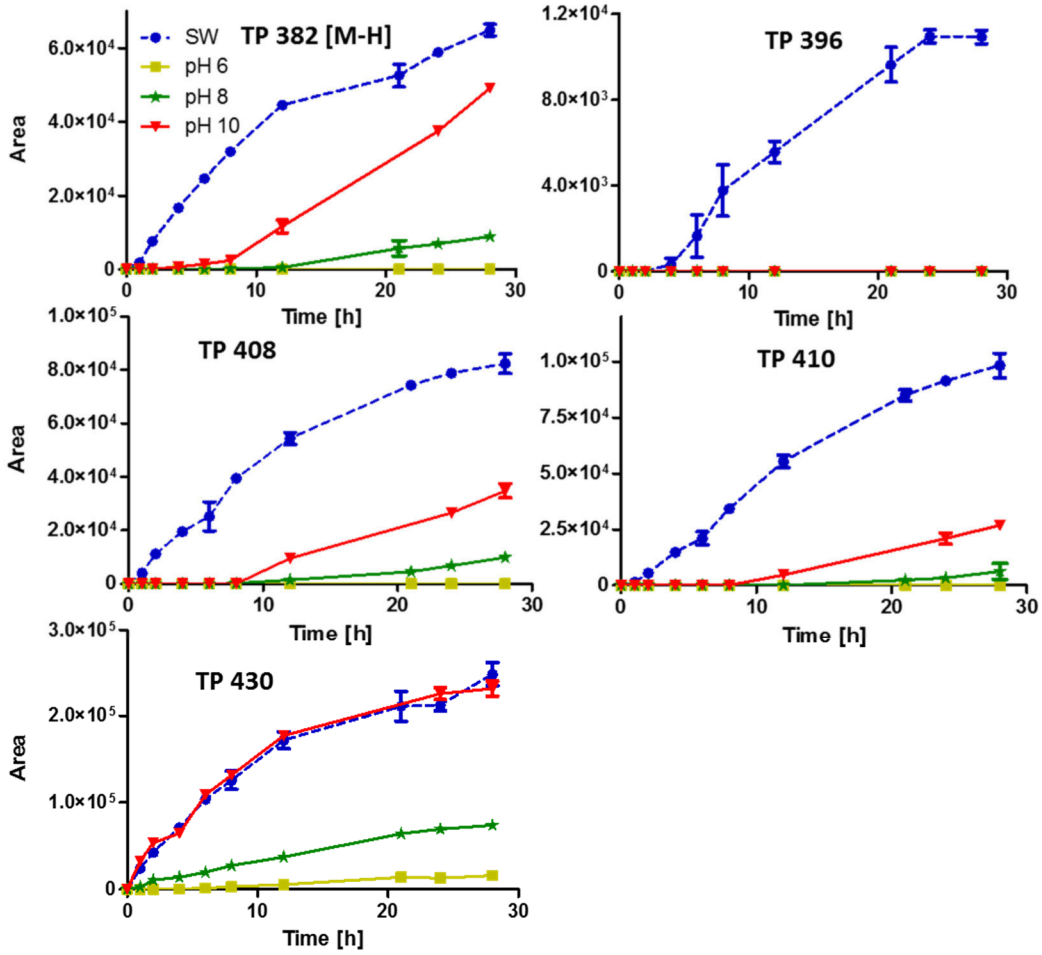

Figure S 8: Progress of transformation products via *N*-acylation with carboxylic acids in direct photolysis experiment (pH 6, 8, and 10) and in indirect photolysis experiment (SW). Note that scalings of y-axes are different.

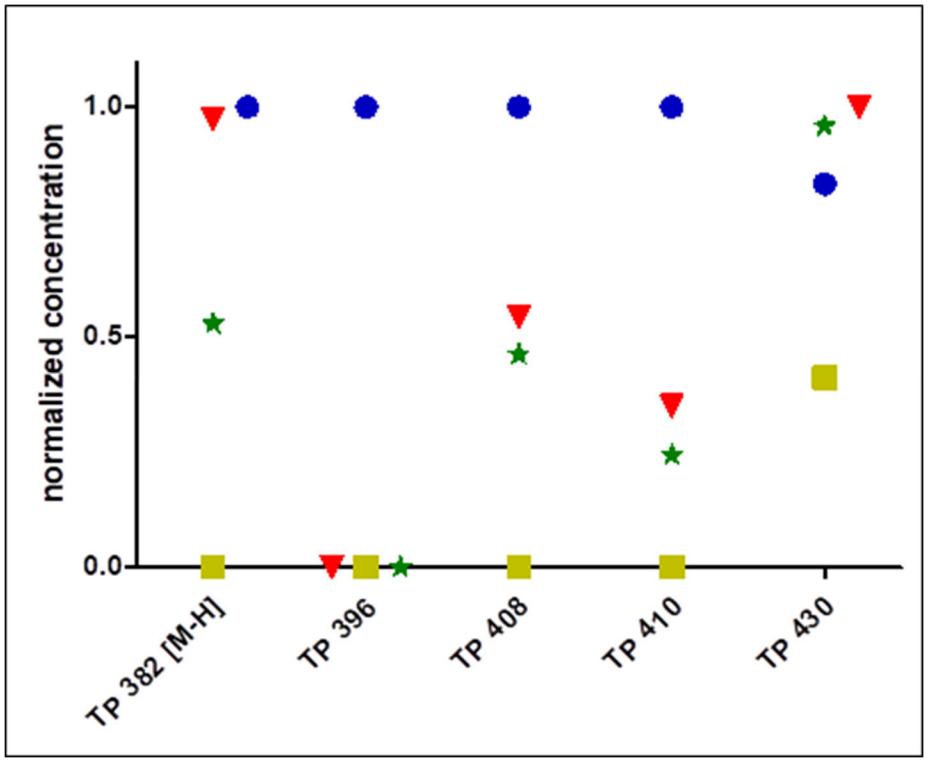

Figure S 9: Progress of the normalized peak areas of TPs via N-acylation with carboxylic acids in direct photolysis (pH 6,8 and 10) and in indirect photolysis (SW) during 28 h.

S. 5 List of all identified TPs

Name: TP 296.1257 (NFLX) (4.42 min)

MS2 Spectra (positive)

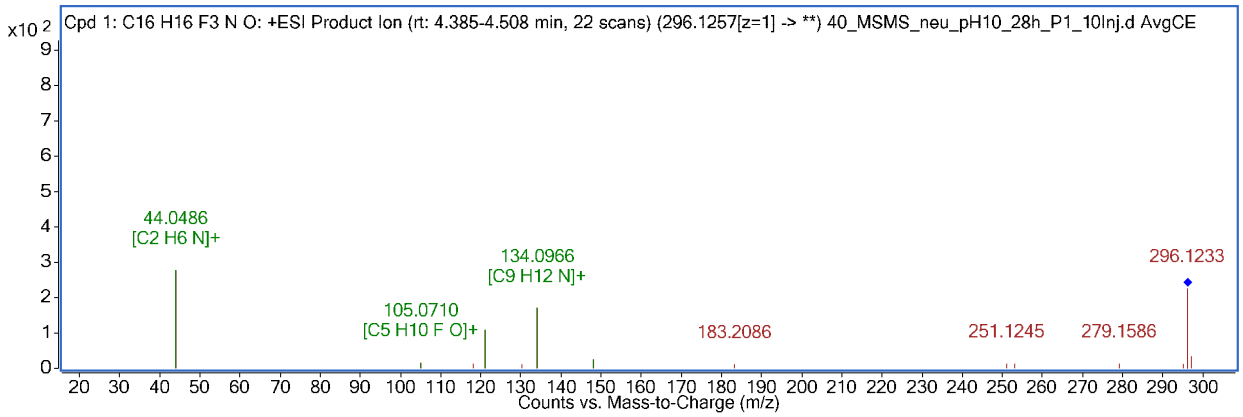

Formula (neutral): C16H16F3NO

Atomic Modification: -CH2

Confidence level: 1

Proposed Structure:

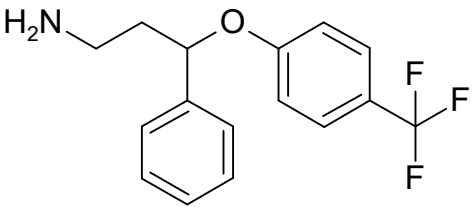

In-source:

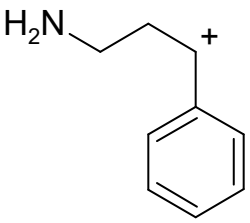

Additional evidence for structure interpretation:

- confirmed with standard

Attributed reaction from the parent compound to this TP:

- demethylation of FLX

Name: TP 161.022 (Trifluormethylphenol) (5.02 min)

MS2 Spectra (negative)

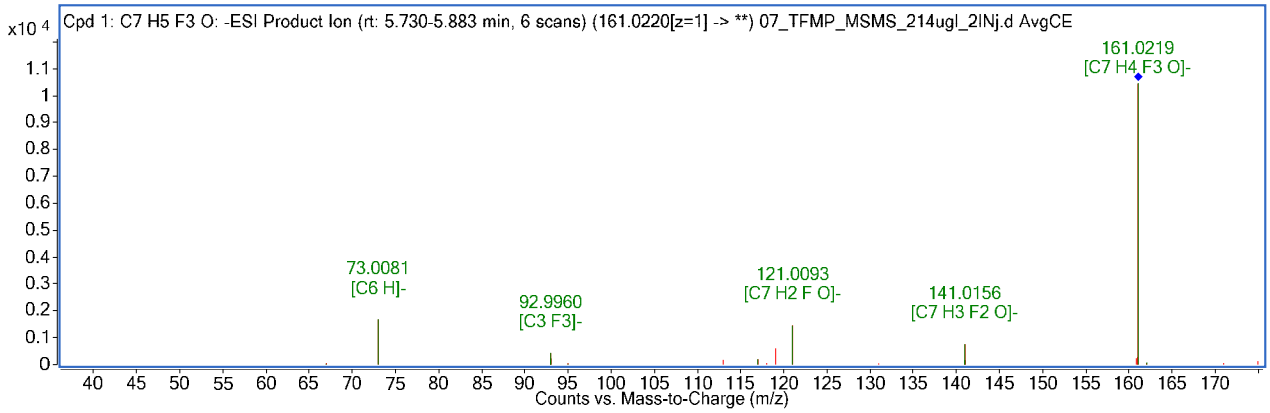

Formula (neutral): C7H5F3O

Atomic modification: – C10H13N

Confidence level: 1

Structure:

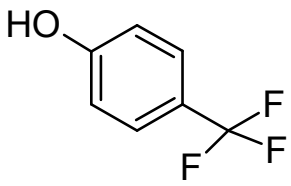

Additional evidence for structure interpretation:

- confirmed with analytical standard

Attributed reaction from the parent compound to this TP:

- cleavage of TFMP

Name: TP 137.024 [M-H] / TP 139 (2.79 min)

MS2 Spectrum (negative)

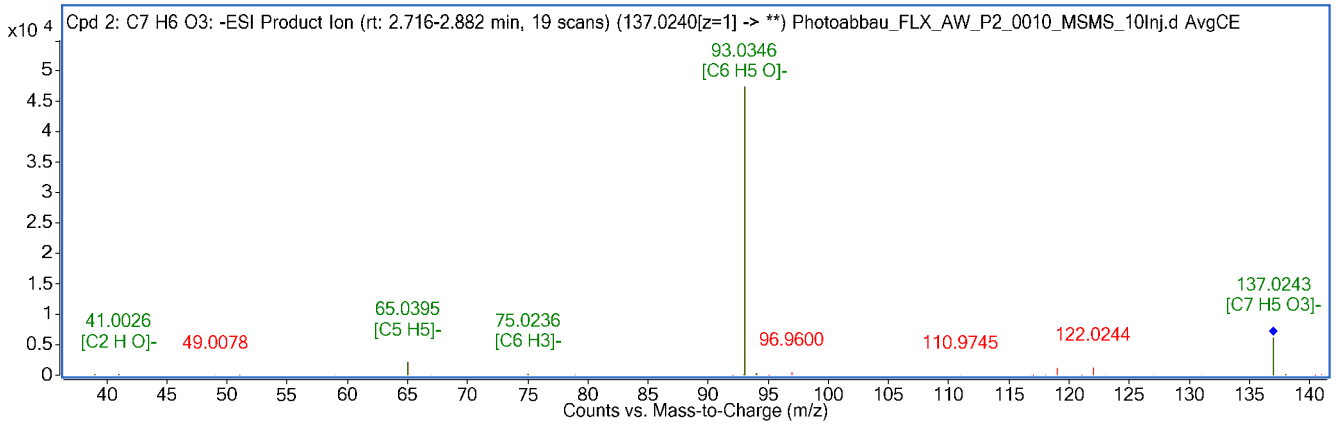

Formula (neutral): C7H6O3

Atomic Modification: -C10H12F3N +O2

Confidence level: 2

Structure:

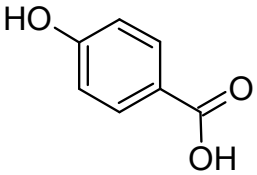

Additional evidence for structure interpretation:

- fragment 93 similar to TP 284
- negative ionization → OH-Group

Attributed reaction from the parent compound to this TP:

- cleavage of TFMP
- CF3 hydrolyzed to –COOH

Name: TP 146.06

MS2 Spectrum (positive)

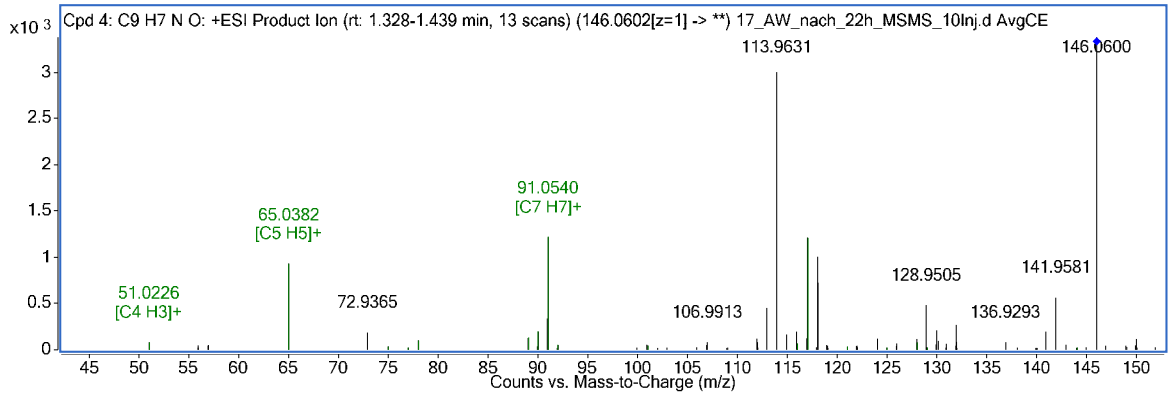

Formula (neutral): C9H7NO

Atomic Modification: -C8H11F3

Confidence level: 2b

(Proposed) Structure:

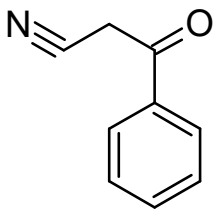

Additional evidence for structure interpretation:

- same fragment m/z 91.0540 than TP 150

Attributed reaction from the parent compound to this TP:

- cleavage of TFMP
- unsaturatio

Name: TP 148.1121 (3.077 min)

MS2 Spectrum (positive)

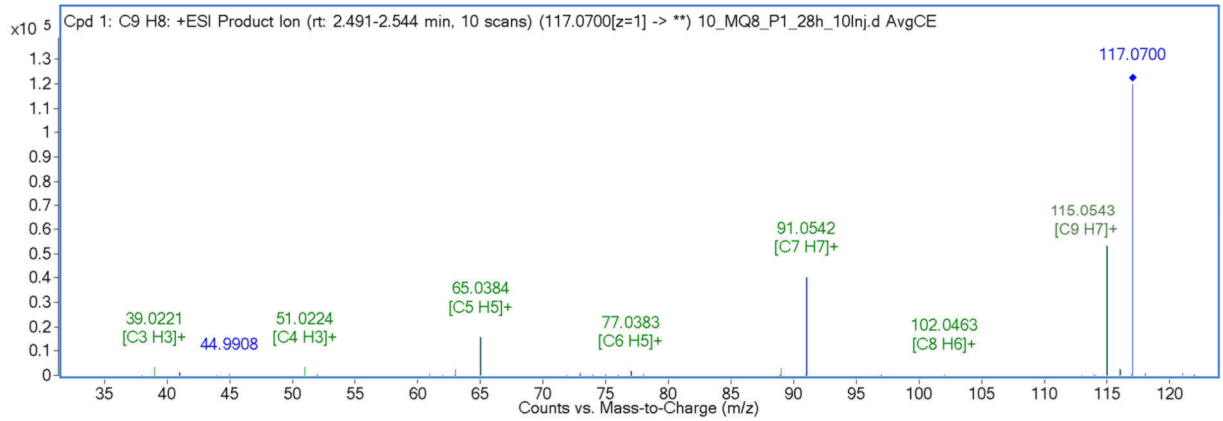

Formula (neutral): C10H13N

Atomic Modification: -C7H5F3O

Confidence level: 2a

Proposed Structure:

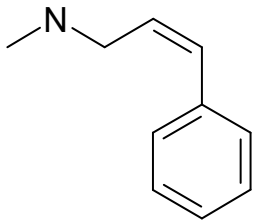

In-source (higher than precursor):

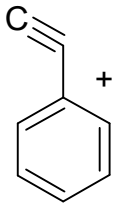

Additional evidence for structure interpretation:

- TP is also a (in-source) fragment of FLX

Attributed reaction from the parent compound to this TP:

- loss of water from TP 166

Name: TP 150.0913 (2.35 min)

MS2 Spectrum (positive)

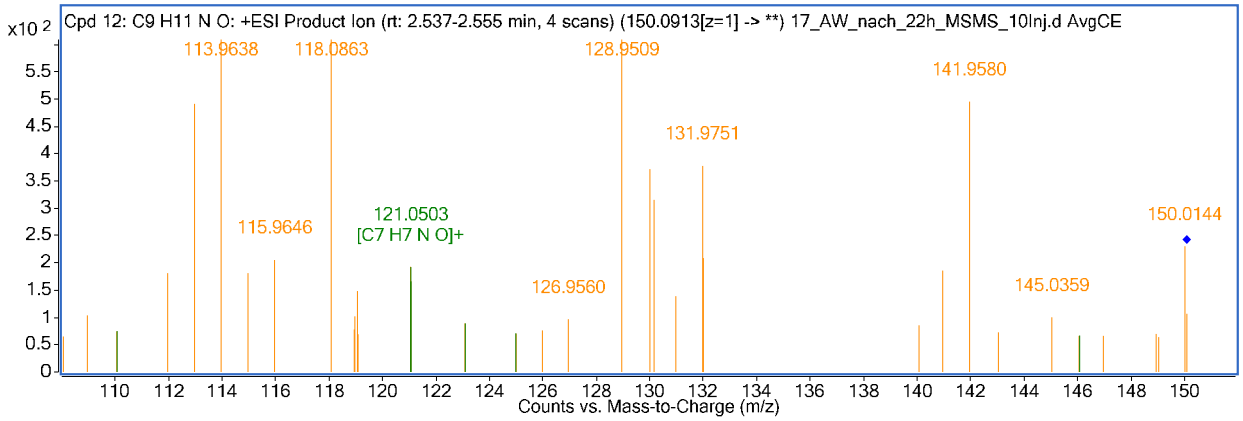

Formula (neutral): C9H11NO

Atomic Modification: -C8H7F3

Confidence level: 2b

(Proposed) Structure:

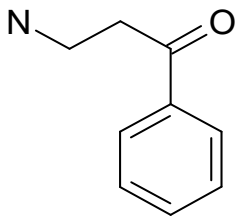

Additional evidence for structure interpretation:

- TP of NFX ozonation in literature [2]

Attributed reaction from the parent compound to this TP:

- demethylation
- cleavage of TFMP
- unsaturation

Name: TP 152.107

MS2 Spectrum (positive)

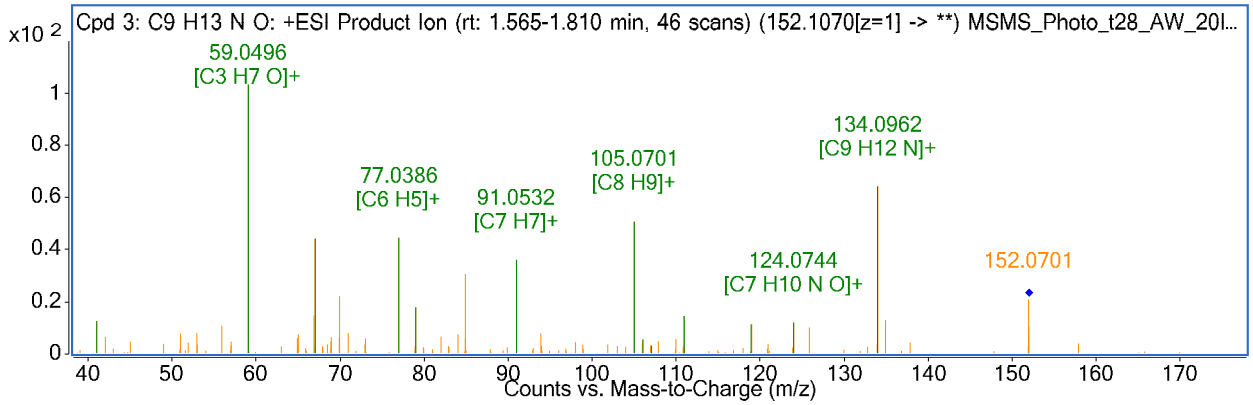

Formula (neutral): C9H13NO

Atomic Modification: -C8H9F3

Confidence level: 2a

(Proposed) Structure:

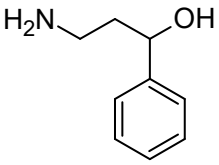

Additional evidence for structure interpretation:

- TP of NFX ozonation in literature [2]

Attributed reaction from the parent compound to this TP:

- demethylation
- cleavage of TFMP
- unsaturation

Name: TP 166.1226 (Methyl-amino-ethyl-benzyl alcohol)

MS2 Spectrum (positive)

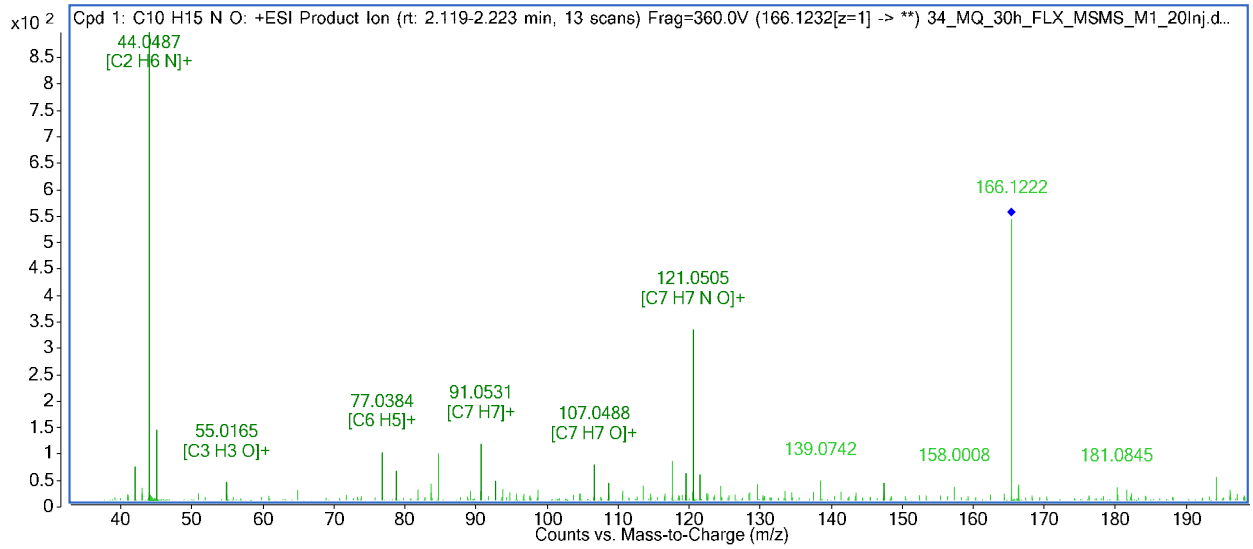

Formula (neutral): C10H15NO

Atomic Modification: -C7H4F3

Confidence level: 1

(Proposed) Structure:

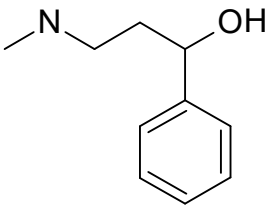

Additional evidence for structure interpretation:

- Confirmed with analytical standard

Attributed reaction from the parent compound to this TP:

- cleavage of TFMP (trifluormethylphenol group) → O-Dealkyation

Name: TP 182.1176 a (1.27 min)

MS2 Spectrum (positive)

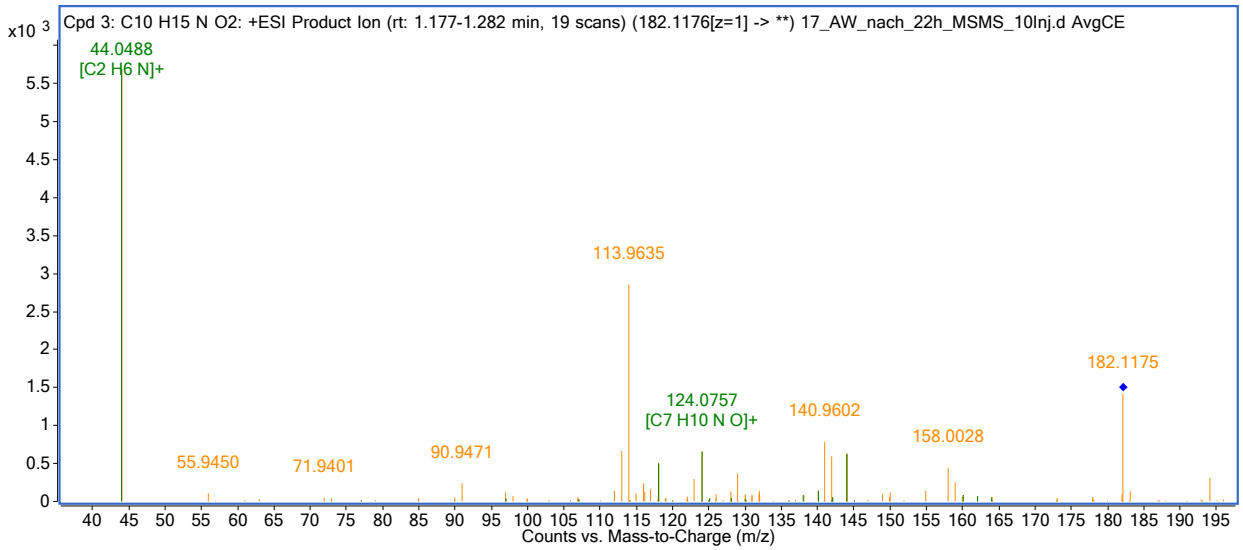

Formula (neutral): C10H15NO2

Atomic Modification: -C7H4F3 +O

Confidence level: 2a

(Proposed) Structure:

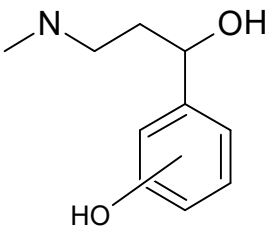

Additional evidence for structure interpretation:

- also identified in literature with “electron beam irradiation” of FLX [1]

Attributed reaction from the parent compound to this TP:

- cleavage of TFMP
- hydroxylation

Name: TP 182.1176 b (1.60 min)

MS2 Spectrum (positive)

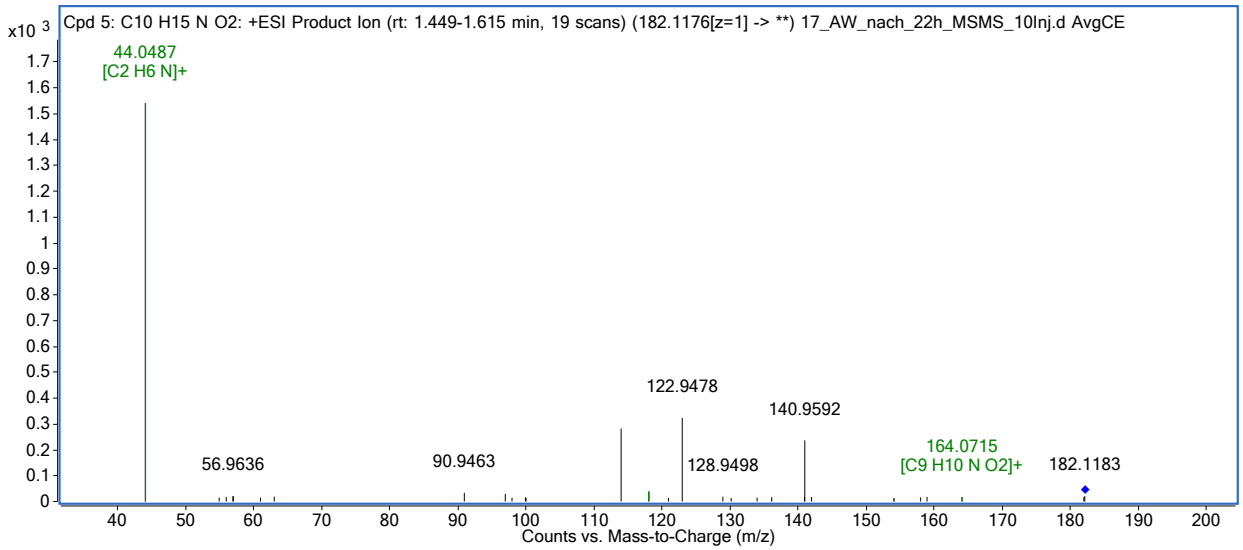

Formula (neutral): C10H15NO2

Atomic Modification: -C7H4F3 +O

Confidence level: 2a

(Proposed) Structure:

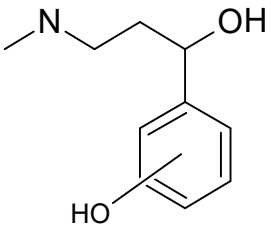

Additional evidence for structure interpretation:

- also identified in literature with “electron beam irradiation” of FLX [1]

Attributed reaction from the parent compound to this TP:

- cleavage of TFMP
- hydroxylation

Name: TP 272.1281 (3.22 min)

MS2 Spectrum (positive)

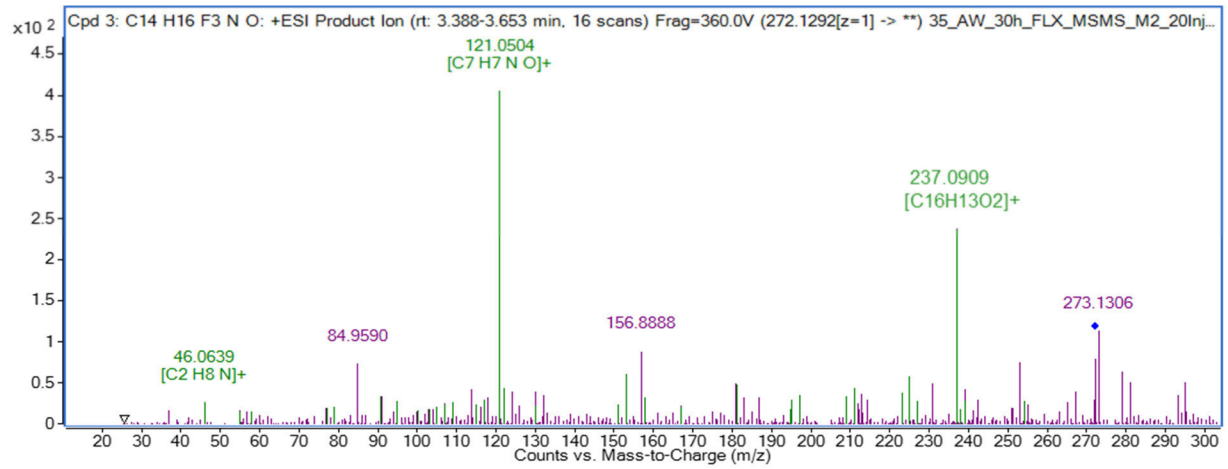

Formula (neutral): C16H17NO3

Atomic Modification: -CHF3 +2O

Confidence level: 2b

Proposed Structure:

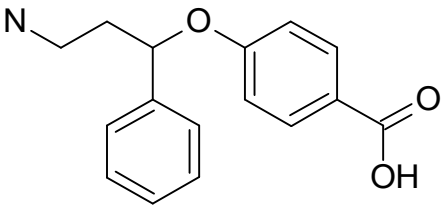

In-source:

Additional evidence for structure interpretation:

- N-demethylation due to no 44 fragment
- TP 272+Methyl= TP 286, TP 286 mentioned in literature (photodegradation of FLX) [3]
- similar fragment 237 than TP 286
- ionization negative and positive

Attributed reaction from the parent compound to this TP:

- CF3 oxidized to –COOH
- demethylation

Name: TP 286.1438 a (2.93 min)

MS2 Spectra (positive)

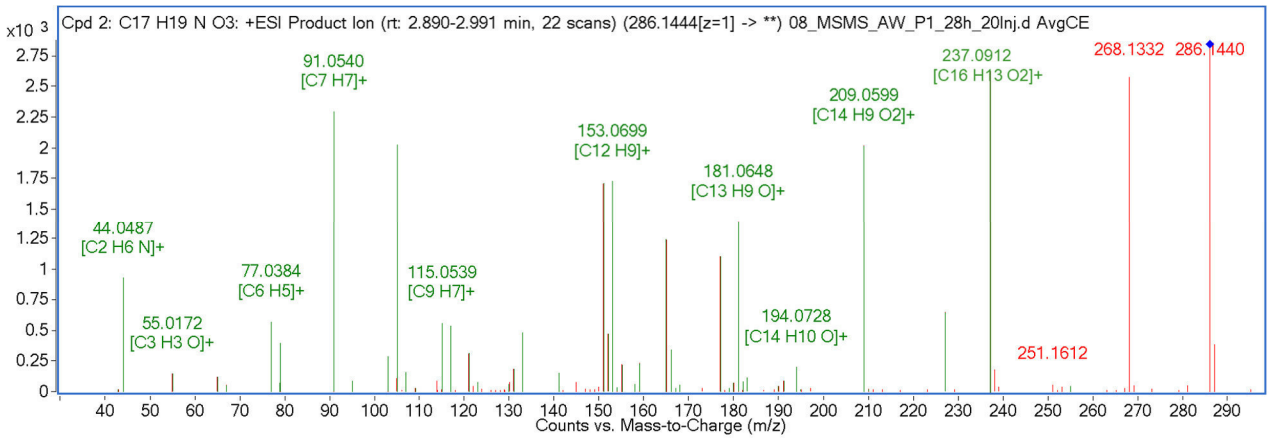

Formula (neutral): C17H19NO3

Atomic Modification: -F3 +HO2

Confidence level: 2a

Proposed Structure:

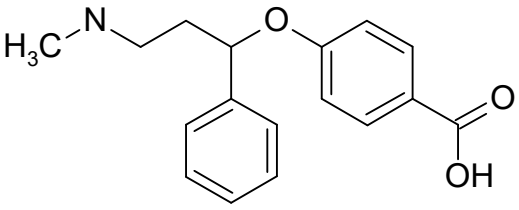

In-source:

Additional evidence for structure interpretation:

- COOH-Group: negative ionization
- sec. amine: positive ionization
- literature [3]
- 237 → same fragment than TP 272

Attributed reaction from the parent compound to this TP:

- CF3 oxidized to –COOH

Name: TP 286.1438 b (3.72 min)

MS2 Spectrum (positive)

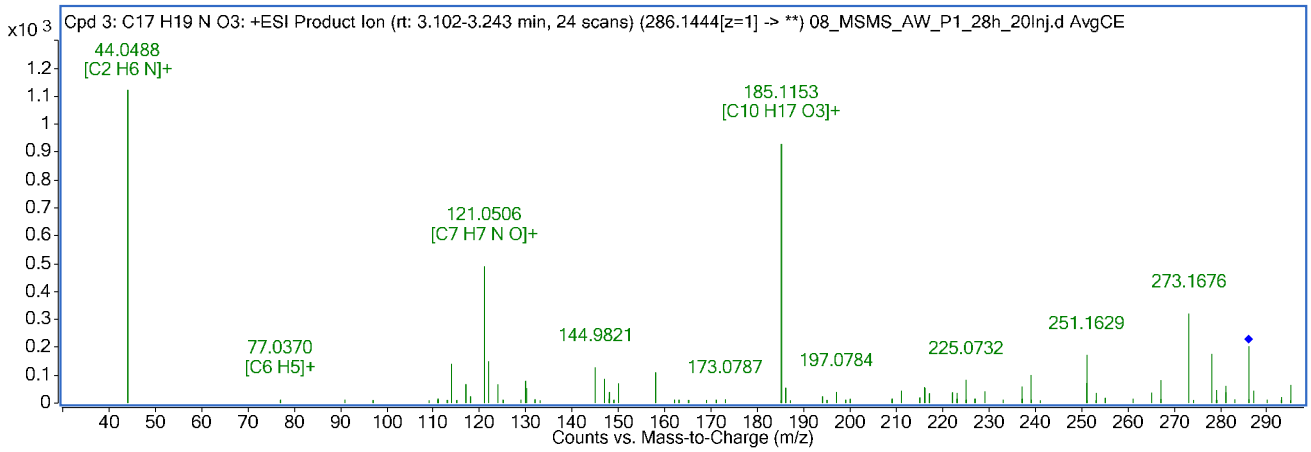

Formula (neutral): C17H19NO3

Atomic Modification: -F3 +HO2

Confidence level: 2b

Proposed Structure:

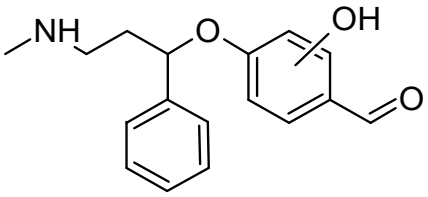

In-source:

Additional evidence for structure interpretation:

- no negative ionization (that means structural difference to 286a)
- fragment 44 unchanged (no OH attached to sec. amine moiety)
- fragment 185 → comparable with Fragment 237 from TP 286a. But with 1 O more and without aromatic ring of the phenylpropylamine moiety → no OH attached to the phenyl ring

Attributed reaction from the parent compound to this TP:

- CF3 oxidized to –COH
- hydroxylation of aromatic ring

Name: TP 284.1292/TP 286c (4.33 min)

MS2 Spectrum (negative)

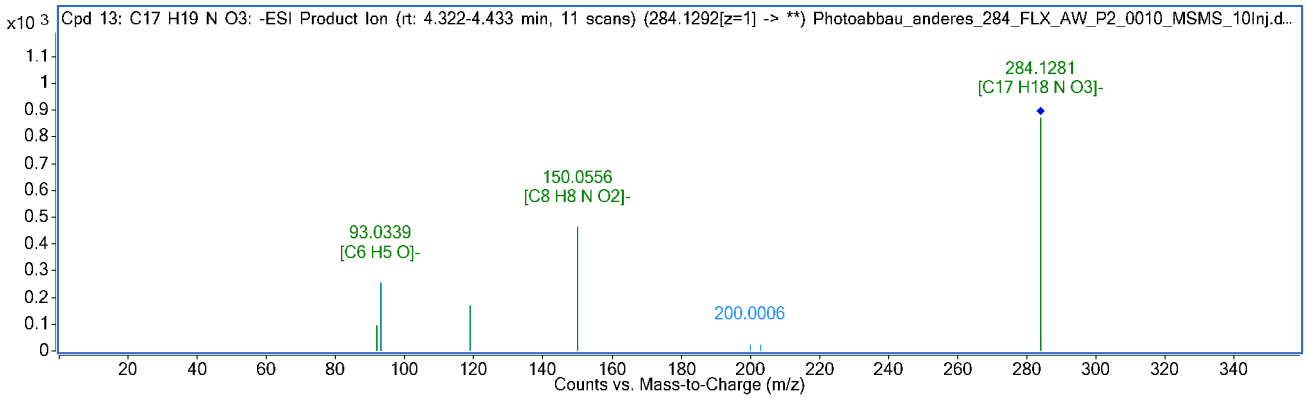

Formula (neutral): C17H19NO3

Atomic Modification: -F3 +HO2

Confidence level: 2b

Proposed Structure:

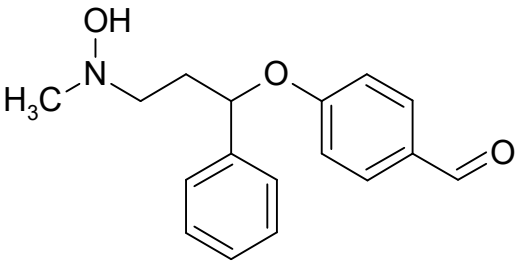

In-source:

Additional evidence for structure interpretation:

- larger retention time → oxidation occurs on N, not on C (N-oxide) [4]
- fragment with 2O and N (150)

Attributed reaction from the parent compound to this TP:

- CF3 oxidized to –COH
- N-hydroxylation

Name: TP 316.119 a [M-H]/ TP 316a (3.19 min)

MS2 Spectrum (negative)

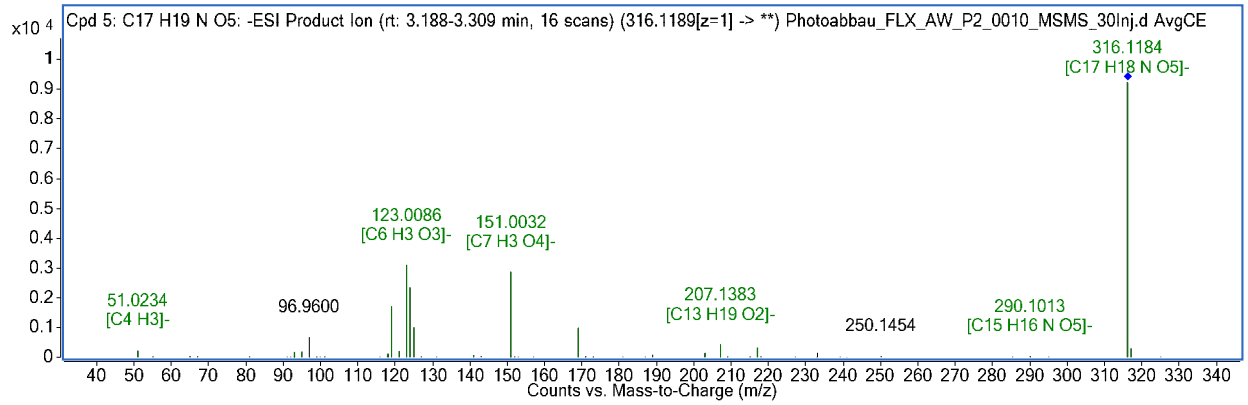

Formula (neutral): C17H19NO5

Atomic Modification: -F3 +HO4

Confidence level: 3

Proposed Structure:

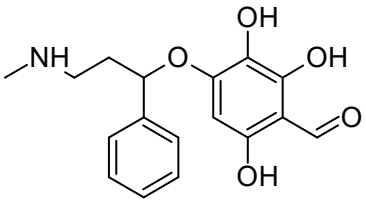

Additional evidence for structure interpretation:

- fragment C7H5O5 (m/z 169.0139+) → 3 O attached to aromatic ring of carboxyl side

Attributed reaction from the parent compound to this TP:

- CF3 hydrolyzed to –COOH (Lam 2005)
- 2 x hydroxylation

Name: TP 316.119 b [M-H]/ TP 316b (3.43 min)

MS2 Spectrum (negative)

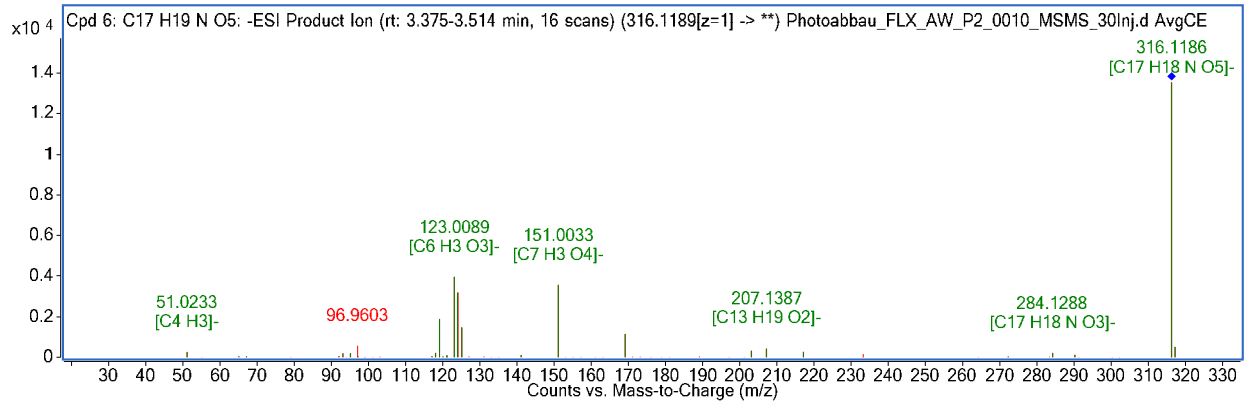

Formula (neutral): C17H19NO5

Atomic Modification: -F3 +HO4

Confidence level: 3

Proposed Structure:

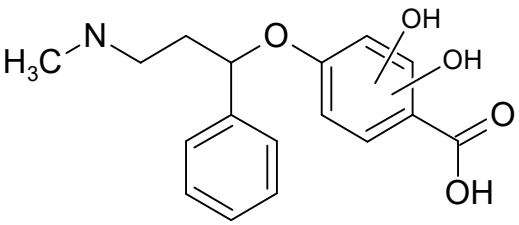

Additional evidence for structure interpretation:

- fragment C7H5O5 (m/z 169.0139+) → 3 O attached to aromatic ring of carboxyl side
- fragment m/z 286.1288 → TP 286a is a fragment of TP 316b

Attributed reaction from the parent compound to this TP:

- CF3 hydrolyzed to –COOH (Lam 2005)
- 2 x hydroxylation

Name: TP 324.157 (4.59 min)

MS2 Spectrum (positive)

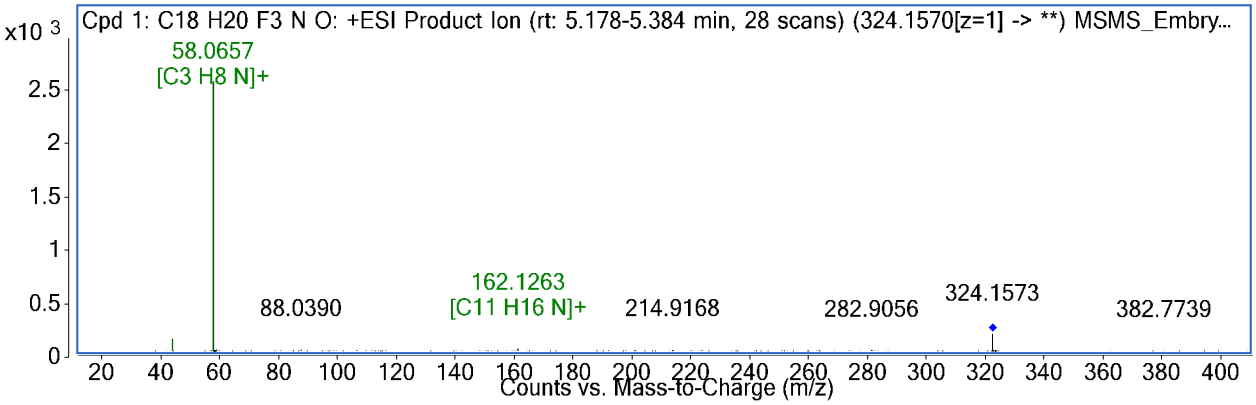

Formula (neutral): C18H20F3NO

Atomic Modification: +CH2

Confidence level: 2b

Proposed Structure:

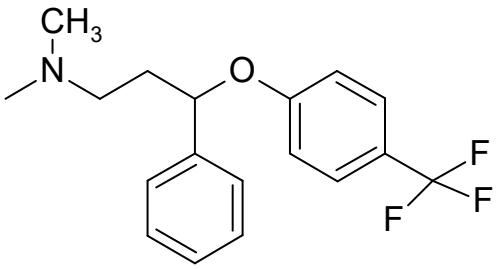

In-source:

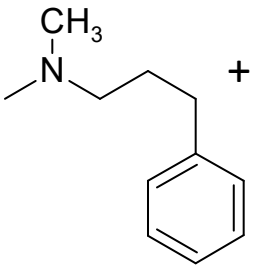

Additional evidence for structure interpretation:

- fragment C3H8N (m/z 58.0657)→ CH2 attached to m/z 44.05 (C2H6N)

Attributed reaction from the parent compound to this TP:

Name: TP 326.1362 a (4.69 min)

MS2 Spectra (positive and negative)

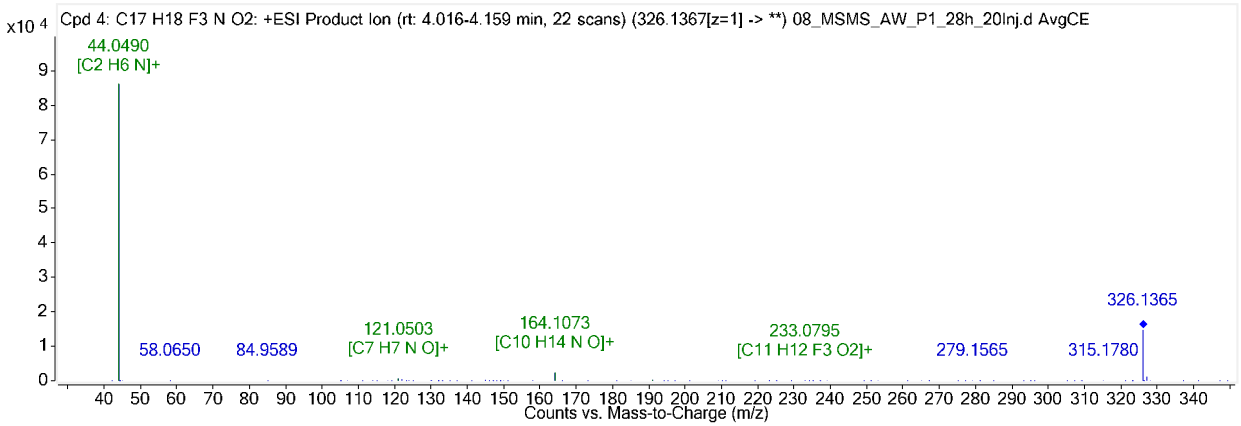

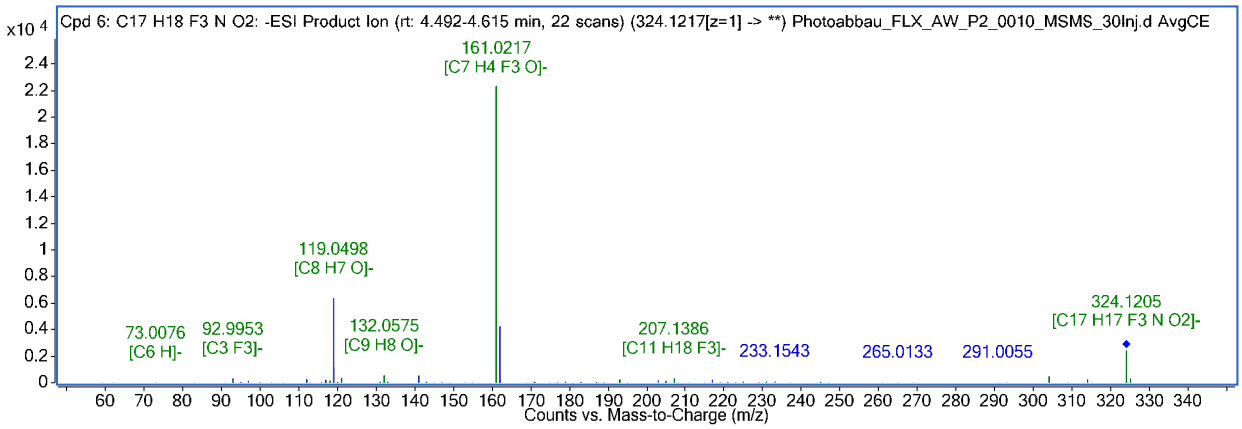

Formula (neutral): C17H18NO2F3

Atomic Modification: +O

Confidence level: 2a

Proposed Structure:

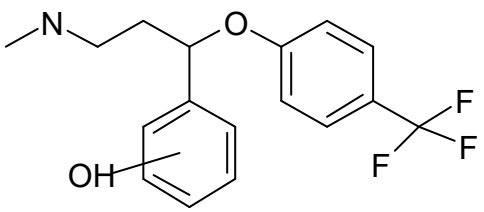

Additional evidence for structure interpretation:

- TFMP is unimpaired (fragment m/z 161.0217)

Name: TP 326.1367 b (4.91 min)

MS2 Spectra (positive)

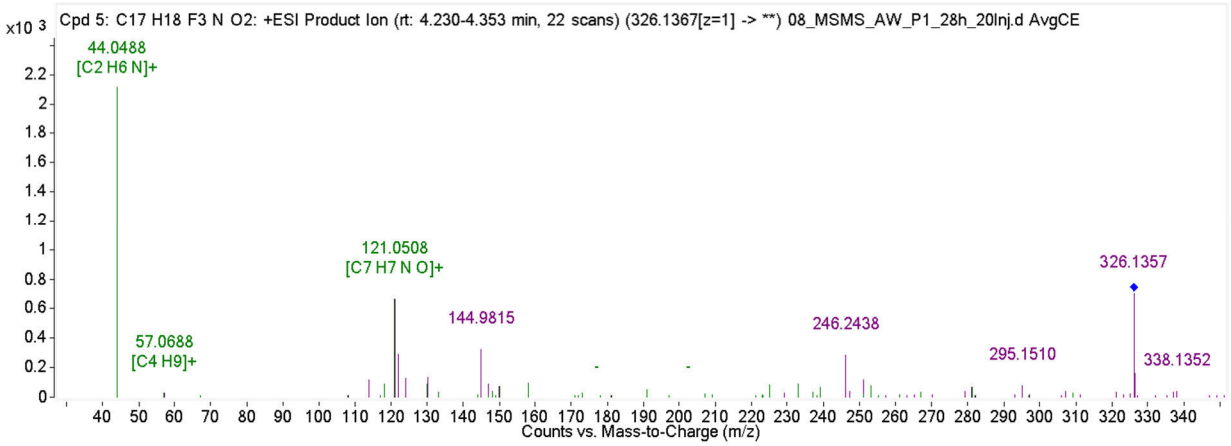

Formula (neutral): C17H18NO2F3

Atomic Modification: +O

Confidence level: 2a

Proposed Structure:

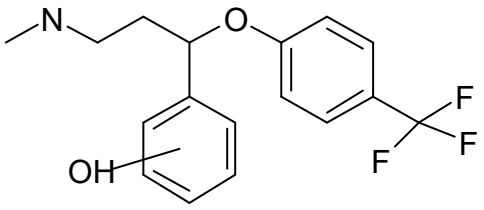

In-source:

Additional evidence for structure interpretation:

- no differences in MS/MS Spectra → same ring, ring position from literature [3]
- smaller area, maybe the reason for no detection in negative

Name: TP 326.1367 c (5.5 min)

MS2 Spectra (positive)

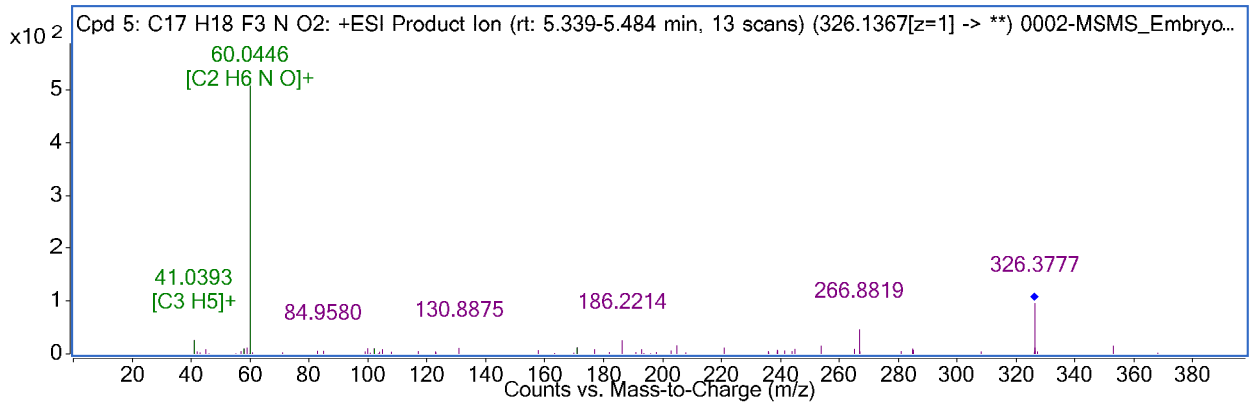

Formula (neutral): C17H18NO2F3

Atomic Modification: +O

Confidence level: 2a

Proposed Structure:

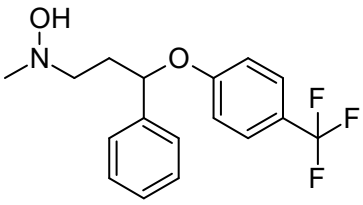

Additional evidence for structure interpretation:

➔ N-oxide due to fragment 60.0446 instead of fragment 44 (O in addition)

Name: TP 338.1362 (6.83 min)

MS2 Spectra (positive)

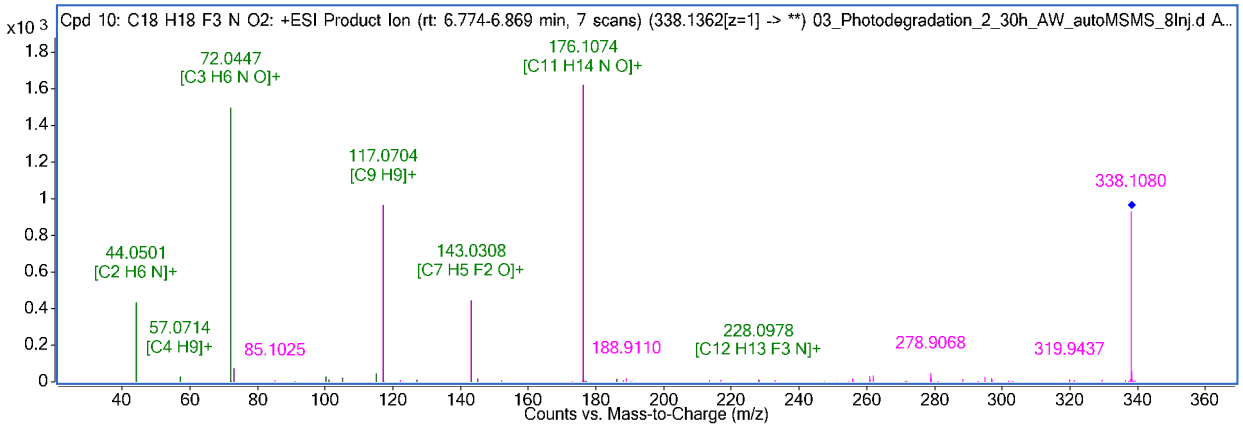

Formula (neutral): C18H18F3NO2

Atomic Modification: +CO

Confidence level: 2a

Proposed Structure:

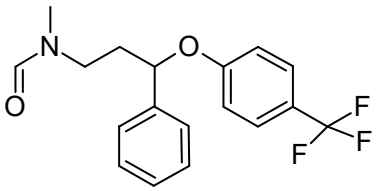

In-source:

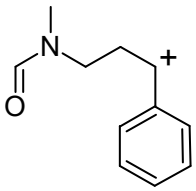

Additional evidence for structure interpretation:

- M+H and M+Na precursor detected
- in-source fragment
- precursor and in-source fragment identified in biotransformation of NFLX [5]

Attributed reaction from the parent compound to this TP:

- N-formylation (formaldehyde attached)

Name: TP 352.152 (6.87 min)

MS2 Spectra (positive)

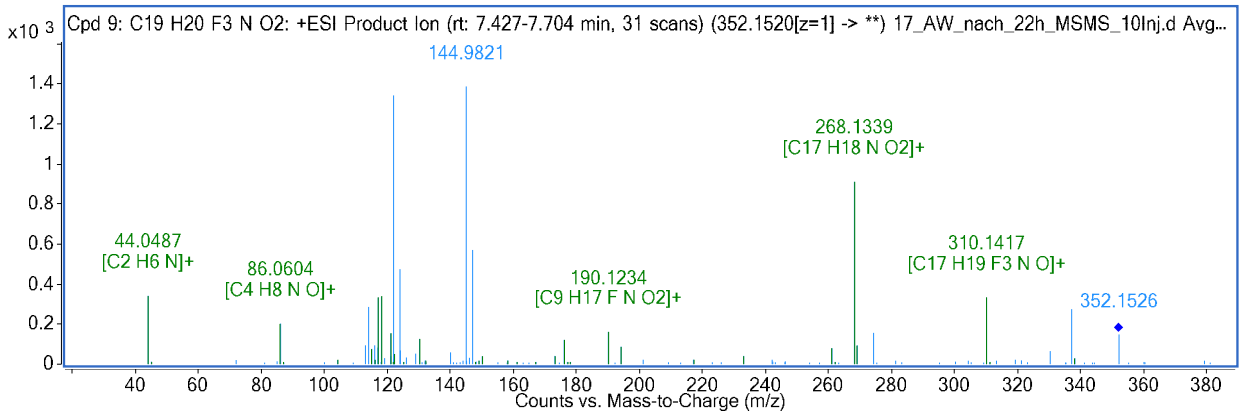

Formula (neutral): C19H20NO2F3

Atomic Modification: +C2H2O

Confidence level: 2a

Proposed Structure:

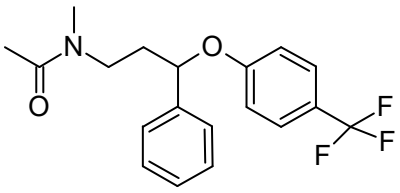

In-source:

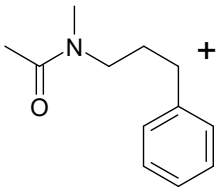

Additional evidence for structure interpretation:

- cleavage of TFMP (smiliar to insource of the other compounds)
- precursor and in-source fragment (300% intensity of precursor) identified in biotransformation [5]

Attributed reaction from the parent compound to this TP:

N-acetylation or the combination of N-demethylation and N-propionylation [5]

Name: TP 364.1519 (6.63 min)

MS2 Spectra (positive)

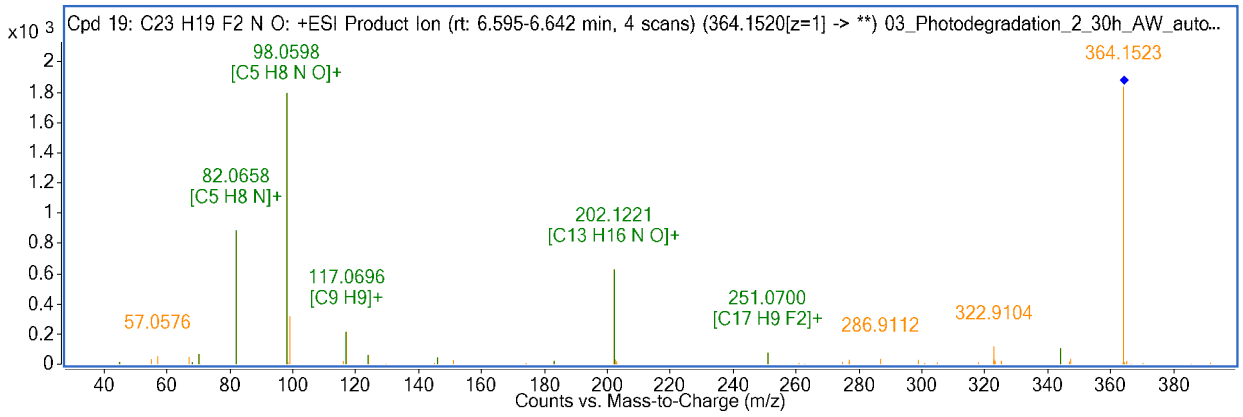

Formula (neutral): C20H20NO2F3

Atomic Modification: +C3H2O

Confidence level:

Proposed Structure:

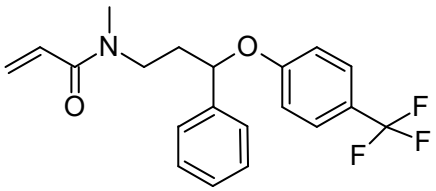

In-source:

Additional evidence for structure interpretation:

- cleavage of TFMP (smiliar to insource of the other compounds)
- M+H and M+Na Precursor

Attributed reaction from the parent compound to this TP:

- N-propionylation and unsaturation (-2H) or acrylaldehyde attached

TP 366.1672 (5.05 min)

Formula (neutral): C20H22NO2F3

Too small for fragmentation

Atomic Modification: +C3H4O

Confidence level: 2b

Proposed Structure:

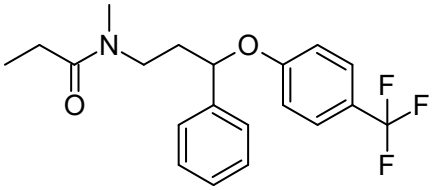

In-source:

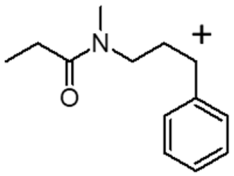

Additional evidence for structure interpretation:

- cleavage of TFMP (smiliar to insource of the other compounds)
- M+H and M+Na Precursor

Attributed reaction from the parent compound to this TP:

- N-propionylation and unsaturation (-2H) or acrylaldehyde attached

Name: TP 378.1675 a (5.78 min)

MS2 Spectra (positive)

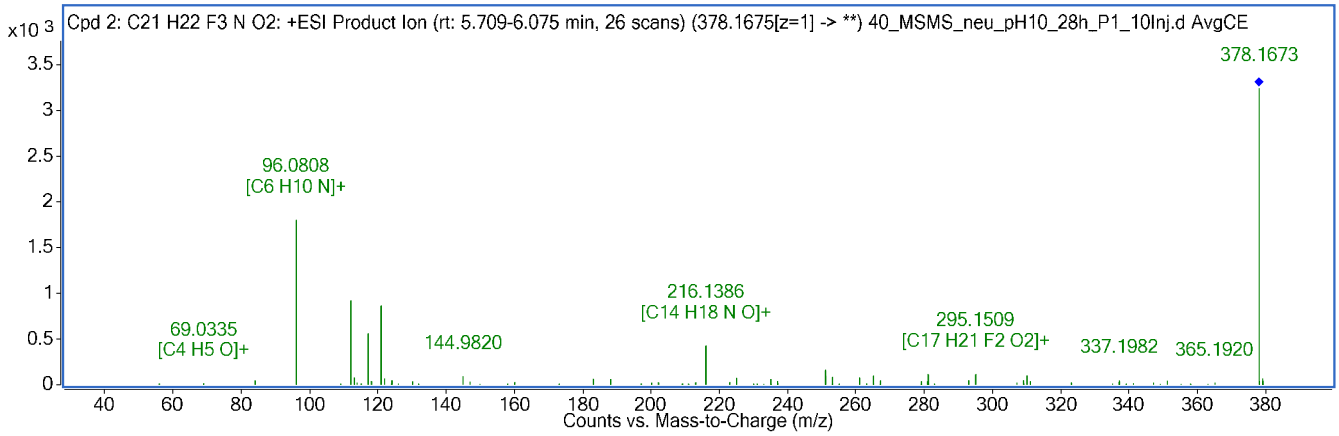

Formula (neutral): C21H22NO2F3

Atomic Modification: +C4H4O

Confidence level: 3

Proposed Structure:

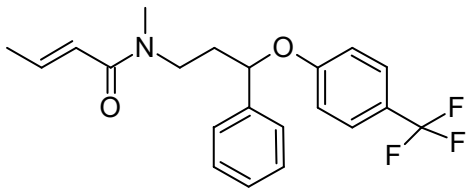

Additional evidence for structure interpretation:

- fragment: cleavage of TFMP (similar to insource of the other compounds)

Attributed reaction from the parent compound to this TP:

- croton aldehyde, 3-butenal or methacrolein attached

Name: TP 378.1675 b (6.82 min)

MS2 Spectra (positive)

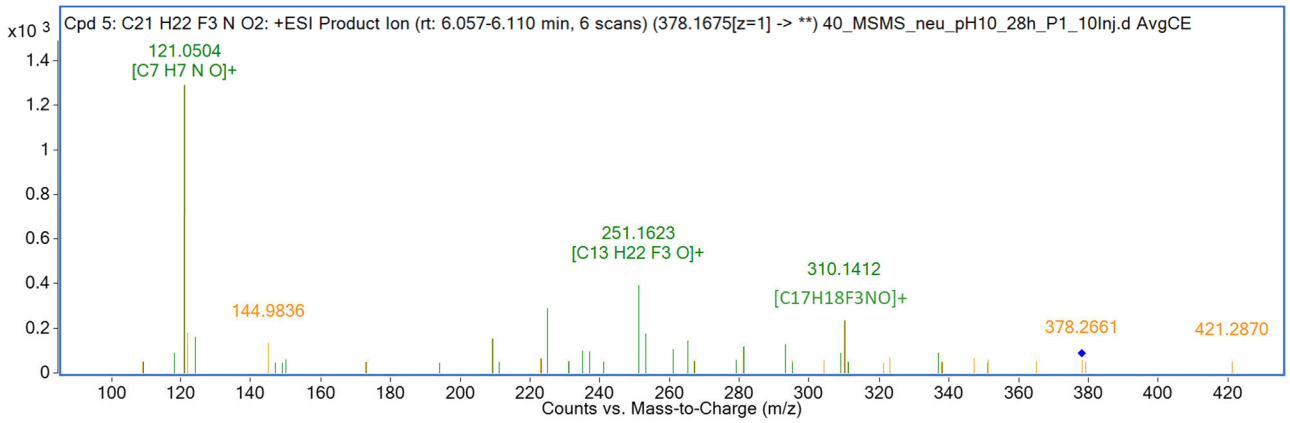

Formula (neutral): C21H22NO2F3

Atomic Modification: +C4H4O

Confidence level: 3

Proposed Structure:

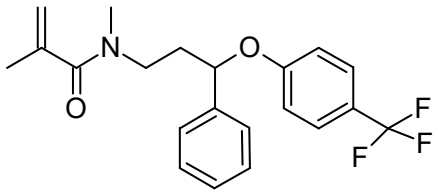

In-source:

Additional evidence for structure interpretation:

- FLX as a fragment

Attributed reaction from the parent compound to this TP:

- croton aldehyde, 3-butenal or methacrolein attached

Name: TP 380.1115 [M-H]/ TP 382 (6.18)

MS2 Spectrum (negative)

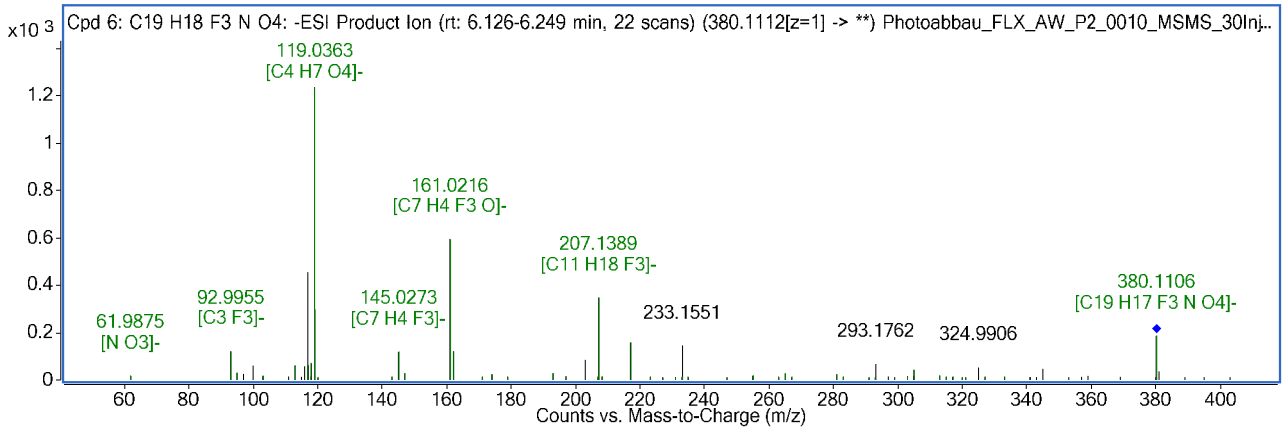

Formula (neutral): C19H18F3NO4

Atomic Modification +C2O3

Confidence level: 2b

Proposed Structure:

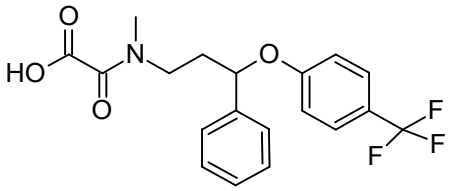

In-source:

Additional evidence for structure interpretation:

- reaction on left side (TFMP unimpaired)

Attributed reaction from the parent compound to this TP:

- oxalic acid attached

Name: TP 396.1419 (6.60 min)

MS2 Spectrum (positive)

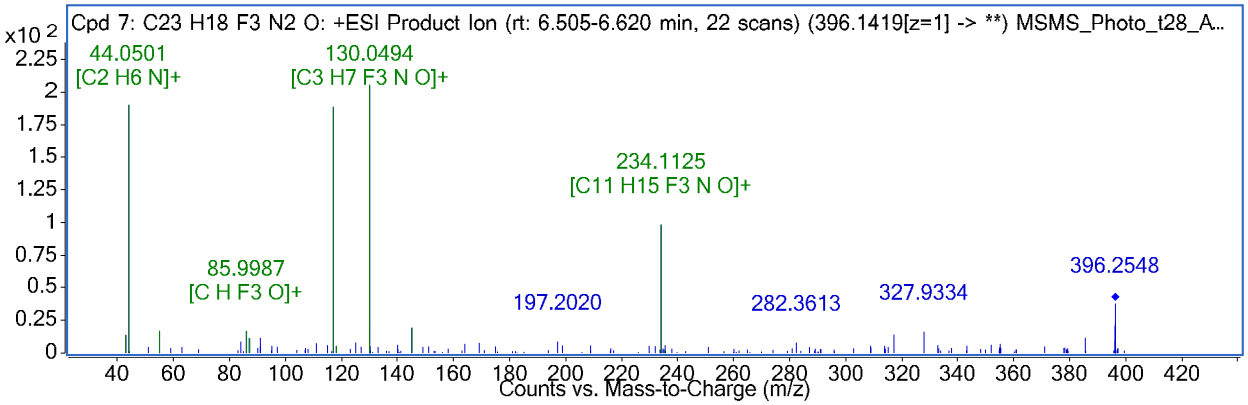

Formula (neutral): C20H21NO4F3

Atomic Modification: +C4H4O3

Confidence level: 2b

Proposed Structure:

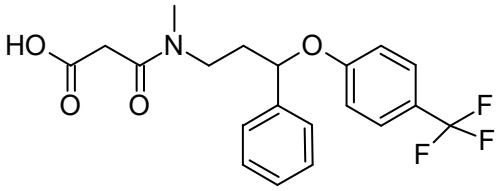

In-source:

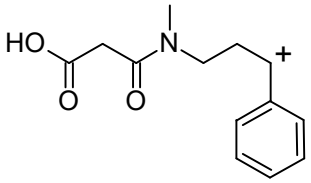

Additional evidence for structure interpretation:

- in-source: loss of TFMP (smiliar to in-source of the other compounds)
- in literature: only in-source 234.1126 was detected →assumption of 396.1419 as precursor. N-succinylation of NFLX (biotransformation) [5]

Attributed reaction from the parent compound to this TP:

- N-malonylation (malonic acid attached)

Name: TP 408.1417 (6.62 min)

MS2 Spectrum (positive)

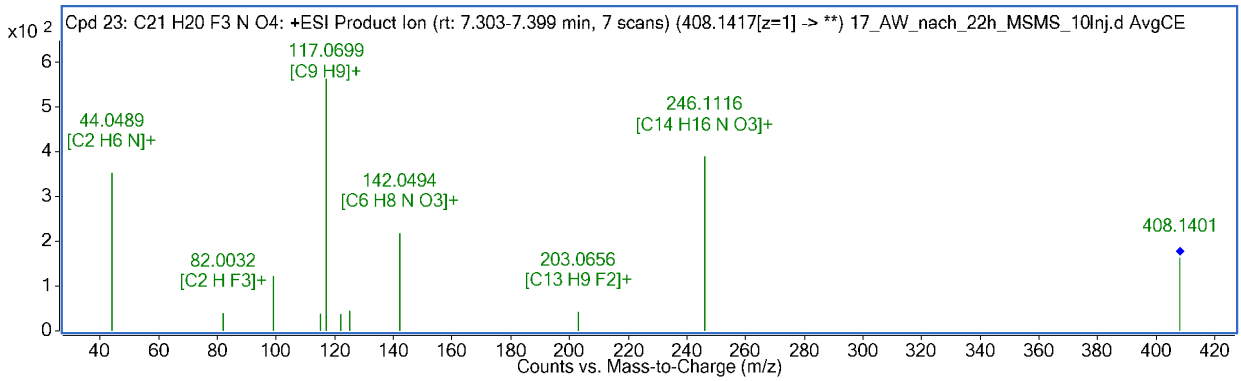

Formula (neutral): C21H20F3NO4

Atomic Modification: +C4H2O3

Confidence level: 2b

Proposed Structure:

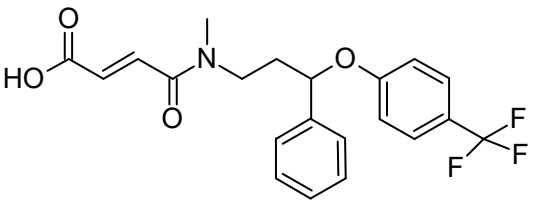

In-source:

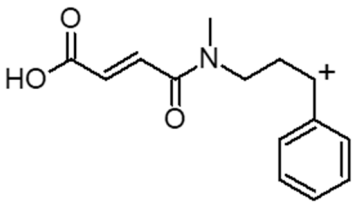

Additional evidence for structure interpretation:

- cleavage of TFMP (smiliar to insource of the other compounds)

Attributed reaction from the parent compound to this TP:

- fumaric acid attached

Name: TP 409.2071 (5.72 min)

MS2 Spectrum (positive)

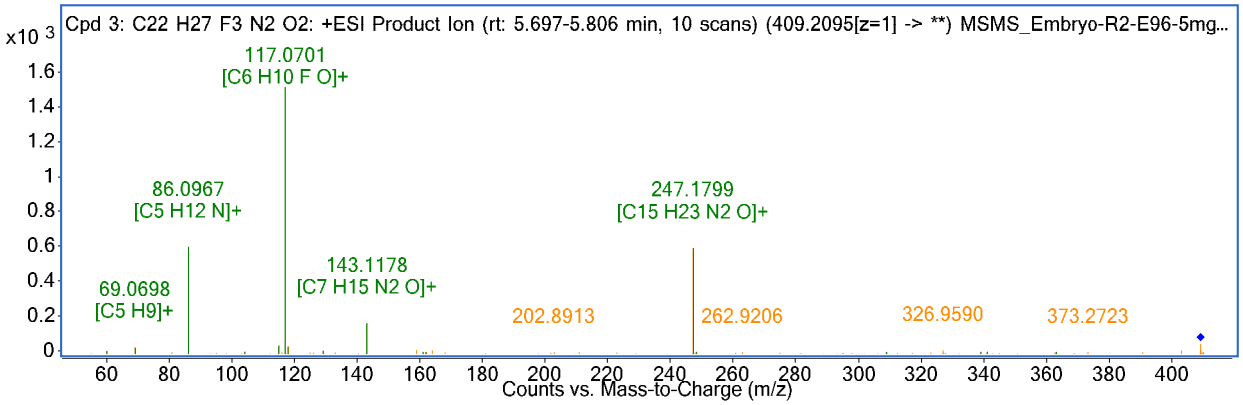

Formula (neutral): C22H27F3N2O2

Atomic Modification: +C5H9NO

Proposed Structure:

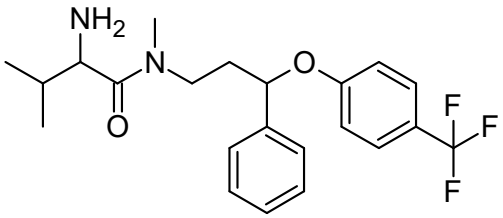

In-source:

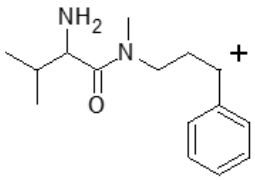

Additional evidence for structure interpretation:

- M+H and M+Na
- MSMS –> IF as a fragment. N on the left side

Name: TP 410.1547 (6.55 min)

MS2 Spectrum (positive)

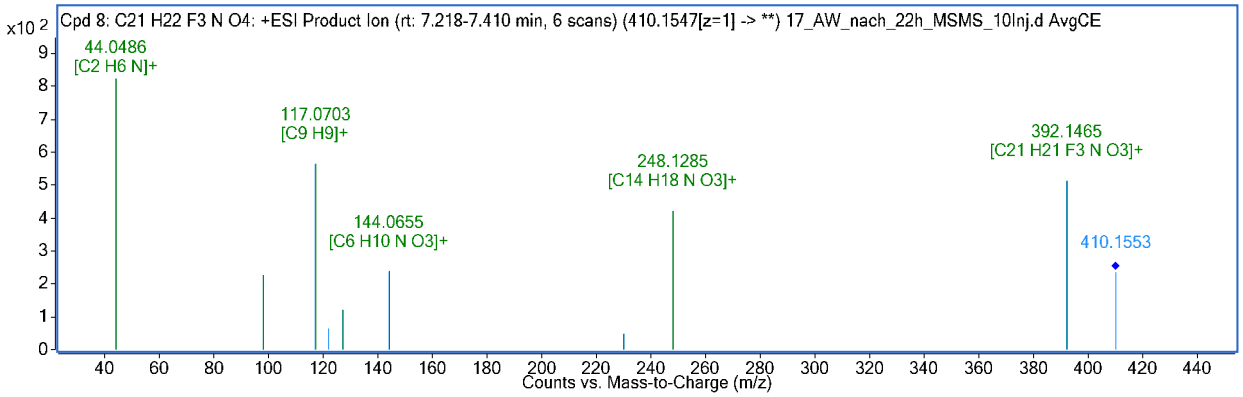

Formula (neutral): C21H22F3NO4

Atomic Modification: +C4H4O3

Confidence level: 2a

Proposed Structure:

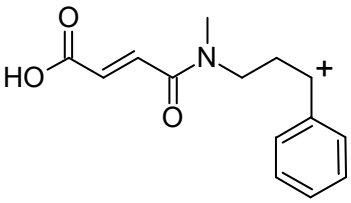

In-source:

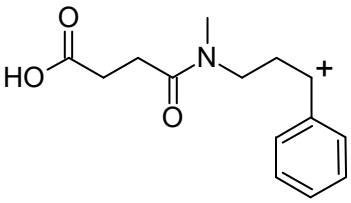

Additional evidence for structure interpretation:

- cleavage of TFMP (smiliar to insource of the other compounds)
- precursor and in-source fragment (170% intensity of precursor) identified in biotransformation [5]

Attributed reaction from the parent compound to this TP:

- N-succinylation (succinic acid)

Name: TP 430.1625 (6.87 min)

MS2 Spectrum (positive and negative)

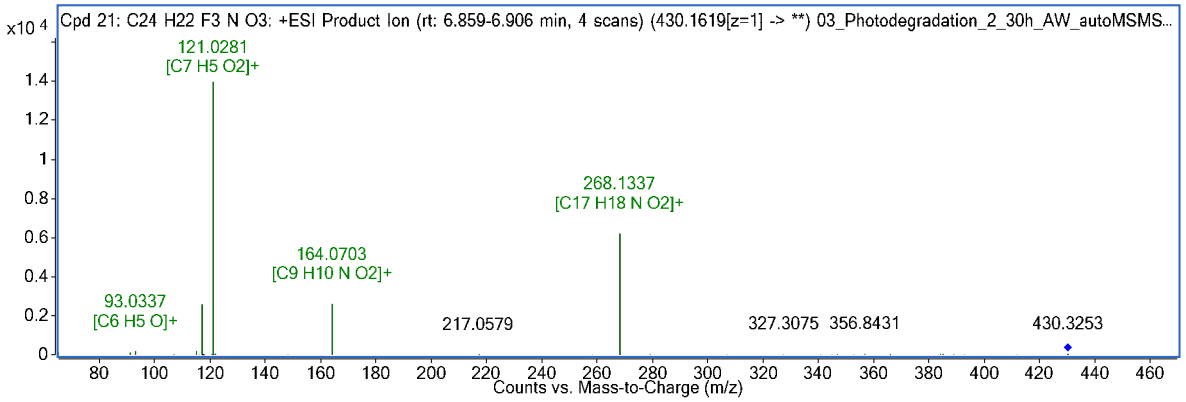

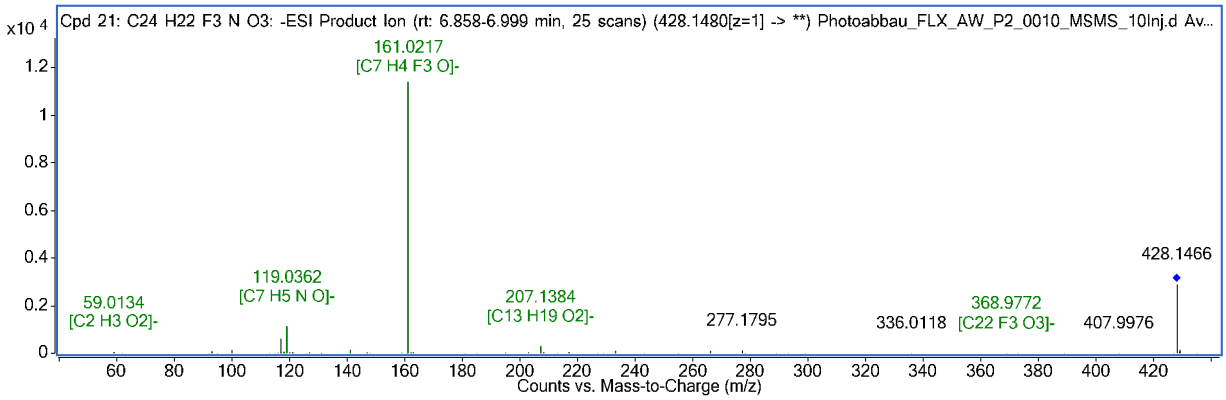

Formula (neutral): C24H22F3NO3

Atomic Modification: +C7H4O2

Confidence level: 3

Proposed Structure:

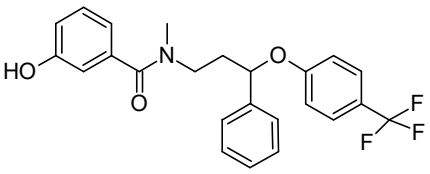

Additional evidence for structure interpretation:

- cleavage of TFMP as a fragment (268)
- positive and negative → OH Group on the left side (TFMP is a fragment (unimpaired)